Aus dem CharitéCentrum 13 für Innere Medizin
mit Gastroenterologie und Nephrologie,
Medizinische Klinik für Gastroenterologie, Infektiologie und Rheumatologie
(einschl. Arbeitsbereich Ernährungsmedizin)

Leiter: Prof. Dr. Jörg-Dieter Schulzke

Habilitationsschrift

Pathomechanismen epithelialer Barrieredysfunktion durch bakterielle Enteropathogene

zur Erlangung der Lehrbefähigung
für das Fach Experimentelle Biomedizin

vorgelegt dem Fakultätsrat der Medizinischen Fakultät
Charité – Universitätsmedizin Berlin

von

Dr. Roland Bücker

geboren am **in Hagen**

Eingereicht: **Januar 2015**

Dekan: **Prof. Dr. Axel Radlach Pries**

1. Gutachter/in: Prof. Dr. Jörg Hacker, Halle (Saale)

2. Gutachter/in: Prof. Dr. Steffen Backert, Erlangen

Inhaltsverzeichnis

Abkürzungsverzeichnis der Habilitationsschrift

A/E	Attaching & Effacing-Läsionen
CED	Chronisch-entzündliche Darmerkrankungen
CRP	C-reaktives Protein
Da	Dalton
DNA	Desoxyribonukleinsäure
EHEC	Enterohämorrhagische *Escherichia coli*
EPEC	Enteropathogene *Escherichia coli*
FITC	Fluoresceinisothiocyanat
HDM	Hämolysin-defiziente Mutante
HlyA	α-Hämolysin
HRP	Horseradish Peroxidase, Meerrettichperoxidase
HT-29/B6	B6-Klon der humanen Kolonkarzinom-Zelllinie HT-29
IL-10$^{-/-}$	Interleukin-10-defiziente Maus
LDH	Lactatdehydrogenase
LPS	Lipopolysaccharide
MA	Monoassoziation
MLCK	Myosin-Light Chain Kinase, Myosin-Leichte-Ketten-Kinase
mRNA	Boten-Ribonukleinsäure
MyD88	Myeloid Differentiation Faktor 88
PCR	Polymerase-Kettenreaktion
PFT	Porenbildendes Toxin
R^t	Transepithelialer elektrischer Widerstand
SIRS	Systemic Inflammatory Response Syndrome
spp.	Spezies (plural)
TAMP	Tight Junction-associated MARVEL proteins
TNFα	Tumornekrosefaktor-alpha
UPEC	Uropathogene *Escherichia coli*
WT	Wildtyp

Prolog

Der Aufbau dieser kumulativen Habilitationsschrift gliedert sich in zwei Unterthemen, die insgesamt fünf Originalarbeiten umfassen, wobei das zentrale Thema beide Bereiche umfasst. Im Mittelpunkt der Untersuchungen steht die **Barrierestörung** an intestinalen Epithelien, die, wie im ersten Teil der eigenen Arbeiten 2.1 beschrieben, durch **invasive Bakterien** aus der Familie der *Campylobacteraceae* (Klasse: Epsilon-Proteobacteriae) oder, wie im zweiten Teil 2.2 dargestellt, durch sezernierte **porenbildende Toxine**, sogenannte Hämolysine, aus der Familie der *Enterobacteriacea*e (Klasse: Gamma-Proteobacteriae) ausgelöst werden kann. Welcher Art die Barrierestörung ist oder auf welche Weise die pathologischen Veränderungen am Epithel mediiert werden, ist Gegenstand der ausgewählten Publikationen. In diesen Arbeiten werden zwei pathomechanistisch geprägte Termini verwendet, die inzwischen Eingang in die wissenschaftliche Literatur gefunden haben: **Leckflux** und **Leaky Gut**.

Beide Begriffe stehen für Konzepte, die Erklärungsansätze für die Entstehung von Diarrhö oder für Entzündungen des Darms als Folge einer epithelialen Barrierestörung mit gesteigerter intestinaler Permeabilität von Wasser und Ionen bis zu größeren Antigenen als gemeinsames Pathophänomen liefern.

1. Einleitung

1.1 Barrierefunktion und Diarrhö

Prinzipiell kann jede Diarrhö unabhängig von ihrer Genese als gestörtes Gleichgewicht von intestinaler Resorption und Sekretion beschrieben werden. Während lange Zeit die Charakterisierung von Funktionsstörungen der Motilität (motilitätsbedingte Diarrhö), aktiver Resorptionsprozesse (z.B. bei malabsorptiven Diarrhöen wie der Zöliakie) oder aktiver Sekretionsprozesse (wie bei infektiösen Diarrhöen) im Vordergrund stand, ist in den letzten Jahren auch der Einfluss der epithelialen Barrierefunktion eingehender untersucht worden. So ist inzwischen belegt, dass eine isolierte epitheliale Barrierestörung infolge eines ins Lumen gerichteten passiven Fluxes von kleinmolekularen Soluten und Wasser eine Diarrhö hervorrufen kann. Diese Form wird als **Leckflux-Diarrhö** bezeichnet. Es konnte gezeigt werden, dass dieser Mechanismus bei der Infektion mit *Clostridium difficile* eine Rolle spielt (Hecht et al., 1992) und sogar zu der profusen Diarrhö bei *Vibrio cholerae* beiträgt, wie aus dem diarrhöischen Effekt von Impfstämmen von *Vibrio cholerae* hervorgeht (Fasano et al., 1991). Letzteres wurde besonders evident in Untersuchungen von Choleratoxin-Gen deletierten Impfstämmen, die natürlich keine aktive elektrogene Chlorid-Sekretion via zyklisches Adenosinmonophosphat (cAMP) mehr induzieren können, aber trotzdem eine Diarrhö hervorrufen. Für diesen Effekt konnte eine von diesen Impfstämmen induzierte epitheliale Barrierestörung als Ursache identifiziert werden und zwar durch ein zweites unabhängiges Toxin vermittelt,

das Zonula occludens-Toxin. Da bei vielen Darmerkrankungen, die zu einer Diarrhö führen, inzwischen auch Störungen der epithelialen Barrierefunktion gefunden wurden, stellt der **Leckflux-Mechanismus** offenbar einen wichtigen Pathomechanismus dar.

Ein zweiter bedeutender Aspekt der intestinalen Barrierefunktion des Epithels betrifft seine Funktion als immunologische Barriere. Eine erhöhte Permeabilität für Makromoleküle stellt einen zentralen Pathomechanismus bei einer Vielzahl von lokal und systemisch entzündlichen Erkrankungen dar. Vor diesem Hintergrund ist verständlich, weshalb die Barrierefunktion des Darmes inzwischen in vielen Arbeitsgruppen intensiv erforscht wird (Shen & Turner, 2006). Bei entzündlichen Erkrankungen des Gastrointestinaltraktes geht mit der Entzündung eine Barrierestörung einher, was in der Folge eine Translokation von Bakterien und Antigenen forciert (Porras et al., 2006). Der Übertritt von immunogenen Substanzen über ein "leckes" Epithel vom Darmlumen in den Organismus als Auslöser entzündlicher Reaktionen wird auch **Leaky Gut** genannt (Ma, 1997). Die Wirkung der residenten Mikrobiota auf den Darm ist dabei ein Erklärungsansatz für die Fehlregulation des Immunsystems bei chronisch-entzündlichen Darmerkrankungen (CED) (Packey & Sartor, 2008).

1.2 Epitheliale Barriere des Darmes

Die epitheliale Barriereeigenschaft des Darmes wird durch das komplexe Zusammenspiel der Epithelzellen und ihrer Zell-Zell-Verbindungen, insbesondere der *Tight Junction*, bestimmt (Turner et al., 2014), wobei in Abhängigkeit von der betrachteten Stoffklasse auch andere Phänomene wie Transzytose eine Rolle spielen (Schumann et al., 2012). Zu den weiteren modulierenden Faktoren werden Veränderungen der Apoptoserate im Epithelverband gezählt. Kann z.B. das Epithel im Rahmen einer Entzündung nicht ausreichend schnell remodelliert werden, resultiert daraus ebenfalls ein Barrieredefekt. Hier sind also auch Wachstumsfaktoren relevant, welche die Epithelregeneration fördern können. Der Endpunkt eines Ungleichgewichts von Epitheldestruktion und -regeneration ist dann die Entstehung von Epithelläsionen wie Erosionen und Ulzerationen.

1.3 Tight Junction und Tight Junction-Proteine

Bei intaktem Epithelzellverband ist die Integrität der *Tight Junction*-Domäne der Zelle für die ionale Leitfähigkeit eines Epithels von ausschlaggebender Bedeutung. Der molekulare Aufbau der *Tight Junction* ist seit einigen Jahren genauer bekannt (zur Übersicht vgl. Günzel & Fromm, 2012; Günzel & Yu, 2013). Am Aufbau der *Tight Junction*-Strängen im Sinne eines Heteropolymers sind zwei Familien von vierfach-membrandurchspannenden Proteinen beteiligt, Claudine und *Tight Junction-associated MARVEL proteins* (TAMPs) (Günzel & Fromm, 2012).

Die **Claudin-Familie** besteht bei Mammalia aus 27 Mitgliedern (Claudin-1 bis Claudin-27) (Günzel & Yu, 2013). Kürzlich ist mit Claudin-15 die erste Kristallstruktur eines *Tight Junction*-Proteins aufgeklärt worden (Suzuki et al., 2014). Aber wie sich die Heteropolymere von *Tight Junction*-Proteinen konkret ausbilden ist bisher unbekannt. Trotz molekularer Ähnlichkeit besitzen sie hinsichtlich ihrer Barrierefunktion unterschiedliche Eigenschaften: Einige Claudine haben eine rein abdichtende Funktion, andere bilden parazelluläre Kanäle für kleine Ionen oder Wasser (Übersicht: Krug et al., 2012). Dabei gibt es Claudine, die eine erhöhte Leitfähigkeit für Kationen oder Anionen besitzen. So stellt beispielsweise Claudin-2 einen Kanal für Natrium-Ionen und auch für Wasser dar (Amasheh et al., 2002, Rosenthal et al., 2010). Als abdichtende Claudine werden im humanen Kolon, sowie auch in dem von unserer Gruppe entwickelten intestinalen Epithelzellmodell HT-29/B6, u.a. Claudin-1, -3, -4, -5, und -8 exprimiert. Die **TAMP-Familie** besteht aus den drei Proteinen Occludin, Tricellulin und MarvelD3 (Raleigh et al., 2010). Ihr gemeinsames Motiv ist die MARVEL-Domäne ("MAL and related proteins for vesicle trafficking and membrane link") (Sanchez-Pulido et al., 2002). Eine besondere Rolle spielt Tricellulin, das hauptsächlich in trizellulären Zellkontaktpunkten lokalisiert ist. Diese trizelluläre *Tight Junction* stellt eine potentielle Schwachstelle der gesamten *Tight Junction* dar (Ikenouchi et al., 2005). Es konnte gezeigt werden, dass der Durchtritt von kleinen Makromolekülen mit einem Molekulargewicht von bis zu 20 kDa durch ein Zellmonolayer erhöht ist, wenn Tricellulin nur gering exprimiert ist (Krug et al., 2009a). Dieses Phänomen spielt möglicherweise eine Rolle beim Eindringen von luminalen Noxen bei intestinaler Inflammation.

Im Rahmen von gastrointestinalen Infektionen kann es zu entzündlichen Reaktionen in der Darmwand kommen, die durch pro-inflammatorische Zytokine vermittelt die epithelialen *Tight Junction*–Proteine beeinflussen (zur Übersicht vgl. Bücker et al., 2010). Ein solcher Einfluss auf die *Tight Junction*–Proteine ist z.B. für das pro-inflammatorische Zytokin Tumornekrosefaktor-alpha (TNFα) aufgezeigt worden (Schmitz et al., 1999), wobei die beteiligten Mechanismen u.a. eine Herabregulation der Expression des *Tight Junction*-Proteins Occludin umfassen (Mankertz et al., 2000). Daneben wird das Kanal-bildende *Tight Junction*-Protein Claudin-2 durch TNFα und Interleukin-13 in seiner Expression im Darmepithel heraufreguliert (Mankertz et al., 2009; Heller et al., 2005).

1.4 Epitheliale Apoptose

Neben Veränderungen der epithelialen *Tight Junction* induzieren pro-inflammatorische Zytokine auch eine gesteigerte epitheliale Apoptoserate. Deren funktionelle Bedeutung für das Epithel ist jedoch noch weniger gut definiert. So konnte gezeigt werden, dass Apoptosen in der Nierenepithelzelllinie LLC-PK1 ohne funktionelle Barriereauswirkungen bleiben können (Peralta Soler et al., 1996). Das hieße, dass die Nachbarzellen die Abdichtung der apoptoti-

schen Zelle während ihrer Extrusion aus dem Epithelverband garantieren können. Hochauflösende funktionelle Untersuchungen zum Barriere-Effekt von epithelialen Apoptosen unter entzündlichen Bedingungen haben inzwischen aber belegt, dass relevante Barrierestörungen als Folge von Apoptoseinduktion auftreten können (Gitter et al., 2000). Dies ist wahrscheinlich auch für verschiedene gastrointestinale Infektionen wie z.B. die Lambliasis oder die Campylobacter-Infektion anzunehmen.

1.5 Gastrointestinale Infektionen durch *Campylobacter* spp.

Campylobacter jejuni (*C. jejuni*) und *Campylobacter coli* (*C. coli*) gehören zu den häufigsten Vertretern bakterieller Enteritiden und Enterokolitiden weltweit. Die *Campylobacter*-Infektion (Campylobacteriose) ist charakterisiert durch meist blutige Diarrhöen. Eine Bedeutung über die intestinale Entzündung hinaus besitzt der Erreger durch potentielle postinfektiöse Komplikationen wie reaktive Arthritis, Guillain-Barré- und Reiter-Syndrom. Dennoch ist das Wissen um seine Pathomechanismen bzw. spezifische Pathogenitätsfaktoren bis heute fragmentarisch. Dies liegt vor allem auch daran, dass es noch nicht gelungen ist, ein Tiermodell zu etablieren, in dem die Pathomechanismen ausreichend beschrieben werden konnten (Young et al., 2000, Masanta et al., 2013). In den meisten Mausmodellen zeigt sich eine Kolonisationsresistenz und diarrhöische Krankheitszustände können nur mit zusätzlicher chemischer Behandlung oder genetischer Modifikation der Tiere experimentell erreicht werden (Masanta et al., 2013). Es ist auch nicht hinreichend bekannt, welche funktionellen epithelialen Veränderungen am menschlichen Darm mit der *Campylobacter*-Enteritis einhergehen. Ebenso unklar war längere Zeit, welchen Beitrag zur Diarrhö bekannte Virulenzfaktoren des Keims leisten, die Adhärenz und Invasivität vermitteln (Bereswill & Kist, 2003).

Während *C. jejuni* bzw. *C. coli* als Zoonose bekanntermaßen meist durch den Verzehr von kontaminierten Lebensmitteln, z.B. vom Huhn bzw. Schwein, in den Menschen gelangen und so zu Erkrankungen führen, ist für ***Campylobacter concisus*** (*C. concisus*) bisher kein solches Tierreservoir gefunden worden. *Campylobacter concisus* ist vornehmlich im Mundraum und im Darm des Menschen zu finden, wobei bisher nicht erwiesen war, dass *C. concisus* überhaupt als humanpathogen eingestuft werden muss.

1.6 Infektion mit *Arcobacter butzleri*

Arcobacter spp. sind Bakterien aus der Familie der *Camylobacteraceae*, die erstmalig 1977 beschrieben wurden (Ellis et al., 1977). Zunächst rechnete man sie zur *Campylobacter*-Gattung bis 1991 eine neue Taxonomie eingeführt wurde und sie seitdem als eigene Gattung gelten (Vandamme et al., 1991). *Arcobacter*-Infektionen wurden in der Vergangenheit vor allem mit Aborten und Enteritiserkrankungen in Viehbeständen in Verbindung gebracht. *Arcobacter cryaerophilus* und *Arcobacter butzleri* (*A. butzleri*) stehen allerdings auch im

Verdacht humanpathogen zu sein und wurden bei Patienten mit Diarrhö und Sepsis gefunden (Kiehlbauch et al., 1991). Die mögliche Beteiligung der Bakterien an der Entstehung von Diarrhöen war lange unbekannt. Man nahm aufgrund der phylogenetischen Ähnlichkeiten zu *Campylobacter* spp. ein ähnliches Verhalten an, ging also von einer Invasivität als dem wichtigsten Pathomechanismus aus (Wesley et al., 1996, Black et al., 1988). Befunde unserer eigenen Arbeitsgruppe lieferten inzwischen direkte Hinweise auf die Induktion einer epithelialen Barrierestörung durch diese Bakterien.

1.7 Infektiöse Diarrhö durch *Aeromonas* spp.

Aeromonas hydrophila (*A. hydrophila*) ist ein Gastroenteritis-Erreger, der in der städtischen deutschen Population mit seiner Fallhäufigkeit derjenigen von *Yersina enterocolitica* (*Y. enterocolitica*) gleicht (Liesenfeld et al., 1993). Aktuelle epidemiologische Befunde fehlen, sporadische Ausbrüche und fatale Fälle belegen aber die pathogene Bedeutung des Erregers. Welche epitheliale Teilfunktion bei der *Aeromonas*-induzierten Diarrhö vorrangig beeinträchtigt ist, war lange unbekannt. Obwohl mehrere teils zellständige und teils sekretorische Virulenzfaktoren in verschiedenen *Aeromonas*-Spezies beschrieben worden sind (Janda et al., 1991), war bisher unklar, ob die Störung der epithelialen Funktion durch eine direkte Interaktion von Aeromonaden mit den Enterozyten oder durch die Wirkung eines löslichen Toxins (z.B. des porenbildenden Toxin **Aerolysin**) ausgelöst wird. Befunde unserer Arbeitsgruppe konnten direkte Hinweise für die Toxin-abhängige Induktion einer intestinalen Sekretion erbringen (Epple et al., 2004). Daneben spielt aber auch eine epitheliale Barrierestörung eine Rolle, wie aus Widerstandsmessungen evident wurde, deren strukturelles Korrelat und auslösende Mechanismen bisher aber nicht weiter charakterisiert worden sind.

1.8 Translokation von *Escherichia coli*

Neben der ionalen Permeabilität und Durchlässigkeit für Antigene ist auch die Abdichtung gegen die luminale Darmflora ein wichtiger Teilaspekt der intestinalen Barrierefunktion. Diesem Barriereaspekt wird z.B. in der Chirurgie große Bedeutung beigemessen, da eine peri- und postoperative bakterielle Translokation als Auslöser von SIRS ("*systemic inflammatory response syndrome*") und postoperativer Sepsis angesehen wird. Natürlich sind auch inflammatorische Prozesse, die im Rahmen von gastrointestinalen Infektionen auftreten, ein potentieller Ausgangspunkt dafür. Experimentelle Befunde, die vor allem mit dem *Escherichia coli* (*E. coli*)-Stamm C25 in epithelialen Zellkulturen erhoben wurden, deuten auf eine transzelluläre Route in der initialen Phase bakterieller Translokation hin (Macutkiewicz et al, 2008). Daneben können, wie für die hämolysierende *E. coli*-Stämme O4 und 536 belegt, dann auch parazelluläre Wege in Form der Ausbildung von fokalen Läsionen ("*Focal Leaks*") daran beteiligt sein, wobei auch hier ein transzellulärer Translokationsweg initial beteiligt sein dürfte (Troeger et al. 2007a). Inzwischen gibt es eine Reihe von experimentellen Hinweisen,

dass ein transzellulärer Durchtritt nicht nur für Bakterien, sondern allgemein für Makromoleküle und Antigene funktionell relevant ist und ebenfalls einer entzündlichen Regulation unterliegt (Schumann et al., 2008; Matysiak-Budnik et al., 2008). Da auch für CED intestinale Barrieredefekte beschrieben wurden, könnte dies durchaus auch für die Unterhaltung einer Schubaktivität etwa bei der Colitis ulcerosa relevant sein.

Unter diesem Aspekt potentiell relevante Keime sind uropathogene *E. coli*-Stämme, die bei einem Teil der Menschen als Mitglied der intestinalen Mikrobiota gefunden werden und für die eine Translokation unter inflammatorischen Konditionen im Darm nachgewiesen wurde. Ob diese Hämolysin-tragende *E. coli*-Stämme aber signifikant gehäuft bei Colitis ulcerosa vorkommen oder z.B. in Tiermodellen mit intestinaler Inflammation pathophysiologische Bedeutung haben können, ist bisher nicht sicher geklärt. Es gab in der Vergangenheit bereits Studien zu *E. coli* und seiner Prävalenz bei Patienten mit CED, die einen Hinweis auf eine höhere Prävalenz der hämolysierenden *E. coli* bei Patienten mit Morbus Crohn oder Colitis ulcerosa gefunden haben (Giaffer et al., 1992), während andere Studien *E. coli* **α-Hämolysin** (HlyA) mittels Polymerase Kettenreaktion (PCR) nicht darstellen konnten (Kotlowski et al., 2007). Studien, die gezielt hämolysierende Bakterien in Stuhl oder Darm-Biopsien aus entzündeten und nicht-entzündeten Darmsegmenten bei diesen Patienten kulturell und mit molekularer Charakterisierung untersuchen, sind daher von besonderem Interesse.

1.9 Fragestellung

Infektionen des Gastrointestinaltrakts durch bakterielle Enteropathogene sind, neben dem Befall der Haut und der Atemwege, die häufigsten bakteriellen Infektionserkrankungen des Menschen und können schwere Komplikationen nach sich ziehen. Die verschiedenen molekularen Mechanismen, die dabei zu Diarrhö und Entzündung führen, sind komplex und nur teilweise verstanden. Neben sekretorischen Mechanismen wie z.B. bei der Diarrhö durch *Vibrio cholerae*, können Pathogene auch die Barrierefunktion des Intestinums beeinflussen oder zu malabsorptiven Störungen führen. In der Humanmedizin sind die diarrhöauslösenden Mechanismen vieler klinisch relevanter Enteropathogene bisher noch nicht ausreichend charakterisiert. Die folgenden Arbeiten vereint die zentrale Fragestellung nach der Pathogenität von bakteriellen Diarrhöerregern bzw. von Bakterien, die im Verdacht stehen Enteritiserreger zu sein. Untersucht wird dabei, ob diese Keime wirklich humanpathogen sind bzw. ob sie ein pathogenes Potential besitzen, welches sich im experimentellen Modellsystem nachvollziehen lässt. Mit der generellen Analyse der Pathogenität der Bakterien wird auch untersucht, welche spezifischen Pathomechanismen die Effekte mediieren, also wie sich z.B. die epitheliale Barriere bei intestinalen Infektionen verhält und auf welche Weise verschiedene Erreger oder ihre Toxine die physiologische Funktion unseres Darmes verändern können. Bakterien aus der *Campylobacteraceae*-Familie, bei denen von einem ähnlichen pathogenen Potential wie vom häufigen Erreger *Campylobacter jejuni* ausgegangen wird, werden im ersten Thementeil der Habilitationsschrift mit der Frage behandelt:

Welche pathogenen Veränderungen durch invasive Bakterien führen zur Diarrhö?

Neben Bakterien, die durch ihre Invasivität ihr pathogenes Potential entfalten, können toxintragende Bakterien durch die Sekretion bakterieller Virulenzfaktoren pathogene Effekte vermitteln ohne selbst direkt mit der Mukosa zu interagieren. Die spezifische Frage zum zweiten Thementeil rückt sezernierte Toxine aus der *Enterobacteriaceae*-Familie, von denen bereits bekannt ist, dass sie eine epitheliale Barrierestörung hervorrufen können, in den Mittelpunkt. Hierzu wird gefragt:

Wie verändern porenbildende Toxine die Barrierefunktion und welche Rolle spielen dabei epitheliale Läsionen?

Die Methodik der hier zusammengefassten Publikationen beinhaltet u.a. funktionelle elektrophysiologische Messungen an Zellmodellen (Ussing-Kammer), an denen zusammen mit morphologischen und molekularen Analysen (Mikroskopie, Western-Blot-Analyse, PCR, Inhibition von Zellsignalen) pathophysiologische Veränderungen dargestellt werden. Auch können zellphysiologische Beobachtungen gemacht werden, die dann als Grundlage für einen pathologischen Prototyp auch am Tiermodell *in vivo* mit diesen Techniken überprüft werden.

2. Eigene Arbeiten

2.1 Invasive Bakterien der *Campylobacteraceae*

Im ersten Thementeil 2.1 werden Bakterien aus der *Campylobacteraceae*-Familie behandelt, von denen angenommen wird, dass ihre Pathogenität nur durch direkten Kontakt mit dem Epithel, also durch Adhäsion und Invasion, vermittelt wird. Neben dem häufigsten zoonotischen bakteriellen Gastroenteritis-Erreger *C. jejuni*, werden weitere Bakterienspezies aus der Bakterienfamilie verdächtigt, ihr pathogenes Potential im menschlichen Darm mit der Folge von Diarrhö und Entzündung zu entwickeln.

2.1.1 Leckflux als Diarrhömechanismus am Beispiel von *Arcobacter butzleri*

Die nachfolgende Orginalarbeit: Bücker et al., „*Arcobacter butzleri* induces barrier dysfunction in intestinal HT-29/B6 cells“, 2009 erschienen im *Journal of Infectious Diseases*, behandelt die pathogenen Eigenschaften einer Bakterienspezies, die im Verdacht steht, Diarrhöen beim Menschen auszulösen.

Um die Diarrhömechanismen, die der gastrointestinalen Infektion durch das „emerging human pathogen“ *A. butzleri* zugrundeliegen, zu beschreiben, wurden humane intestinale Epithelzellen mit den Bakterien *in vitro* infiziert und dann die Antwort der Zellen mit elektrophysiologischen und molekularbiologischen Methoden analysiert.

Im Epithelzellmodell HT-29/B6, einer humanen Kolonkarzinomzelllinie, konnte gezeigt werden, dass durch das Bakterium *A. butzleri* der transepitheliale elektrische Widerstand auf 30% des Ausgangswertes reduziert wurde, wobei parallel dazu die parazelluläre Permeabilität für Fluoreszein (332 Da) (10,8 ± 3,5 versus 1,8 ± 0,6 $\cdot 10^{-6}$ cm/s bei Kontrollen, $P<0,05$) und Fluoresceinisothiocyanat-(FITC)-Dextran-4000 (4 kDa) (0,036 ± 0,005 versus 0,015 ± 0,002 $\cdot 10^{-6}$ cm/s bei Kontrollen, $P<0,01$) zunahm. Dieser Effekt war zeit- und dosisabhängig und auch durch Bakterienlysate auslösbar, wobei letztere Hitze- und Proteinase K-sensitiv waren. Als strukturelles Korrelat fand sich eine reduzierte Expression der *Tight Junction*-Proteine Claudin-1, -5 und -8 sowie eine Umverteilung der *Tight Junction*-Proteine Claudin-1 und -8 aus der *Tight Junction* heraus, woraufhin in der Folge intrazelluläre Aggregate von *Tight Junction*-Proteinen in der Epithelzelle detektierbar wurden. Außerdem induzierte *A. butzleri* epitheliale Apoptosen. Die Anzahl der Apoptosen war in den infizierten Zellmonolayern um den Faktor drei gegenüber der Kontrolle erhöht. Insgesamt sind diese Veränderung also geeignet, die bei einer *Arcobacter*-Infektion beobachtete Diarrhö auf einen Leckflux-Mechanismus zurückzuführen (Bücker et al., 2009).

MAJOR ARTICLE

Arcobacter butzleri Induces Barrier Dysfunction in Intestinal HT-29/B6 Cells

Roland Bücker,[1,a] Hanno Troeger,[1,a] Josef Kleer,[4] Michael Fromm,[3] and Jörg-Dieter Schulzke[2]

Departments of [1]Gastroenterology, Infectious Diseases and Rheumatology, and [2]General Medicine, and [3]Institute of Clinical Physiology, Charité Berlin; and [4]Institute of Food Hygiene, Freie Universität, Berlin, Germany

Background. *Arcobacter butzleri* causes watery diarrhea and bacteremia. Although, recently, more cases of diarrhea have been caused by *Arcobacter* species, very little is known about its pathogenesis, the identification of which is the aim of this study.

Methods. Human HT-29/B6 colonic epithelial monolayers were apically inoculated with *A. butzleri.* Transepithelial resistance and macromolecule fluxes were measured in Ussing chambers. Tight junction protein expression was analyzed by Western blotting, and subcellular distribution was analyzed by confocal laser-scanning microscopy.

Results. Infection of HT-29/B6 caused a decrease in transepithelial resistance to 30% and an increase in paracellular permeability to fluorescein ($10.8 \pm 3.5\ 10^{-6}$ cm/s vs. $1.8 \pm 0.6\ 10^{-6}$ cm/s in control; $P < .05$) and dextran-4 kDa ($0.036 \pm 0.005\ 10^{-6}$ cm/s vs. $0.015 \pm 0.002\ 10^{-6}$ cm/s in control; $P < .01$). This effect was time and dose dependent and was also caused by bacterial lysates showing heat and proteinase-K sensitivity. As structural correlate, expression of the tight junctional proteins claudin-1, -5, and -8 was reduced, and claudin-1 and -8 were redistributed off the tight junctional strands forming intracellular aggregates. Furthermore, *A. butzleri* induced epithelial apoptosis (3-fold).

Conclusions. *A. butzleri* induces epithelial barrier dysfunction by changes in tight junction proteins and induction of epithelial apoptosis, which are mechanisms that are consistent with a leak flux type of diarrhea in *A. butzleri* infection.

Arcobacter are gram-negative, motile and spiral-shaped bacteria with a length of ~4 μm. *Arcobacter* were described for the first time in 1977 as aerotolerant *Campylobacter*-like micro-organisms [1] and were assigned to the *Campylobacter* group [2, 3]. However, in 1991, the taxonomy was revised, and *Arcobacter* was introduced as a new genus belonging to the epsilon-proteobacteria [4]. The complete genome sequence of *Arcobacter butzleri* was recently published [5].

A. butzleri is considered to be an emerging human pathogen that can cause severe diarrhea and bacteremia [6–8]. In humans, *A. butzleri* causes diarrheal illness associated with abdominal pain and, in some cases, nausea, vomiting, and fever [6, 9]. In addition, watery and persistent diarrheic stools are characteristic of *A. butzleri* infection [9]. Besides the currently most frequent notifiable *Campylobacter* infection in Europe [10], *Arcobacter* are known to be the fourth most common *Campylobacter*-like organisms isolated from diarrheic stool samples from patients in Belgium and France [9, 11]. The association of *A. butzleri* with human gastroenteritis was also reported from other countries, and such gastroenteritis is considered to be increasing in incidence [12]. The global prevalence of *Arcobacter* infection is rather underestimated, because no routine diagnostic of these bacteria has been performed [11]. The exact routes of transmission are unknown. *Arcobacter* have been considered as food- and water-borne pathogens [13, 14]. The organisms were detected in feces and meat of livestock animals, drinking water, seawater plankton, and pets [15–18]. An epidemic of *Arcobacter* infection was assumed to spread through contaminated meat (mainly poultry) [19, 20].

Although evidence was found for the association of

Received 10 December 2008; accepted 11 March 2009; electronically published 15 July 2009.

Potential conflicts of interest: none reported.

Financial support: Deutsche Forschungsgemeinschaft (Schu 559/10-1 and KFO 104/2).

[a] R.B. and H.T. contributed equally to this article.

Reprints or correspondence: Dr. Jörg-Dieter Schulzke, Medizinische Klinik I, Gastroenterologie, Infektiologie und Rheumatologie, Charité–Universitätsmedizin Berlin, Campus Benjamin Franklin, Hindenburgdamm 30, 12200 Berlin, Germany (joerg.schulzke@charite.de).

The Journal of Infectious Diseases 2009; 200:756–64

0022-1899/2009/20005-0014$15.00

DOI: 10.1086/600868

Arcobacter with human and animal illness, there is almost no information on the pathophysiology of this disease. In general, intestinal pathogens can induce diarrhea by induction of active ion secretion, via malabsorption, or by impairment of the epithelial barrier function of the intestine. Barrier impairment is often caused by structural changes of the epithelial tight junction (TJ) or by induction of epithelial gross lesions, including induction of apoptosis and necrosis, erosions, or ulcer-type lesions [21], all of which lead to a passive efflux of water and solutes from the circulation into the lumen of the intestine (leak flux diarrhea). The dysfunction of the TJ is characterized either by expression changes or by redistribution or disruption of TJ proteins that seal the paracellular space between neighboring epithelial cells [22, 23].

MATERIAL AND METHODS

***Growth conditions of* A. butzleri.** Clinical isolates of *A. butzleri* ATCC 49616 (from human diarrheal stool) and CCUG 10373 (from human blood) were cultured in Mueller-Hinton media with selective supplement (cefoperazone, amphotercin B, teicoplanin, selective supplement; Oxoid) for 72 h at 30°C under microaerobic conditions (CampyGen; Oxoid). For quantification of *A. butzleri,* the liquid-cultured bacteria were microscopically counted.

Lysates. *A. butzleri* were harvested from log-phase cultures (200 mL), washed with phosphate-buffered saline, and resuspended in 5 mL of ice-cold bathing solution (RPMI 1640 cell culture medium; PAA Laboratories). The intracellular content of the bacteria was released into the bathing solution after cell wall disruption by means of a hydraulic press (FRENCH Press; Thermo Spectronic). After cell lysis, cell debris and cell membrane remnants were removed by centrifugation (20,000 *g* for 30 min at 4°C).

Epithelial cell culture. HT-29/B6 cells were cultured as described elsewhere [24] and were seeded on polycarbonate filters with a pore size of 3 μm (effective membrane area, 0.6 cm^2; Millicell-PCF; Millipore). Monolayers of HT-29/B6 cells form an epithelial barrier between the apical compartment within the insert and the basolateral compartment outside. Confluent monolayers were used for the experiments 7 or 8 days after seeding, when transepithelial electrical resistance was 500–800 Ohm cm^2. Cells were shifted to antibiotic-free RPMI 1640 before infection. In parallel to the infection with *A.butzleri* strains, 4 following types of controls were performed: (1) without adding bacteria and/or bacterial lysates, (2) with addition of heat-inactivated *A. butzleri* and/or *A. butzleri* lysates (60 min at 56°C), (3) with *Escherichia coli* K12, and (4) with *Campylobacter jejuni* ATCC 33560.

Electrophysiological studies. After bacterial infection with *A. butzleri* (MOI of 10) for 40 h, HT-29/B6 cell monolayers were mounted into modified Ussing-type chambers, as described elsewhere [25]. Short circuit current and transepithelial electrical resistance (R^t) were determined by using a computerized automatic clamp device (Fiebig Hard & Software).

Epithelial permeability. Unidirectional tracer flux studies from mucosal to serosal were performed under short-circuit conditions in Ussing chambers with fluorescein and fluorescein isothiocyanate (FITC)–labeled dextran-4000 (Sigma), as described elsewhere [26]. The medium in the basolateral chamber was initially free of dyes. Medium was withdrawn from the basolateral chamber at specific intervals, and fluorescence was measured in a spectrofluorimeter (SpectraMaxGemini; Molecular Devices). Permeability was calculated from flux over concentration difference.

Cytotoxicity. Lactate dehydrogenase (LDH) release from HT-29/B6 cells was measured according to the method of Madara and Stafford [27]. The MTT assay (MTT Cell Proliferation Kit; Roche) was performed on subconfluent HT-29/B6 cells in 96-well plates in accordance with manufacturer's instructions and was measured by a spectrophotometer (SpectraMax340PC; Molecular Devices). TUNEL staining (In situ Cell Death Detection Kit; Roche) was performed in accordance with the manufacturer's instructions.

Western blot analyses. Immunoblots were performed and analyzed as described elsewhere [23]. Detergent-soluble protein fractions were prepared from monolayers incubated with or without *A. butzleri.* HT-29/B6 cells were lysed in ice-cold lysis buffer (10 mmol/L Tris; pH, 7.5; 150 mmol/L sodium chloride, 0.5% Triton X-100, 0.1% SDS, and complete protease inhibitor mixture [Roche]) and were incubated for 30 min on ice. The lysate was centrifuged (15,000 *g* for 15 min at 4°C), and the supernatant was used as whole cell extract. The following antibodies were used: anti-occludin (1:2000; Zymed), anti–claudin-1–5 and -8 (1:1000; Zymed), anti–β-actin (1:5000; Sigma), and anti–caspase-3 (1:1000; Cell Signaling Technology).

Immunofluorescence. To test for the integrity of the TJ meshwork, the proteins occludin, claudins, and *Zonula occludens* protein-1 were visualized using confocal laser-scanning microscopy (Zeiss LSM 510) and were analyzed with Carl Zeiss LSM Image Examiner software according to prior descriptions [23]. The length of the TJ meshwork per exposed tissue area was measured microscopically using ImageJ software with NeuronJ plug-in by tracking the TJ. For detection, antibodies raised against TJ proteins (1:50; Zymed) were used.

Quantitative polymerase chain reaction (PCR). Total RNA was obtained from HT-29/B6 cells with use of RNAzol reagent (WAK Chemie). Complementary DNA (cDNA) was synthesized by reverse-transcription PCR with use of the High-Capacity cDNA Archive Kit (Applied Biosystems) with oligo(dT) primer. Real-time PCR was performed according to the manufacturer's instructions with an ABI 7900HT PCR device using the TaqMan Gene Expression Assay (no. Hs00533949_s1; clau-

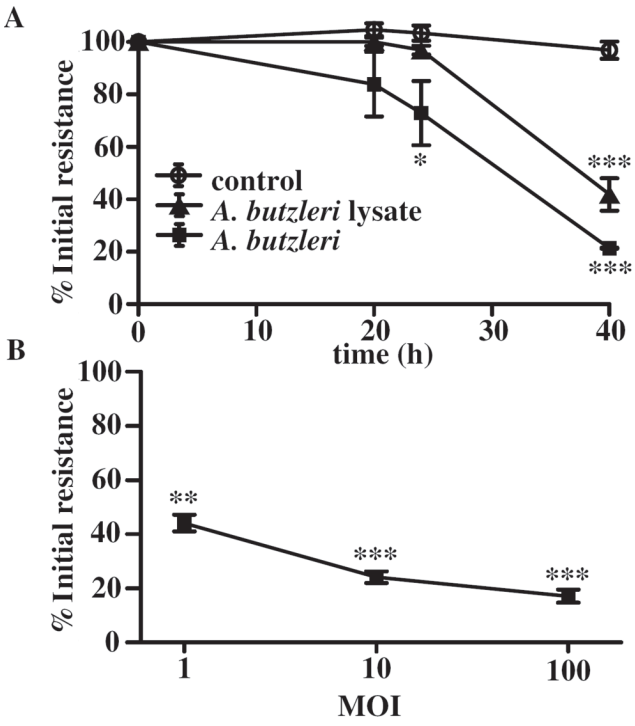

Figure 1. Effects of *Arcobacter butzleri* on transepithelial resistance. *A,* Time-dependent decrease in transepithelial resistance of HT-29/B6 monolayers. Confluent HT-29/B6 cells grown on permeable supports were apically infected with *A. butzleri* at a multiplicity of infection (MOI) of 10 or with *A. butzleri* lysate by FRENCH Press with proteins >50 kDa (residue after ultrafiltration with 50,000 MWCO Millipore filter unit). *B,* Dose-dependent decrease in transepithelial resistance of HT-29/B6 monolayers. Confluent HT-29/B6 cells were apically infected with *A. butzleri* at initial MOIs of 1, 10, and 100. Data (mean values ± standard error of the mean; $n = 4$ for each group) were analyzed using Student's *t* test, and asterisks indicate statistically significant differences between controls and infected cell samples. $*P < .05$, $**P < .01$, and $***P < .001$.

din-5) with FAM dye-labeled primers. Glyceraldehyde 3-phosphate dehydrogenase cDNA was quantified using VIC reporter dyes as endogenous control (all Applied Biosystems). Differential expression was calculated according to the $2^{-\Delta\Delta CT}$ method [28].

Statistical analysis. Data were analyzed using GraphPad software. Data are expressed as mean values ± standard error of the mean. Statistical analysis was performed using Student's *t* test, adjusted by Holm-Bonferroni correction for multiple comparisons. $P < .05$ was considered to be statistically significant.

RESULTS

***Infection with* A. butzleri *reduces* R^t.** To investigate the effect of *A. butzleri* on epithelial integrity, R^t of polarized HT-29/B6 monolayers was measured after *A. butzleri* infection. Highly motile bacteria were subcultured in RPMI liquid medium and were added to the apical compartment of confluent HT-29/B6 cell monolayers to yield an initial concentration of 1×10^7 colony-forming units per mL, equaling a multiplicity of infection of 10. As shown in figure 1, there was an incremental decrease in R^t that began 24 h after bacterial inoculation (at 24 h, $P < .05$; at 40 h, $P < .001$; $n = 4$ each) with both strains used. All control groups remained at stable R^t values. *A. butzleri* 49616 showed the strongest effects on R^t and was used in subsequent studies. Lysates from *A. butzleri* caused a similar effect on R^t as viable, motile bacteria (figure 1*A*). HT-29/B6 monolayers, which were apically infected with *A. butzleri* at multiplicities of infection of 1, 10, and 100, showed a dose-dependent decrease in R^t after 48 h (figure 1*B*).

Physicochemical properties of* Arcobacter *lysate. *A. butzleri* lysate derived after FRENCH Press treatment led to a dose-dependent decrease in R^t. After 48 h of incubation with diluted *A. butzleri* lysate, R^t was reduced to 58% ± 2% (1:5) and 73% ± 3% (1:10) of initial resistance ($P < .01$; $n = 4$). By ultrafiltration, the major active compound of the bacterial lysates was found to have a molecule mass >50 kDa. The activity of this bacterial compound was tested for heat sensitivity. *A. butzleri* lysate treated at 56°C for 60 min did not further affect R^t after 48 h of incubation with HT-29/B6 cells. Likewise, proteinase-K treatment abolished the effect of *A. butzleri* lysate on R^t. *A. butzleri* supernatants had no effect on R^t (figure 2).

Functional analyses of epithelial permeability. To further characterize epithelial barrier function, the permeability to fluorescein (332 Da) and FITC-dextran-4000 (4 kDa) was measured

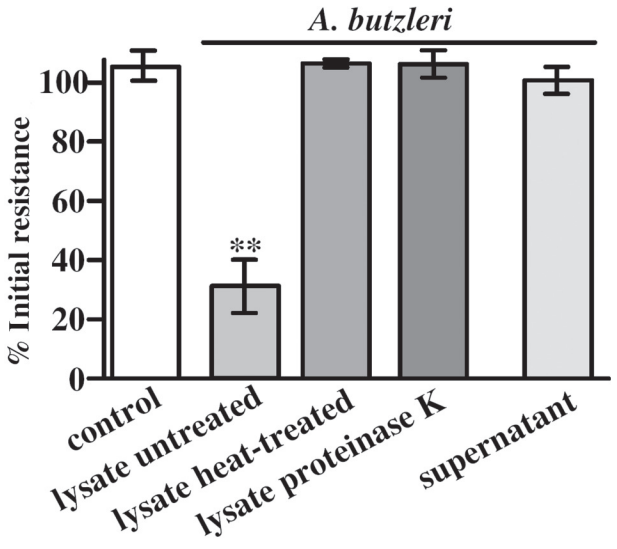

Figure 2. Transepithelial electrical resistance of HT-29/B6 monolayers. Confluent HT-29/B6 cells were apically treated with *Arcobacter butzleri* lysate by FRENCH Press with proteins >50 kDa or with *A. butzleri* supernatants. Heat treatment (60 min at 56°C) or proteinase-K treatment on *A. butzleri* lysate abolished the effect on transepithelial resistance ($n = 4$ for each group). $**P < .01$.

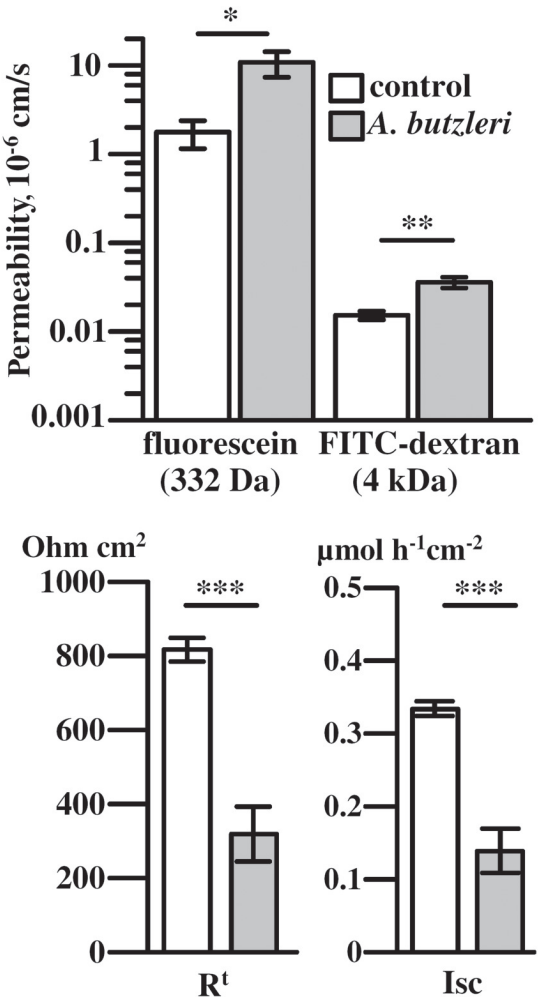

Figure 3. Effects of *Arcobacter butzleri* on paracellular permeability. Paracellular permeability after 40 h of *A. butzleri* infection when transepithelial resistance (R^t) and short circuit current (Isc) were decreased. Fluxes of tracer macromolecules (fluorescein, $n = 6$; fluorescein isothiocyanate (FITC)–dextran-4000, $n = 4$) through *A. butzleri* infected HT-29/B6 monolayers were measured in Ussing chambers. $^*P < .05$, $^{**}P < .01$, and $^{***}P < .001$.

as tracer flux from the apical to the basolateral compartment in Ussing chambers. After 40 h of mucosal exposure to *A. butzleri*, R^t of the HT-29/B6 monolayers had decreased to 30%, whereas the short circuit current was not induced but rather was slightly diminished (0.14 ± 0.03 μmol h^{-1} cm^{-2} after *A. butzleri* infection vs. 0.33 ± 0.01 μmol h^{-1} cm^{-2} in control; $P < .001$; $n = 6$). Concomitantly, permeability to fluorescein and FITC-dextran-4000 was increased after *A. butzleri* infection (for fluorescein, from 1.8 ± 0.6 10^{-6} cm/s in control to 10.8 ± 3.5 10^{-6} cm/s [$P < .05$; $n = 6$]; for FITC-dextran, from 0.015 ± 0.002 10^{-6} cm/s in control to 0.036 ± 0.005 10^{-6} cm/s [$P < .01$; $n = 4$]) (figure 3).

***Structural alteration of TJ organization after infection with* A. butzleri.** In Western blot analysis, expression of claudin-1, -5, and -8 was decreased 40 h after infection (figure 4). To investigate the cellular distribution of these TJ proteins, HT-29/B6 monolayers were stained at the same time, when the R^t had decreased to 30% of the initial value. The localization of endogenous claudins was determined by immunofluorescence with use of confocal laser-scanning microscopy (figure 5). First, visualization of the TJ proteins *Z. occludens* protein-1 and occludin showed an intact tight junctional meshwork without any gaps or other types of gross lesions (data not shown). Then,

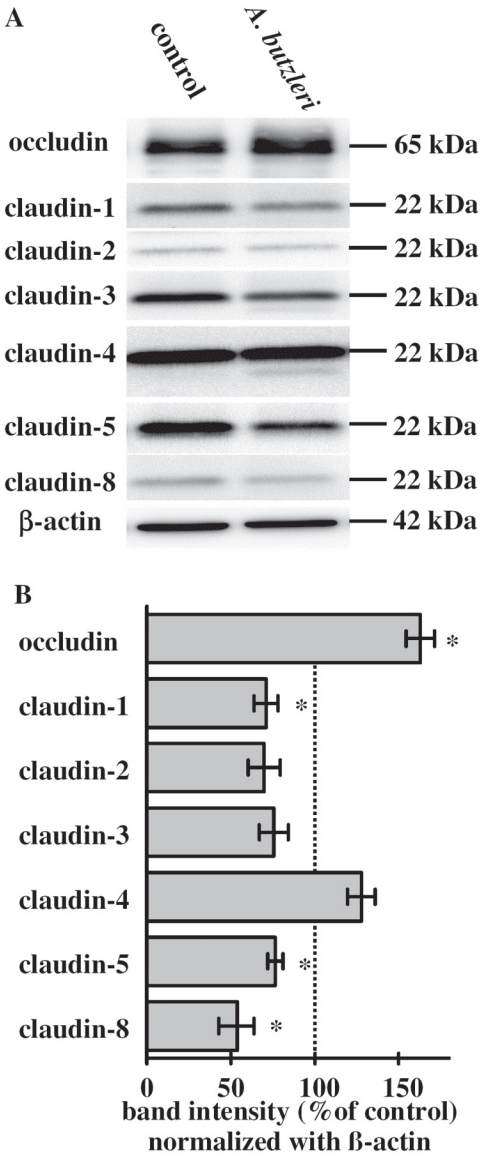

Figure 4. *A,* Effects on the expression of tight junction proteins in HT-29/B6 cells 40 h after *Arcobacter butzleri* infection. Western blots revealed an obvious increase of occludin, whereas claudin-1, -3, -5, and -8 were decreased. *B,* Densitometry on occludin and claudins showed a decrement in claudin-1, claudin-5, and claudin-8 and an increase of occludin expression after normalization with β-actin. $^*P < .05$ ($n = 4$; Student's t test).

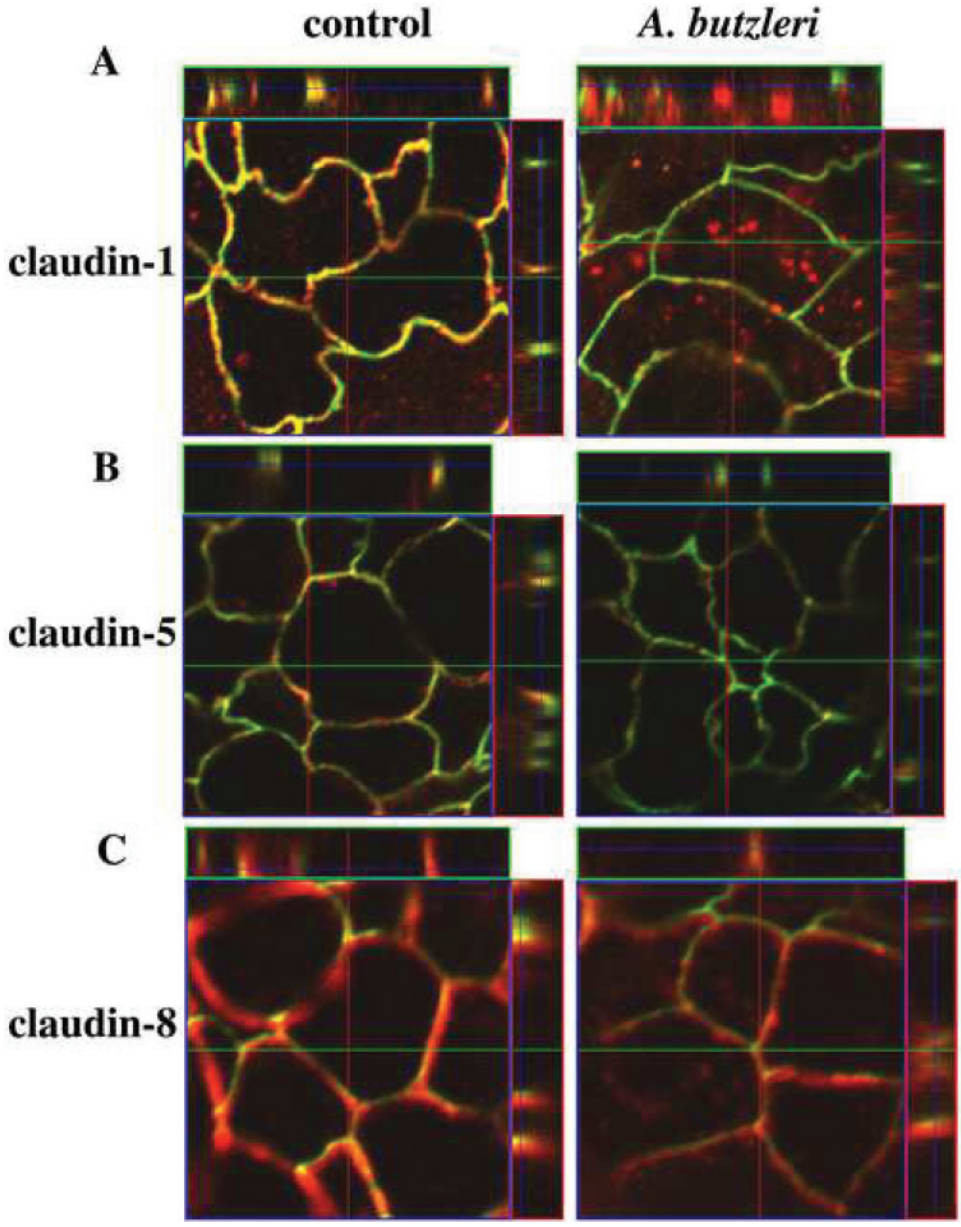

Figure 5. Confocal laser-scanning microscopy (*z*-axis stack) of HT-29/B6 monolayers 40 h after infection with *Arcobacter butzleri* immunostaining with anti–*Zonula occludens* protein-1 *(green)* or anti-claudin *(red)* antibodies (merge is shown in yellow) illustrates characteristic loss of claudin-1 *(A)* and claudin-8 *(C)* off the tight junction, as well as accumulation of claudin-1 and -8 in the cytosol and a strong reduction of claudin-5 *(B).*

the length of the TJ network per exposed tissue area was measured and was not altered in infected monolayers (11.1 ± 0.5 μm/cell after *A. butzleri* infection vs. 10.5 ± 0.2 μm/cell in control; $n = 3$; the difference was not statistically significant). This is important, because an altered cell size with a change in the exposed TJ length would have caused a change in tightness of the monolayer, even if TJ protein measurements per mg protein in Western blots were unaltered. Thereafter, TJ proteins were quantified by densitometry of Western blots. As the main result, claudin-1, -5, and -8 expression levels were decreased, and furthermore, cellular distribution of these claudins was altered. *Z*-axis scans (*xz* plane) of control monolayers revealed that these tight junctional proteins were present in colocalization with *Z. occludens* protein-1 within the TJ strands of HT-29/B6 cells, whereas immunostaining of infected monolayers revealed a reduction of these claudins in the TJ, most pronounced for claudin-1 and -5 (figure 5*A* and 5*B*) and a redistribution of claudin-1 and claudin-8 off the TJ, with a concomitant appearance of intracellular claudin aggregates (figure 5*A* and 5*C*). Claudin-2, -3, and −4 showed no obvious alterations (data not shown). Twenty-four hours after infection, the claudin-5 messenger RNA level measured by real-time reverse-transcriptase PCR was

reduced to 57% ± 10% ($P < .05$; $n = 4$), indicating expression regulation from the gene.

Cytotoxicity. The barrier dysfunction after infection could result, on the one hand, from changes or disruption of TJ strands but, on the other hand, also from a loss of epithelial cells by necrosis or apoptosis induction. Therefore, LDH release was determined as a marker for cytotoxicity. We found a slight increase in LDH release, which suggests moderate cytotoxic effects caused by *A. butzleri*. Two days after infection, LDH release was elevated to 1.4% ± 0.2%, compared with 0.6% ± 0.2% in control ($P < .001$; $n = 6$ (figure 6*A*). In subconfluent HT-29/B6 cells, viability was decreased to 60% ± 2% of control, as measured by MTT assay after 1 day· of exposure to *A. butzleri* lysate ($P < .001$; $n = 12$) (figure 6*B*). Furthermore, apoptosis was examined histologically in TUNEL staining (figure 7*A* and 7*B*), indicating an increased apoptotic rate in *A. butzleri*–infected HT-29/B6 monolayers. Twenty-four hours after infection, the apoptotic rate was still similar to the control level (0.9% ± 0.2%); however, after 48 h, infected monolayers showed a 3-fold increase in epithelial apoptoses to 3.4% ± 0.9% ($P < .05$; $n = 5$) (figure 7*B*). In parallel, pro-caspase-3 band intensity decreased to 68% ± 8% of the control level ($P < .05$; $n = 3$) (figure 7*D*). The caspase inhibitor N-benzyloxycarbonyl-Val-Ala-Asp-fluoromethyl-ketone (Z-VAD-FMK; 50 μmol/L) attenuated the *A. butzleri* lysate-induced effect on R^t at 48 h (*A. butzleri* reduced R^t to 39% ± 1%, and the decrease in R^t was partially blocked by Z-VAD-FMK, resulting in a R^t of 53% ± 3%; $P < .01$; $n = 4$ each) (figure 7*C*). In parallel, apoptosis induction was blocked by Z-VAD-FMK to the control level (figure 7*B*).

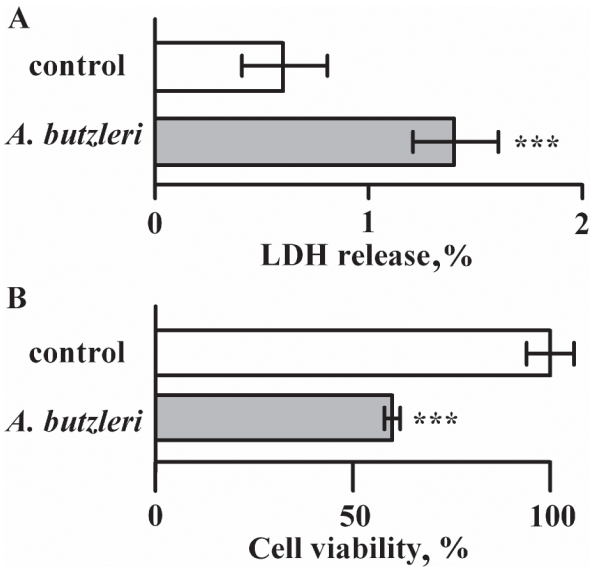

Figure 6. Effects of *Arcobacter butzleri* on epithelial necrosis. Cell death (epithelial necrosis) was induced in *A. butzleri*–exposed HT-29/B6 cells. *A, A. butzleri* increased lactate dehydrogenase (LDH) release as a marker for necrosis after 48 h of coincubation ($n = 6$). *B, A. butzleri* lysate (1:10) decreased cell viability on subconfluent HT-29/B6 cells (measured with MTT cell viability assay; $n = 12$). ***$P < .001$.

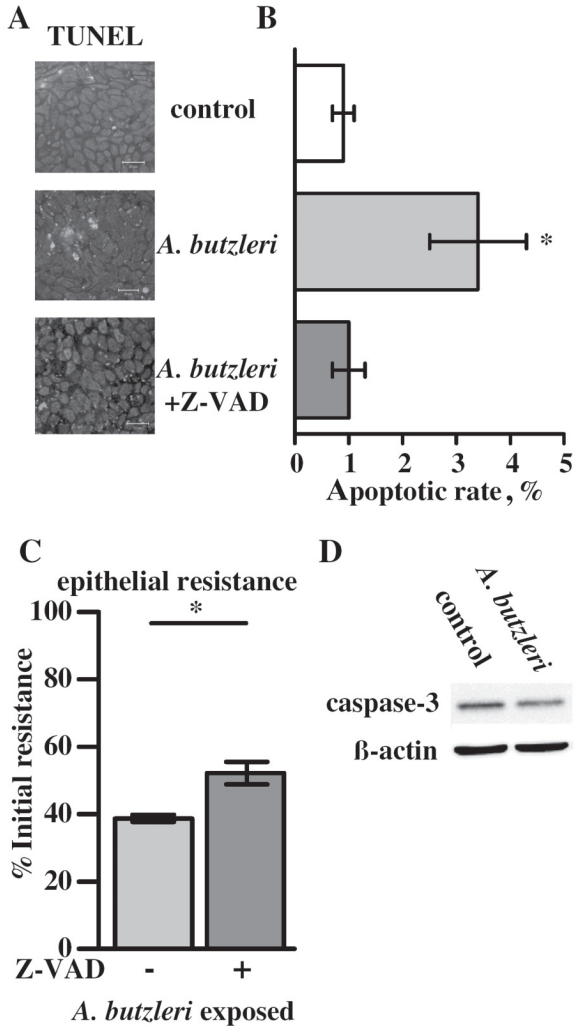

Figure 7. Effects of *Arcobacter butzleri* on epithelial apoptosis. *A,* Apoptotic effects of *A. butzleri* on confluent HT-29/B6 cells visualized with TUNEL staining and fluorescence microscopy. Approximately 2 days after *A. butzleri* infection, the number of cell rosette formations was increased, condensed or fragmentized nuclei were visible, and a more generalized loss of cells was observed. *B,* After 48 h of incubation with *A. butzleri,* TUNEL staining of confluent HT-29/B6 monolayers revealed an increase in the number of apoptotic cells ($P < .05$; $n = 5$). Caspase inhibitor (N-benzyloxycarbonyl-Val-Ala-Asp-fluoromethyl-ketone [Z-VAD]) completely inhibits apoptotic cell death, and transepithelial resistance was partially although not completely reconstituted by Z-VAD (50 μmol/L; *C*). *D,* Western analysis. Increased apoptosis was indicated by caspase-3 activation 48 h after infection. Band intensity of pro-caspase-3 (35 kDa) was significantly diminished ($P < .05$; $n = 3$).

DISCUSSION

In taxonomy, *A. butzleri* is a relative of *C. jejuni*, one of the most common causes of bacterial diarrhea in humans. From

a microbiological perspective, both species show some homology, share similar hosts, and are regarded as pathogens in humans but as commensals in animals. In particular, poultry is thought to be the main reservoir of both pathogens [15, 29]. Despite the close relationship between the pathogens, they are unique organisms with independent factors of pathogenicity, although *C. jejuni* has also been shown to down-regulate the function of the epithelial TJs [30]. It is well known that several enteropathogenic bacteria can change sealing properties of the epithelial TJ, leading to diarrhea, as caused by, for example, *Clostridium difficile* [31] or the attenuated *Vibrio cholerae* strain CVD101. The latter, depleted of the chloride secretion-inducing cholera toxin gene, still induced diarrhea in human volunteers, and this is caused by a second toxin (*Z. occludens* toxin), which affects TJ structure; consequently, ions and water are passively transported from the circulation into the intestinal lumen [32]. Also, epithelial barrier dysfunction in human immunodeficiency virus enteropathy and in *Giardia lamblia* infection contributes to diarrhea by a leak flux mechanism [33, 34].

As the first important result of our present study, *A. butzleri* was shown to be capable of inducing epithelial barrier impairment, which has been shown here for the first time to our knowledge. In our cell culture model, increased macromolecular permeability via the paracellular pathway and a decrease in epithelial resistance was observed. Of importance, infection with *A. butzleri* was not accompanied by an increase in short circuit current, which is a direct measure of active anion secretion. On the one hand, this excludes an opening of apical chloride channels as source of the R^t change, and on the other hand, it suggests that diarrheal mechanisms other than secretion are important (e.g., leak flux diarrhea induction).

As a structural correlate of the barrier impairment, a change in TJ protein composition and distribution was identified, which is the second important finding of the present study. With respect to barrier function, the claudin protein family is most important, even if not all claudins have sealing properties [35]. Some claudins are even pore forming, and the individual role of a single claudin will also depend on the background of the other TJ proteins in a TJ strand. Claudin-1, for example, has important sealing properties [22], which is supported by functional analysis of claudin-1 knock-out mice showing severe transepidermal water loss, which points to a crucial role for barrier function [36]. We found claudin-1 expression to be reduced by *A. butzleri,* and furthermore, its cellular distribution changed significantly. Claudin-1 was redistributed off the TJ and internalized. A similar effect on TJs was obtained by Muza-Moons et al [37] for claudin-1 disruption in enteropathogenic *E. coli*–infected human intestinal T84 monolayers. The intracellular claudin-1 protein aggregation in response to *A. butzleri* may be the result of changes in TJ assembly and/or turnover. Ubiquitinylation as a mechanism of claudin assembly and disassembly has recently been discussed to play a central role in posttranslational claudin regulation [38].

In contrast to claudin-1, claudin-2 induces the formation of cation-selective channels and is thereby able to increase epithelial permeability [39]. This has been discussed to represent a protective mechanism when expressed in the inflamed intestinal mucosa, by which noxious agents are rinsed off from the mucosal surface, but clearly contributes to leakiness of the epithelium. Claudin-3 and claudin-4 have sealing function and have receptor function for *Clostridium perfringens* enterotoxin [40, 41]. *C. perfringens* enterotoxin is a well-characterized modulator of barrier integrity. It binds to claudins and induces disruption of the TJ strands. However, claudins-2, -3, and -4 were not altered by *A. butzleri* in our HT-29/B6 cell model. As shown in MDCK cells, *C. perfringens* enterotoxin can remove claudin-4 from the TJ [41].

A. butzleri specifically caused removal of claudin-5 from the TJ. Claudin-5 is also a sealing TJ protein. Overexpression of claudin-5 in Caco-2 cells with low R^t background led to sealing of the barrier [23]. In *A. butzleri*–treated HT-29/B6 cells, claudin-5 expression was reduced in Western blots, and this seemed to also be the case in immunofluorescence microscopy, even if this is not a quantitative method and can yield only indirect evidence. Investigation of the regulatory influences revealed that the claudin-5 mRNA level in real-time reverse-transcriptase PCR analysis was reduced, which paralleled the diminished claudin-5 protein expression and gives evidence for *A. butzleri* to affect claudin-5 via transcriptional regulation from the gene.

Finally, we investigated claudin-8, which also has sealing properties within the TJ and which represents a paracellular barrier protein for cations [42]. Similar to expression of claudin-1, claudin-8 expression was found to be diminished in *A. butzleri*–exposed HT-29/B6 cells, and its distribution in immunostainings was changed from the TJ strands toward intracellular aggregates.

Although expression of the TJ protein occludin was up-regulated, R^t could not be maintained at its original level in infected monolayers. However, this was not surprising, because the function of occludin is not sealing of the TJ, even if it is present within TJ strands. This is directly supported by experimental evidence showing that epithelial barrier function was not significantly affected in occludin-deficient mice [43, 44].

Confocal laser-scanning microscopy showed that the length of the TJ meshwork per exposed serosal area in our measuring chamber was not affected by *A. butzleri.* Therefore, we could rule out that an increase in exposed TJ strand length as the result of a decrease in cell size has contributed to the reduction in R^t. Taken together, the reduction of claudin-1, -5, and -8 levels and their redistribution off the TJ are responsible for the functional changes after *A. butzleri* infection and may contribute to diarrhea by a leak flux mechanism. This is also in line

with the clinical experience of watery diarrhea being the main manifestation of *Arcobacter* infection [9, 45, 46].

In addition to TJ alteration, effects on epithelial apoptosis were observed 48 h after infection, which is an additional relevant observation of this study. In general, apoptosis can be induced via death receptors, which activate caspase-8 as the first step. Then, activation of the caspase network occurs through caspase-3 activation. In addition, caspase-independent apoptosis can be induced by bacterial pathogens through activation of p38 or by interference with NF-κB signaling. In our study, *A. butzleri* was shown to induce apoptosis in a caspase-3–dependent manner. However, the functional relevance of epithelial apoptosis for the barrier function of an epithelium has often been a matter of debate. For the colon, our group has yielded direct evidence in the past that an increased apoptotic rate of this extent is important for epithelial barrier function [47] and that apoptotic foci directly contribute to barrier dysfunction under inflammatory conditions (ulcerative colitis) [21]. This interpretation is also supported by our present finding of a partial reconstitution of *A. butzleri*–induced barrier dysfunction by inhibition of apoptosis with Z-VAD-FMK, which enabled us to distinguish the barrier impairment caused by TJ disruption from apoptotic influences. Both play a significant role in the late effect of *A. butzleri* on R^t, but the effect on TJs appears to be predominant.

A. butzleri also hampered the viability of subconfluent HT-29/B6 cells, as indicated by MTT assay. In other cell culture models, *A. butzleri* lysate had few toxic effects, and it does not possess a cytolethal-distending toxin, as does *C. jejuni* [48]. Cytotoxic effects of *A. butzleri* were first described by Musmanno et al [49] and could be confirmed in this study. LDH release from confluent monolayers increased 48 h after infection, providing evidence for a late necrotic effect.

Lysate of *A. butzleri* had a similar effect on R^t, TJs, and the viability of HT-29/B6 cells as intact bacteria. This has been indicated in experiments in which the effect of the lysate was abolished under protein-degrading conditions, as well as by exposure to heat (heat sensitivity), and this implicates that the active compound of *A. butzleri* lysate is a protein. Bacterial supernatants showed no effect on R^t, which indicates that a toxin is cell associated, rather than secreted. In general, for the mechanisms of TJ regulation in response to pathogens, different types of signaling have been described thus far (e.g., changes in half-life time, cleavage of claudins, ubiquitinylation, and gene regulation). We were able to show that *A. butzleri* can affect claudin expression from the gene. Furthermore, *A. butzleri* compounds can activate the caspase pathway, as outlined above.

Moreover, we can presume that the virulence of *A. butzleri* has 2 phases. First, an initial effect on TJs was observed, and then, we observed a late effect on cytotoxicity because of necrosis and induction of apoptosis. The inherent pathomechanisms of *Arcobacter* enteritis are, thus far, still unknown. Our findings provide evidence for *A. butzleri* to be a host-adapted pathogen, characterized by defined interactions with human epithelial cells and distinct pathomechanisms. In summary, we have demonstrated for the first time to our knowledge that *A. butzleri* induces impairment of the intestinal barrier function via TJ regulation and apoptosis induction, which are mechanisms that are well known to cause leak flux diarrhea.

Acknowledgments

We thank Anja Fromm, Nicole Held, and Martin Voss, for excellent technical assistance, and Prof. Chakraborty, for his helpful comments.

References

1. Ellis WA, Neill SD, O'Brien JJ, Ferguson HW, Hanna J. Isolation of *Spirillum/Vibrio*-like organisms from bovine fetuses. Vet Rec **1977**; 100: 451–2.
2. Neill SD, Ellis WA, O'Brien JJ. Designation of aerotolerant *Campylobacter*-like organisms from porcine and bovine abortions to the genus *Campylobacter.* Res Vet Sci **1979**; 27:180–6.
3. Neill SD, Ellis WA, O'Brien JJ. The biochemical characteristics of *Campylobacter*-like organisms from cattle and pigs. Res Vet Sci **1978**; 25: 368–72.
4. Vandamme P, Falsen E, Rossau R, et al. Revision of *Campylobacter, Helicobacter,* and *Wolinella* taxonomy: emendation of generic descriptions and proposal of *Arcobacter* gen. nov. Int J Syst Bacteriol **1991**; 41: 88–103.
5. Miller WG, Parker CT, Rubenfield M, et al. The complete genome sequence and analysis of the epsilonproteobacterium *Arcobacter butzleri.* PLoS ONE **2007**; 2:e1358.
6. Vandamme P, Pugina P, Benzi G, et al. Outbreak of recurrent abdominal cramps associated with *Arcobacter butzleri* in an Italian school. J Clin Microbiol **1992**; 30:2335–7.
7. On SL, Stacey A, Smyth J. Isolation of *Arcobacter butzleri* from a neonate with bacteraemia. J Infect **1995**; 31:225–7.
8. Yan JJ, Ko WC, Huang AH, Chen HM, Jin YT, Wu JJ. *Arcobacter butzleri* bacteremia in a patient with liver cirrhosis. J Formos Med Assoc **2000**; 99:166–9.
9. Vandenberg O, Dediste A, Houf K, et al. *Arcobacter* species in humans. Emerg Infect Dis **2004**; 10:1863–7.
10. The community summary report on trends and sources of zoonoses, zoonotic agents, antimicrobial resistance and foodborne outbreaks in the European Union in 2005. The EFSA Journal **2006**:94.
11. Prouzet-Mauléon V, Labadi L, Bouges N, Ménard A, Mégraud F. *Arcobacter butzleri:* underestimated enteropathogen. Emerg Infect Dis **2006**; 12:307–9.
12. Kiehlbauch JA, Brenner DJ, Nicholson MA, et al. *Campylobacter butzleri* sp. nov. isolated from humans and animals with diarrheal illness. J Clin Microbiol **1991**; 29:376–85.
13. Atabay HI, Corry JE, On SL. Diversity and prevalence of *Arcobacter* spp. in broiler chickens. J Appl Microbiol **1998**; 84:1007–16.
14. Assanta MA, Roy D, Lemay MJ, Montpetit D. Attachment of *Arcobacter butzleri,* a new waterborne pathogen, to water distribution pipe surfaces. J Food Prot **2002**; 65:1240–7.
15. Houf K, De Zutter L, Van Hoof J, Vandamme P. Occurrence and distribution of *Arcobacter* species in poultry processing. J Food Prot **2002**; 65:1233–9.
16. Jacob J, Lior H, Feuerpfeil I. Isolation of *Arcobacter butzleri* from a drinking water reservoir in eastern Germany. Zentralbl Hyg Umweltmed **1993**; 193:557–62.
17. Maugeri TL, Carbone M, Fera MT, Irrera GP, Gugliandolo C. Distri-

bution of potentially pathogenic bacteria as free living and plankton associated in a marine coastal zone. J Appl Microbiol **2004**; 97:354–61.
18. Houf K, De Smet S, Baré J, Daminet S. Dogs as carriers of the emerging pathogen *Arcobacter.* Vet Microbiol **2008**; 130:208–13.
19. Houf K, De Zutter L, Verbeke B, Van Hoof J, Vandamme P. Molecular characterization of *Arcobacter* isolates collected in a poultry slaughterhouse. J Food Prot **2003**; 66:364–9.
20. Ho HT, Lipman LJ, Gaastra W. The introduction of *Arcobacter* spp. in poultry slaughterhouses. Int J Food Microbiol **2008**; 125:223–9.
21. Gitter AH, Wullstein F, Fromm M, Schulzke JD. Epithelial barrier defects in ulcerative colitis: characterization and quantification by electrophysiological imaging. Gastroenterology **2001**; 121:1320–8.
22. Inai T, Kobayashi J, Shibata Y. Claudin-1 contributes to the epithelial barrier function in MDCK cells. Eur J Cell Biol **1999**; 78:849–55.
23. Amasheh S, Schmidt T, Mahn M, et al. Contribution of claudin-5 to barrier properties in tight junctions of epithelial cells. Cell Tissue Res **2005**; 321:89–96.
24. Kreusel KM, Fromm M, Schulzke JD, Hegel U. Cl-secretion in epithelial monolayers of mucus-forming human colon cells (HT-29/B6). Am J Physiol **1991**; 261:C574–82.
25. Epple HJ, Kreusel KM, Hanski C, Schulzke JD, Riecken EO, Fromm M. Differential stimulation of intestinal mucin secretion by cholera toxin and carbachol. Pflugers Arch **1997**; 433:638–47.
26. Schulzke JD, Fromm M, Bentzel CJ, Zeitz M, Menge H, Riecken EO. Ion transport in the experimental short bowel syndrome of the rat. Gastroenterology **1992**; 102:497–504.
27. Madara JL, Stafford J. Interferon-gamma directly affects barrier function of cultured intestinal epithelial monolayers. J Clin Invest **1989**; 83:724–7.
28. Livak KJ, Schmittgen TD. Analysis of relative gene expression data using real-time quantitative PCR and the $2(-\Delta\Delta C(T))$ method. Methods **2001**; 25:402–8.
29. Lee MD, Newell DG. *Campylobacter* in poultry: filling an ecological niche. Avian Dis **2006**; 50:1–9.
30. Chen ML, Ge Z, Fox JG, Schauer DB. Disruption of tight junctions and induction of proinflammatory cytokine responses in colonic epithelial cells by *Campylobacter jejuni.* Infect Immun **2006**; 74:6581–9.
31. Hecht G, Koutsouris A, Pothoulakis C, LaMont JT, Madara JL. *Clostridium difficile* toxin B disrupts the barrier function of T84 monolayers. Gastroenterology **1992**; 102:416–23.
32. Fasano A, Baudry B, Pumplin DW, et al. *Vibrio cholerae* produces a second enterotoxin, which affects intestinal tight junctions. Proc Natl Acad Sci U S A **1991**; 88:5242–6.
33. Stockmann M, Fromm M, Schmitz H, Schmidt W, Riecken EO, Schulzke JD. Duodenal biopsies of HIV-infected patients with diarrhoea exhibit epithelial barrier defects but no active secretion. AIDS **1998**; 12:43–51.
34. Troeger H, Epple HJ, Schneider T, et al. Effect of chronic *Giardia lamblia* infection on epithelial transport and barrier function in human duodenum. Gut **2007**; 56:328–35.
35. Van Itallie CM, Anderson JM. Claudins and epithelial paracellular transport. Annu Rev Physiol **2006**; 68:403–29.
36. Furuse M, Hata M, Furuse K, et al. Claudin-based tight junctions are crucial for the mammalian epidermal barrier: a lesson from claudin-1-deficient mice. J Cell Biol **2002**; 156:1099–111.
37. Muza-Moons MM, Schneeberger EE, Hecht GA. Enteropathogenic *Escherichia coli* infection leads to appearance of aberrant tight junctions strands in the lateral membrane of intestinal epithelial cells. Cell Microbiol **2004**; 6:783–93.
38. Lui WY, Lee WM. Regulation of junction dynamics in the testis—transcriptional and post-translational regulations of cell junction proteins. Mol Cell Endocrinol **2006**; 250:25–35.
39. Amasheh S, Meiri N, Gitter AH, et al. Claudin-2 expression induces cation-selective channels in tight junctions of epithelial cells. J Cell Sci **2002**; 115:4969–76.
40. Katahira J, Sugiyama H, Inoue N, Horiguchi Y, Matsuda M, Sugimoto N. *Clostridium perfringens* enterotoxin utilizes two structurally related membrane proteins as functional receptors in vivo. J Biol Chem **1997**; 272:26652–8.
41. Sonoda N, Furuse M, Sasaki H, et al. *Clostridium perfringens* enterotoxin fragment removes specific claudins from tight junction strands: evidence for direct involvement of claudins in tight junction barrier. J Cell Biol **1999**; 147:195–204.
42. Yu AS, Enck AH, Lencer WI, Schneeberger EE. Claudin-8 expression in Madin-Darby canine kidney cells augments the paracellular barrier to cation permeation. J Biol Chem **2003**; 278:17350–9.
43. Saitou M, Furuse M, Sasaki H, et al. Complex phenotype of mice lacking occludin, a component of tight junction strands. Mol Biol Cell **2000**; 11: 4131–42.
44. Schulzke JD, Gitter AH, Mankertz J, et al. Epithelial transport and barrier function in occludin-deficient mice. Biochim Biophys Acta **2005**; 1669: 34–42.
45. Lerner J, Brumberger V, Preac-Mursic V. Severe diarrhea associated with *Arcobacter butzleri.* Eur J Clin Microbiol Infect Dis **1994**; 13:660–2.
46. Higgins R, Messier S, Daignault D, Lorange M. *Arcobacter butzleri* isolated from a diarrhoeic non-human primate. Lab Anim **1999**; 33:87–90.
47. Bojarski C, Gitter AH, Bendfeldt K, et al. Permeability of human HT-29/B6 colonic epithelium as a function of apoptosis. J Physiol **2001**; 535:541–52.
48. Johnson LG, Murano EA. Lack of a cytolethal distending toxin among *Arcobacter* isolates from various sources. J Food Prot **2002**; 65:1789–95.
49. Musmanno RA, Russi M, Lior H, Figura N. In vitro virulence factors of *Arcobacter butzleri* strains isolated from superficial water samples. New Microbiol **1997**; 20:63–8.

2.1.2 Klinik der *Campylobacter*-Infektion

Während es zum klinischen Verlauf der *Arcobacter*-Infektion bislang nur Einzelfallbeschreibungen und Beschreibungen von sporadischen Ausbrüchen gibt, sind im Genus *Campylobacter* aufgrund der höheren Patientenzahlen mehr Daten vorhanden. Neben der Infektion mit *C. jejuni / coli*, die zu den häufigsten meldpflichtigen Erkrankungen in Deutschland zählen, rücken auch Infektionen mit weiteren „emerging human pathogens", wie der Spezies *C. concisus* immer mehr in den Vordergrund.

In einer internationalen Kooperation mit dem Department of Infectious Diseases, Aalborg, Dänemark konnten die pathologischen Veränderungen, die für die Barrierestörung und Diarrhö bei der *C. concisus*-Infektion verantwortlich sind, beleuchtet werden (Nielsen, ..., Bücker, 2011, *PLoS ONE* sowie Nielsen, ..., Bücker, et al., 2012, *Clin. Microbiol. Infect.*). In der folgenden Publikation: Nielsen, ..., Bücker, et al. „Short-term and medium-term clinical outcomes of *Campylobacter concisus* infection", 2012 erschienen in *Clinical Microbiology and Infection*, konnte in klinischen Untersuchungen festgestellt werden, dass die *C. concisus*-Enteritis eher durch langanhaltende Diarrhöen mit geringerer systemischer Immunaktivierung charakterisiert ist, indem sie im Vergleich zur *Campylobacter jejuni*-Infektion bei einer geringen Zahl von Patienten mit Fieber und Erhöhung des C-reaktiven Proteins (CRP) in Erscheinung trat (Nielsen et al., 2012a). Die *C. concisus*-Infektion zeigte eine ähnlich hohe Prävalenz wie die *C. jejuni*-Infektion, was bereits in vorangegangenen Untersuchungen belegt werden konnte (Samie et al., 2007; Nielsen et al., 2012b).

Mit der Beschreibung der klinischen Parameter bei einer *C. concisus*-Infektion konnte ein weiterer Beitrag zur Darstellung der Bakterien als ein Humanpathogen geleistet werden. Im Rahmen dieser Untersuchungen fielen auch Indizien einer möglichen assoziierten Folgeerkrankung der *C. concisus*-Infektion auf. Im Follow-up der Patienten in dieser Studie konnte bei 11% der *C. concisus*-Infizierten nach 6 Monaten eine *Mikroskopische Kolitis* als Erstmanifestation einer CED ermittelt werden (Nielsen et al., 2012a). In wieweit *C. concisus* für die Entstehung der *Mikroskopischen Kolitis* als möglicher ätiologischer Faktor in Frage kommt, erfordert weitere Untersuchungen. Im Follow-up zeigte sich allerdings in beiden Gruppen ein gehäuftes Auftreten von Symptomen des postinfektiösen Reizdarmsyndroms, was für die *C. jejuni*-Infektion bereits bekannt war. Für die akute Phase der Infektion kann jedoch zusammenfassend festgestellt werden, dass die *C. concisus*-Infektion einen milderen, aber längeren Verlauf einer Gastroenteritis zeigt als die *C. jejuni*-Infektion (Nielsen et al., 2012a).

ORIGINAL ARTICLE 10.1111/j.1469-0691.2012.03990.x

Short-term and medium-term clinical outcomes of *Campylobacter concisus* infection

H. L. Nielsen[1], J. Engberg[2], T. Ejlertsen[3], R. Bücker[4] and H. Nielsen[1]

1) *Department of Infectious Diseases, Aalborg Hospital, Aarhus University Hospital, Aalborg,* 2) *Department of Clinical Microbiology, Slagelse Hospital, Slagelse,* 3) *Department of Clinical Microbiology, Aalborg Hospital, Aarhus University Hospital, Aalborg, Denmark and* 4) *Department of Gastroenterology, Infectious Diseases and Rheumatology, Division of Nutritional Medicine, Charité – Universitätsmedizin Berlin, Germany*

Abstract

There are only sparse data on the short-term and medium-term clinical impacts of *Campylobacter concisus* infection. A clinical study was performed during a 2-year period to determine the clinical manifestations in *C. concisus*-positive adult patients. A case patient was defined as an adult patient (≥18 years) with a *C. concisus*-positive stool sample during the study period. Clinical data were obtained with use of a questionnaire supplemented with the patients' medical records, if any. The short-term and medium-term clinical manifestations in these patients were compared with those of patients with *Campylobacter jejuni/Campylobacter coli* infection. One hundred and seventy-four *C. concisus* patients and 196 *C. jejuni/C. coli* patients participated in the study. Patients with pre-existing inflammatory bowel disease or microscopic colitis or enteric co-infection were excluded from review of the clinical manifestations. Comparison of the short-term clinical manifestations in 139 *C. concisus* patients with those in 187 *C. jejuni/C. coli* patients showed a significantly lower prevalence of fever, chills, mucus and blood in stools, and weight loss. However, 80% of *C. concisus* patients, but only 32% of *C. jejuni/C. coli* patients, had diarrhoea for >2 weeks. After a 6-month follow-up period, 12% of *C. concisus* patients were diagnosed with microscopic colitis, whereas no *C. jejuni/C. coli* patients were diagnosed with non-infective colitis. Irritable bowel symptoms were common in both groups at follow-up. *C. concisus* infection seems to cause a milder course of acute gastroenteritis than *C. jejuni/C. coli* infection, but is associated with more prolonged diarrhoea.

Keywords: *Campylobacter coli*, *Campylobacter concisus*, *Campylobacter jejuni*, clinical manifestations, diarrhoea, gastroenteritis, microscopic colitis

Original Submission: 12 April 2012; **Revised Submission:** 22 June 2012; **Accepted:** 30 June 2012

Editor: S. Cutler

Clin Microbiol Infect

Corresponding author: H. L. Nielsen, Department of Infectious Diseases, Aalborg Hospital, Aarhus University Hospital, Hobrovej 18-22, DK-9000 Aalborg, Denmark
E-mail: halin@rn.dk

Introduction

Campylobacter jejuni is the most commonly reported infectious agent in gastrointestinal disease in the EU (http://ecdc.europa.eu). A related species, *Campylobacter concisus*, was first isolated from human periodontal lesions in 1981, but it is commonly isolated from saliva in healthy individuals [1,2].

Earlier studies have cultured *C. concisus* in diarrhoeic stools samples from children and immunocompromised adult patients [3–5]. However, the bacterium has also been reported in stools from healthy children [6]. Therefore, the precise role of *C. concisus* as a primary intestinal pathogen has yet to be established, and the overall clinical importance of *C. concisus* infection remains unclear. Recently, an association between *C. concisus* and inflammatory bowel disease (IBD) has been found [7–10]. *In vitro*, *C. concisus* has shown the capability for epithelial invasion as well to cause apoptotic leaks, and these findings support the hypothesis that *C. concisus* is an intestinal pathogen [11–14]. However, *C. concisus* is a very heterogeneous species that may vary in pathogenic potential. Patients with IBD are colonized with specific *C. concisus* strains in intestinal tissues, resulting from endogenous colonization of the patients' oral *C. concisus* [15].

A recent study from Denmark reported a high incidence of *C. concisus*, almost equal to that of *C. jejuni/Campylobacter coli*, in diarrhoeic stool samples from patients in an unselected population-based community [16]. Here, we present the first report of the short-term and medium-term clinical outcomes in *C. concisus*-positive adult patients, and compare the clinical outcomes with those of a cohort of *C. jejuni/C. coli*-positive adult patients.

Materials and Methods

The study was conducted prospectively, in North Denmark Region, located in northern Jutland, with a population of 580 515 inhabitants, from January 2009 to December 2010, with a 6-month follow-up. Diarrhoeic stool samples were cultured at the Department of Clinical Microbiology, Aalborg Hospital, Aarhus University Hospital, with the filter method as well as routine diagnosis. Identification of *Campylobacter* species was performed as described elsewhere [11,16]. *C. jejuni* and *C. coli* were not speciated, although most infections (>90%) were probably caused by *C. jejuni* [17].

A case patient was defined as an adult patient (≥18 years) with a *C. concisus*-positive stool sample. Comparison patients were patients infected with *C. jejuni/C. coli*. The study was unmatched. Whenever a faecal sample culture that was positive for either *C. concisus* or *C. jejuni/C. coli*, the patient was invited by telephone by the clinical investigator to participate in a questionnaire study. Patients were excluded if they could not be contacted by telephone, declined to participate, were unable to participate, resided outside North Denmark Region, or had a terminal illness. All patients signed a written informed consent form.

Two questionnaires (non-validated) were mailed to the patients on the same day as the telephone interview. The first concerned baseline characteristics such as marital status, smoking, drinking habits, medication, and chronic diseases. For all patients, medical records were used simultaneously to record their International Classification of Diseases (ICD)-10 diagnoses. This was used for calculation of the Charlson comorbidity index for each patient [18]. Biochemical data from each patient were included if they had the same index date as the positive faecal sample, or an index date of up to 2 days before. To assess the short-term clinical outcome, the following symptoms were used: fever (≥38°C), chills, nausea, vomiting, headache, dizziness, abdominal pain, muscle aches, the peak number of stools passed during a 24-h period, appearance of stools (watery, mucous, or bloody), weight loss, prescriptions of antibiotics, and duration (in days) of diarrhoeal disease. Duration was categorized as ≤7 days, 8–14 days, and >14 days. Patients with co-pathogens in their faecal sample or diagnosed with IBD (ICD-10: K50.X or K51.X) or other non-infective colitis (ICD-10: K52.X) at baseline were excluded from analysis of the clinical outcomes.

The second questionnaire had to be completed and returned within 6 months from the date of the positive stool sample. Participants were asked to report persisting or emerging symptoms (e.g. abdominal problems and joint pains), use of new medications, and additional visits to the general practitioner or hospitalization within the 6 months. Diagnoses of hospitalized patients were recorded by use of the medical records. Additionally, patients were asked about abdominal symptoms within the last week.

Questionnaires were analysed with Stata software, version 10 (Stata, College Station, TX, USA). Relative prevalence proportions (RPPs) with corresponding 95% CIs were calculated to estimate differences in baseline variables. Because of the small sample size and a frequent outcome for dichotomous variables, a modified Poisson regression analysis was used to estimate relative risks for clinical outcome variables [19]. Estimates were adjusted for possible confounders: age, gender, and comorbidity. Scientific and ethics approval for the study was obtained from the Ethics Committee for North Denmark Region (N-20080056).

Results

A total of 8939 faecal samples from 6432 adult patients were cultured, and 315 *C. concisus* patients (median 60 years; interquartile range (IQR) 40–72 years) and 380 *C. jejuni/C. coli* patients (median 40 years; IQR 27–54 years) were identified. Two hundred and thirteen (68%) *C. concisus* patients and 256 (67%) *C. jejuni/C. coli* patients accepted the invitation to participate in the survey (Fig. 1). However, only 174 of 315 (55%) *C. concisus* patients and 196 of 380 (52%) *C. jejuni/C. coli* patients actually returned the first questionnaire. Baseline characteristics are presented in Table 1. Forty-nine *C. concisus* patients (median 65 years; range 31–90 years) had comorbidities, as compared with only 23 *C. jejuni/C. coli* patients (median 63 years; range 45–79 years) (RPP 2.4; 95% CI 1.5–3.8). Seven patients in each group had ulcerative colitis (UC), five *C. concisus* patients had Crohn's disease (CD) and two *C. concisus* patients had microscopic colitis (MC) (collagenous colitis) (ICD-10: K52.8D1) at the time of sampling. There were no *C. jejuni/C. coli* patients with CD or MC. The use of intestinal anti-inflammatory agents, glucocorticoids and antineoplastic agents did not differ between the two groups. However, the use of proton pump inhibitors

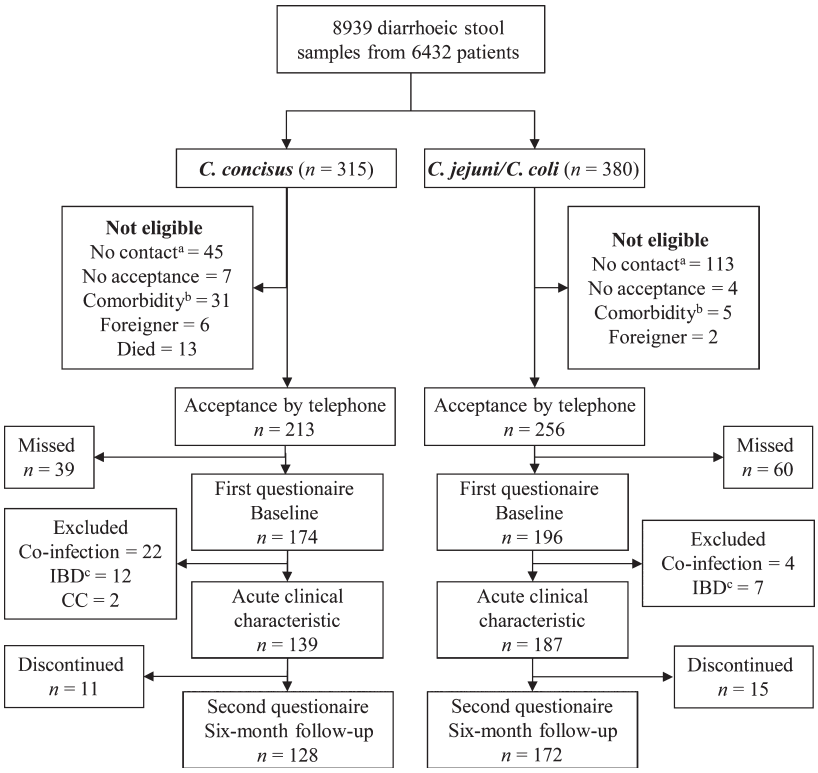

FIG. 1. Flow diagram of *Campylobacter concisus* and *Campylobacter jejuni/Campylobacter coli* patients participating in the study from January 2009 to December 2010. [a]No telephone number available or attempt at contact unsuccessful. [b]Dementia, stroke, and cancer. [c]One inflammatory bowel disease (IBD) patient with *C. concicus* infection and two IBD patients with *C. jejuni/C. coli* infection had a co-infection. CC = Collagenous Colitis (ICD-10: K52.8DI).

TABLE 1. Baseline characteristics of adult patients with *Campylobacter concisus* or *Campylobacter jejuni/Campylobacter coli* gastroenteritis

Variable	*C. concisus* (*n* = 174)	*C. jejuni/C. coli* (*n* = 196)	p-value[a]
Age (years)			
Mean	55.7	43.8	<0.001
Median (IQR)	59 (41–70)	42 (31–58)	
Male sex	37.9	51.5	<0.001
Marital status			
Married or cohabiting	71.8	70.4	0.82
Never married, divorced, or widowed	27	26	0.91
Unknown	1.2	3.6	0.18
Current smokers	18.4	21.9	0.44
Alcohol (average intake per week)			
Low (0–4 units[b])	79.9	70.4	<0.05
Medium (5–14 units)	16.1	18.9	0.50
High (>14 units)	4.0	5.7	0.63
Charlson comorbidity index[c]			
Low (0)	71.8	88.3	<0.001
Medium (1–2)	24.7	10.2	<0.001
High (>2)	3.5	1.5	0.32
Inflammatory bowel disease[d]	6.9	3.6	0.16
Daily medication[e]	66.6	49	<0.001
Use of PPIs[f]	18.4	10.2	<0.05

Data are percentage of patients, unless otherwise indicated.
[a]Fisher's exact test was used for dichotomous variables, and Student's *t*-test was used for continuous variables that followed a standard normal distribution under the null hypothesis.
[b]A Danish alcohol unit is 12 g (0.42 ounces).
[c]Three levels of comorbidity were defined: 0 (low), corresponding to patients with no recorded underlying diseases implemented in the Charlson index; 1–2 (medium); and >2 (high).
[d]Including Crohn's disease (ICD-10: K50.X) and ulcerative colitis (ICD-10: K51.X).
[e]Only drugs with an ATC code were included.
[f]Proton pump inhibitors (ATC code: A02BC).

was higher in the *C. concisus* group (18.4%) than in *C. jejuni/C. coli* group (10.2%) (RPP 1.8; 95% CI 1.1–3). There was also a clear difference in the number of co-pathogens; four *C. jejuni/C. coli* patients had a co-pathogen in their stool samples (*Clostridium difficile*, *C. concisus*, and *Salmonella enterica*, *n* = 2), in contrast to 22 *C. concisus* patients (*Clostridium difficile*, *n* = 11, or *S. enterica*, *n* = 11).

The acute clinical characteristics are presented in Table 2. A high proportion of *C. jejuni/C. coli* patients (69.7%) reported fever (≥38°C) and chills during their acute illness, whereas only 23.9% of *C. concisus* patients reported fever (p <0.001). More than three-quarters of all patients (81.6% for *C. concisus* and 79.0% for *C. jejuni/C. coli*) reported abdominal pain. The maximum number of stools in a 24-h period was, on average, 11.7 for *C. jejuni/C. coli* patients and 9.2 for *C. concisus* patients (p <0.001). Both groups reported a high frequency of watery diarrhoea, whereas *C. jejuni/C. coli* patients had a significantly higher frequency of mucus and macroscopic blood in their stools (p <0.05). Many *C. concisus* patients (71.6%) had weight loss (mean 4.4 kg; range 1–13 kg) during their gastroenteritis, but the number of patients with weight loss was significantly higher (87.1%) in the *C. jejuni/C. coli* group (mean 4.4 kg; range 1–13 kg) (p <0.01). On assessment of duration of diarrhoea, 92% of *C. jejuni/C. coli* patients reported an end date with a median duration of 10 days (IQR 7–15 days). Half of the *C. concisus*

TABLE 2. Clinical characteristics of patients with *Campylobacter concisus* and *Campylobacter jejuni/Campylobacter coli* gastroenteritis; only patients with no co-infection and no prior gastrointestinal disease (inflammatory bowel disease or microscopic colitis) are shown

Variable	*C. concisus* (*n* = 139)	*C. jejuni/C. coli* (*n* = 187)	RR (95% CI)[a]	p-value	Adjusted RR (95% CI)[b]	p-value
Symptoms						
Fever	23.9	69.7	0.34 (0.25–0.47)	<0.001	0.39 (0.28–0.54)	<0.001
Chills	34.1	71.0	0.48 (0.37–0.62)	<0.001	0.50 (0.39–0.66)	<0.001
Nausea	67.4	73.6	0.92 (0.79–1.06)	0.2	0.94 (0.81–1.09)	0.4
Vomiting	40.6	35.9	1.13 (0.85–1.51)	0.4	1.19 (0.85–1.66)	0.2
Headache	50.8	61.8	0.82 (0.67–1.01)	0.06	0.92 (0.75–1.13)	0.4
Dizziness	50.8	59.9	0.85 (0.69–1.05)	0.1	0.88 (0.70–1.09)	0.2
Abdominal pain	81.6	79.0	1.03 (0.92–1.16)	0.6	1.13 (1.00–1.26)	0.05
Muscle aches	51.5	63.0	0.82 (0.67–1.00)	0.05	0.85 (0.69–1.05)	0.1
Consistency of stools						
Watery	91.7	98.4	0.93 (0.88–0.98)	<0.05	0.94 (0.89–0.99)	<0.05
Mucus in stool	47.4	67.2	0.70 (0.57–0.87)	<0.01	0.73 (0.59–0.90)	<0.01
Blood in stool	9.9	24.7	0.40 (0.22–0.71)	<0.01	0.45 (0.25–0.82)	<0.05
Weight loss	71.6	87.1	0.82 (0.73–0.93)	<0.01	0.83 (0.73–0.94)	<0.01
Duration of diarrhoea (days)[c]						
≤7	6.2	30.4	0.20 (0.10–0.41)	<0.001	0.22 (0.10–0.47)	<0.001
8–14	13.9	37.6	0.37 (0.23–0.59)	<0.001	0.43 (0.26–0.71)	<0.001
>14	79.9	32	2.49 (1.98–3.14)	<0.001	2.26 (1.77–2.90)	<0.001

RR, relative risk.
Data are percentage of patients, unless otherwise indicated.
[a]A modified Poisson regression analysis was used to obtain estimates on RRs.
[b]Adjusted for age, sex, and comorbidity. Age was stratified into three groups (18–39 years, 40–59 years, and ≥60 years), and comorbidities were separated into two strata: patients with no comorbidities and those with one or more comorbidities.
[c]Nine patients in each group had an unknown duration of diarrhoea, and were excluded.

patients had diarrhoea at the time of answering the questionnaire, and the other half of the *C. concisus* patients (*n* = 66) with fixed start and end dates had a median duration of diarrhoea of 16 days (IQR 11–29 days). Thirty-eight *C. jejuni/C. coli* patients (median 40 years; range 18–79 years) and 31 *C. concisus* patients (median 69 years; range 18–90 years) were hospitalized because of their acute gastroenteritis. The average numbers of days of hospitalization were 4 and 8 for *C. jejuni/C. coli* and *C. concisus* patients, respectively (p <0.001).

Blood parameters were obtained from 60 *C. concisus* patients and 55 *C. jejuni/C. coli* patients (Table 3). Only one-third of *C. jejuni/C. coli* patients (*n* = 19) and one-quarter of *C. concisus* patients (*n* = 14) had leukocytosis. Half of the *C. concisus* patients (52%) had normal C-reactive protein (CRP) levels (<10 mg/L), whereas most (94%) of the *C. jejuni/C. coli* patients had elevated CRP levels.

TABLE 3. Blood parameters from patients[a] with *Campylobacter concisus* and *Campylobacter jejuni/Campylobacter coli* gastroenteritis

Biochemical data[b]	*C. concisus* (*n* = 60)	*C. jejuni/C. coli* (*n* = 55)	p-value
Na^+ (mM)	140 (121–147)	139 (129–147)	0.4
K^+ (mM)	4 (1.5–5.2)	3.9 (2.9–4.8)	0.2
CRP (mg/L)	<10 (<10–191)	65 (<10–336)	<0.001
Leukocytes ($\times 10^9$/L)	7.5 (2.5–19)	8.9 (3.1–31.2)	0.1
Creatinine (μM)	76 (46–1131)	75 (53–417)	0.3

CRP, C-reactive protein.
Data are presented as medians (range).
[a]Thirty-one *C. concisus* (52%) and 38 *C. jejuni/C. coli* (69%) patients were hospitalized.
[b]Leukocytes were measured in EDTA blood. Na^+, K^+, CRP and creatinine were measured in plasma.

Antibiotic sensitivities were determined as described by Nielsen *et al.* [16]. Clinicians received the antimicrobial susceptibility data for *C. jejuni/C. coli*, whereas the data for *C. concisus* were only sent by specific request, owing to uncertainty regarding the pathogenic potential of the bacterium. Fifty-five per cent of *C. jejuni/C. coli* patients (*n* = 102) reported being treated with antibiotics, whereas only 31% of *C. concisus* patients (*n* = 43) had antibiotic treatment (p <0.001). *C. jejuni/C. coli* patients were treated with ciprofloxacin (50%), a macrolide antibiotic (30%), or other antibiotics (20%). *C. concisus* patients were mainly treated with either ciprofloxacin (42%) or a macrolide (42%). Twelve per cent of patients in both groups reported the use of antipropulsives (loperamide).

Fifteen *C. jejuni/C. coli* patients and 11 *C. concisus* patients were lost to follow-up 6 months after their positive stool sample (Table 4). Thirty-four per cent of *C. concisus* patients and 25.3% *C. jejuni/C. coli* patients reported having trouble with abdominal pain at 6 months, and more than half of all patients reported having symptoms with loose stools during the last week. Thirty-two *C. concisus* patients and 14 *C. jejuni/C. coli* patients had a follow-up in an outpatient hospital setting because of gastrointestinal illnesses, and almost

TABLE 4. Overall clinical outcome after 6 months follow-up in adult patients with gastroenteritis with *Campylobacter concisus* or *Campylobacter jejuni/Campylobacter coli*

Variable	*C. concisus* (*n* = 128)	*C. jejuni/C. coli* (*n* = 172)	p-value
Enteric symptoms[a]			
Abdominal pain	34.4	25.3	0.1
Loose stools	54.6	52.4	0.8
Pain on defecation	11	11	1
Different consistency of stools from day to day	63.3	46.4	<0.01
Mucus in stools	9.7	8.1	0.7
Visiting GP with GI disorder	12.5	6.3	0.1
Visiting GP because of arthralgia	4.7	3.5	0.8
Hospitalized with GI disorder	25	8.1	<0.001
Lower endoscopy	23.4	5.8	<0.001
Diagnoses[b]			
Inflammatory bowel disease[c]	2.3	0	0.08
Microscopic colitis[d]	12.5	0	<0.001
Irritable bowel syndrome	4.7	1.2	0.08
Other	5.5	6.9	0.6

GI, gastrointestinal; GP, general practitioner.
Data are percentage of patients, unless otherwise indicated.
[a]Self-reported symptoms from the GI system within the last week 6 months after the positive stool sample.
[b]Patients' diagnoses in the time interval between the positive stool sample and the 6-month follow-up.
[c]Two *C. concisus* patients were diagnosed with Crohn's disease, and one patient was diagnosed with ulcerative colitis.
[d]Fourteen patients were diagnosed with collagenous colitis, and two patients were diagnosed with lymphocytic colitis.

one-quarter of *C. concisus* patients had a lower endoscopy examination. No *C. jejuni/C. coli* patients were diagnosed with non-infective colitis during follow-up. In contrast, two *C. concisus* patients were diagnosed with CD and one with UC. Sixteen *C. concisus* patients were diagnosed with MC during follow-up. Six patients from each group, with no arthritis at baseline, consulted their general practitioner because of emerging arthralgia in one of the major joints (knee and ankle). No patient was hospitalized because of reactive arthritis (ReA) during the study period.

Discussion

Earlier reports regarding the clinical symptoms caused by *C. concisus*, besides diarrhoea, were limited to children and immunocompromised adult patients [3,20,21]. The present report is the first to describe the clinical characteristics of *C. concisus* infection in adult patients in an unselected population-based community. *C. concisus* infection was almost as prevalent as infection with the common *C. jejuni/C. coli* throughout the 2-year study period, as described previously [16].

C. concisus patients had a higher frequency of comorbidities than *C. jejuni/C. coli* patients, probably because of their higher age. The higher frequency of comorbidities may explain the high number of *C. concisus* patients who could not participate in the study. A high number of *C. jejuni/C. coli* patients were excluded because of lack of telephone contact. However, for both groups, the overall age distributions among the included and excluded cohorts were not different.

Our results show that *C. concisus* infection causes a milder course of acute gastroenteritis than *C. jejuni/C. coli* infection. However, we cannot rule out the effect of age on symptomatology. *C. concisus* patients reported fewer fevers and chills, as well as a lower frequency of mucus and blood in their stools, than *C. jejuni/C. coli* patients. Furthermore, a higher percentage of *C. jejuni/C. coli* patients reported weight loss. Like *C. jejuni/C. coli* infection, *C. concisus* infection resulted in upper gastrointestinal symptoms, such as vomiting, in many patients. This emphasizes that *C. concisus* infection may be interpreted as gastroenteritis and not only as simple enteritis. For nausea, headache, dizziness, abdominal pain, and muscle aches, there were no significant differences between the two groups. Almost all *C. jejuni/C. coli* patients (94%) from whom we obtained blood parameters had elevated CRP levels in serum, whereas only half (48%) of *C. concisus* patients had elevated CRP levels. The lower CRP response seen in *C. conicisus* infection, together with less frequent fever and chills, may present an escape mechanism from the immune response, e.g. by interfering with host cell immune signalling or by masking immunological recognition patterns via molecular mimicry, as it is known for *Helicobacter pylori* [22]. The reservoir for *C. concisus* might be the oral cavity, and proton pump inhibitors resulting in an increase in gastric pH may lead to intestinal infection with *C. concisus*.

In agreement with previous data, only a few *C. jejuni/C. coli* patients had prolonged diarrhoea [17,23,24]. In contrast, 80% of *C. concisus* patients reported prolonged diarrhoea of >2 weeks. In general, oral fluid replacement is the cornerstone of treatment of most cases of *C. jejuni/C. coli* enteritis, but antibiotics may shorten the duration of symptoms if administered early [17]. However, antibiotic therapy in *C. jejuni/C. coli* patients cannot explain the large difference in duration of diarrhoea between the groups. We have no evidence regarding the efficacy of antimicrobial treatment of a *C. concisus* infection, and randomized clinical trials are needed to investigate the role of antibiotics in *C. concisus* infection.

A high number of patients in both groups reported abdominal pain and loose stools, and more than half of all *C. concisus* patients reported a different consistency of stools from day to day. These questions, among others, were asked to assess whether the patients had post-infectious irritable bowel syndrome (IBS) as shown for *C. jejuni/C. coli* patients [25]. Although our self-reported data do not fulfil the Rome III diagnostic criteria for IBS, the results show that

C. concisus patients have the same degree of late gastrointestinal complaints as patients diagnosed with *C. jejuni/C. coli*. During the study period, there were also more *C. concisus* patients than *C. jejuni/C. coli* patients diagnosed with IBS, although the numbers were small.

Six patients from each group visited their general practitioner because of emerging arthralgia in one of the major joints, which could be interpreted as possible ReA. However, these percentages of patients with ReA seem low in comparison with other studies [26–28]. The reason for this may be recall bias, owing to the time difference between the occurrence of symptoms in ReA, which occur in the weeks following the *Campylobacter* infection, and the 6-month follow-up questionnaire.

Epidemiological studies with long observation periods have focused on the possible association between *C. jejuni/C. coli* infection and the risk of IBD [17,18]. Likewise, studies have recently focused on the potential association between *C. concisus* infection and IBD [7–10]; however, only two *C. concisus* patients with CD and one patient with UC were diagnosed during the 6-month study period. Clinical studies including more *C. concisus* patients with a longer clinical follow-up period are urgently needed.

For MC, we found a possible association with *C. concisus* infection, as >12% of the infected patients were diagnosed with this disorder during the follow-up period. All patients were diagnosed in hospital after a colonoscopy including biopsies of the colonic mucosa. Patients with MC were all treated with oral anti-inflammatory agents, and recovered. An increased risk of MC following a stool sample positive for *C. concisus* seems possible. However, the risk of MC following a negative stool sample also has to be investigated, to evaluate the risk of detection bias, which cannot be excluded in our study.

Our study participants were not matched by age and gender, and, as for any retrospective study, there is potential for recall bias among respondents, although this seems less likely in our case-comparison study, as both clinical and follow-up data were collected similarly from both groups with the structured questionnaires.

In conclusion, *C. concisus* infection seems to cause a milder course of acute gastroenteritis than *C. jejuni/C. coli* infection. However, *C. concisus* infections were associated with more prolonged diarrhoea, and *C. concisus* patients seemed to have the same gastrointestinal complaints following the acute gastroenteritis as patients diagnosed with *C. jejuni/C. coli* infection. Our follow-up period of 6 months was too short to allow any conclusions to be drawn regarding the risk of IBD, but we found a possible association between *C. concisus* infection and MC.

Acknowledgements

We gratefully acknowledge the assistance of the microbiology staff in the faeces laboratory at the Department of Clinical Microbiology, Aalborg Hospital, K. Koch for assisting with the statistical analysis, and all patients who took part in the study.

Transparency Declaration

This work was supported by grants from the Hertha Christensen Foundation, Heinrich Kopp's legate, and the A. P. Møller Foundation for the Advancement of Medical Science. The authors declare that they have no conflicting interests in relation to this work.

References

1. Tanner AC, Dzink JL, Ebersole JL, Socransky SS. *Wolinella recta*, *Campylobacter concisus*, *Bacteroides gracilis*, and *Eikenella corrodens* from periodontal lesions. *J Periodontal Res* 1987; 22: 327–330.
2. Zhang L, Budiman V, Day AS *et al.* Isolation and detection of *Campylobacter concisus* from saliva of healthy individuals and patients with inflammatory bowel disease. *J Clin Microbiol* 2010; 48: 2965–2967.
3. Aabenhus R, Permin H, On SL, Andersen LP. Prevalence of *Campylobacter concisus* in diarrhoea of immunocompromised patients. *Scand J Infect Dis* 2002; 34: 248–252.
4. Engberg J, On SL, Harrington CS, Gerner-Smidt P. Prevalence of *Campylobacter*, *Arcobacter*, *Helicobacter*, and *Sutterella* spp. in human fecal samples as estimated by a reevaluation of isolation methods for campylobacters. *J Clin Microbiol* 2000; 38: 286–291.
5. Lastovica AJ. Emerging *Campylobacter* spp.: the tip of the iceberg. *Clin Microbiol Newslett* 2006; 28: 49–56.
6. Van ER, Breynaert J, Revets H *et al.* Isolation of *Campylobacter concisus* from feces of children with and without diarrhea. *J Clin Microbiol* 1996; 34: 2304–2306.
7. Mahendran V, Riordan SM, Grimm MC *et al.* Prevalence of *Campylobacter* species in adult Crohn's disease and the preferential colonization sites of *Campylobacter* species in the human intestine. *PLoS One* 2011; 6: e25417.
8. Man SM, Zhang L, Day AS, Leach ST, Lemberg DA, Mitchell H. *Campylobacter concisus* and other *Campylobacter* species in children with newly diagnosed Crohn's disease. *Inflamm Bowel Dis* 2010; 16: 1008–1016.
9. Mukhopadhya I, Thomson JM, Hansen R, Berry SH, El-Omar EM, Hold GL. Detection of *Campylobacter concisus* and other *Campylobacter* species in colonic biopsies from adults with ulcerative colitis. *PLoS One* 2011; 6: e21490.
10. Zhang L, Man SM, Day AS *et al.* Detection and isolation of *Campylobacter* species other than *C. jejuni* from children with Crohn's disease. *J Clin Microbiol* 2009; 47: 453–455.
11. Nielsen HL, Nielsen H, Ejlertsen T *et al.* Oral and fecal *Campylobacter concisus* strains perturb barrier function by apoptosis induction in HT-29/B6 intestinal epithelial cells. *PLoS One* 2011; 6: e23858.
12. Kalischuk LD, Inglis GD. Comparative genotypic and pathogenic examination of *Campylobacter concisus* isolates from diarrheic and non-diarrheic humans. *BMC Microbiol* 2011; 11: 53.

13. Man SM, Kaakoush NO, Leach ST *et al.* Host attachment, invasion, and stimulation of proinflammatory cytokines by *Campylobacter concisus* and other non-*Campylobacter jejuni Campylobacter* species. *J Infect Dis* 2010; 202: 1855–1865.
14. Kaakoush NO, Deshpande NP, Wilkins MR *et al.* The pathogenic potential of *Campylobacter concisus* strains associated with chronic intestinal diseases. *PLoS One* 2011; 6: e29045.
15. Ismail Y, Mahendran V, Octavia S *et al.* Investigation of the enteric pathogenic potential of oral *Campylobacter concisus* strains isolated from patients with inflammatory bowel disease. *PLoS One* 2012; 7: e38217.
16. Nielsen HL, Engberg J, Ejlertsen T, Bucker R, Nielsen H. High incidence of *Campylobacter concisus* in gastroenteritis in North Jutland, Denmark: a population-based study. *Clin Microbiol Infect* 2012; Mar 27 [Epub ahead of print].
17. Blaser MJ, Engberg J. Clinical aspects of *Campylobacter jejuni* and *Campylobacter coli* infections. In: Nachamkin I, Szymanski CM, Blaser MJ, eds. *Campylobacter*, 3rd edn. Washington, DC: ASM Press, 2008; 99–121.
18. Charlson ME, Pompei P, Ales KL, MacKenzie CR. A new method of classifying prognostic comorbidity in longitudinal studies: development and validation. *J Chronic Dis* 1987; 40: 373–383.
19. Zou G. A modified poisson regression approach to prospective studies with binary data. *Am J Epidemiol* 2004; 159: 702–706.
20. Aabenhus R, Permin H, Andersen LP. Characterization and subgrouping of *Campylobacter concisus* strains using protein profiles, conventional biochemical testing and antibiotic susceptibility. *Eur J Gastroenterol Hepatol* 2005; 17: 1019–1024.
21. Lastovica AJ, Allos BM. Clinical significance of *Campylobacter* and related species other than *Campylobacter jejuni* and *Campylobacter coli*. In: Nachamkin I, Szymanski CM, Blaser MJ, eds. *Campylobacter*, 3rd edn. Washington, DC: ASM press, 2008; 123–149.
22. Appelmelk BJ, Vandenbroucke-Grauls CMJE. Lipopolysaccharide Lewis antigens. In: Mobley HLT, Mendz GL, Hazell SL, eds. *Helicobacter pylori: physiology and genetics*. Washington, DC: ASM Press, 2001; 35: 418–428.
23. Evans MR, Northey G, Sarvotham TS, Rigby CJ, Hopkins AL, Thomas DR. Short-term and medium-term clinical outcomes of quinolone-resistant *Campylobacter* infection. *Clin Infect Dis* 2009; 48: 1500–1506.
24. Schonberg-Norio D, Sarna S, Hanninen ML, Katila ML, Kaukoranta SS, Rautelin H. Strain and host characteristics of *Campylobacter jejuni* infections in Finland. *Clin Microbiol Infect* 2006; 12: 754–760.
25. Spiller RC. Role of infection in irritable bowel syndrome. *J Gastroenterol* 2007; 42 (suppl 17): 41–47.
26. Hannu T, Mattila L, Rautelin H *et al. Campylobacter*-triggered reactive arthritis: a population-based study. *Rheumatology (Oxford)* 2002; 41: 312–318.
27. Schiellerup P, Krogfelt KA, Locht H. A comparison of self-reported joint symptoms following infection with different enteric pathogens: effect of HLA-B27. *J Rheumatol* 2008; 35: 480–487.
28. Townes JM. Reactive arthritis after enteric infections in the United States: the problem of definition. *Clin Infect Dis* 2010; 50: 247–254.

2.1.3 Bakterielle Pathogenität am Beispiel von *Campylobacter concisus*

In der folgenden Publikation: Nielsen, ..., Bücker, „Oral and fecal *Campylobacter concisus* strains perturb barrier function by apoptosis induction in HT-29/B6 intestinal epithelial cells“, 2011 erschienen bei *PLoS ONE*, sollten an der humanen Epithelzelllinie HT-29/B6 die pathogenen Veränderungen durch *C. concisus* auf zellulärer Ebene experimentell charakterisiert werden (analog zu dem experimentellen Ansatz wie bei der Arbeit zu *Arcobacter butzleri* 2.1.1). Hierbei zeigten sich allerdings mildere Expressionsunterschiede in den *Tight Junction*-Proteinen. Nur in fokalen Schädigungsbereichen von apoptotischen Läsionen, wo auch die Bakterien vermehrt zu finden waren, zeigten sich *Tight Junction*-Protein-Umverteilungen in den infizierten Zellen. Dabei war insbesondere Claudin-5 mit 66% ± 8% gegenüber der Kontrolle ($P<0,05$) expressionsverändert, was sich ebenfalls auf mRNA Ebene nachvollziehen ließ. Gleichzeitig zeigte sich im Laktatdehydrogenase (LDH)-Assay eine Steigerung zytotoxischer Effekte. So war LDH im Zellkulturüberstand auf 3,1% ± 0,3% versus 0,7% ± 0,1% in der Kontrolle erhöht ($P<0,001$). Darüber hinaus wurden verschiedene Bakterienisolate aus dem Mundraum oder aus Fäzes in ihrem pathogenen Potential verglichen. Die Invasivität der verschiedenen Bakterienstämme war ähnlich und es konnte sowohl durch fäkale als auch durch orale *C. concisus*-Stämme eine Apoptoseinduktion auf das 5-fache des Kontrollwerts festgestellt werden. *C. concisus*-infizierte Monolayer zeigten dementsprechend eine Erhöhung der Permeabilität gegenüber Fluoreszein ($1,74 \pm 0,13 \cdot 10^{-6}$ cm/s versus $0,56 \pm 0,17 \cdot 10^{-6}$ cm/s in der Kontrolle, $P<0,05$), aber keinen Unterschied in der 4 kDa FITC-Dextran Permeabilität. Dieses Muster der Permeabilitätsunterschiede fand sich bereits in unseren früheren Publikationen in selektiv Apoptoserate-gesteigerten Epithelien (Bojarski et al., 2001). Bei den Barrieredefekten, die hauptsächlich auf vermehrte Apoptose-Ereignissen im Epithel beruhen, gibt es in Permeabilitätsmessungen einen Cut-off von Molekülgrößen über 4 kDa. So ließ sich auch hier die Permeabilitätssteigerung gegenüber dem Fluxmarker Fluoreszein (332 Da) durch die Behandlung mit Camptothecin, einem Apoptoseinduktor, experimentell imitieren und so die funktionell messbare Störung auf eine gesteigerte Apoptoseinduktion in der infizierten Zellkultur zurückführen. Die Pathogenität ist definiert als die Kapazität einer Mikrobe, einen Schaden im Wirt zu erzeugen. Ihr pathogenes Potential bzw. ihre Virulenz beschreibt ihre relative Kapazität, einen Schaden zu erzeugen (z.B. Zellschaden, Barriereschaden), was in Relation zu einem bekannten Pathogen gestellt wird. Die große Ähnlichkeit der beobachteten Virulenz der hier untersuchten Bakterienstämme weist auf eine generelle Pathogenität der Bakterienspezies *C. concisus* hin. Zusammenfassend lässt sich sagen, dass die epitheliale Barrierestörung durch *C. concisus* hauptsächlich durch apoptotische Leck-Bildung bedingt ist, was zusammen mit den *Tight Junction*-Veränderungen auf einen Leckflux-Mechanismus der dabei beobachteten Diarrhö hindeutet.

OPEN ACCESS Freely available online

PLoS one

Oral and Fecal *Campylobacter concisus* Strains Perturb Barrier Function by Apoptosis Induction in HT-29/B6 Intestinal Epithelial Cells

Hans Linde Nielsen[1], Henrik Nielsen[1], Tove Ejlertsen[2], Jørgen Engberg[3], Dorothee Günzel[4], Martin Zeitz[5], Nina A. Hering[5], Michael Fromm[4], Jörg-Dieter Schulzke[5]*, Roland Bücker[5]

1 Department of Infectious Diseases, Aalborg Hospital, Aarhus University Hospital, Aalborg, Denmark, **2** Department of Clinical Microbiology, Aalborg Hospital, Aarhus University Hospital, Aalborg, Denmark, **3** Department of Clinical Microbiology, Slagelse Hospital, Slagelse, Denmark, **4** Institute of Clinical Physiology, Charité Universitätsmedizin Berlin, Berlin, Germany, **5** Department of Gastroenterology, Infectious Diseases and Rheumatology, Division of General Medicine and Nutrition, Charité Universitätsmedizin Berlin, Berlin, Germany

Abstract

Campylobacter concisus infections of the gastrointestinal tract can be accompanied by diarrhea and inflammation, whereas colonization of the human oral cavity might have a commensal nature. We focus on the pathophysiology of *C. concisus* and the effects of different clinical oral and fecal *C. concisus* strains on human HT-29/B6 colon cells. Six oral and eight fecal strains of *C. concisus* were isolated. Mucus-producing HT-29/B6 epithelial monolayers were infected with the *C. concisus* strains. Transepithelial electrical resistance (R^t) and tracer fluxes of different molecule size were measured in Ussing chambers. Tight junction (TJ) protein expression was determined by Western blotting, and subcellular TJ distribution was analyzed by confocal laser-scanning microscopy. Apoptosis induction was examined by TUNEL-staining and Western blot of caspase-3 activation. All strains invaded confluent HT-29/B6 cells and impaired epithelial barrier function, characterized by a time- and dose-dependent decrease in R^t either after infection from the apical side but even more from the basolateral compartment. TJ protein expression changes were sparse, only in apoptotic areas of infected monolayers TJ proteins were redistributed. Solely the barrier-forming TJ protein claudin-5 showed a reduced expression level to 66±8% ($P<0.05$), by expression regulation from the gene. Concomitantly, Lactate dehydrogenase release was elevated to 3.1±0.3% versus 0.7±0.1% in control ($P<0.001$), suggesting cytotoxic effects. Furthermore, oral and fecal *C. concisus* strains elevated apoptotic events to 5-fold. *C. concisus*-infected monolayers revealed an increased permeability for 332 Da fluorescein (1.74±0.13 vs. 0.56±0.17 10^{-6} cm/s in control, $P<0.05$) but showed no difference in permeability for 4 kDa FITC-dextran (FD-4). The same was true in camptothecin-exposed monolayers, where camptothecin was used for apoptosis induction. In conclusion, epithelial barrier dysfunction by oral and fecal *C. concisus* strains could mainly be assigned to apoptotic leaks together with moderate TJ changes, demonstrating a leak-flux mechanism that parallels the clinical manifestation of diarrhea.

Citation: Nielsen HL, Nielsen H, Ejlertsen T, Engberg J, Günzel D, et al. (2011) Oral and Fecal *Campylobacter concisus* Strains Perturb Barrier Function by Apoptosis Induction in HT-29/B6 Intestinal Epithelial Cells. PLoS ONE 6(8): e23858. doi:10.1371/journal.pone.0023858

Editor: Vladimir N. Uversky, University of South Florida College of Medicine, United States of America

Received May 19, 2011; **Accepted** July 26, 2011; **Published** August 24, 2011

Funding: This work was supported by the Deutsche Forschungsgemeinschaft [DFG Schu 559/11-1 to MZ, JDS, RB]. The funders had no role in study design, data collection and analysis, decision to publish, or preparation of the manuscript.

Competing Interests: The authors have declared that no competing interests exist.

* E-mail: joerg.schulzke@charite.de

Introduction

Campylobacter concisus, first isolated from the human oral cavity, has been proposed as an emerging human enteric pathogen [1]. In contrast to other *Campylobacter* species no primary animal reservoir has been found for *C. concisus*, although it has been detected in diarrheic fecal samples from domestic dogs [2]. Recently, Zhang and coworkers found a very high prevalence of *C. concisus* in saliva from healthy individuals and patients with Crohn's disease suggesting it is an oral commensal rather than a clinical significant oral pathogen [3]. A potential role of emerging *C. concisus* in human gastrointestinal disease has been proposed, and recent studies describe a high incidence of *C. concisus* in pediatric diarrheic stool samples as well as in immunocompromised patients with diarrhea in a tertiary hospital setting [1], [4], [5]. However, the overall prevalence of *C. concisus* in feces is underreported because an easy-to-handle standardized selective culture medium is not available and the time-consuming filter method is not included in standard diagnostics. In a mouse model *C. concisus* induced weight loss and microabscesses in the liver [6], whereas there is only sparse data on the pathophysiology when the microorganism is introduced to the human intestine. *C. concisus* possesses virulence factors including secreted and cell-bound hemolytic activities as well as several putative virulence factors e.g. cytolethal distending toxin [7], [8]. Recently, *C. concisus* genes coding for a presumed Zonula occludens toxin (ZOT) as well as a surface-layer protein belonging to the RTX (repeats in toxin) toxins has been identified [8]. Even though these toxins are recognized as important virulence factors their pathogenic role in *C. concisus* infection is unknown. In a recent work by Kalischuk and Inglis the ZOT gene was detected more often in *C. concisus* isolates from healthy individuals than in isolates from diarrheic humans [9]. In consistence with earlier reports [10], the authors identified two main genetically distinct clusters which differed with respect to

their pathogenic properties. ALFP cluster 2 isolates were predominantly found in diarrheic patients and showed higher ability in epithelial invasion and translocation. In contrary, *C. concisus* ALFP cluster 1 were mainly found in fecal isolates from healthy individuals and are present in the oral reference strain ATCC 33237. These strains harbor hemolytic activity and can induce apoptotic DNA fragmentation. Man and coworkers reported recently that *C. concisus* is able to attach to and invade intestinal epithelial cells, and moreover *C. concisus* was observed to invade adjacent to the tight junction (TJ) [11]. In the current study we focus on the pathophysiology of *C. concisus* and describe the effects on epithelial barrier function of different oral and fecal clinical *C. concisus* strains, using the human colon cell line HT-29/B6.

Results

As shown in Figure 1*A* the incremental decrease in R^t, beginning 22 h after bacterial inoculation ($P<0.05$, and at 48 h: $P<0.001$; Student's *t*-test) showed the same characteristic with all strains used, including ATCC 33237. HT-29/B6 monolayers that were apically or basolaterally infected with *C. concisus* at MOIs between 10 and 100 showed a dose-dependent decrease in R^t after 48 h, whereas infection from the basal side revealed a stronger response in R^t (Figure 1*B*). All oral and fecal strains had similar effects on R^t as shown in Figure 1*C*.

The expression of TJ proteins claudin-1 to -3, -8, occludin and zonula occludens protein-1 (ZO-1) was not changed 48 h postinfection. Only claudin-5 showed a reduced expression level to 66±8% of the control value in whole cell lysate protein preparations ($P<0.05$, n = 9), whereas claudin-4 showed a tendency towards upregulation which did not reach statistical significance (194±37% of control, n = 9, *n.s.*) (Figure 2). ZO-1 distribution in *C. concisus*-infected cells differs only with respect to Triton-X 100 (TX)-soluble and TX-insoluble protein fractions [11], therefore we checked this feature also for the claudins. All claudins showed a slight drift from TX-insoluble to TX-soluble protein preparations. This drift of claudins out of the TJ to intracellular compartments could not be confirmed in confocal laser-scanning microscopy of immunostainings (data not shown). However, 24 h postinfection claudin-5 mRNA level was reduced to 49±16% ($P<0.05$, n = 4), suggesting expression regulation from the gene, likewise in *Arcobacter butzleri* infection [12]; a close relative, belonging to the epsilon-proteobacteria.

To further characterize epithelial barrier function, the permeability to fluorescein or FD-4 was measured. After 48 h of mucosal exposure to *C. concisus*, R^t of the HT-29/B6 monolayers had decreased to 60%, whereas the short-circuit current was not induced but rather slightly diminished (2.9±0.2 after *C. concisus* infection versus 3.2±0.2 μmol h^{-1} cm^{-2} in control, *n.s.*, n = 5). Concomitantly, permeability for fluorescein was increased after *C. concisus* infection (from 0.56±0.17 in control to 1.74±0.13 10^{-6} cm/s, $P<0.01$, n = 4) and permeability for FD-4 was unchanged (from 0.14±0.06 in control to 0.29±0.11 10^{-6} cm/s, *n.s.*, n = 4) (Figure 3*A*). To simulate the effects of *C. concisus* in apoptosis induction we used camptothecin (20 μg/ml) as positive control for 48 h. Camptothecin treatment of HT-29/B6 monolayers revealed similar apoptotic effects, with no changes in TJ integrity [13]. Fluorescein permeability was increased to the same extent as *C. concisus*-infected cells (from 0.84±0.33 in control to 3.09±0.38 10^{-6} cm/s, $P<0.01$, n = 4), whereas permeability to FD-4 was unchanged (from 0.15±0.06 in control to 0.21±0.03 10^{-6} cm/s, *n.s.*, n = 4, Figure 3*B*).

The barrier dysfunction after infection could on the one hand result from changes or disruption of TJ strands but on the other hand also from a loss of epithelial cells by apoptosis or necrosis induction. Apoptosis as examined histologically in TUNEL staining indicated an increased apoptotic ratio in *C. concisus*-infected cells (Figure 4*A*). Furthermore, LDH release was determined as marker for cytotoxicity. LDH release was elevated to 3.1±0.3% versus 0.7±0.1% in control ($P<0.001$; n = 5) suggesting cytotoxic effects caused by *C. concisus* (Figure 4*B*). After 48 h infected monolayers showed a 5-fold increase in epithelial apoptosis (5.2±0.9% vs. 1.0±0.3% in control; $P<0.01$; n = 5). In Western blots, pro-caspase-3 band intensity decreased to 70±2% in infected monolayers ($P<0.05$, n = 7, Figure 4*C*), but the caspase-3 activation was weaker when compared to the effects of *C. jejuni* ATCC 33560, where pro-caspase-3 was decreased to 52±6% of

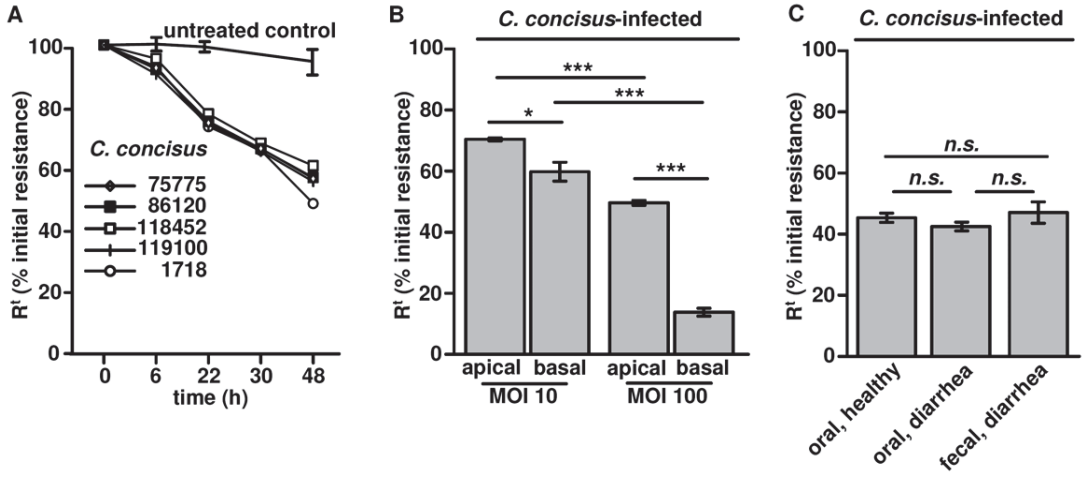

Figure 1. Effect of *Campylobacter concisus* on epithelial barrier function. *(A)* Different *Campylobacter concisus* strains on HT-29/B6 cells. Time-dependent decrease in transepithelial electrical resistance (R^t). *(B)* Dose-dependent effects on R^t after infection with *C. concisus* 1718 from either apical or basal side in HT-29/B6 monolayers 48 h postinfection. *(C)* Comparison of the effect on R^t of *C. concisus* isolates from oral or fecal source 48 h p.i. Isolates were grouped depending on source in "healthy" (strain no. K2 oral, K4 oral, M2 oral) and "diarrhea" (strain no. 112100 fecal & oral, 113332 fecal & oral, 115605 fecal & oral) as listed in table 1. (*n.s.* = not significant; *$P<0.05$; *** $P<0.001$).
doi:10.1371/journal.pone.0023858.g001

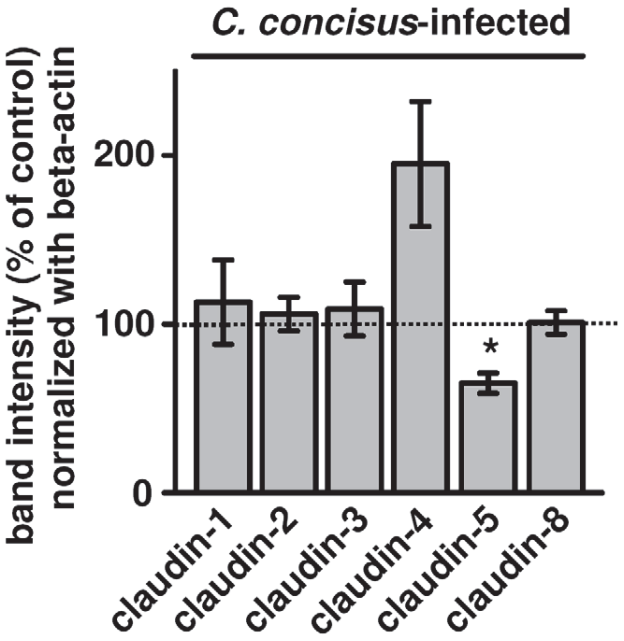

Figure 2. Effects on tight junction proteins. Western blot analysis on the expression of tight junction proteins in HT-29/B6 cells 48 h after infection with *C. concisus*. Densitometry on claudin-1 to -4 and -8 showed no significant difference to control values. Solely claudin-5 expression was reduced with **P*<0.05; each n = 9. HT-29/B6 cells were infected with either oral or fecal strains *C. concisus* K2 oral, K4 oral, M2 oral, 75775 fecal, 86120 fecal, 118452 fecal, 119100 fecal, 1718 fecal or ATCC 33237.
doi:10.1371/journal.pone.0023858.g002

control values (*P*<0.01, *C. concisus* vs. *C. jejuni*, n = 4), while the apoptotic ratio was equal between *C. concisus*- and *C. jejuni*-infected cells (4.6±0.3%, *n.s.* vs. *C. concisus*, n = 4). Fecal and oral strains did not differ in their ability to induce apoptosis in HT-29/B6 cells with 4.8±1.4% by oral strains vs. 4.7±0.5% apoptosis by fecal strains (*n.s.*, n = 5; Figure 4*D*). Pre-treatment with the apoptosis inhibitor Z-VAD showed a reduced loss of R^t in *C. concisus*-infected cells (at 48 h, *C. concisus* 112100 fecal & oral; without Z-VAD 63.5±1.5% vs. with Z-VAD 86.7±2.9% of initial resistance, *P*<0.001; n = 8; Figure 4*E*). Moreover, when we prolonged the incubation time to 72 h, we detected *C. concisus* next to or in epithelial lesions with restitutional purse-string formation in confocal laser-scanning micrographs (Figure 5 and Figure S1). Also, patchy distributed apoptotic areas with TJ changes were found beside largely unaffected areas in each monolayer (Figure 6). As an example it is shown in Figure 6 that claudins of infected monolayers were not clearly redistributed towards intracellular compartments.

Discussion

As a main finding, we demonstrated that *C. concisus* was able to induce barrier dysfunction in confluent HT-29/B6 cells from apical but even more from the basolateral compartment. Although controversially discussed [9], [11], also oral *C. concisus* strains, even from healthy carriers, had the ability to impair epithelial barrier function. Man and coworkers demonstrated the polar flagellum of *C. concisus* to be involved in attachment and invasion of Caco-2-cells [11]. We found similar invasion abilities for our *C. concisus* strains in HT-29/B6 as well as Caco-2-cells (data not shown). Recently, it was also reported that *C. concisus* translocated across the Caco-2 monolayers and suggested that the concomitant increase in permeability for 44 kDa horseradish peroxidase (HRP) 6 h postinfection was through a paracellular pathway [11]. In contrast to this, Söderholm and coworkers reported that HRP fluxes through the epithelium were due to a transcytotic pathway via HRP-containing endosomes [14], at least in intact epithelial layers. Therefore it might be that *Campylobacter* invasion is rather correlated with the transcytosis ratio (macropinocytosis) and not with a paracellular disruption, but perhaps a spatial TJ redistribution is accelerated by this process. However, the causal link between the barrier dysfunction of *C. concisus*-infected cells and a pathomechanism via the paracellular pathway by apoptosis induction and/or TJ affection (= leak-flux dysfunction) is supported by our data. We investigated the protein expression of barrier-forming claudins. The claudin protein family is most important for epithelial barrier function even though not all claudins have sealing properties. We did only find a weak influence on claudin-4 and -5 and no effect on claudin-1 to -3, -8, occludin

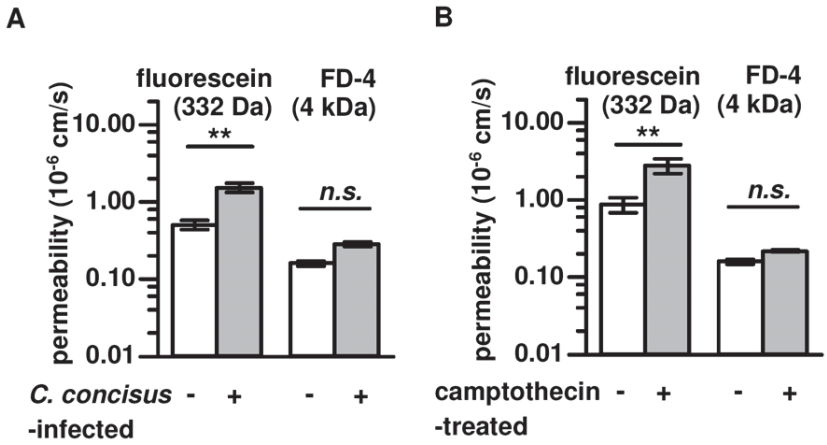

Figure 3. Epithelial permeability. Paracellular permeability was characterized by determining 332 Da fluorescein or 4 kDa FITC-dextran (FD-4) fluxes through (***A***) *C. concisus*-infected 48 h p.i. or (***B***) 48 h camptothecin-treated HT-29/B6 monolayers in Ussing chamber experiments (Student's *t*-test with **P*<0.05, ***P*<0.01;****P*<0.001; each n = 4). Infection with pooled *C. concisus* strains (oral & fecal) vs. untreated control monolayers were performed.
doi:10.1371/journal.pone.0023858.g003

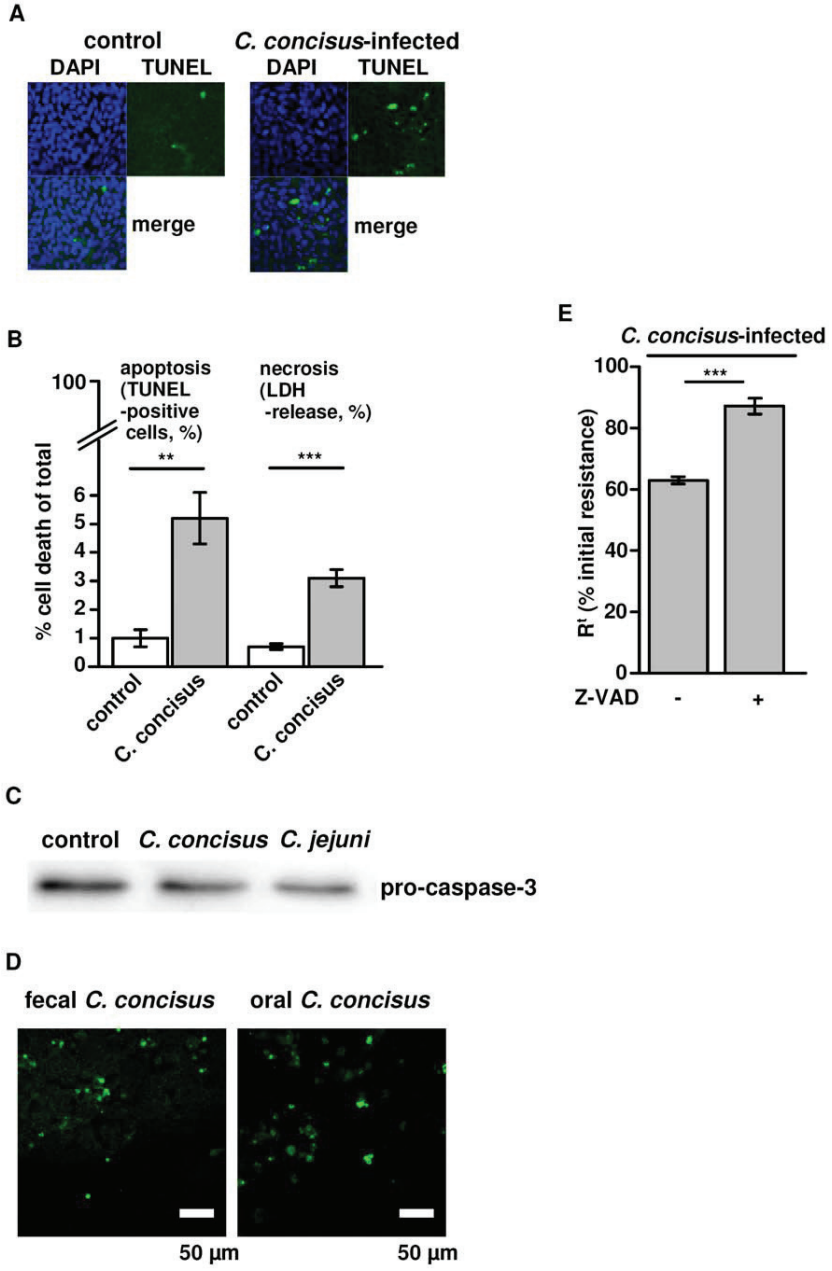

Figure 4. Effects of *C. concisus* on epithelial apoptosis. *(A)* Apoptotic effects of *C. concisus* on confluent HT-29/B6 cells visualized with TUNEL staining and fluorescence microscopy 48 h after infection, the number of cell rosette formations was increased, condensed or fragmentized nuclei were visible, and a more generalized loss of cells was observed. *(B)* After 48 h of incubation with *C.concisus* TUNEL staining of confluent HT-29/B6 monolayers revealed an increase in the number of apoptotic cells and LDH release was measured as a sign of necrosis induction (Student's *t*-test with $^{**}P<0.01$; $^{***}P<0.001$; each n = 5). *(C)* Increased apoptosis was indicated by caspase-3 activation 48 h after infection. Band intensity of pro-caspase-3 (35 kDa) was significantly diminished ($P<0.05$, n = 7). *C. jejuni* ATCC 33560 served as positive control. *(D)* After 48 h of incubation with *C. concisus* from oral or fecal source apoptotic cell number was equal in TUNEL staining of confluent HT-29/B6 monolayers (*n.s.*, n = 5). *(E)* For verification of *C. concisus*-induced apoptosis effects on barrier function, HT-29/B6 monoalyers were pre-treated with 50 µM Z-VAD (N-benzyloxycarbonyl-Val-Ala-Asp-fluoromethyl-ketone), a caspase inhibitor that completely blocks caspase-mediated cell death. Transepithelial resistance was partially although not completely reconstituted by Z-VAD. Isolates were grouped depending on source in "oral" and "fecal" as listed in table 1.
doi:10.1371/journal.pone.0023858.g004

or ZO-1. This is contrary to other enteric pathogens with a stronger impact on TJs, e.g. enteropathogenic *Escherichia coli* or *Arcobacter butzleri* [12]. Our results did not display an overall alteration of the TJ. The only reduction in the sealing TJ protein claudin-5 was rather weak, thus it seems likely that the TJ is functionally only moderately affected. However, infected epithelial cells were destroyed, as demonstrated by a release of LDH and an increase in apoptotic events. The most important result of our study was that both, oral and fecal strains induced apoptotic leaks leading to an increase in epithelial permeability to fluorescein. Pre-treatment with the apoptosis inhibitor Z-VAD showed a reduced loss of R^t over 48 h and confirms the impact of *C. concisus*-induced

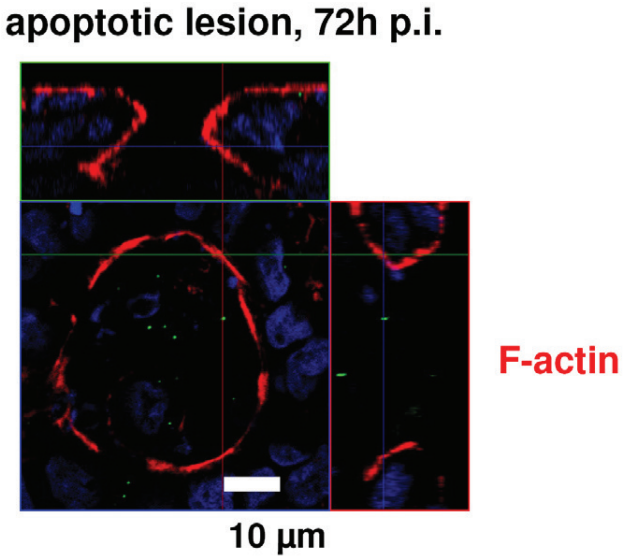

Figure 5. Apoptotic leaks. Confocal laser-scanning microscopy (*Z*-axis scans, *XY* plane) of an apoptotic lesion in HT-29/B6 monolayers infected with *C. concisus*. Cytoskeletal F-actin is marked red by Phalloidin-Alexa-Fluor[594], the blue staining with DAPI (=4′-6-diamidino-2-phenylindole dihydrochloride) marks the nuclei of epithelial cells and *C. concisus* is marked green by anti-*Campylobacter* antibody. Details are presented in Figure S1. In controls, superficial single cell lesions were closed within 16 min, accompanied by formation of an actin ring (''*purse-string*'') that is essential for restitution. Recovery of apoptotic lesions, induced by *C. concisus*, seems unaffected as the purse-string actin formation is clearly visible.
doi:10.1371/journal.pone.0023858.g005

apoptosis on barrier function. Interestingly, a similar experiment with *A. butzleri*, which shows more impact on the TJ and also an effect on apoptosis, results in a partial reconstitution of *A. butzleri*–induced barrier dysfunction by inhibition of apoptosis with Z-VAD. This enabled us to distinguish the barrier impairment caused by TJ disruption from apoptotic influences [12]. The comparison of tracer fluxes in *C. concisus*- or camptothecin-exposed monolayers revealed an increase in 332 Da fluorescein permeability but no difference for 4 kDa dextran in the same time period with both treatments, suggesting that apoptosis induction could be the main cause of *C. concisus*-induced barrier dysfunction. This result correlates to previous results of our group that revealed increased permeability in apoptotic monolayers to the same characteristic molecule size cut-off at 4 kDa. In these experiments camptothecin-induced apoptosis in HT-29/B6 monolayers showed also an increased permeability towards intermediate molecule size of 344 Da (H^3-lactulose) and no change for 4 kDa tracer molecules (H^3-polyethylene glycol) [13]. Thus, the apoptosis induction by *C. concisus* seems to be the prominent feature of infection. The induction of epithelial cell death could be caspase-dependent but also caspase-independent as already shown for *C. jejuni* [15]. As shown for the hemolytic toxin aerolysin from *Aeromonas hydrophila*, the pore-forming activity of aerolysin interferes with restitutional purse-string formation [16] of small epithelial lesions via MLCK-dependent actomyosin constriction [17]. However, this rapid inhibitory consequence on epithelial recovery was not the case with *C. concisus*. Here, purse-string formation was still visible even 72 h p.i. The hemolytic activity of *C. concisus* is low, compared to typical hemolytic bacteria, but all *C. concisus* strains used in our study showed some hemolytic activity (data not shown), measured by the contact hemolysin assay [7].

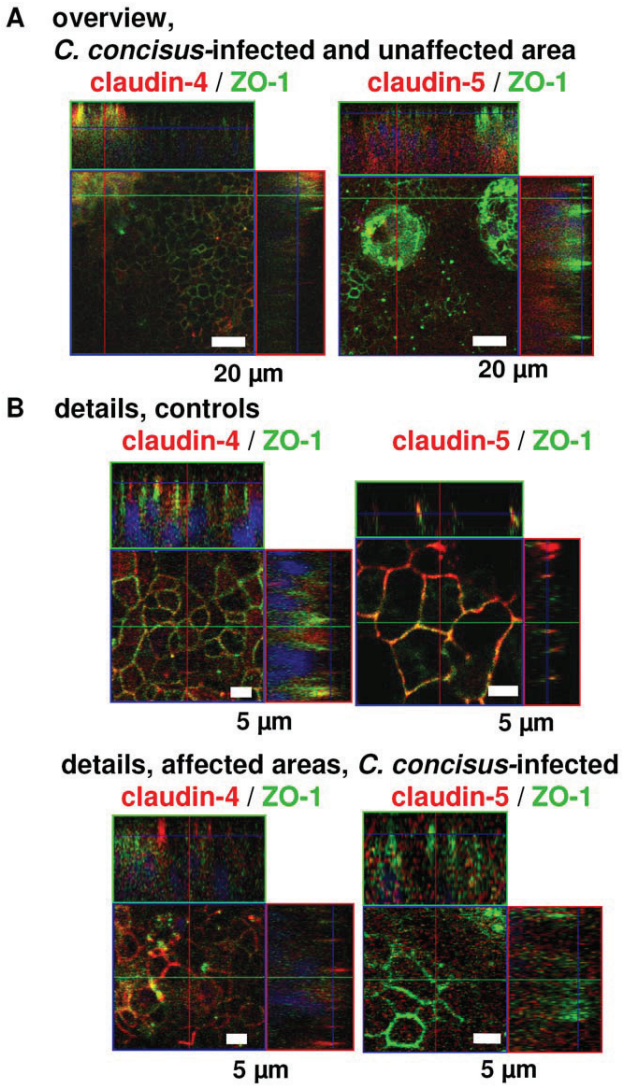

Figure 6. Apoptosis and tight junctions. Confocal laser-scanning microscopy of HT-29/B6 monolayers revealed patchy distributed areas with tight junction changes and apoptotic events as well as largely unaffected areas in *(A)* overviews with low magnification and *(B)* details with higher magnifcation. Immunostaining with green signal for ZO-1; and claudin-4 and -5 marked red; merge appears yellow. Nuclei are stained blue with DAPI.
doi:10.1371/journal.pone.0023858.g006

Our findings suggest *C. concisus* as an enteric pathogen, characterized by defined spatial interactions with human epithelial cells. We demonstrate that both oral and fecal *C. concisus* strains induce impairment of the intestinal barrier function. The epithelial necrosis and apoptosis induction are mechanisms that can contribute to a leak-flux type of diarrhea. Also, this leads to a higher amount of antigens passing the mucosa that can accelerate inflammatory processes. Campylobacteriosis is a well-known zoonosis, mostly caused by *C. jejuni* through contaminated food. In our study eight patients with diarrhea had *C. concisus* in their feces, whereas three healthy individuals had *C. concisus* only in saliva samples. Investigations on biofilm formation in the oral cavity and on the ecological niche of *C. concisus* would be worthwhile also for research on the route of transmission (oral-oral and/or fecal-oral). Humans might be the main reservoir for *C.*

concisus infection, as known from *Helicobacter pylori* infection. There is a need for extensive investigation of veterinary samples in search for possible additional reservoirs of *C. concisus*. Furthermore, there is an urgent need for clinical data with a proper follow-up period to ascertain, if this emerging pathogen is an etiologic factor in the development of chronic diarrhea or inflammatory bowel diseases as recently proposed for *Salmonella* or *Campylobacter* enteritis [18].

Materials and Methods

Isolation and growth condition of *C. concisus*

Six oral and eight fecal strains of *C. concisus* were selected for the study. Fecal strains were sampled from eight patients with diarrhea (age 2–63 years). Three of the patients were also asked to deliver saliva samples from which *C. concisus* was cultivated. The remaining three oral strains were cultivated from saliva samples of three healthy individuals (age 25–31 years) who had no *C. concisus* in their fecal samples and no history of gastrointestinal disease (Table 1). This study adhered to the Declaration of Helsinki, and ethics approval for research was obtained from The Ethics Committee for Region Nordjylland, Denmark (Den Videnskabsetiske Komité for Region Nordjylland; N-20080056). All patients who participated in the investigation signed written informed consent forms. For children written informed consent forms were signed by their parents. All strains were analyzed at the Department of Clinical Microbiology, Aalborg Hospital, Aarhus University Hospital, Denmark. *C. concisus* was isolated by the filter technique on 5% horse blood agar plates, containing 1% yeast extract (SSI Diagnostica, Hillerød, Denmark), and incubated at 37°C in a microaerobic atmosphere with 3% hydrogen [19]. Final confirmation was obtained through a species-specific real-time PCR based on the cpn60 gene, as described elsewhere [20]. No other pathogen was isolated in the patients' fecal samples. All strains were stored in nutrient beef broth with 10% glycerin (SSI Diagnostica) at −80°C until use. Prior to experimental infection of epithelial cell cultures, bacteria were grown on 5% horse blood agar plates, containing 1% yeast extract (SSI Diagnostica) at 37°C in microaerobic atmosphere with 3% hydrogen for 48 h. Then bacteria cells were transfered to liquid culture medium RPMI 1640 (PAA Laboratories, Pasching, Austria) and cultured again for 48 h to log-phase. Bacterial density was counted microscopically and adjusted to a choosen multiplicity of infection (MOI). The *C. concisus* reference strain ATCC 33237 from human gingival sulcus was cultured in the same way.

Epithelial cell culture

HT-29/B6 cells represent an established cell model for studies on bacterial infection [12], [17], [21]. HT-29/B6 cells were established and described by Kreusel et al. in 1991, as a stable and highly differentiated subclone derived from wild-type HT-29 cells by glucose deprivation [22]. The cells were cultured in RPMI cell culture medium (RPMI 1640, PAA Laboratories, Pasching, Austria) as described previously [22]. Cells were grown to confluence on polycarbonate filter supports (Millicell-PCF^{TM}, effective membrane area 0.6 cm^2, pore size 3 μm, Millipore, Billerica, MA., USA), and formed high-ohmic epithelial monolayers with a transepithelial electrical resistance (R^t) between 500 and 800 Ohm·cm^2 eight days after seeding. In parallel to the infection with all *C. concisus* strains, three types of controls were performed: (i) without adding bacteria, (ii) with addition of heat-inactivated *C. concisus* or *C. concisus* lysates (60 min at 75°C) and (iii) with *Escherichia coli* K12.

Electrophysiological studies

In order to investigate the effect of the oral and fecal *C. concisus* strains on epithelial integrity, R^t of polarized HT-29/B6 monolayers was measured after infection with chopstick electrodes (Word Precision Instruments, Sarasota, FL., USA) combined with an ohmmeter (manufactured by D. Sorgenfrei at the Institute of Clinical Physiology, Charité, Berlin) in the cell culture dish under sterile conditions at 37°C. Bacteria were added to the apical compartment of confluent HT-29/B6 cell monolayers to yield an initial concentration of 2×10^7 cfu/ml equaling a MOI of 20. Infected HT-29/B6 cell monolayers were mounted into modified Ussing-type chambers (manufactured by the Institute of Clinical Physiology, Charité, Berlin) [22] after 48 h. Short circuit current (Isc) and R^t were determined by using a computerized automatic clamp device (Fiebig Hard & Software, Berlin, Germany). Infections were done in an atmosphere with 5% CO_2 in ambient air in favor for the HT-29/B6 cell line. For an additional assay concerning dose-dependent effects, monolayers were apically or basolaterally infected with *C. concisus* at MOIs between 10 and 100.

Table 1. Proband data at time of *Campylobacter concisus* isolation.

Age	Sex	Clinical characteristic	Source	Isolate no.
25	Female	Healthy	oral	K2
31	Female	Healthy	oral	K4
26	Male	Healthy	oral	M2
29	Male	Crohn's disease	fecal	75775
60	Male	Diarrhea	fecal	86120
19	Female	Crohn's disease	fecal	118452
63	Female	Collagenous colitis	fecal	119100
2	Female	Bloody diarrhea	fecal	1718
36	Female	Crohn's disease	fecal & oral	112100
57	Female	Diarrhea	fecal & oral	113332
42	Male	Diarrhea	fecal & oral	115605

doi:10.1371/journal.pone.0023858.t001

Epithelial permeability

Unidirectional tracer flux studies were performed from the apical to the basolateral compartment under short-circuit conditions in Ussing chambers with fluorescein (332 Da) and fluorescein isothiocyanate-labeled 4 kDa dextran (FD-4) (Sigma, St. Louis, MO., USA) according to previous described protocols [23], [24]. Medium in the basolateral compartment was initially free of dyes. At specific intervals, medium was withdrawn from the basolateral chamber and fluorescence was measured in a spectrophotometer (Tecan Infinite M200, Durham, NC., USA). Permeability was calculated from flux over concentration difference. Camptothecin-treated monolayers were also investigated by tracer flux measurements, in order to quantify barrier disturbance by apoptosis induction.

Western blot analysis

TJs play a key role in epithelial integrity and may be affected during infection. We investigated the TJ protein expression of barrier-forming claudins after infection with *C. concisus*. Western blot analysis TJ proteins were quantified by densitometry. Immunoblots were performed and analyzed as described elsewhere [25]. Detergent-soluble protein fractions were prepared from infected monolayers. The following antibodies were used: anti-ZO-1, anti-occludin (1:2000; Zymed, San Francisco, CA., USA), anti–claudin-1–5 and -8 (1:1000; Zymed), anti–β-actin

(1:5000; Sigma), and anti–caspase-3 (1:1000; Cell Signaling Technology, Beverly, MA., USA).

Immunofluorescence microscopy

To test for the integrity of the TJ meshwork, TJ proteins ZO-1, occludin, claudin-1 to 5 and claudin-8 were visualized using confocal laser-scanning microscopy (Zeiss LSM510, Jena, Germany), analyzed by Carl Zeiss LSM Image Examiner software according to prior descriptions [25]. For detection, antibodies raised against TJ proteins (1:50; Zymed) or *Campylobacter* (Santa Cruz Biotechnology Inc, Santa Cruz, CA. USA) were used. For cytoskeletal F-actin, staining with Phalloidin-Alexa-Fluor^{594} (Sigma) was performed.

Cytotoxicity. LDH release assay

Lactate dehydrogenase (LDH) release from HT-29/B6 cells was measured according to the method of Madara and Stafford [26]. ***TUNEL staining*** was performed according to manufacturer's protocol (In-situ Cell Death Detection Kit, Roche, Mannheim, Germany). Stained apoptoses were counted microsopically. We investigated the properties of oral and fecal *C. concisus* isolates in apoptosis induction by TUNEL staining and Western blotting on caspase-3 activation.

Invasion assay

Bacteria were harvested from agarplates (5% horse blood agar +1% yeast extract; SSI Diagnostica) after 48 h and equally diluted in 3 ml RPMI-media, vortexed, and incubated another 48 h in a 37°C microaerobic atmosphere with 3% hydrogen. Monolayers were infected from the apical side with a MOI of 10 and treated (i) with gentamicin (100 µg/ml) prior to infection, (ii) with gentamicin after 2 hours of incubation, or (iii) without gentamicin. Bacterial supernatants were proven for bacterial count. The monolayers were then washed three times with PBS and flooded with 300 µl 0.5% Triton-X 100. *C. jejuni* ATCC 33560 was used as positive control.

Quantitative Realtime-PCR

Total RNA was obtained from HT-29/B6 cells by phenol-chloroform extraction and complementary DNA (cDNA) was synthesized by reverse-transcription PCR with High-Capacity cDNA Archive Kit (Applied Biosystems, Mannheim, Germany) with random primers. Real-time PCR was performed according to manufacturer's instructions with an ABI-7900HT PCR device using the TaqMan Gene Expression Assay (no. Hs00533949_s1; claudin-5) with FAM dye-labeled primers. Glyceraldehyde 3-phosphate dehydrogenase cDNA was quantified using VIC reporter dyes as endogenous control (all Applied Biosystems). Differential expression was calculated according to the $2^{-\Delta\Delta CT}$ method [27].

Statistical analysis

Data are expressed as means ± standard error of the mean (SEM). Statistical analysis was performed using the Student *t*-test. $P<0.05$ was considered significant.

Supporting Information

Figure S1 Apoptotic leaks. 360° view of the confocal laser-scanning micrograph of an apoptotic lesion in HT-29/B6 monolayers infected with *C. concisus*, based on Figure 5 (Z-axis scans, XY plane). Cytoskeletal F-actin is marked red by Phalloidin-Alexa-Fluor^{594}, the blue staining with DAPI (= 4′-6-diamidino-2-phenylindole dihydrochloride) marks the nuclei of epithelial cells and *C. concisus* is marked green by anti-*Campylobacter* antibody. In controls, superficial single cell lesions were closed within 16 min, accompanied by formation of an actin ring ("*purse-string*") that is essential for restitution. Recovery of apoptotic lesions, induced by *C. concisus*, seems unaffected as the purse-string actin formation is clearly visible.
(MPG)

Acknowledgments

The excellent technical assistance of In-Fah Lee, Claudia May, Detlef Sorgenfrei and Anja Fromm is gratefully acknowledged.

Author Contributions

Conceived and designed the experiments: RB J-DS HLN HN. Performed the experiments: HLN RB. Analyzed the data: RB HLN NAH DG J-DS MF. Contributed reagents/materials/analysis tools: HLN HN MF RB TE JE MZ. Wrote the paper: HLN RB.

References

1. Newell DG (2005) *Campylobacter concisus*: an emerging pathogen? Eur J Gastroenterol Hepatol 17(10): 1013–1014.
2. Chaban B, Ngeleka M, Hill JE (2010) Detection and quantification of 14 *Campylobacter* species in pet dogs reveals an increase in species richness in feces of diarrheic animals. BMC Microbiol 10: 73.
3. Zhang L, Budiman V, Day AS, Mitchell H, Lemberg DA, et al. (2010) Isolation and detection of *Campylobacter concisus* from saliva of healthy individuals and patients with inflammatory bowel disease. J Clin Microbiol 48(8): 2965–2967.
4. Aabenhus R, Permin H, On SL, Andersen LP (2002) Prevalence of *Campylobacter concisus* in diarrhoea of immunocompromised patients. Scand J Infect Dis 34(4): 248–252.
5. Lastovica AJ (2009) Clinical relevance of *Campylobacter concisus* isolated from pediatric patients. J Clin Microbiol 47(7): 2360.
6. Aabenhus R, Stenram U, Andersen LP, Permin H, Ljungh A (2008) First attempt to produce experimental *Campylobacter concisus* infection in mice. World J Gastroenterol 14(45): 6954–6959.
7. Istivan TS, Coloe PJ, Fry BN, Ward P, Smith SC (2004) Characterization of a haemolytic phospholipase A(2) activity in clinical isolates of *Campylobacter concisus*. J Med Microbiol 53(Pt 6): 483–493.
8. Kaakoush NO, Man SM, Lamb S, Raftery MJ, Wilkins MR, et al. (2010) The secretome of *Campylobacter concisus*. FEBS J 277(7): 1606–1617.
9. Kalischuk LD, Inglis GD (2011) Comparative genotypic and pathogenic examination of *Campylobacter concisus* isolates from diarrheic and non-diarrheic humans. BMC Microbiol 11: 53.
10. Engberg J, Bang DD, Aabenhus R, Aarestrup FM, Fussing V, et al. (2005) *Campylobacter concisus*: an evaluation of certain phenotypic and genotypic characteristics. Clin Microbiol Infect 11(4): 288–295.
11. Man SM, Kaakoush NO, Leach ST, Nahidi L, Lu HK, et al. (2010) Host Attachment, Invasion, and Stimulation of Proinflammatory Cytokines by *Campylobacter concisus* and Other Non-*Campylobacter jejuni Campylobacter* Species. J Infect Dis 202(12): 1855–1865.
12. Bücker R, Troeger H, Kleer J, Fromm M, Schulzke JD (2009) *Arcobacter butzleri* induces barrier dysfunction in intestinal HT-29/B6 cells. J Infect Dis 200(5): 756–764.
13. Bojarski C, Gitter AH, Bendfeldt K, Mankertz J, Schmitz H, et al. (2001) Permeability of human HT-29/B6 colonic epithelium as a function of apoptosis. J Physiol 535(Pt 2): 541–552.
14. Soderholm JD, Streutker C, Yang PC, Paterson C, Singh PK, et al. (2004) Increased epithelial uptake of protein antigens in the ileum of Crohn's disease mediated by tumour necrosis factor alpha. Gut 53(12): 1817–1824.
15. Kalischuk LD, Inglis GD, Buret AG (2007) Strain-dependent induction of epithelial cell oncosis by *Campylobacter jejuni* is correlated with invasion ability and is independent of cytolethal distending toxin. Microbiology 153(Pt 9): 2952–2963.
16. Florian P, Schöneberg T, Schulzke JD, Fromm M, Gitter AH (2002) Single-cell epithelial de-fects close rapidly by an actinomyosin purse string mechanism with functional tight junctions. J Physiol 545(Pt 2): 485–499.
17. Bücker R, Krug SM, Rosenthal R, Günzel D, Fromm A, et al. (2011) Aerolysin from *Aeromonas hydrophila* perturbs tight junction integrity and cell lesion repair in intestinal epithelial HT-29/B6 cells. J Infect Dis. In Press.
18. Gradel KO, Nielsen HL, Schonheyder HC, Ejlertsen T, Kristensen B, et al. (2009) Increased short- and long-term risk of inflammatory bowel disease after salmonella or campylobacter gastroenteritis. Gastroenterology 137(2): 495–501.

19. Engberg J, On SL, Harrington CS, Gerner-Smidt P (2000) Prevalence of *Campylobacter*, *Arcobacter*, *Helicobacter*, and *Sutterella* spp. in human fecal samples as estimated by a reevaluation of isolation methods for Campylobacters. J Clin Microbiol 38(1): 286–291.
20. Chaban B, Musil KM, Himsworth CG, Hill JE (2009) Development of cpn60-based real-time quantitative PCR assays for the detection of 14 *Campylobacter* species and application to screening of canine fecal samples. Appl Environ Microbiol 75(10): 3055–3061.
21. Troeger H, Richter JF, Beutin L, Günzel D, Dobrindt U, et al. (2007) *Escherichia coli* alpha-haemolysin induces focal leaks in colonic epithelium: a novel mechanism of bacterial translocation. Cell Microbiol 9(10): 2530–2540.
22. Kreusel KM, Fromm M, Schulzke JD, Hegel U (1991) Cl- secretion in epithelial monolayers of mucus-forming human colon cells (HT-29/B6). Am J Physiol 261(4 Pt 1): C574–C582.
23. Epple HJ, Kreusel KM, Hanski C, Schulzke JD, Riecken EO, et al. (1997) Differential stimulation of intestinal mucin secretion by cholera toxin and carbachol. Pflugers Arch 433(5): 638–647.
24. Schulzke JD, Fromm M, Bentzel CJ, Zeitz M, Menge H, et al. (1992) Ion transport in the experimental short bowel syndrome of the rat. Gastroenterology 102(2): 497–504.
25. Amasheh S, Schmidt T, Mahn M, Florian P, Mankertz J, et al. (2005) Contribution of claudin-5 to barrier properties in tight junctions of epithelial cells. Cell Tissue Res 321(1): 89–96.
26. Madara JL, Stafford J (1989) Interferon-gamma directly affects barrier function of cultured intestinal epithelial monolayers. J Clin Invest 83: 724–727.
27. Livak KJ, Schmittgen TD (2001) Analysis of relative gene expression datausing real-time quantitative PCR and the $2(-\Delta\Delta C(T))$ method. Methods 25: 402–408.

2.2 Porenbildende Toxine der Enterobacteriaceae

Während die Bakterien aus der *Campylobacteraceae*-Familie im Thementeil 2.1 durch direkten Kontakt mit dem Epithel (Adhärenz und Invasivität) ihre Pathogenität entfalten, fokussieren sich die Arbeiten im Thementeil 2.2 auf sezernierte bakterielle Toxine, die Hämolysine aus der *Enterobacteriaceae*-Familie, wobei die pathologischen Veränderungen am Epithel hierbei hauptsächlich auf die Toxinwirkung zurückzuführen sind.

2.2.1 Aerolysin, ein bakterielles porenbildendes Hämolysin

Die Auswirkung von Hämolysinen wird standardmäßig an Erythrozyten zur Bestimmung der hämolytischen Aktivität bzw. auf Blutagarplatten getestet, woher sich ihr Name ableitet. Die Wirkungsweise dieser Toxine, die zu den porenbildenden Toxinen (pore-forming toxins = PFTs) zählen, auf Zielzellen im Darm, wo Hämolysin-tragende Bakterien vermehrt zu finden sind, blieb längere Zeit eher unbeachtet. Der Einfluss von *Aeromonas hydrophila* und des von ihm sezernierten PFTs Aerolysin auf die epitheliale Barriere sowie die zugrunde liegenden Signalwege wurde am HT-29/B6-Zellmodell analysiert. Hiermit beschäftigt sich die folgende Veröffentlichung: Bücker et al., „Aerolysin from *Aeromonas hydrophila* perturbs tight junction integrity and cell lesion repair in intestinal epithelial HT-29/B6 cells“, erschienen im *Journal of Infectious Diseases* im Jahr 2011. Bei der durch das darmpathogene Bakterium *A. hydrophila* an der intestinalen Epithelzelllinie HT-29/B6 hervorgerufenen Störung konnte ebenfalls ein Leckflux-Mechanismus als zentraler Pathomechanismus beleuchtet werden, der auf eine Calcium-abhängige Aktivierung der Myosin-Light Chain Kinase (MLCK) zurückzuführen war. Durch die Aerolysin-Wirkung wurden durch eine zytoskeletale Aktin-Myosin-Kontraktion im HT-29/B6-Zellmonolayer *Tight Junction*-Proteine aus der Zellmembran mobilisiert und somit eine Undichtigkeit des gesamten Epithels hervorgerufen (Bücker et al., 2011). Hierbei kam auch erstmals die Zwei-Wege-Impedanzspektroskopie bei Untersuchungen zum Einfluss von Infektionserregern zum Einsatz (Krug et al., 2009b). Die dargestellte Messtechnik ermöglicht eine Unterscheidung zwischen trans- und parazellulärem Anteil der Barrierestörung. Auf diese Weise konnte eine direkte Zuordnung des Effekts des porenbildenden Aerolysins zum parazellulären Weg aufgezeigt werden. Es konnte gezeigt werden, dass durch die Aerolysin-Porenbildung während der *Aeromonas*-Infektion die epitheliale Integrität durch eine *Tight Junction*-Umverteilung ausgelöst wird, was auch eine Störung des schnellen Wundverschluß kleiner Läsionen zur Folge hat. Die Diarrhö durch *Aeromonas* konnte mehreren Mechanismen zugeordnet werden, die hauptsächlich auf der Toxinwirkung beruhen. Zum Einen konnte eine transzelluläre Sekretion gezeigt werden, wie sie zuvor auch schon beschrieben wurde (Epple et al., 2004), und zum Anderen wurde eine parazelluläre Störung, der Leckflux durch Umverteilung der *Tight Junction*-Proteine als Pathomechanismus, identifiziert.

MAJOR ARTICLE

Aerolysin From *Aeromonas hydrophila* Perturbs Tight Junction Integrity and Cell Lesion Repair in Intestinal Epithelial HT-29/B6 Cells

Roland Bücker,[1,2] Susanne M. Krug,[3] Rita Rosenthal,[3] Dorothee Günzel,[3] Anja Fromm,[3] Martin Zeitz,[1] Trinad Chakraborty,[4] Michael Fromm,[3] Hans-Jörg Epple,[1] and Jörg-Dieter Schulzke[1,2]

[1]Department of Gastroenterology, Infectious Diseases, and Rheumotology, [2]Division of Nutritional Medicine, and [3]Institute of Clinical Physiology, Charité Berlin; and [4]Department of Medical Microbiology, Justus-Liebig University, Giessen, Germany

Background. Aeromonads cause a variety of infections, including gastroenteritis, sepsis, and wound necrosis. Pathogenesis of *Aeromonas hydrophila* and its hemolysin has been characterized, but the mechanism of the epithelial barrier dysfunction is currently poorly understood.

Methods. Human colon epithelial monolayers HT-29/B6 were apically inoculated with clinical isolates of *A. hydrophila* or with the secreted pore-forming toxin aerolysin. Epithelial resistance and permeability for several markers were determined in Ussing chambers, using 2-path impedance spectroscopy. The subcellular distribution of tight junction (TJ) and cytoskeleton proteins was analyzed by Western blotting and confocal laser-scanning microscopy.

Results. *A. hydrophila* infection induces chloride secretion with a small decrease in transcellular resistance. However, the major effect of *A. hydrophila,* mediated by its toxin aerolysin, was a sustained reduction of paracellular resistance by retracting sealing TJ proteins from the TJ strands. Aerolysin-treated monolayers showed increased paracellular permeability to FITC-dextran-4000 (0.104 ± 0.014 vs 0.047 ± 0.001 10^{-6} cm/s in control; $P < .05$). Moreover, restitution of epithelial lesions was impaired. The effects were myosin light chain kinase (MLCK) dependent and mediated by intracellular Ca^{2+} signaling.

Conclusions. During *Aeromonas* infection, pore formation by aerolysin impairs epithelial integrity by promoting TJ protein redistribution and consequently affecting wound closure. Thus, *Aeromonas*-induced diarrhea is mediated by 2 mechanisms, transcellular secretion and paracellular leak flux.

The gamma-proteobacteriacea *Aeromonas* spp. are widely distributed and can be isolated from soil, fresh water, and seawater [1]. Aeromonads are food- and water-borne bacteria and are considered to be zoonotic human pathogens that can cause severe diarrhea, dysentery, and bacteremia [2, 3]. In human and veterinary medicine, strains of *Aeromonas* are mostly isolated from stool, wounds, and aborts [4]. The main route of transmission for *Aeromonas* gastroenteritis is considered to be fecal–oral. Studies on the etiology of travelers' diarrhea revealed *Aeromonas* to have a prevalence of about 3% in diarrheic patients returning from Asia and Africa [5]. Among other clinically relevant aeromonads like *Aeromonas caviae*, *A. trota*, and *A. veronii* biovar sobria, the most frequently isolated pathogen *A. hydrophila* is mainly associated with diarrheal illness accompanied by abdominal pain and nausea, but *A. hydrophila* also plays a significant role in wound infection with necrotization. Moreover, there are reports of fatal sequelae, including septicemia and myonecrosis [6].

Aeromonads harbor a variety of virulence factors and enterotoxins like cytotoxic Act, cytotonic Alt and Ast, as well as various hemolysins (for example, aerolysin [AerA], HlyA, Ahh1, and Asa1). Aerolysin has been studied for at least 3 decades and thus is well characterized [7]. The 54-kDa pore-forming toxin (PFT) is secreted as pro-aerolysin that binds with high affinity to glycosylphosphatidylinositol (GPI)-anchored proteins

Received 20 September 2010; accepted 13 July 2011.

Correspondence: Jörg-Dieter Schulzke, MD, Medizinische Klinik für Gastroenterologie, Infektiologie und Rheumatologie, Bereich Ernährungsmedizin, Charité CC 13, Campus Benjamin Franklin, Hindenburgdamm 30, 12203 Berlin, Germany (joerg.schulzke@charite.de).

The Journal of Infectious Diseases 2011;204:1283–92

0022-1899 (print)/1537-6613 (online)/2011/2048-0018$14.00
DOI: 10.1093/infdis/jir504

on target cells to integrate into the plasma membrane [8]. The proteins build stable heptameric aerolysin complexes that form β-barrel pores [9]. In a systemic infection mouse model with aeromonads, aerolysin was found to be the main factor for lethality [10]. Aerolysin action on the epithelial barrier has been described in 2 studies. Abrami and coworkers [11] have shown in human colon carcinoma (Caco-2) cells, Madin-Darby canine kidney (MDCK) cells, and Fischer rat thyroid epithelial (FRT) cells that aerolysin decreases transepithelial resistance and increases cellular potassium efflux, indicating pore formation via the transcellular pathway. Our previous studies demonstrated that aerolysin induced active chloride secretion in human intestinal epithelia, derived from short-circuit current as well as ^{22}Na and ^{36}Cl flux measurements. This activation of electrogenic chloride secretion was accompanied by a decrease in transepithelial resistance [12]. However, there was a discrepancy between the permanent reduction in transepithelial resistance after *Aeromonas* infection or exposure to aerolysin and the rather transient secretory response.

In general, intestinal pathogens cause diarrhea by induction of active ion secretion, via malabsorptive mechanisms or by impairment of the epithelial barrier. Barrier impairment is often caused by structural changes of the epithelial tight junction (TJ) or by induction of epithelial gross lesions [13]. Both lead to passive back-leakage of water and solutes from the blood circulation to the intestinal lumen (leak flux diarrhea). Dysfunction of the TJ is characterized either by altered expression, subcellular redistribution, or degradation of TJ proteins. The barrier properties of the TJ are mainly defined by claudins, tetraspan transmembrane proteins that seal the paracellular space between adjacent cells [14, 15]. At least 8 of the 24 claudins are present in human intestinal epithelium, regulating the paracellular barrier along the gastrointestinal tract by the molecular compositions of the TJ strands. Claudins are linked to F-actin of the perijunctional cytoskeleton via cytosolic accessory proteins as zonula occludens protein-1 (ZO-1). In case of redistribution of TJ proteins, endocytosis or direct sorting of TJ proteins to the cytosolic fraction can be induced by actomyosin contraction [16].

In the present study, we characterized 2 mechanisms of aerolysin-induced epithelial barrier dysfunction, one involving disturbed TJ integrity and another leading to a defective restitution of epithelial lesions. This adds up to a dual concept for the diarrheal mechanism in *Aeromonas* infection caused by its pore-forming toxin, aerolysin.

MATERIAL AND METHODS

Epithelial Cell Culture

Human colonic HT-29/B6 cells, which represent an established cell model for studies on bacterial infection [17, 18], were cultured in Roswell Park Memorial Institute (RPMI 1640) cell culture medium (PAA Laboratories, Pasching, Austria) as described previously [19]. Cells were grown to confluence on polycarbonate filter supports (Millicell-PCF, effective membrane area 0.6 cm^2, pore size 3 μm, Millipore, Billerica, MA), and formed high-ohmic epithelia with an epithelial resistance (R^t) of ~650 Ω cm^2 8 days after seeding. Cells were shifted to serum- and antibiotic-free RPMI medium prior to infection with hemolytic bacteria. In parallel with the infection with *A. hydrophila*, 4 types of controls were performed: (1) without adding bacteria or bacterial supernatants, (2) with the aerolysin (AerA)-deficient *Aeromonas* strain AB3-5 [10], (3) with *Escherichia coli* TOP10F_pQE-40 or its lysate (vector control), and (4) after preincubation of AerA-containing preparations with zinc (500 μM $ZnCl_2$, pH 7.4).

Growth Conditions of Bacteria

Clinical isolate of *A. hydrophila* GI, from human diarrheal stool (Campus Benjamin Franklin, Berlin), reference strain *A. hydrophila* ATCC 7966, *Aeromonas* strain AH2, and its AerA-negative derivate *Aeromonas* strain AB3-5 were cultured in RPMI media overnight (o/n) at 37°C under aerobic conditions.

Supernatants and Aerolysin Preparation

Bacteria were grown in RPMI medium to log-phase, then centrifuged with 4000g for 15 minutes. Supernatants were concentrated and sterile-filtered, and the extracellular content of the bacteria released into medium was measured for hemolytic activity. All probes were adjusted to 350 hemolytic units (HU). Then, preparations were diluted and used according to the infection experiments by addition of appropriate sublytic concentrations to the apical compartment of the epithelial cell monolayers. *E. coli* TOP10F_pQE-40_AerA (aerolysin overexpressing) and its vector control were cultured in lysogeny broth (LB) medium o/n at 37°C to log phase and then harvested by centrifugation (4000g, 15 minutes). Bacteria were shifted to RPMI medium and lysed through cell wall disruption by means of hydraulic pressure (French Press, Thermo Spectronic, Cambridge, UK) to release AerA into the medium. Hemolytic activity was adjusted to 350 HU and the preparations were diluted according to *Aeromonas* supernatant preparations. Lactate dehydrogenase (LDH) release from HT-29/B6 cells was performed as a measure of cytotoxicity.

Electrophysiological Studies

HT-29/B6 cell monolayers were mounted in modified Ussing chambers as described previously [20] and apically treated with either the aeromonads (multiplicity of infection [MOI] of 10, 1, and <1) or with the supernatant/aerolysin preparations. Short-circuit current (I_{SC}) and transepithelial resistance (R^t, "TER") were determined by a computerized automatic clamp device (Fiebig Hardware & Software, Berlin, Germany).

Epithelial Permeability

Unidirectional tracer flux studies (mucosal to serosal) were performed under short-circuit conditions in Ussing chambers

with fluorescein and fluorescein-isothiocyanate (FITC)-dextran-4000 (Sigma-Aldrich, St. Louis, MO) as previously described [20]. At specific intervals, samples were taken from the basolateral chamber and fluorescence was measured in a spectrophotometer (Tecan Infinite-M200, Durham, NC). Permeability was calculated from flux over concentration difference.

Two-Path Impedance Spectroscopy

Epithelial monolayers were mounted in Ussing-type impedance chambers, bathed with Ringer's solution, and experiments were performed as published in detail elsewhere [21]. Briefly, an electric circuit model was used to describe the epithelial properties. Overall epithelial resistance (R^{epi}) consists of 2 parallel resistors: transcellular resistance (R^{trans}), representing the resistive properties of the cell membranes; and paracellular resistance (R^{para}), representing the properties of the TJ. Application of alternating currents resulted in voltage changes from which complex impedance values were calculated. For calculation of R^{trans} and R^{para}, impedance spectra and fluxes of the paracellular marker fluorescein were obtained before and after chelating extracellular cations with ethylene glycol tetraacetic acid (EGTA), which has been shown to reversibly open the TJ and to alter fluorescein flux reciprocally to R^{epi} changes [21].

Western Blot

Immunoblots were analyzed as described elsewhere [15]. Detergent-soluble protein fractions were prepared from monolayers incubated with aeromonads/AerA or controls. The following antibodies were used: anti-occludin, anti-claudin-1, -4, and -5 (Zymed, San Francisco, CA); anti–β-actin (Sigma-Aldrich, St. Louis, MO); anti–Myosin-Light-Chain (MLC)-II; and anti–MLC-II-phospho-Ser19 (Cell Signaling Technology, Beverly, MA).

Immunofluorescence Microscopy

Integrity of the TJ meshwork was visualized by confocal laser-scanning microscopy (LSM; Zeiss LSM510, Jena, Germany) of immunostained occludin, claudins, ZO-1, and E-cadherin according to previous descriptions [15]. For cytoskeletal F-actin, staining with phalloidin-Alexa-Fluor^{594} was performed.

Calcium Measurements

Confluent HT-29/B6 cells on coverslips were incubated in HEPES-buffered solution with 10^{-5} M of the Ca^{2+}-sensitive dye FURA-2-AM prior to the experiments. Intracellular calcium ($[Ca^{2+}]_i$) was measured as described previously [22].

Induction of Single-Cell Lesions

Epithelial lesions were induced by iontophoretic KCl injection with a microelectrode [23]. The time interval between 2 lesions was 180 seconds; time between the induction of the last lesion and fixation was 30 seconds. Monolayers were fixed in 4% paraformaldehyde for 15 minutes, then permeabilized with 0.5% Triton-X-100 for 7 minutes, and F-actin was stained with phalloidin-Alexa-Fluor^{594}.

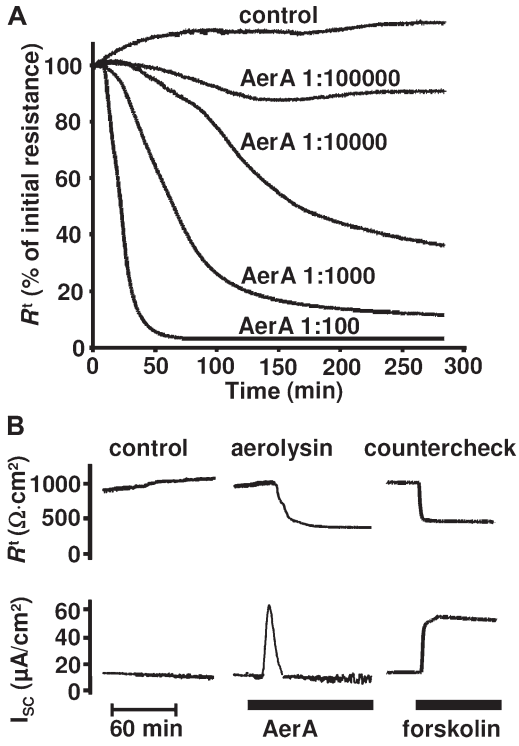

Figure 1. Effect of aerolysin (AerA) on HT-29/B6 cells. *A,* Time- and dose-dependent decrease in transepithelial resistance (R^t). *B,* Time course of R^t and short-circuit current (I_{SC}) after AerA (1:5000 dilution) or forskolin treatment in HT-29/B6 monolayers.

Statistical Analysis

Data are expressed as means ± standard error of the mean. Statistical analysis was performed using the Student *t* test, adjusted by Bonferroni-Holm correction for multiple testing. $P < .05$ was considered significant.

RESULTS

Functional Analysis of Epithelial Barrier Function During Aeromonas Infection

Polarized epithelial HT-29/B6 cells were apically treated with either (1) *A. hydrophila*, (2) supernatant from *Aeromonas* cultures, (3) AerA preparations, or (4) controls (*Aeromonas*-AB3-5 or *E. coli*). Monolayers treated with the virulent *Aeromonas* strains or with AerA showed an incremental decrease in R^t, starting after an incubation period of at least 30 minutes. In the following hours, resistance was reduced to near the baseline of empty filter supports, whereas all controls exhibited stable resistances. Experiments with different AerA concentrations also revealed a characteristic drop in R^t (Figure 1*A*), whereas in controls, the preincubation with zinc could effectively block the effects of AerA-containing preparations.

In the time course of Figure 1*B*, HT-29/B6 cells showed a rapid and permanent decrease in R^t after AerA treatment. In addition, a rapid but transient increase in I_{SC} was observed, which

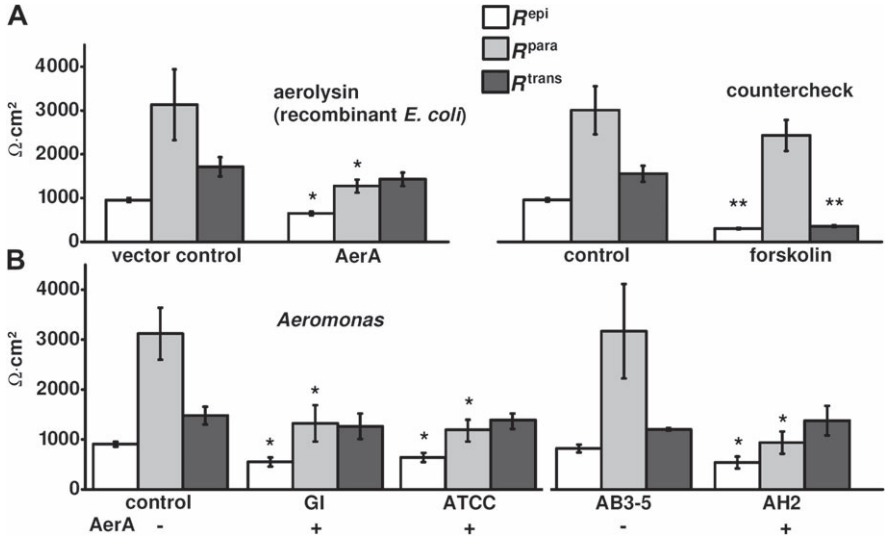

Figure 2. Two-path impedance spectroscopy for differentiation of para- and transcellular resistance changes for the effect of *A. hydrophila* and of its hemolysin AerA in HT-29/B6 monolayers. *A*, Epithelial resistance (R^{epi}) and paracellular resistance ($R^{para} \Rightarrow$ TJ) of HT-29/B6 decreased after AerA treatment, whereas the transcellular part ($R^{trans} \Rightarrow$ membrane) was not significantly affected in the measurement period. Forskolin treatment served as countercheck for induction of a transcellular effect. *B*, Supernatants in sublytic concentrations of *A. hydrophila* GI (patient isolate) and ATCC reference strain also revealed a characteristic resistance change as induced by AerA alone (1:1000 dilution, $^*P > .05$, n = 6). Negative controls were performed using *E. coli* TOP10F vector controls or the AerA-negative strain *Aeromonas*-AB3-5 compared with the AerA-containing isogenetic *Aeromonas* strain AH2. Transepithelial resistance (R^t) consists of R^{epi} (overall epithelial resistance) and R^{sub} (filter support). $1/R^{epi}$ is the summation of $1/R^{trans}$ and $1/R^{para}$.

was already characterized in more detail by our group earlier [12]. This set of experiments, however, yielded direct evidence not only that the decrease in R^t was due to the transient I_{SC} response, but also that it indicates a permanent barrier impairment. In contrast, in experiments with forskolin, a permanent I_{SC} increase by opening of chloride channels via increased cyclic adenosine monophosphate (cAMP) was accompanied by a parallel R^t decrease of identical duration. To examine whether the barrier defect on HT-29/B6 monolayers produced by *A. hydrophila* or by aerolysin was due to transcellular (eg, apical membrane channel opening) or paracellular alterations (eg, disorganization of TJs), we performed 2-path impedance spectroscopy (2PI) to distinguish R^{trans} from R^{para}. Apical treatment of HT-29/B6 monolayers with either *A. hydrophila* supernatant or with AerA led to a decrease in the overall resistance R^{epi}. This was mainly the result of paracellular effects, as R^{para} was reduced to about half of its original value (Figure 2). As a countercheck, forskolin-treated monolayers showed a clear reduction in R^{trans}, when forskolin induced a permanent opening of chloride channels (Figure 2*A*). Measurement of all AerA-harboring strains showed the same characteristic change in resistance as seen with aerolysin alone (Figure 2*B*). For further evaluation of the paracellular effects, fluxes of different paracellular markers were measured. AerA-treated monolayers exhibited 5-fold increased epithelial permeability to fluorescein (4.7 ± 0.6 vs $0.8 \pm 0.1\ 10^{-6}$ cm/s in control; $P < .01$, $n = 3$), and showed doubled permeability to FITC-dextran-4000 (0.104 ± 0.014 vs $0.047 \pm 0.001\ 10^{-6}$ cm/s in control; $P < .05$, $n = 3$; Figure 3). To examine whether cell death is involved in the barrier impairment, we tested for cytotoxicity. Within the first hours after treatment of HT-29/B6 cells with the AerA-containing preparations, we found no cytotoxic effects. LDH release was $0.7\% \pm 0.1\%$ of total LDH (1:100 AerA dilution, 3 hours, n = 5) with no difference to control values ($0.7\% \pm 0.05\%$). Moreover, no morphological changes or cytotoxic effects, such as cell swelling, vacuolation, or any signs of cell death, were observed after *Aeromonas* infection. Thus, the decrease in resistance is pronounced, permanent, and not due to

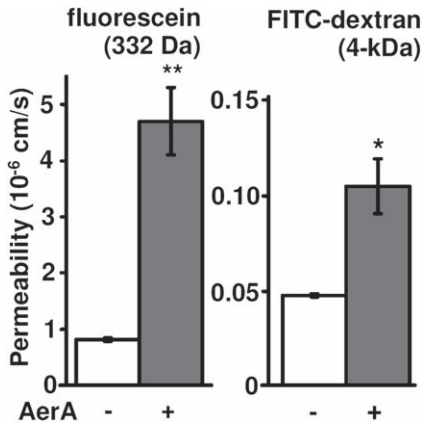

Figure 3. Epithelial permeability. Paracellular permeability was characterized by determining 332 Da fluorescein or 4-kDa FITC-dextran fluxes through AerA-treated HT-29/B6 monolayers in Ussing chamber experiments ($^*P < .05$, $^{**}P < .01$; n = 3).

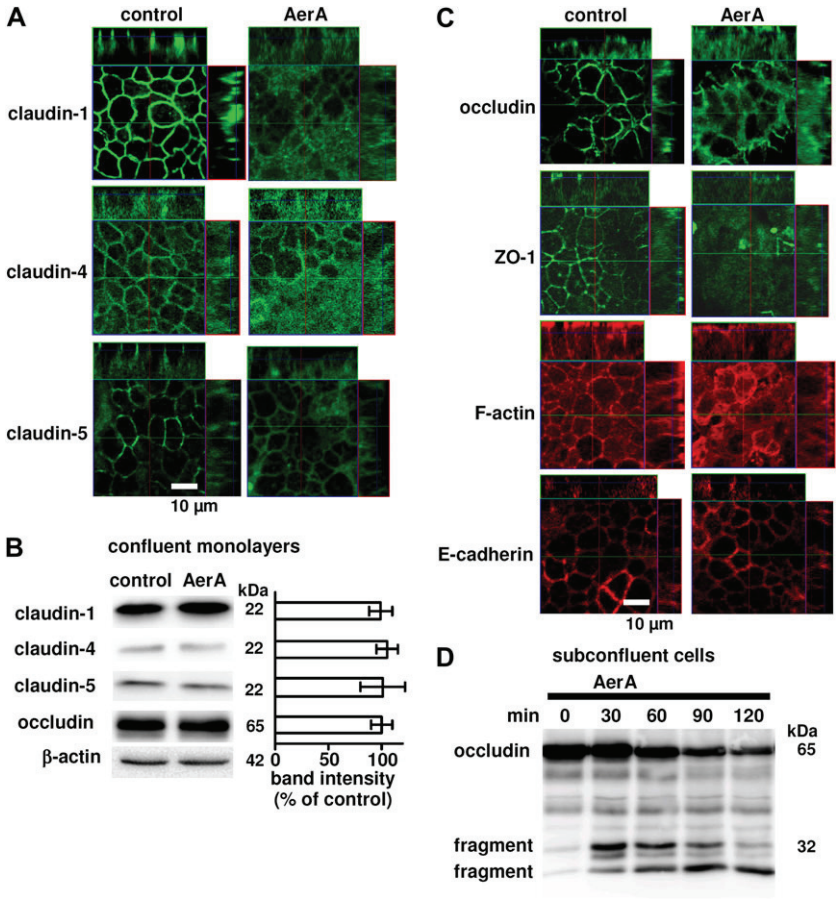

Figure 4. Analysis of TJ protein expression. HT-29/B6 monolayers were incubated with aerolysin or *Aeromonas* supernatant (1:1000 dilution) for 3 hours. *A*, Subcellular distribution of sealing TJ proteins claudin-1, -4, and -5 was studied by confocal laser-scanning microscopy (LSM). *B*, Western blots of sealing claudins and occludin from confluent monolayers with β-actin as loading control and densitometric analysis (not significant; n = 4). *C*, LSM for structural TJ proteins occludin and ZO-1, cytoskeletal F-actin, and adherens junction protein E-cadherin. White bar = 10 µm. *D*, Cleavage of occludin with subsequent fragmentation in subconfluent HT-29/B6 cells after treatment with *Aeromonas* supernatant (high AerA dose; 1:10 dilution).

impaired cell viability. Because of this, these sublytic concentrations of AerA-preparations (<1 HU, 1:1000 to 1:5000 dilution) have been used throughout all experiments defining barrier properties.

Structural Alteration of TJ Organization

For investigation of subcellular distribution of TJ proteins, HT-29/B6 monolayers were stained at different time points when epithelial resistance had dropped. Three hours after *Aeromonas* infection, or treatment with supernatant or aerolysin, opening of the TJ was indicated in confocal LSM, as sealing TJ proteins like claudin-1, -4, and -5 were redistributed off the TJ (Figure 4*A*), whereas no change in cellular TJ protein expression or cleavage of TJ proteins could be detected in Western blots (Figure 4*B*). LSM of control monolayers revealed TJ proteins to be present mainly within the TJ strands, whereas immunostaining of AerA-treated monolayers revealed a reduction of all investigated claudins in the TJ strands and a concomitant intracellular (cytoplasmic) appearance of claudin-positive material (Figure 4*A*). In Figure 4*C*, further *Z*-stack scans obtained for occludin and ZO-1 also revealed a redistribution of these proteins. At the same time, F-actin appeared more condensed and constricted, whereas cell–cell contacts remained stable in AerA-treated monolayers, as shown by E-cadherin staining as control for intact epithelial morphology. In contrast to the results in confluent monolayers, cleavage of occludin could be observed in subconfluent cells treated with *Aeromonas* supernatant (Figure 4*D*).

Cell Signaling via Intracellular Calcium

Fura-2-acetoxymethyl ester (Fura-2-AM) measurements revealed an increase in $[Ca^{2+}]_i$, starting about 10 minutes after the addition of AerA and remaining elevated until termination of the experiment (Figure 5*A*). Because elevation of $[Ca^{2+}]_i$ and subsequent calcium signaling can affect epithelial barrier function, we characterized the AerA-induced effects using respective inhibitors. Chelation of $[Ca^{2+}]_i$ by 1,2-bis-(2-amino-phenoxy)-ethane-N,N,N′,N′-tetraacetic acid acetoxymethyl ester (BAPTA-AM; Figure 5*B*) as well as the myosin light chain kinase

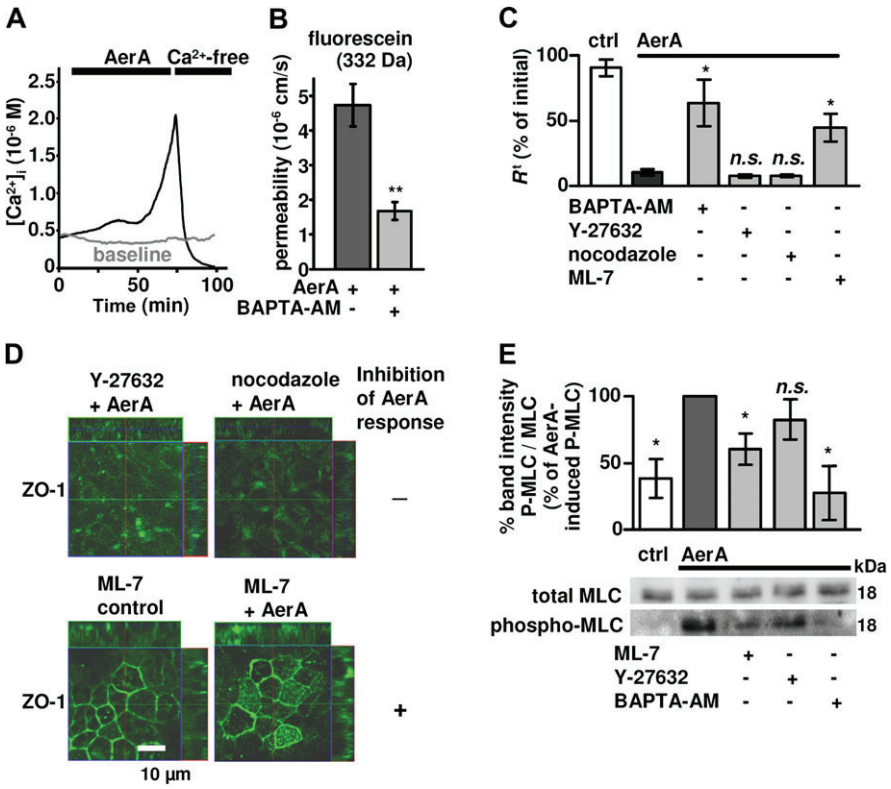

Figure 5. Calcium signaling. *A*, Intracellular calcium of HT-29/B6 cells after aerolysin treatment (1:5000 dilution) obtained by Fura-2-AM measurements. $[Ca^{2+}]_i$ increase is shown as one representative result of 4 independent experiments. *B*, Epithelial permeability for fluorescein was elevated after AerA treatment and the intracellular Ca^{2+} chelator BAPTA-AM (10 μM) attenuated this effect (**$P < .01$, n = 4). *C*, Inhibition of AerA response on R^t at 180 minutes is shown for respective blockers of Ca^{2+}-signaling pathways leading to TJ redistribution; with BAPTA-AM (by intracellular Ca^{2+} chelation), ML-7 (inhibitor of MLCK), Y-27632 (inhibitor of Rho/ROCK), and nocodazole (microtubule blocker; each 10 μM). Controls with inhibitors alone had stable resistances (*$P < .05$, n = 3). *D*, Confocal laser-scanning micrographs (ZO-1) of AerA-treated monolayers on coverslips with inhibition of MLCK (ML-7), which attenuated the AerA-response, whereas ROCK-II inhibition (Y-27632) and endocytosis inhibition by microtubule blockage (nocodazole) did not. See ZO-1 staining in Fig 4*C* for comparison. *E*, Western blot and densitometric analyses on the phosphorylation status of the myosin light-chain (MLC) after treatment with AerA in the presence of ML-7 or Y-27632 or BAPTA-AM (*$P < .05$, n = 3).

(MLCK) inhibitor ML-7 attenuated the AerA effect on epithelial barrier function. In contrast to ML-7, the ROCK-II inhibitor Y-27632 or the endocytosis inhibitor nocodazole did not affect the AerA response (Figure 5*C*). For structural correlation, the functional findings were complemented by immunostainings of ZO-1 (Figure 5*D*) and Western blotting on the phosphorylation state of MLC after treatment with AerA, in presence of ML-7, BAPTA-AM, or Y-27632, which also did not yield any evidence for a blocking effect (Figure 5*E*).

Wound Closure

To investigate the relevance of *Aeromonas* on epithelial restitution, single-cell lesions were induced and followed by LSM in the presence of either the supernatant of *A. hydrophila* or the aerolysin preparation. In parallel, measurements were performed with nonhemolytic controls or with AerA when inhibited by zinc. In controls, restitution was comparable to untreated monolayers and the lesions were closed within 16 minutes after induction of single-cell lesions. A ring-shaped actin accumulation around the lesions, which is part of the "purse-string" mechanism for restitution [23–25], was visible in control monolayers 10–13 minutes after induction of a single-cell lesion. When monolayers were treated with active AerA-containing preparations for at least 3 hours, all lesions remained clearly visible and the monolayers did not show any restitutional purse-string formation (Figure 6). Thus, TJ redistribution and disruption of wound closure take place simultaneously.

DISCUSSION

Aerolysin as Main Effector of Aeromonas-Induced Barrier Impairment

Dysregulation or functional impairment of TJs is found in many intestinal diseases, including gastrointestinal (GI) infectious diseases. The leak flux mechanism is one reason for diarrhea, and in addition, leak flux is thought to be a central pathomechanism of antigen entry into the "leaky gut" during gastroenteritis. As the first result of this study, we demonstrated that the hemolysin

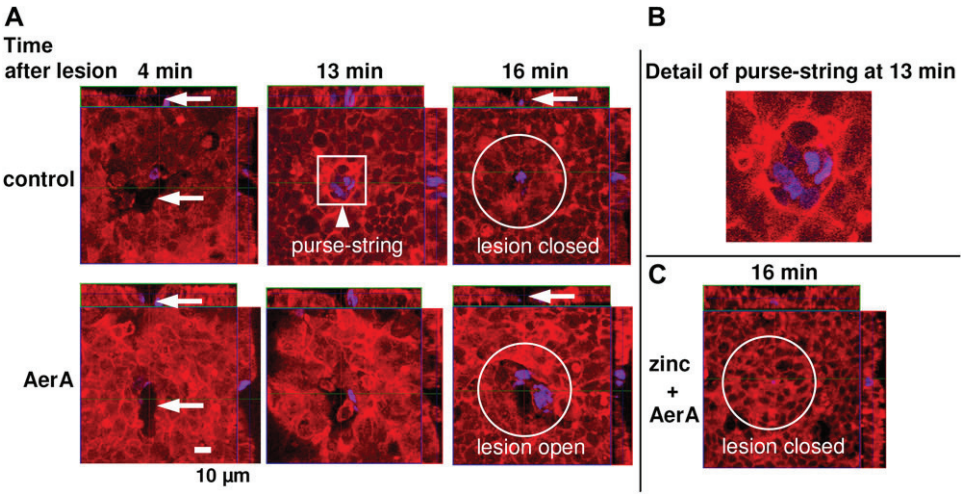

Figure 6. Wound closure. Confocal laser-scanning micrographs of single-cell lesions in HT-29/B6 monolayers (*Z*-axis scans, *XY* plane). *A*, In controls, single-cell lesions were closed within 16 minutes, accompanied by formation of an actin ring (``purse-string'') at 13 minutes after induction. F-actin is marked red by Phalloidin-Alexa-Fluor^{594} and appears more condensed in AerA-treated cells. Three hours after application of either *Aeromonas* supernatant or aerolysin (1:1000 dilution), the restitution after induction of single-cell lesions was defective. The fluorescence dye 4',6-diamidino-2-phenylindole dihydrochloride (DAPI; blue) marks the nuclei in the area of the lesion. The microelectrode for induction of lesions was also filled with 30 µM of DAPI for staining the nuclei of the damaged cells. This enabled us to retrieve the lesions in subsequent microscopic analyses. Restitution was evaluated by analysis of lesion closure (recovery time), lesion shape, and actin formation that could be identified by LSM. *B*, Details of purse-string in controls: F-actin appears only slightly condensed (much less than after Aeromonas exposure) and a restitutional purse-string was formed around the lesion. *C*, The aerolysin response could be abolished by pretreatment with zinc. White bar = 10 µm.

aerolysin is a main effector of *Aeromonas*-induced barrier impairment, as bacteria, supernatants, or aerolysin alone caused similar barrier effects. Up to now, the action of aerolysin on the intestine was ascribed on the one hand to secretory dysfunction and on the other hand to cytolethal effects. In concordance with previous reports, here we present evidence that cell death is probably a feature of the late phase of infection [26, 27], and that other mechanisms of barrier disturbance exist.

Epithelial resistance was shown to decrease in dose- and time-dependent manners. In the first period after aerolysin exposure, we measured a slight and transient drop in R^{trans} as the result of opening of chloride channels in the apical enterocyte membrane, described previously by our group [12]. Thereafter, a continuous decrease in R^{para} clearly represents the major pathway effecting barrier impairment. This is surprising because PFTs are thought to solely reduce R^{trans} by the opening of ion channels and/or pore formation [11, 12]. The 2PI method allowed us to distinguish the different effects of PFTs, namely a reduction in R^{para} and along with the involvement of TJs in this effect, which became apparent in the period after the transient chloride secretion. As a structural correlate for the reduced R^{para}, TJ proteins were redistributed off the TJ toward intracellular compartments. These effects were observed within 3 hours after treatment, which indicates that this relatively fast process is not the result of longer-lasting expression regulation changes. This conclusion is supported also by the unchanged claudin expression in immunoblots. Cleavage of TJ proteins was also not detectable in confluent monolayers. However, occludin was cleaved in subconfluent cells, providing further evidence for the concept that TJ proteins are protected against proteolysis in the confluent epithelium due to their presence in confined junctions [28, 29].

Ca^{2+} Signaling Leading to Actomyosin Constriction of the Perijunctional Cytoskeleton

The second major result of this study is that TJ redistribution and the subsequent leak flux are mediated via Ca^{2+} signaling leading to actomyosin constriction of the perijunctional cytoskeleton, as revealed by F-actin staining. In this mechanistic process, actomyosin is assumed to retract TJ proteins from the TJ strands and the plasma membrane into the cytosol [16, 30]. Following the electrophysiological findings, the TJ protein redistribution became visible in LSM only after the scattering into the cytosol was pronounced. Constriction of the perijunctional cytoskeleton leads to ZO-1 and subsequently claudin redistribution by spatial high calcium concentrations in the microdomains where the aerolysin-pore is integrated. A Ca^{2+}-induced Ca^{2+} release from intracellular stores by aerolysin was shown for granulocytes [31]. A pronounced Ca^{2+} release can lead to activation of Ca^{2+}-dependent Cl^- channels, as shown for the cholesterol-dependent cytolysin listeriolysin-O [32] or for the hemolysin from *Vibrio parahaemolyticus* [33].

In the case of aerolysin, MLC phosphorylation was shown to be induced and could be blocked by MLCK inhibition. In contrast, inhibition of the Rho and Rho-associated protein kinase (Rho/ROCK) pathway had no protective effect on TJ

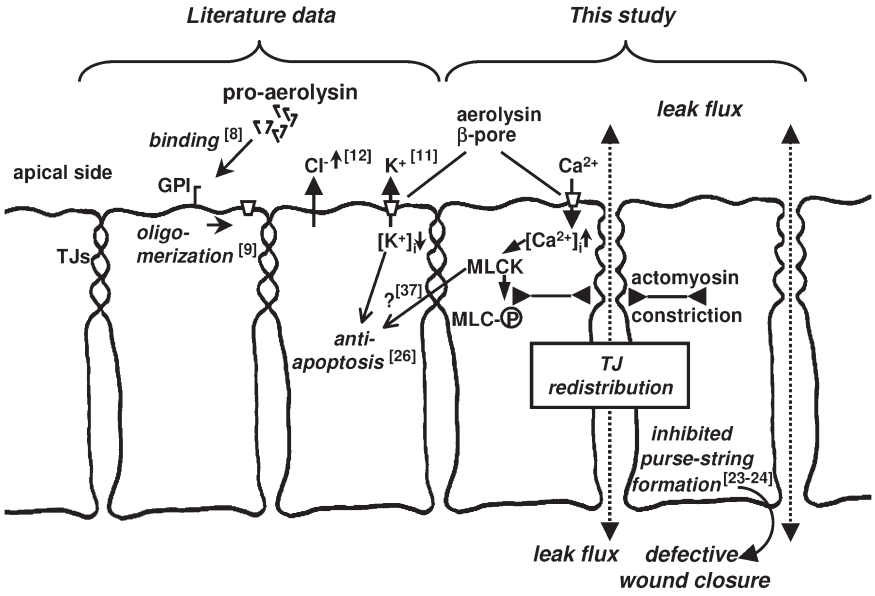

Figure 7. Schematic model of the aerolysin-induced cellular response. The secreted proaerolysin monomer binds to raft-associated glycosylphosphatidylinositol (GPI) anchors on the apical membrane [8, 46] and oligomerizes into a heptameric β-barrel pore [9]. Pore formation leads to active chloride secretion [12] and potassium efflux [11]; the latter was shown to have anti-apoptotic effects [26]. There is a possible involvement of MLCK in pro-survival signaling [37]. The aerolysin pore is permeable to calcium [31]. This study shows that AerA increased $[Ca^{2+}]_i$, leading to MLCK activation, which triggers myosin light-chain (MLC) phosphorylation and actomyosin constriction. The subsequent tight junction (TJ) redistribution causes a leak flux. After cytoskeleton rearrangement, purse-string formation is inhibited [23, 24], resulting in our observation of defective wound closure.

stability. Moreover, endocytosis, as a part of an actin-dependent mechanism [34], seems also not to be primarily involved in TJ redistribution, as inhibition of this mechanism by microtubule blockage with nocodazole could not attenuate the aerolysin response. On the other hand, internalization of PFTs by endocytosis could be a mechanism of cellular protection [35]. In addition, anti-apoptotic signaling by aerolysin was already shown, as it inhibits Akt/protein kinase B pathways or activates processing of caspase-1 via inflammasomes [26, 36]. The possible influence of MLCK activity on anti-apoptosis [37, 38] in the context of aerolysin-mediated prosurvival signaling needs further investigations.

However, the mechanistic process of actomyosin-mediated sorting of TJs has been well described [38] and seems to be the predominant effect of aerolysin action on epithelial integrity, as demonstrated by 2PI measurements here. Contrary to this, other toxins from gram-positive pathogens acting on the cytoskeleton show different mechanisms, as, for example, that the cytoskeleton is affected via inactivation of Rho-GTPases by glucosyltransferase toxins from *Clostridium difficile*, leading to a variety of consequences [39], or that *C. botulinum* toxins affect actin filaments by ADP-ribosylation of G-actin [40]. Furthermore, the *C. perfringens* enterotoxin (CPE) is a well-described effector in TJ pathogenesis. CPE is also a β-PFT with structural similarities to aerolysin, and was shown to assemble via a lipid-raft-independent mechanism into the host cell membrane, leading to rapid cell death [41, 42]. CPE binds to the extracellular loop 2 of claudin-3 and claudin-4. Molecular analysis revealed a noncytotoxic fragment of CPE that contains the claudin-binding site and removes specific claudins from the TJ strands [43, 44]. In contrast to CPE, aerolysin has been shown to affect all claudins as a more global event. Despite the structural homologies of β-PFTs [45], sequence alignments with BLAST revealed no similarities of the CPE claudin-binding motif within aerolysin protein sequence. For aerolysin as well as for other β-PFTs, no direct claudin binding has been described as yet. Aerolysin requires GPI anchors for successful insertion into the membrane [8]. These are not present in the TJ, but the local association to GPI-containing rafts in the apical membrane near the TJ is conceivable [46]. The obvious difference of the molecular targets and the specific actions of these toxins on the host cells clearly point to a different pathogenesis.

Aerolysin Blocks Restitution of Single-Cell Lesions

As a third important finding, our study clearly proves that wound healing was defective, as *A. hydrophila* supernatant and aerolysin effectively blocked restitution of single-cell lesions. It is known that after superficial wounding, restitution of lesions is promoted by GTP-binding protein Rac1 in a Ca^{2+}-dependent manner [47]. Intact actin and TJ arrangements are essential for rapid closure of small lesions [24], but in response to aerolysin, TJ and cytoskeletal disorganization impede the restitutional process of purse-string formation [25]. Similarly, our group previously reported delayed wound closure of lesions in intestinal

epithelium treated with supernatants from HlyA-containing *E. coli* O4 [26], but the underlying cellular mechanisms for the action of the β-PFT have not been identified [17]. Hence, besides direct cytotoxic effects of PFTs, defective wound healing could contribute to necrotizing processes in wound infections and intestinal epithelial lesions.

All aerolysin effects were sensitive to zinc. The protective role of zinc is well known, as it is essential for metabolism and has a variety of protective effects on the epithelium, including TJ upregulation [48]. However, the ability of divalent cations such as zinc to inhibit hemolysis has not been properly considered. As already reported, zinc efficiently represses pore formation induced by aerolysin and other β-PFTs [49, 50]. Thus, zinc treatment can protect the host cell from all underlying pathological effects of these toxins. Zinc has therapeutic implications in treatment of diarrhea or as a topical adjuvant for lesions (eg, sticking-plaster, zinc paste).

In summary (Figure 7), we have demonstrated that a mucus-permeable β-PFT, integrated into the apical host cell membrane, indirectly induces a barrier defect by inducing TJ redistribution. We found that, following initial resistance effects as a result of pore formation by the toxin and membrane channel opening, elevated intracellular calcium activates MLCK-dependent actomyosin constriction of the perijunctional cytoskeleton, which is mainly responsible for the paracellular resistance effect. Moreover, this dysfunction leads to defective restitution of epithelial lesions.

Notes

Acknowledgments. The excellent technical assistance of Nicole Held, In-Fah Lee, and Detlef Sorgenfrei is gratefully acknowledged.

Financial support. This work was supported by grants from Deutsche Forschungsgemeinschaft (DFG Schu 559/11).

Potential conflicts of interest. All authors: No reported conflicts.

All authors have submitted the ICMJE Form for Disclosure of Potential Conflicts of Interest. Conflicts that the editors consider relevant to the content of the manuscript have been disclosed.

References

1. Albert MJ, Ansaruzzaman M, Talukder KA, et al. Prevalence of enterotoxin genes in *Aeromonas* spp. isolated from children with diarrhea, healthy controls, and the environment. J Clin Microbiol **2000**; 38:3785–90.
2. Trower CJ, Abo S, Majeed KN, von Itzstein M. Production of an enterotoxin by a gastro-enteritis-associated *Aeromonas* strain. J Med Microbiol **2000**; 49:121–6.
3. Blair JE, Woo-Ming MA, McGuire PK. *Aeromonas hydrophila* bacteremia acquired from an infected swimming pool. Clin Infect Dis **1999**; 28:1336–7.
4. Martins LM, Marquez RF, Yano T. Incidence of toxic *Aeromonas* isolated from food and human infection. FEMS Immunol Med Microbiol **2002**; 32:237–42.
5. Shah N, DuPont HL, Ramsey DJ. Global etiology of travelers' diarrhea: systematic review from 1973 to the present. Am J Trop Med Hyg **2009**; 80:609–14.
6. Adamski J, Koivuranta M, Leppänen E. Fatal case of myonecrosis and septicaemia caused by *Aeromonas hydrophila* in Finland. Scand J Infect Dis **2006**; 38:1117–9.
7. Bernheimer AW, Avigad LS. Partial characterization of aerolysin, a lytic exotoxin from *Aeromonas hydrophila*. Infect Immun **1974**; 9: 1016–21.
8. Brodsky RA, Mukhina GL, Nelson KL, Lawrence TS, Jones RJ, Buckley JT. Resistance of paroxysmal nocturnal hemoglobinuria cells to the glycosylphosphatidylinositol-binding toxin aerolysin. Blood **1999**; 93: 1749–56.
9. Wilmsen HU, Leonard KR, Tichelaar W, Buckley JT, Pattus F. The aerolysin membrane channel is formed by heptamerization of the monomer. EMBO J **1992**; 11:2457–63.
10. Chakraborty T, Huhle B, Hof H, Bergbauer H, Goebel W. Marker exchange mutagenesis of the aerolysin determinant in *Aeromonas hydrophila* demonstrates the role of aerolysin in *A. hydrophila*-associated systemic infections. Infect Immun **1987**; 55:2274–80.
11. Abrami L, Fivaz M, Glauser PE, Sugimoto N, Zurzolo C, van der Goot FG. Sensitivity of polarized epithelial cells to the pore-forming toxin aerolysin. Infect Immun **2003**; 71:739–46.
12. Epple HJ, Mankertz J, Ignatius R, et al. *Aeromonas hydrophila* beta-hemolysin induces active chloride secretion in colon epithelial cells (HT-29/B6). Infect Immun **2004**; 72:4848–58.
13. Gitter AH, Wullstein F, Fromm M, Schulzke JD. Epithelial barrier defects in ulcerative colitis: characterization and quantification by electrophysiological imaging. Gastroenterology **2001**; 121:1320–8.
14. Inai T, Kobayashi J, Shibata Y. Claudin-1 contributes to the epithelial barrier function in MDCK cells. Eur J Cell Biol **1999**; 78:849–55.
15. Amasheh S, Schmidt T, Mahn M, et al. Contribution of claudin-5 to barrier properties in tight junctions of epithelial cells. Cell Tissue Res **2005**; 321:89–96.
16. Schwarz BT, Wang F, Shen L, et al. LIGHT signals directly to intestinal epithelia to cause barrier dysfunction via cytoskeletal and endocytic mechanisms. Gastroenterology **2007**; 132:2383–94.
17. Troeger H, Richter JF, Beutin L, et al. *Escherichia coli* alpha-haemolysin induces focal leaks in colonic epithelium: a novel mechanism of bacterial translocation. Cell Microbiol **2007**; 9:2530–40.
18. Bücker R, Troeger H, Kleer J, Fromm M, Schulzke JD. *Arcobacter butzleri* induces barrier dysfunction in intestinal HT-29/B6 cells. J Infect Dis **2009**; 200:756–64.
19. Kreusel KM, Fromm M, Schulzke JD, Hegel U. Cl-secretion in epithelial monolayers of mucus-forming human colon cells (HT-29/B6). Am J Physiol **1991**; 261:C574–82.
20. Epple HJ, Kreusel KM, Hanski C, Schulzke JD, Riecken EO, Fromm M. Differential stimulation of intestinal mucin secretion by cholera toxin and carbachol. Pflügers Arch **1997**; 433:638–47.
21. Krug SM, Fromm M, Günzel D. Two-path impedance spectroscopy for measuring paracellular and transcellular epithelial resistance. Biophys J **2009**; 97:2202–11.
22. Grynkiewicz G, Poenie M, Tsien RY. A new generation of Ca^{2+} indicators with greatly improved fluorescence properties. J Biol Chem **1985**; 260:3440–50.
23. Florian P, Schöneberg T, Schulzke JD, Fromm M, Gitter AH. Single-cell epithelial defects close rapidly by an actinomyosin purse string mechanism with functional tight junctions. J Physiol **2002**; 545:485–99.
24. Russo JM, Florian P, Shen L, et al. Distinct temporal-spatial roles for rho kinase and myosin light chain kinase in epithelial purse-string wound closure. Gastroenterology **2005**; 128:987–1001.
25. Günzel D, Florian P, Richter JF, et al. Restitution of single-cell defects in the mouse colon epithelium differs from that of cultured cells. Am J Physiol Regul Integr Comp Physiol **2006**; 290:R1496–507.
26. Gurcel L, Abrami L, Girardin S, Tschopp J, van der Goot FG. Caspase-1 activation of lipid metabolic pathways in response to bacterial pore-forming toxins promotes cell survival. Cell **2006**; 126:1135–45.
27. Couto CR, Oliveira SS, Queiroz ML, Freitas-Almeida AC. Interactions of clinical and environmental *Aeromonas* isolates with Caco-2 and HT29 intestinal epithelial cells. Lett Appl Microbiol **2007**; 45:405–10.
28. Casas E, Barron C, Francis SA, et al. Cholesterol efflux stimulates metalloproteinase-mediated cleavage of occludin and release of ex-

tracellular membrane particles containing its C-terminal fragments. Exp Cell Res **2010**; 316:353–65.
29. Lischper M, Beuck S, Thanabalasundaram G, Pieper C, Galla HJ. Metalloproteinase mediated occludin cleavage in the cerebral microcapillary endothelium under pathological conditions. Brain Res **2010**; 1326:114–27.
30. Ivanov AI, McCall IC, Parkos CA, Nusrat A. Role for actin filament turnover and a myosin II motor in cytoskeleton-driven disassembly of the epithelial apical junctional complex. Mol Biol Cell **2004**; 15: 2639–51.
31. Krause KH, Fivaz M, Monod A, van der Goot FG. Aerolysin induces G-protein activation and Ca^{2+} release from intracellular stores in human granulocytes. J Biol Chem **1998**; 273:18122–9.
32. Richter JF, Gitter AH, Günzel D, et al. Listeriolysin O affects barrier function and induces chloride secretion in HT-29/B6 colon epithelial cells. Am J Physiol Gastrointest Liver Physiol **2009**; 296:G1350–9.
33. Raimondi F, Kao JP, Kaper JB, Guandalini S, Fasano A. Calcium-dependent intestinal chloride secretion by *Vibrio parahaemolyticus* thermostable direct hemolysin in a rabbit model. Gastroenterology **1995**; 109:381–6.
34. Utech M, Ivanov AI, Samarin SN, et al. Mechanism of IFN-gamma-induced endocytosis of tight junction proteins: myosin II-dependent vacuolarization of the apical plasma membrane. Mol Biol Cell **2005**; 16:5040–52.
35. Husmann M, Beckmann E, Boller K, et al. Elimination of a bacterial pore-forming toxin by sequential endocytosis and exocytosis. FEBS Lett **2009**; 583:337–44.
36. Wiles TJ, Dhakal BK, Eto DS, Mulvey MA. Inactivation of host Akt/protein kinase B signaling by bacterial pore-forming toxins. Mol Biol Cell **2008**; 19:1427–38.
37. Connell LE, Helfman DM. Myosin light chain kinase plays a role in the regulation of epithelial cell survival. J Cell Sci **2006**; 119:2269–81.
38. Zolotarevsky Y, Hecht G, Koutsouris A, et al. A membrane-permeant peptide that inhibits MLC kinase restores barrier function in in vitro models of intestinal disease. Gastroenterology **2002**; 123:163–72.
39. Kelly CP, Pothoulakis C, LaMont JT. *Clostridium difficile* colitis. N Engl J Med **1994**; 330:257–62.
40. Wilde C, Aktories K. The Rho-ADP-ribosylating C3 exoenzyme from *Clostridium botulinum* and related C3-like transferases. Toxicon **2001**; 39:1647–60.
41. Caserta JA, Hale ML, Popoff MR, Stiles BG, McClane BA. Evidence that membrane rafts are not required for the action of *Clostridium perfringens* enterotoxin. Infect Immun **2008**; 76:5677–85.
42. Chakrabarti G, McClane BA. The importance of calcium influx, calpain and calmodulin for the activation of CaCo-2 cell death pathways by *Clostridium perfringens* enterotoxin. Cell Microbiol **2005**; 7: 129–46.
43. Sonoda N, Furuse M, Sasaki H, et al. *Clostridium perfringens* enterotoxin fragment removes specific claudins from tight junction strands: evidence for direct involvement of claudins in tight junction barrier. J Cell Biol **1999**; 147:195–204.
44. Fujita K, Katahira J, Horiguchi Y, Sonoda N, Furuse M, Tsukita S. *Clostridium perfringens* enterotoxin binds to the second extracellular loop of claudin-3, a tight junction integral membrane protein. FEBS Lett **2000**; 476:258–61.
45. Cole AR, Gibert M, Popoff M, Moss DS, Titball RW, Basak AK. *Clostridium perfringens* epsilon-toxin shows structural similarity to the pore-forming toxin aerolysin. Nat Struct Mol Biol **2004**; 11:797–8.
46. Polishchuk R, Di Pentima A, Lippincott-Schwartz J. Delivery of raft-associated, GPI-anchored proteins to the apical surface of polarized MDCK cells by a transcytotic pathway. Nat Cell Biol **2004**; 6: 297–307.
47. Rao JN, Liu SV, Zou T, et al. Rac1 promotes intestinal epithelial restitution by increasing Ca^{2+} influx through interaction with phospholipase C-(gamma)1 after wounding. Am J Physiol Cell Physiol **2008**; 295:C1499–509.
48. Zhang B, Guo Y. Supplemental zinc reduced intestinal permeability by enhancing occludin and zonula occludens protein-1 (ZO-1) expression in weaning piglets. Br J Nutr **2009**; 102:687–93.
49. Avigad LS, Bernheimer AW. Inhibition of hemolysis by zinc and its reversal by L-histidine. Infect Immun **1978**; 19:1101–3.
50. Wilmsen HU, Pattus F, Buckley JT. Aerolysin, a hemolysin from *Aeromonas hydrophila*, forms voltage-gated channels in planar lipid bilayers. J Membr Biol **1990**; 115:71–81.

15 October 2011
Volume 204
Number 8

The Journal of Infectious Diseases

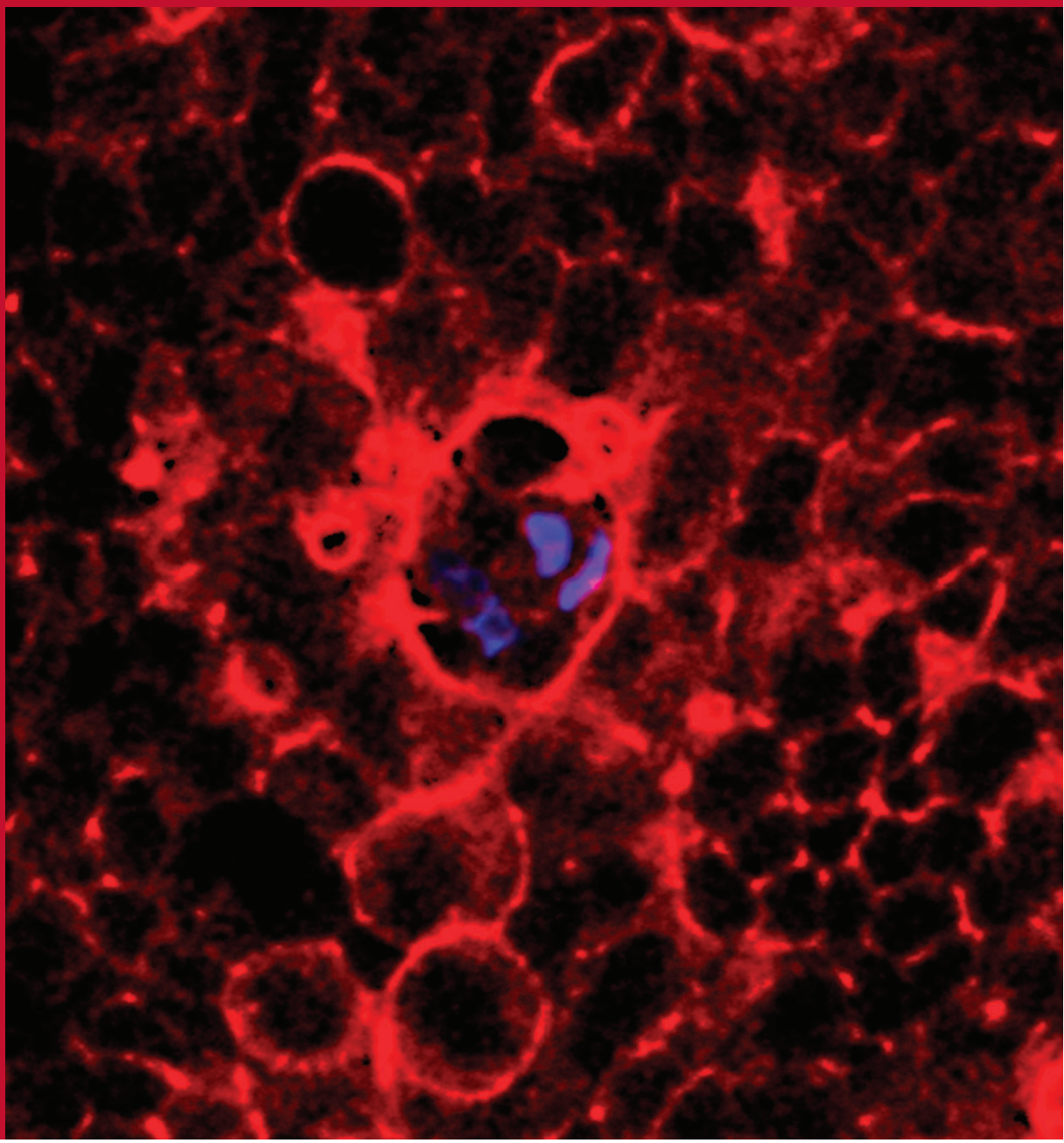

IDSA Infectious Diseases Society of America

hivma

OXFORD UNIVERSITY PRESS

Cover image

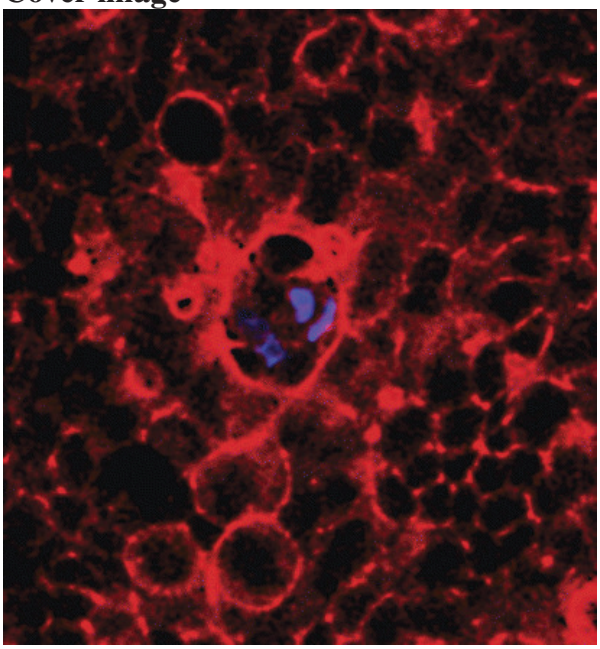

On the cover: Image shows epithelial wound repair after induction of an artificial lesion in an intestinal cell monolayer. The nuclei in the area of the lesion are marked in blue. Cytoskeleton F-actin is marked red and appears condensed around the lesion. This actin ring (purse-string formation) is part of the restitutional mechanism in epithelial wound closure of small lesions and can be impaired by microbial toxins. (See Buecker et al, pp 1283–92)

2.2.2 Entstehung fokaler Läsionen durch den Virulenzfaktor *E. coli* α-Hämolysin

Während bei der experimentellen Infektion mit *Aeromonas*-Kulturen bzw. bei der Behandlung der Epithelzellen mit Aerolysin die Wirkung des Hämolysins als ein globaler Effekt auf die Epithelzellen zu beobachten war, zeigen andere Erreger eher fokale Effekte auf das Epithel wie z.B. bei *C. concisus* (Punkt 2.1.3). Der fokale Charakter bakterieller Translokation über die epitheliale Barriere war in besonderer Weise auch bei uropathogenen *Escherichia coli* O4 oder *E. coli* 536 zu beobachten, wobei insbesondere ein Virulenzfaktor, das α-Hämolysin (HlyA) eine entscheidende Rolle bei der Entstehung von fokalen Läsionen (‚*Focal Leak*') zu spielen scheint (Troeger et al., 2007a). Der von uns neu beschriebene Pathomechanismus der Entstehung von *Focal Leaks* im Darmepithel, der charakteristische Läsionen durch α-Hämolysin-tragende *E. coli*-Stämme bezeichnet (Troeger et al., 2007a), wurde in der folgenden Publikation: Bücker et al., „α-Haemolysin of Escherichia coli in IBD: a potentiator of inflammatory activity in the colon", erschienen 2014 in *GUT*, unter definierten Bedingungen in der Maus *in vivo* weiter charakterisiert. Hierzu wurden Mäuse mit α-Hämolysin tragenden *E. coli*-Stämmen intestinal kolonisiert. Drei verschiedene Mausmodelle wurden verwendet: (i) Wildtyp-Mäuse (WT), (ii) IL-10 defiziente-Mäuse (*IL-10*$^{-/-}$) und (iii) keimfreie Mäuse zur Monoassoziation (MA) entweder mit α-Hämolysin-tragenden *E. coli* 536 (HlyA) oder mit der isogenen *E. coli* 536-Hämolysin-defizienten Mutante (HDM).

Die mit HlyA-produzierendem *E. coli* 536-infizierten Mäuse zeigten im Dickdarm eine Zunahme von *Focal Leaks* in allen drei experimentellen Modellen. Dies führte in Ussing-Kammer-Experimenten jeweils zu einer Verminderung des transepithelialen Widerstandes im Kolon der Tiere. Dabei war die epitheliale Permeabilität auch gegenüber dem Makromolekül HRP (Horseradish Peroxidase, 44 kDa) in allen drei Tiermodellen erhöht (z.B. bei HlyA-monoassoziierten Mäusen 1,98 ± 0,54 nmol·h^{-1}·cm^{-2} *versus* HDM mit 0,32 ± 0,07 nmol·h^{-1}·cm^{-2}, P<0,05). Als Folge davon war der Entzündungsaktivitätsindex bei den HlyA-behandelten Tieren höher als bei den HDM-infizierten Kontrollen und zwar in den mit Entzündung einhergehenden Modellen: *IL-10*$^{-/-}$-Tiere sowie bei Tieren mit Monoassoziation, nicht aber in den nicht-entzündeten WT-Mäusen. Somit konnten wir im Tiermodell *in vivo* erstmalig zeigen, dass der neuartige Pathomechanismus der *Focal Leak*-Induktion, durch vermehrte Translokation von Antigenen und Bakterien in den Organismus, eine inflammatorische Antwort zur Folge hat.

Neben der experimentellen Darstellung des α-Hämolysin als bakterieller Virulenzfaktor bei intestinalen Entzündungen konnte in dieser Studie die Häufigkeit dieser Bakterienstämme in Kolonbiopsaten von gesunden Menschen und Patienten mit CED gemessen werden. Es fand sich insgesamt eine hohe Prävalenz von HlyA-tragenden *E. coli* bei Patienten mit CED, aber auch bei gesunden Probanden. Mehr als 70% der untersuchten Personen waren in der PCR

positiv für HlyA. Darüber hinaus fand sich aber auch eine erhöhte absolute HlyA-Genhäufigkeit in Kolonbiopsien von Colitis ulcerosa-Patienten im akuten Schub gegenüber den nicht-entzündeten Kontrollen, was auf eine erhöhte Aufnahme in die Mukosa unter diesen Bedingungen hindeutet. Demnach müssen HlyA-exprimierende *E. coli*-Stämme als potentielle Kofaktoren bei der Entstehung von intestinaler Entzündung in Betracht gezogen werden. Dies liefert einen neuen Erklärungsansatz für die Beteiligung der residenten Mikrobiota an der Entstehung von Kolitiden. Darüber hinaus konnte wir mit dieser Studie einen weiteren direkten Beweis für einen Invasions-Mechanismus - vom Lumen in den Organismus - finden und somit einen Mechanismus für die sogenannte ***"Leaky Gut"-Hypothese*** beleuchten. Beim *Leaky Gut* ist die Permeabilität des Darms gegenüber größeren immunogenen Stoffen, die vom Lumen in den Organismus gelangen, erhöht. Der pathogene Mechanismus hinter der Wirkung von *E. coli* α-Hämolysin ist hier der *Focal Leak*-Bildung zuzuschreiben, wohingegen die epitheliale Apoptoseinduktion oder eine *Tight Junction*-Beteiligung eine untergeordnete Rolle zu spielen scheinen.

ORIGINAL ARTICLE

α-Haemolysin of *Escherichia coli* in IBD: a potentiator of inflammatory activity in the colon

Roland Bücker,[1] Emanuel Schulz,[1] Dorothee Günzel,[2] Christian Bojarski,[1] In-Fah M Lee,[2] Lena J John,[1] Stephanie Wiegand,[1] Traute Janßen,[3] Lothar H Wieler,[3] Ulrich Dobrindt,[4] Lothar Beutin,[5] Christa Ewers,[6] Michael Fromm,[2] Britta Siegmund,[1] Hanno Troeger,[1] Jörg-Dieter Schulzke[1]

▶ Additional material is published online only. To view please visit the journal online (http://dx.doi.org/10.1136/gutjnl-2013-306099).

[1]Department of Gastroenterology, Infectious Diseases and Rheumatology, Berlin, Germany
[2]Institute of Clinical Physiology, Charité—Universitätsmedizin Berlin, Campus Benjamin Franklin, Berlin, Germany
[3]Department of Veterinary Medicine, Institute of Microbiology and Epizootics, Freie Universität Berlin, Berlin, Germany
[4]Institute of Hygiene, University of Münster, Münster, Germany
[5]Bundesinstitut für Risikobewertung, Berlin, Germany
[6]Department of Veterinary Medicine, Institute of Hygiene and Infectious Diseases of Animals, Justus-Liebig-Universität Giessen, Giessen, Germany

***Correspondence to**
Professor Jörg-Dieter Schulzke, Medizinische Klinik für Gastroenterologie, Infektiologie und Rheumatologie, Charité—Universitätsmedizin Berlin, Campus Benjamin Franklin, Hindenburgdamm 30, Berlin 12203, Germany; joerg.schulzke@charite.de

Received 17 September 2013
Revised 22 January 2014
Accepted 28 January 2014

To cite: Bücker R, Schulz E, Günzel D, *et al*. *Gut* Published Online First: [*please include* Day Month Year] doi:10.1136/gutjnl-2013-306099

ABSTRACT

Objective α-Haemolysin (HlyA) influences host cell ionic homeostasis and causes concentration-dependent cell lysis. As a consequence, HlyA-producing *Escherichia coli* is capable of inducing 'focal leaks' in colon epithelia, through which bacteria and antigens translocate. This study addressed the role of HlyA as a virulence factor in the pathogenesis of colitis according to the 'leaky gut' concept.

Design To study the action of HlyA in the colon, we performed oral administration of HlyA-expressing *E coli*-536 and its isogenic α-haemolysin-deficient mutant (HDM) in three mouse models: wild type, interleukin-10 knockout mice (*IL-10*$^{-/-}$) and monoassociated mice. Electrophysiological properties of the colonised colon were characterised in Ussing experiments. Inflammation scores were evaluated and focal leaks in the colon were assessed by confocal laser-scanning microscopy. *HlyA* quantity in human colon biopsies was measured by quantitative PCR.

Results All three experimental mouse models infected with HlyA-producing *E coli*-536 showed an increase in focal leak area compared with HDM. This was associated with a decrease in transepithelial electrical resistance and an increase in macromolecule uptake. As a consequence, inflammatory activity index was increased to a higher degree in inflammation-prone mice. Mucosal samples from human colon were *E coli* HlyA-positive in 19 of 22 patients with ulcerative colitis, 9 of 9 patients with Crohn's disease and 9 of 12 healthy controls. Moreover, focal leaks were found together with 10-fold increased levels of HlyA in active ulcerative colitis.

Conclusions *E coli* HlyA impairs intestinal barrier function via focal leak induction in the epithelium, thereby intensifying antigen uptake and triggering intestinal inflammation in vulnerable mouse models. Therefore, HlyA-expressing *E coli* strains should be considered as potential cofactors in the pathogenesis of intestinal inflammation.

Significance of this study

What is already known about this subject?

- Proteobacteria, in particular adherent-invasive *Escherichia coli*, have been associated with the pathogenesis of IBD. In active ulcerative colitis (UC), the microbiota of the large intestine changes towards higher bacterial numbers of *Enterobacteriaceae* with *E coli* as main resident.
- α-Haemolysin-carrying *E coli* (eg, uropathogenic *E coli*; UPEC) are frequently found in the faeces of humans and livestock animals. Patients with active UC develop mucosal microlesions and erosions in the colon.

What are the new findings?

- A novel mechanism of bacterial pathology which initiates lesions in the colon mucosa called 'focal leaks' was identified in vivo in three different mouse models.
- Induction of 'focal leaks' perturbed epithelial barrier function and increased the influx of high molecular weight antigens.
- Colonic mucosal inflammation was accelerated by α-haemolysin-carrying *E coli* in inflammatory mouse models.
- In contrast to earlier observations, the prevalence of α-haemolysin-positive *E coli* in human colon was high, detectable by UPEC-*hlyA*-specific PCR. Haemolysin-carrying *E coli* in human mucosa from patients with active UC were more abundant than in controls.

How might it impact on clinical practice in the foreseeable future?

- Bacteria with the ability to impair mucosal barrier function, as for example, *E coli* carrying haemolysins, may become increasingly important in the epidemiology of IBD.
- New therapeutic concepts like bacteriotherapy (eg, administration of *E coli* Nissle) or vaccination against UPEC could be considered for forthcoming clinical trials in IBD.

INTRODUCTION

Within the gut, most strains of *Escherichia coli* are regarded as commensals, some (eg, *E coli* Nissle 1917) even possessing probiotic properties. However, some strains (eg, enteropathogenic *E coli* (EPEC) or uropathogenic *E coli* (UPEC)) possess virulence factors which cause intestinal and extra-intestinal diseases. Furthermore, other *Enterobacteriaceae*, such as *Salmonella and Campylobacter*, may have a role in the pathogenesis of inflammatory bowel disease (IBD).[1 2] Genome-wide association studies suggest a genetic basis to IBD susceptibility, which may

involve changes in intestinal epithelial barrier function and the intestine's innate immune defence mechanisms.[3 4] In healthy individuals, the spectrum of intestinal microbiota is relatively stable over time. However, a decrease in microbial diversity and a quantitative shift in the balance between different bacterial strains occurs, especially in active ulcerative colitis (UC), in which increases in enterobacteria (particular *E coli*), have been observed.[5–7] Furthermore, *E coli* of the B2 phylogroup frequently reside in the intestinal mucosa of patients with IBD,[8 9] and while these B2 strains are linked to urinary tract infections,[10] they could contribute to disruption of colonic epithelial barrier function.

Intestinal epithelial barrier dysfunction may reflect tight junction (TJ) defects, an increase in apoptosis, the appearance of 'focal leaks' or erosions, or a combination of these factors. Barrier defects such as these increase the permeability of the mucosa to water and small solutes, their resulting 'leak' fluxes into the lumen being one of the pathogenetic mechanisms of diarrhoea in IBD. Increased permeability to small and large molecules, including potentially harmful antigens capable of eliciting immune responses, occurs in IBD.[11 12] Thus, impaired barrier function may be cause and consequence of intestinal inflammation: in UC, apoptotic foci and erosions are early features of colonic inflammation, whereas in Crohn's disease (CD), erosions/ulcers are generally absent early in the inflammatory process.[13]

Luminal antigens are also absorbed transcellularly via endocytosis, which may be influenced by proinflammatory cytokines and/or bacterial virulence factors. *E coli* virulence factors such as fimbriae, enterotoxins and serine protease autotransporters (SPATES, eg, Sat) have been implicated in intestinal disorders.[14 15] By contrast, the role of *E coli* α-haemolysin in the gut is still unclear, despite being well characterised in other respects.[16] Haemolysins are pore-forming toxins (PFTs), *E coli* α-haemolysin (HlyA) belonging to the β-barrel-PFT (β-PFT) group. It forms small cation-permeable channels in the host cell membrane with an inner diameter of approximately 10 Å. Haemolytic bacteria have been shown to induce intestinal malabsorption,[17] secretion[18] and epithelial lesions via necrosis and/or apoptosis.[19] We previously showed that HlyA induced 'focal leaks' in colonic HT-29/B6 cells, within which *E coli* accumulated before undergoing translocation.[20] HlyA-containing supernatants also delayed epithelial restitution after induction of single-cell lesions in mouse colon epithelium.[21] Thus, the aim of the present study was to determine the effect of *E coli* HlyA-induced impairment of colonic epithelial barrier function on antigen translocation and colonic mucosal inflammation.

METHODS

Bacterial culture and intestinal colonisation model

HlyA-producing *E coli*-536 and *E coli*-536 haemolysin-deficient mutant (HDM) (536ΔhlyI_ΔhlyII::cat)[22]were cultured in Luria-Bertani broth at 37°C overnight and grown to log phase. For infection either *E coli*-536 or *E coli*-536 HDM was diluted to 10^6 colony-forming unit (CFU)/100 μL and administered via oral gavage to mice (200 μL) for intestinal colonisation according to previous protocols by pre-conditioning with streptomycin via drinking water to reduce the coliform microbiota.[23] Female C57BL/6J wild type (WT) mice or B6.129P2-IL10<tm1Cgn>J interleukin-10 knockout mice (*IL-10*$^{-/-}$) (Jackson Laboratories, Bar Harbor, Maine, USA) were used for colonisation. Furthermore, germfree C3H/ORL WT mice (Charles River, Sulzfeld, Germany) were inoculated for intestinal monoassociation with a lower infectious dose (10^5 *E coli*/100 μL). Mice were kept under germ-free conditions and were sacrificed 1 week after infection (approval number G0279/08). The intestine was removed and directly used for electrophysiological measurements. Further samples were fixed in parallel in paraformaldehyde or formalin for histological staining. Faeces were plated in different dilutions on selective agar for CFU counting. Faeces were also assessed for consistency and occult blood using hemoccult (CARE Diagnostica, Moellersdorf, Austria). Body weight of each mouse was monitored. Clinical colitis score was assessed as described previously.[24]

Histopathology

The tissues were fixed in a 4% formalin solution for 2 h, paraffin embedded and cut in serial sections (4 μm) for H&E staining. The pathologists were blinded to the assessment of the principal investigator. Epithelial changes were graded as described previously with a scoring range between 0 (healthy) and 12 (inflamed).[25]

Transepithelial electrical resistance, impedance spectroscopy and molecule marker fluxes

Mouse colon samples were mounted into Ussing chambers and total transmural electrical resistance was recorded by a computerised automatic clamp device (Fiebig-Hard&Software, Berlin, Germany). Resistance values were corrected by subtracting resistance of the bathing solution between the voltage-sensing electrodes. The total transepithelial resistance (R^t, TER) of the intestinal barrier consists of two components arranged in series, epithelial (R^{epi}) and subepithelial resistance (R^{sub}). By means of impedance spectroscopy it is possible to distinguish between R^{epi} and R^{sub} as previously described.[26] Concurrently, unidirectional flux measurements were performed from mucosa to serosa under short-circuit conditions. 100 μM fluorescein or 18 μM HRP (Sigma-Aldrich, St Louis, Missouri, USA) was added to the mucosal side of the tissue. At specific intervals, samples were taken from the basolateral hemichamber. Fluorescence or enzymatic activity was measured in a spectrofluorimeter (Tecan, Maennedorf, Switzerland) and permeability was calculated from flux over concentration difference.

Epithelial apoptosis

Immediately after sacrifice of animals, tissues were fixed with 2% paraformaldehyde, embedded in Tissue-Tek O.C.T. medium (Sakura, Alphen, The Netherlands) for cryosectioning and cut into 5 μm cross sections, then permeabilised with 0.2% Triton X-100 and stained with rabbit-anti-cleaved-caspase-3 (1:400, Cell Signalling Technology Inc, Danvers, Massachusetts, USA) and mouse-anti-cytokeratin-20 antibodies (1:100, Invitrogen, Karlsruhe, Germany). Apoptotic cells were counted microscopically.

Visualisation of *E coli* HlyA and epithelial integrity by immunofluorescence

Colon tissues were fixed with 2% paraformaldehyde for 3 h without rinsing the luminal content to fix the bacteria's localisation, followed by quenching the protein linking up with 25 mM glycine. The tissue was stained as whole tissue mount without cutting as recently described.[27] Briefly, the fixed tissue was permeabilised with 1% TritonX-100 in phosphate-buffered saline (PBS) for 2 h at 37°C, and subsequently incubated in blocking solution (10% goat serum, 1% bovine serum albumin, 0.8% TritonX-100 in PBS) for 3 h at room temperature. Incubation with the primary antibody in blocking solution was performed over night at 4°C. The tissue was washed with

blocking solution four times with a prolonged washing time of 1 h each, then incubated over night at 4°C with a secondary IgG antibody and washed again four times. Staining with DAPI and Phalloidin-AlexaFluor647N was performed at room temperature for ½ h (each 1:1000). The following antibodies were used: anti-HlyA, anti-*E coli*-O (1:200 provided by Lothar Beutin), anti-occludin (1:100), anti-E-cadherin (1:250), AlexaFluor-488 goat-anti-mouse, AlexaFluor-488 goat-anti-rabbit, AlexaFluor-594 goat-anti-mouse or AlexaFluor-594 goat-anti-rabbit IgG (1:500; Invitrogen). Antibody sensitivity was evaluated in *E coli*-536-infected HT-29/B6 cell culture. HT-29/B6 monolayers were grown on permeable polycarbonate filters in antibiotic-free RPMI 1640 medium as described previously.[20] Stained tissues were mounted using ProTaqs MountFlour (Biocyc, Luckenwalde, Germany). Stainings were visualised by confocal laser-scanning microscopy (C-LSM, Zeiss LSM510, Jena, Germany) with a 40× water-immersion objective (2 mm working distance for deep optical *XY*-plain sections in *Z*-stacks).

Measurement of *hlyA* in human colon biopsies

Biopsy specimens were taken from sigmoid colon from patients undergoing routine endoscopy (approval number EA4/098/09). In patients with active inflammation the tissue was taken from minor inflamed areas. DNA extraction was performed according to the manufacturer's instruction by bead beating (ZR Fecal DNA MiniPrep, Zymo Research, Irvine, California, USA). Quantitative real-time PCR (qPCR) was performed using SYBR-green with an ABI 7900HT PCR device according to manufacturer's instructions (Applied Biosystems, Mannheim, Germany) with EHEC-*hlyA* type-specific primers[8] or UPEC-*hlyA type*: HlyA536_for: 5′-TTCTGCTGTGACACT GGCAA-3′, HlyA536_rev:5′-TAACAGCACCTACCAGTGCG-3′ and the values were referred to a standard curve and compared with total bacteria/*E coli* with primers used previously (see online supplementary tables S1–S3).[28 29]

Statistical analysis

Data are expressed as mean values±SE of the mean (SEM). Statistical analysis was performed using two-tailed Student's t test or Mann–Whitney U test for non-parametric data, as appropriate. $p<0.05$ was considered statistically significant.

A detailed description of methods can be found in the online supplements.

RESULTS

Intestinal disorder in challenged animals

Oral infection of mice with 10^6 *E coli*-536 or *E coli*-536 HDM revealed colonisation of the gastrointestinal tract between 10^6 and 10^8 CFU/g faeces 48 h after infection. All successfully colonised mice were assessed for their outcome (diarrhoea and colitis activity). Infected mice revealed no or only moderate symptoms, assessed by body weight, faecal consistence and occult blood. Mice infected with the α-haemolysin-expressing *E coli*-536 showed increased colitis activity compared with controls infected with the HDM strain. As already reported, the *E coli*-536 colonised WT mice showed no or only moderate clinical symptoms,[23] whereas an increase in colitis score was measurable in the *IL-10*$^{-/-}$ colitis model and in the monoassociated (MA) mice compared with the HDM-infected animals (figure 1A).

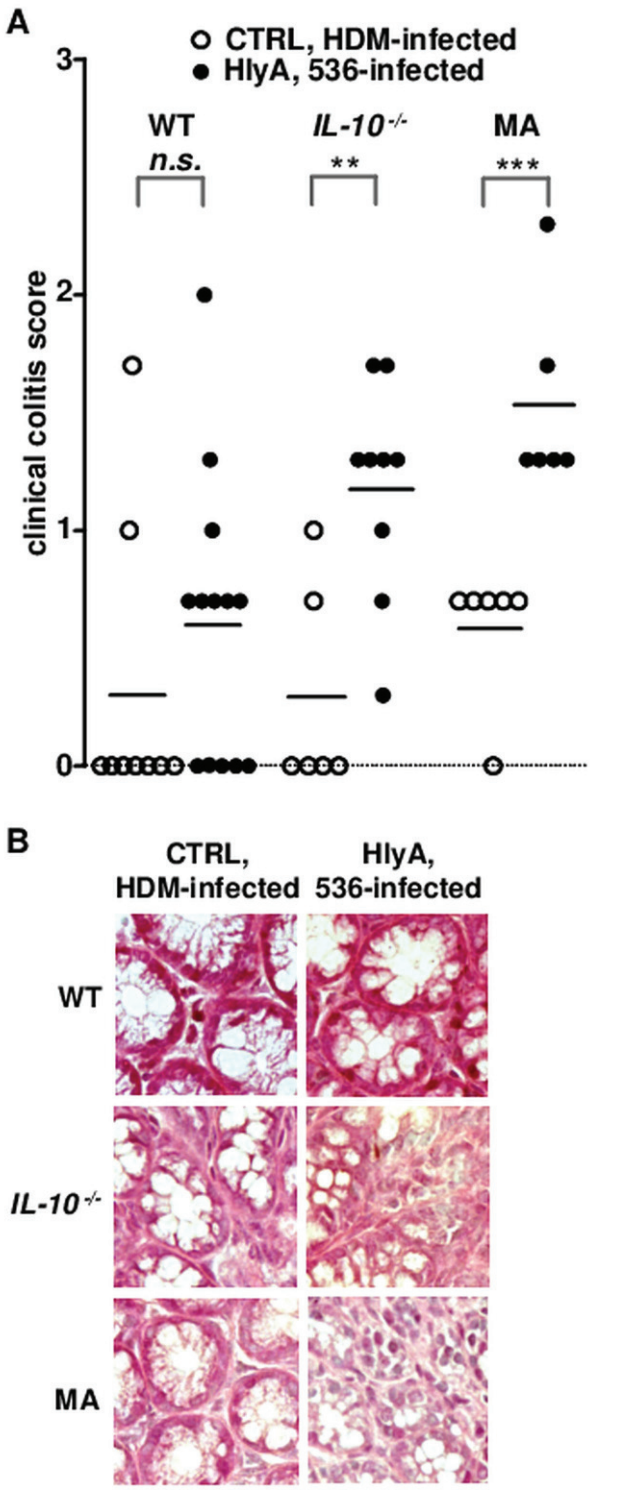

Figure 1 Colitis activity. (A) Colitis scores measured in mice after oral infection with *Escherichia coli*-536, compared with α-haemolysin (HlyA)-deficient *E coli* 536 haemolysin-deficient mutant (HDM) strain, either in wild type (WT), interleukin-10 knockout mice (*IL*−*10*$^{-/-}$) colitis model or monoassociated (MA) WT mice. Dots were single values; bars represent mean values ranging from 0 (healthy) to 4 (maximal activity of colitis). **p<0.01,***p<0.001, n.s., not significant; Student's t test. One of seven HDM-infected *IL-10* mice was not colonised and excluded from analysis. (B) Pathohistology; H&E stainings of colon mucosa of 536-colonised WT, *IL-10*$^{-/-}$ or MA mice. For comparison, healthy mucosa without lymphocyte infiltration: on the left side HDM-colonised WT or MA mouse colon. Depicted is one representative image of each group in quadruplicate. Ctrl, control.

Histopathology of the large intestine colonised with *E coli*-536

The clinical symptoms had their correlate in colon histology. The mucosa of *E coli*-536-challenged mice showed mild changes with sporadic lesions, focal loss of enterocytes, enlarged lymph follicles and slightly increased lymphocyte infiltration into the lamina propria. The histological appearance of colonised WT mice was almost normal, whereas the germfree WT mice exhibited moderate histological changes when infected with *E coli*-536 for monoassociation (figure 1B). Most importantly, the *IL-10*$^{-/-}$ mice showed increased histopathological responses to *E coli*-536 in comparison to HDM. Changes were not as severe as in active colitis, but reflect an initial/early phase of inflammation. The 536-treated *IL-10*$^{-/-}$ mice exhibited a higher colitis score of 1.8±0.4 versus 0.6±0.2 in controls ($p<0.05$, n=5, animals between 3 and 8 days post infectionem). The overall epithelium was intact, fulfilling the prerequisite for subsequent electrophysiological measurements of epithelial barrier function.

Electrophysiological observations on the colon of challenged mice

Barrier function of the mucosal epithelium was assessed in Ussing experiments. Impedance spectroscopy measurements revealed a decrease in overall transepithelial electrical resistance (R^t) in the colon colonised with *HlyA*-harbouring *E coli*-536 compared with mice colonised with strain 536-HDM (figure 2). This loss of electrical resistance of the colon specimens could be due to a drop in epithelial (R^{epi}) and in subepithelial (R^{sub}) resistance. In the case of the MA mouse model, the drop in R^t could be assigned to a drop in R^{epi}, while R^{sub} remained unaffected. In WT and *IL-10*$^{-/-}$ mice, R^t was also decreased and R^{sub} remained almost unaltered but the concomitant reduction in R^{epi} just failed to reach statistical significance.

In parallel, macromolecule permeability measurements with 44 kDa horseradish peroxidase (HRP) were performed and revealed an increase in HRP fluxes in all 536 infected mice compared with HDM controls (figure 3). The already initially increased flux in the *IL-10*$^{-/-}$ mice can be interpreted as the pre-existing pathogenic mechanism for antigen/HRP antigen uptake prior to colitis. Fluorescein (332 Da) was used as an additional marker, which in the case of unaltered macromolecule flux and thus the absence of gross lesions would have been a parameter for disturbed TJs. A slight increase in epithelial fluorescein permeability was observed in WT and MA mice (536-WT mice with 1.04±0.11 vs 0.47±0.17 nmol/cm^2/h^1 HDM-control and 536-MA mice with 0.79±0.10 vs 0.41±0.11 nmol/cm^2/h^1 HDM-control; $p<0.05$, n=5 each). However, this was only a small increase with doubled fluorescein fluxes. In the case of the 536-infected *IL-10*$^{-/-}$ colitis model this increase to 0.91±0.21 nmol/cm^2/h^1 (n=6) even failed to reach statistical significance compared with HDM-control mice (0.51±0.10 nmol/cm^2/h, n=5). Thus, this small increase in fluorescein flux does not point to severe TJ defects but may be explained by the appearance of focal leaks.

Epithelial apoptosis

Investigation of epithelial cell death—specifically the search for focal areas of increased apoptotic cell ratio—was done in the colon after staining of cleaved caspase 3. We could detect only very few sporadic apoptotic foci in *IL-10*$^{-/-}$ and MA HlyA mice, while single apoptotic events were present throughout all specimens (figure 4A). However, the apoptotic ratio in WT, *IL-10*$^{-/-}$ and MA mice infected with *E coli*-536 remained statistically unchanged compared with control HDM mice (figure 4B) and also no difference was obtained between the different models.

Confocal laser-scanning microscopy revealed lesions in the presence of HlyA-positive *E coli*

To detect possible focal leaks as observed in vitro earlier,[20] we searched microscopically for lesions and bacterial signals in immunofluorescence (IF) stainings of unsectioned mouse colon. Lesions and/or erosions in the colonic mucosa of *E coli*-536-colonised mice were observed in IF stainings with co-localisation of invaded *E coli* (figure 5A). The mucosal lesions induced by *E coli*-536 showed the same shape and size as observed earlier in rat colon and HT-29/B6 cell cultures [20] (figure 5B) with a funnel-shaped notch including bacterial signals inside (figure 5C and see online supplemental movie).

Size estimation of focal leaks

For demonstrating bacterial IF signals MA mice were studied in more detail (figure 6A). Focal leaks and bacterial signals could be detected in *E coli*-536 but not in *E coli*-536-HDM-colonised mucosa. For quantification, focal leaks were counted microscopically, digitally marked and sized. We found one to four gross

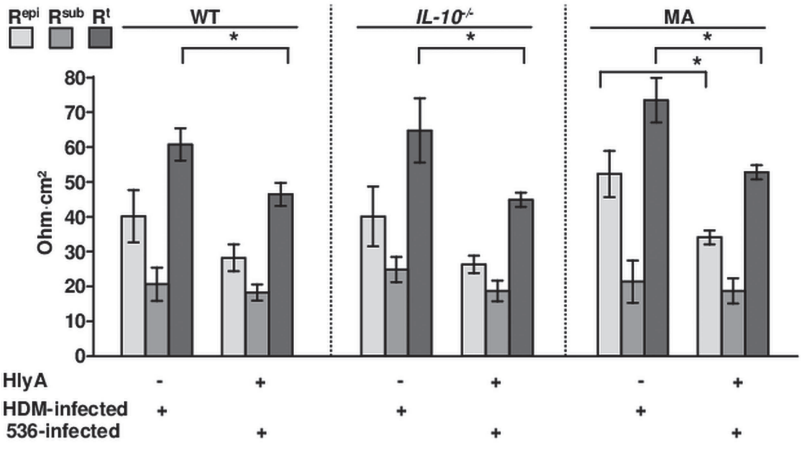

Figure 2 Electrical resistance of mouse colon measured by impedance spectroscopy. Overall transmural electrical resistance (R^t, dark grey bars) consists of epithelial resistance (R^{epi}, light grey bars) and subepithelial resistance (R^{sub}, bright bars). The left panel shows the electrical resistance of wild type (WT) mice infected either with the haemolysin-deficient mutant (HDM) of *Escherichia coli* as control or with the α-haemolysin (HlyA)-carrying *E coli*-536 (n=7 and 8). The middle panel shows the results obtained from interleukin-10 knockout mice (n=6 and 8) and the right panel measurements of monoassociated (MA) WT mice (n=5 and 5) colonised in the same manner by the *E coli* strains. *$p<0.05$ (Student's t test).

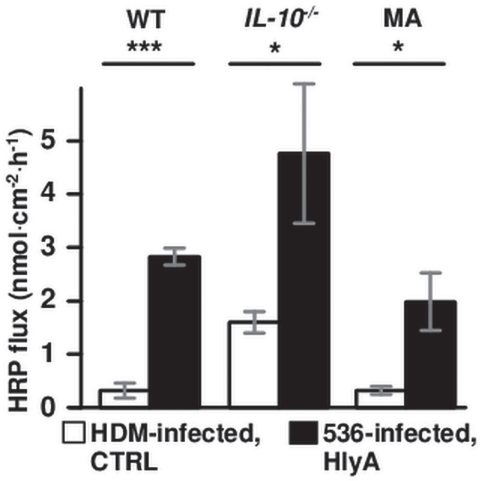

Figure 3 Antigen permeability of mouse colon measured in Ussing chambers. Horseradish peroxidase (HRP) fluxes from mucosal to serosal compartment were assessed by enzymatic reactivity in the serosal compartment. *p<0.05 (three to four animals per group, Student's t -test). Crtl, control; HDM, haemolysin-deficient mutant; HlyA, α-haemolysin; IL-10$^{-/-}$, interleukin 10 knockout; MA, monoassociated; WT, wild type.

leaks with a size range of 2000–50 000 μm^2 per single leak in areas of 0.049 cm^2 (equalling 4 900 000 μm^2; the tissue area of the Ussing experiments). An accumulated mean leak area of 54 000 μm^2 was measured in the 536-MA mice, which is 1.1% of the respective tissue area. Equivalent structures to focal leaks can also be found in the 536-infected WT mice (n=7, figure 6B) but no such leaks were detected in *E coli*-536-HDM-colonised WT mice. However, the *IL-10*$^{-/-}$ mouse model showed a few focal leaks when colonised with HlyA-negative *E coli*, though not as large as observed in the *E coli*-536-infected *IL-10*$^{-/-}$ mouse, probably due to the already ongoing inflammatory stage (n=3, figure 6B). The quantification of leak size revealed an increase for each mouse model with *E coli*-536 versus HDM colonisation. A calculation of epithelial resistance of an affected epithelium (R_{epi_leak}) with 1.1% leak area fits to the measured values in impedance spectroscopy (see online supplemental calculation). Moreover, the overall leak area of *E coli*-536-infected HT-29/B6 cell monolayers increased with bacterial burden (figure 6C).

HlyA increased in human colon mucosa during active UC

As reported previously, *hlyA* was not detected in bacterial cultures from biopsy specimens using EHEC-specific *hlyA*-primers.[8 30] However, in qPCR measurements using our primer for UPEC-specific *hlyA*-type and DNA extraction from biopsy samples without pre-cultivation of bacteria, we found *hlyA*-positive *E coli* in 19 of 22 patients with UC, 9 of 9 patients with active CD and 9 of 12 healthy controls (see online supplementary tables S1–S3). While prevalence between healthy controls and patients with IBD was not different, there was a more than 10-fold increase in *hlyA* level in mucosal biopsies of active UC compared with healthy controls (p<0.05, figure 7A). The total bacterial count was not significantly altered between the groups (7110±3620 copy numbers/ng DNA in active UC vs 4150±3700 copy numbers/ng DNA in healthy controls) but showed a tendency towards an increase in *Enterobacteriacea* as indicated by Eco primer (figure 7A). The increase in bacterial numbers harbouring *E coli* HlyA seemed to be specific for UC,

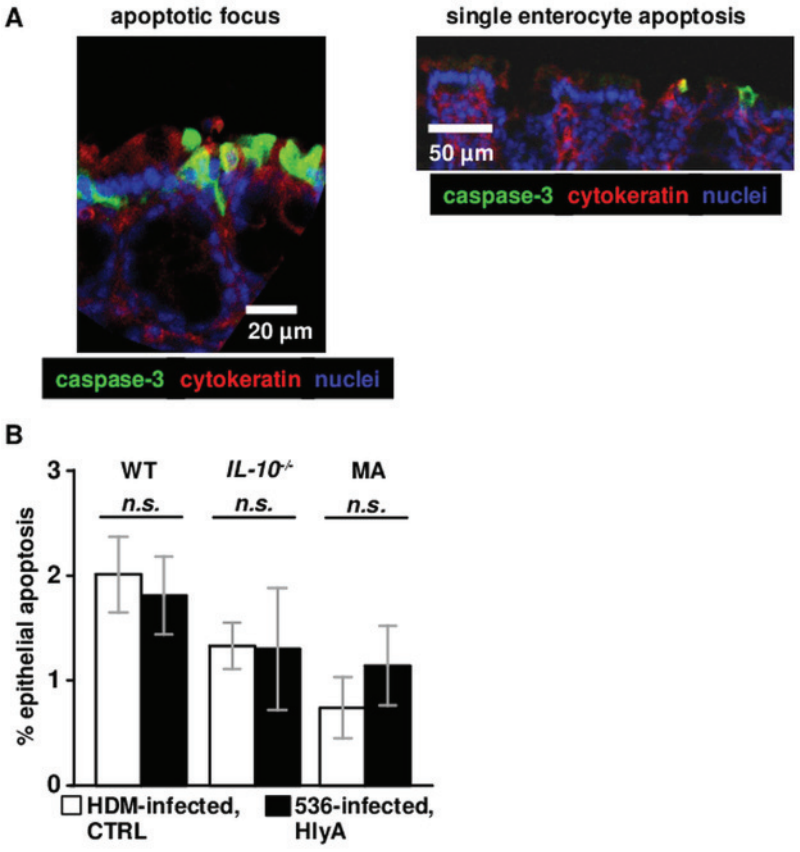

Figure 4 Epithelial apoptosis. (A) Epithelial cell apoptosis in colonic tissue of *Escherichia coli*-536 infected mice detected with anti-caspase-3 immunofluorescence microscopy 5 days after infection. Tissues from infected animals were immediately fixed after sacrification. Single apoptotic events were located evenly throughout the colonic epithelium, whereas apoptotic fociwere detected only sporadically. Depicted is one representative image of at least three animals. (B) Quantification of cleaved caspase-3-stained apoptotic events (apoptotic rate) was performed in wild type (WT) (n=3), interleukin 10 knockout (*IL-10*$^{-/-}$) (n=4), monoassociated (MA) (n=3) mice colon tissue colonised with *E coli* 536 (HlyA) or the haemolysin-deficient mutant (HDM) control strain (given as % apoptotic cells in a low-power field). Four different serial tissue cross sections of each animal were counted with at least 1000 DAPI and cytokeratin-20-positive epithelial cells (n-values represent the number of animals in the analysis). DAPI, 4′-6-diamidino-2-phenylindole dihydrochloride, colours nuclei blue; n.s., not significantly different in Student's t test.

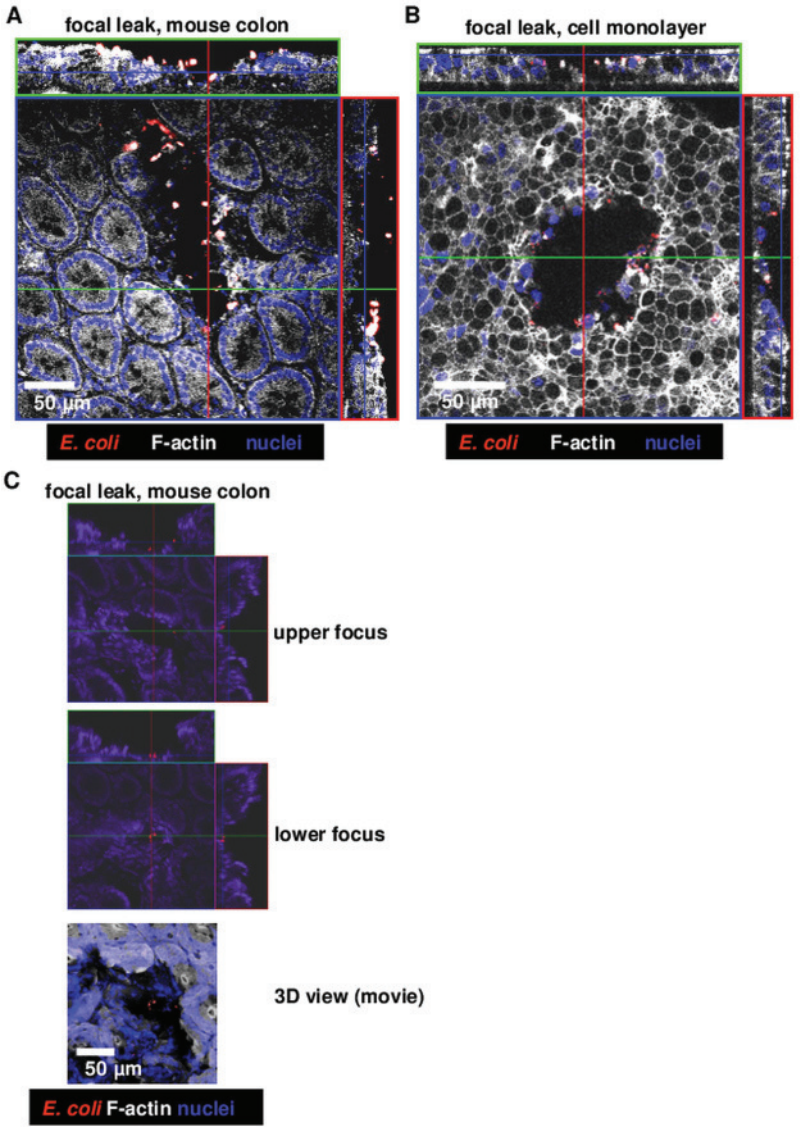

Figure 5 Confocal laser-scanning microscopy of immunfluorescence stainings of *Escherichia coli* α-haemolysin (HlyA)-induced lesions. Whole mount staining of mucosae from challenged mice or epithelial cell monolayers (without sectioning). (A) Focal leak in *E coli*-536-colonised wild type mouse colon, (B) focal leak in a human colon epithelial cell monolayer HT-29/B6, (C) smaller focal leak with concomitant bacterial invasion in mouse colon, see also online supplemental movie for 360° 3D view.

since high concentrations of HlyA were neither found in colon samples from active CD nor in healthy individuals (figure 7B). Moreover, it was possible to find focal leaks in human sigmoid colon in patients with UC by confocal endomicroscopy with biopsy sampling and subsequent IF staining and C-LSM of the tracked biopsies (figure 7C, see online supplementary figure S1). In the colon biopsies of non-inflamed regions from patients with UC small lesions could be pictured which showed HlyA-positive signals inside.

DISCUSSION

Induction of focal leaks by *E coli* HlyA

E coli HlyA-induced focal leaks—originally discovered in HT-29/B6 monolayers[20]—were also detected in three in vivo mouse models. Generally, the UPEC strain 536 used in our present study has a different genetic constitution compared with attaching and effacing (A/E) *E coli*, which produce typical lesions with pedestal actin formation, mediated by effector proteins like intimin or EspF.[31] In contrast to a typical EHEC, *E coli*-536 lacks the pathogenicity island locus of enterocyte effacement for A/E lesions. Thus, we proposed and confirmed an alternative pathomechanism for HlyA in initiating lesions in the intestinal mucosa.

Cellular response mechanisms to HlyA

A/E-typical pedestal actin formation was not seen in microscopic images of *E coli*-536-colonised epithelium. However, HlyA is known to create channels in the host cell membrane that promote potassium efflux, affect Akt/protein kinase B activity [32] and enable calcium influx into the host cell with various consequences resulting from calcium-dependent cell signalling. Regardless of the contribution of host cell calcium channels, a cation-selective pore like HlyA itself can mediate a calcium influx which may lead to cytoskeleton alterations or cell lysis. Rapid calcium oscillations have been described in renal epithelial cells in response to UPEC HlyA.[16] The calcium-dependent response of enterocytes to β-PFT haemolysins in sublytic concentrations shows different cellular characteristics, including impaired epithelial restitution, cytoskeletal and TJ disturbance as reported for aerolysin (AerA) from *Aeromonas hydrophila*.[33] In contrast, characteristic focal leaks as induced by HlyA were not found in AerA-treated intestinal epithelial cells.[33]

The various pathogenic impacts of β-PFTs could be explained by differences in expression or the site of infection, and by toxin polymorphisms. Even strain-specific differences in genomic sequences may have an impact on their different modes of pathogenic action (eg, in *E coli* HlyA only ~70%

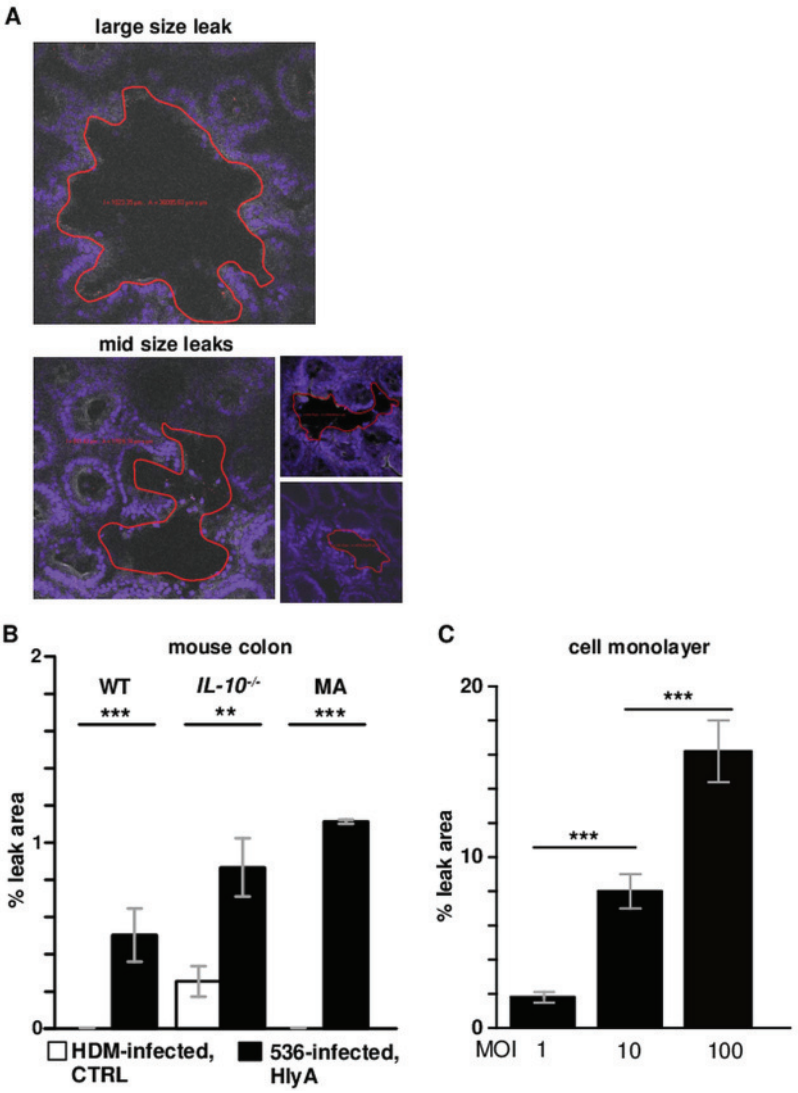

Figure 6 Microscopic size estimation of focal leaks. (A) Examples of large and mid sized leaks, marked (red line) and measured with Zeiss LSM Image Examiner software for focal leak area size calculation. (B) Quantitation of leak area as % of the whole investigated area in a low-power field. In whole mount immunofluorescence staining of uncut mouse colon, an observation area of approximately 0.1 cm^2 was screened microscopically for focal leaks. The identified leaks were digitally marked and the overall area of one to four single leaks was divided by the overall measuring area. In haemolysin-deficient mutant (HDM) treated interleukin 10 knockout (*IL-10*$^{-/-}$) mice focal leaks were revealed, whereas in HDM-treated wild type (WT) and monoassociated (MA) mice no leaks were observed in three independent stainings of at least three animals (n=3). (C) Dose-dependent appearance of focal leaks in a human colonic HT-29/B6 epithelial cell monolayers after 3 h treatment with different multiplicity of infection (MOI) of *Escherichia coli*-536 (n=3 each MOI). **p<0.01,***p<0.001, n.s., not significant; Student's *t*-test. HlyA, α-haemolysin.

sequence identity between EHEC and UPEC HlyA types exists). However, the role of calcium influx through the HlyA pore in epithelial cells, resulting in signalling events which possibly cause focal leak formation, needs further investigations. Hypothetical modes of focal leak creation include epithelial damage (eg, via cell death mechanisms such as necrosis or autophagia, while apoptosis could be excluded), and/or the inhibition of cellular restitution of small lesions.

Disruption of the epithelial barrier by HlyA

Epithelial barrier function of the colon was seriously compromised by HlyA. This was less evident from measurements of electrical resistance, which was only slightly affected in HlyA-positive *E coli* 536-infected mice. However, this was clearly evident from Ussing-chamber flux measurements with larger molecules. We decided to use HRP as antigen influx marker because it has two advantages: it is a suitable marker for passage through leaks as it cannot diffuse paracellularly through the TJ; and it can be measured enzymatically which guarantees that the molecule remains uncleaved and avoids misinterpretation from released labels. Thus, the increased HRP flux measured in this study can be explained by the appearance of focal leaks in all three mouse models after *E coli*-536 colonisation. The size estimation of focal leaks induced by HlyA-carrying *E coli*-536 revealed that approximately 1% of the observed mucosa was affected, and a calculation of the increased conductivity of the leaky epithelium revealed that this focal leak size explains most of the change in epithelial resistance (see online supplemental calculation). However, we cannot exclude that other pathological effects induced by *E coli*-536 such as TJ changes with strand discontinuities may have an additional impact. We also excluded HRP transcytosis as an alternative mechanism of macromolecule uptake by histochemistry. No increase in endocytosis by colonocytes was seen (see online supplementary figure S2), which would have been an electrically silent process, not influencing transepithelial resistance measurements. TJ changes could only be observed around focal leaks (see online supplementary figure S3 as eg, condensation of occludin) and global changes in strand forming TJ proteins, such as claudins 1–3, could be ruled out by Western blot densitometry (see online supplementary figure S4).

Accelerated inflammation by α-haemolysin-expressing *E coli*

In addition, α-haemolysin-expressing *E coli* enhanced inflammation in our inflammatory mouse models. As already reported, this inflammatory response was not measurable in WT mice,[2 3] but was present in the vulnerable *IL-10*$^{-/-}$ colitis model. A difference was also seen in HlyA-carrying versus HDM-*E coli*

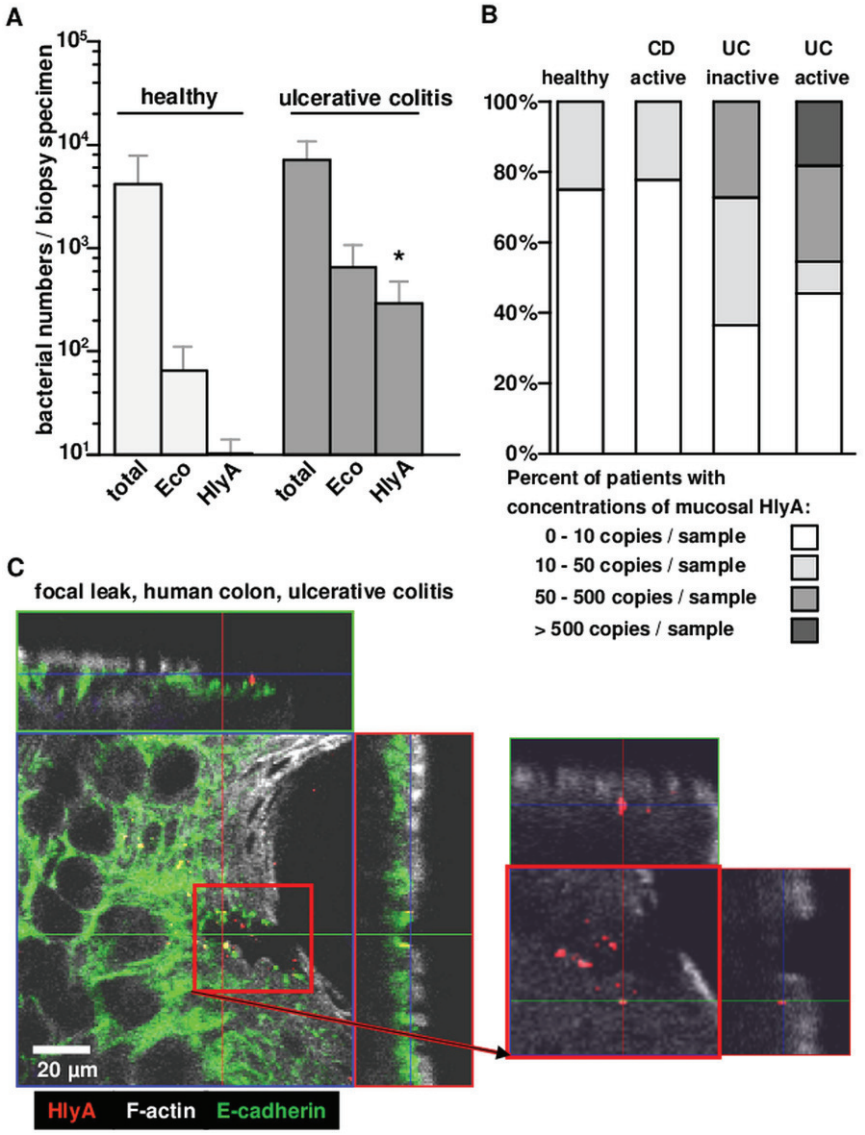

Figure 7 α-Haemolysin (HlyA) in human colon. (A) Haemolysin measurements in human colon biopsies by quantitative PCR. Number of total bacteria (total), of *Escherichia coli* (Eco) or of HlyA 536-positive *E coli* per PCR specimen (1 ng DNA, equalling approx. 10 µg mucosal biopsy) of 12 healthy controls compared with 11 patients with ulcerative colitis with active colitis. *p<0.05 in Mann–Whitney U test. (B) Percentage of patients with concentrations of HlyA-positive mucosal *E coli*. PCR copy numbers as indicated per colon biopsy specimen (1 ng DNA) from 12 healthy controls, 9 patients with active CD, 11 patients with UC in remission and 11 patients with active UC. (C) Focal leak with HlyA-positive signals in human colon mucosa. Detail of a focal leak at the edge of a crypt. Confocal laser-scanning microscopy on whole mount biopsy specimens after immunfluorescence staining obtained from a patient with inactive UC as one representative image in triplicate. Intact endogenous control area without HlyA signal and a focal leak with appearance of HlyA (red), while E-cadherin (green) and F-actin (white) are absent at the edge of a crypt. Nuclei are coloured blue. The insert on the right side shows a detail with F-actin staining and HlyA signals at and in the epithelium. See online supplementary figure S1 for the overview of the affected region within a non-inflamed area and the workflow.

groups in the MA mice in the initial stage of colitis. Such mild but significant effects resulting from the onset of colitis could also be assessed in other studies with mild inflammation in *IL-10*$^{-/-}$ mice.[34]

α-Haemolysin-expressing *E coli* (eg, UPEC) were frequently found in faeces of healthy humans and livestock animals.[35 36] Within the healthy mucosa of the colon, no intraepithelial bacteria should be present. Only in cases of infection (eg, EHEC), or in the presence of inflammation (IBD), do high numbers of mucosa-associated or intraepithelial *E coli* invade the colonic mucosa, but so far without evidence of any correlation between the severity of inflammation and the bacterial count.[37–40]

High prevalence of *hlyA*, especially in UC biopsies

qPCR measurements in human biopsy specimens with UPEC *hlyA*-type specific primers revealed an overall high prevalence of *hlyA* in the colon mucosa, but higher levels in patients with active UC. This is in line with previous findings of high *hlyA* occurrence in human stool samples in a non-inflamed stage.[35] Moreover, Martinez-Medina and colleagues[9] found *hlyA* in about 20% of *E coli* isolates from the biopsies of 10 patients with CD and 12 healthy control patients with similar primers, and in another study using Chip technology for comparative genomics, *E coli* isolates from the biopsies of two of five patients with UC were positive for *hlyA*.[41] Our findings could depict for the first time that HlyA is indeed usually present, but much more frequently in colonic samples of patients with active UC, and thus may play a significant role in intensifying inflammation. HlyA may play a role in initiating lesions in UC, since we could identify HlyA in IF stainings inside and around lesions of endoscopically unaffected tissues from patients with mild inflamed disease. It is conceivable that HlyA-carrying *E coli* have easier access to the colonic mucosa when it is inflamed.[40] In addition, HlyA is frequently associated with bacterial outer membrane vesicles, which may contain a cocktail of various proteins/toxins from the bacterial periplasm, including factors contributing to facilitated access to the mucosa.

CONCLUSION

Our findings suggest that *E coli* HlyA can induce focal leaks in cell models, and in active UC and native mouse colon, and thereby increase antigen invasion as indicated by HRP flux measurements, providing an additional pathological mechanism for antigen influx consistent with the 'leaky gut concept'. Furthermore, this study shows that extra-intestinal pathogenic *E coli*, when colonising the intestine in high numbers, trigger

inflammation or act as inductors prior to inflammation in quiescent colitis. Thus, erosions and ulcers observed in UC could develop from increased apoptosis and/or be initiated via mediators, such as HlyA.

Selective reduction of bacteria with barrier-breaking features (eg, haemolysins) raises the possibility of new treatment options in patients with IBD. Future studies may prove that vaccination against certain *Enterobacteriaceae* (as in chronic cystitis) or bacteriotherapy with (for example) non-pathogenic *E coli* strains, are new and effective alternative therapies for IBD.

Acknowledgements The excellent technical assistance of Detlef Sorgenfrei and Anja Fromm is gratefully acknowledged. We thank Gábor Nagy who constructed *E coli*-536-HDM. This work is dedicated to Professor Martin Zeitz († 26 November 2013).

Contributors Conceived and designed the experiments: RB, JDS, HT. Performed the experiments: RB, ES, I-FML, SW, LJJ, TJ, CE. Acquisition of biopsy material from endoscopy: CB, ES. Analysed the data: RB, ES, I-FML, LHW, J-DS, HT, DG, CB. Important intellectual support: ES, UD, LB, LHW, DG, CE, MF, BS. Contributed reagents/materials/analysis tools: TJ, LHW, UD, LB, LJJ, DG, CB, MF, JDS. Wrote the paper: RB. Critical revision and study supervision: MF, J-DS.

Funding Supported by Deutsche Forschungsgemeinschaft (Schu 559/11 and SFB 852).

Competing interests None.

Patient consent Obtained.

Ethics approval Animal experiments were approved by the local governmental authorities under the approval number G0279/08 (LaGeSo, Landesamt für Gesundheit und Soziales, Berlin, Germany). For the use of human material this study adhered to the Declaration of Helsinki, and ethics approval for research was obtained from The Ethics Committee of the Charité Berlin (approval number EA4/098/09 and EA2/179/05). All patients who participated in the investigation signed written informed consent forms. Children were not included in the study.

Provenance and peer review Not commissioned; externally peer reviewed.

REFERENCES

1 Gradel KO, Nielsen HL, Schønheyder HC, *et al*. Increased short- and long-term risk of inflammatory bowel disease after salmonella or campylobacter gastroenteritis. *Gastroenterology* 2009;137:495–501.
2 Sasaki M, Klapproth JM. The role of bacteria in the pathogenesis of ulcerative colitis. *J Signal Transduct* 2012;2012:704953.
3 Anderson CA, Boucher G, Lees CW, *et al*. Meta-analysis identifies 29 additional ulcerative colitis risk loci, increasing the number of confirmed associations to 47. *Nat Genet* 2011;43:246–52.
4 Franke A, McGovern DP, Barrett JC, *et al*. Genome-wide meta-analysis increases to 71 the number of confirmed Crohn's disease susceptibility loci. *Nat Genet* 2010;42:1118–25.
5 Cooke EM, Ewins SP, Hywel-Jones J, *et al*. Properties of strains of Escherichia coli carried in different phases of ulcerative colitis. *Gut* 1974;15:143–6.
6 Frank DN, St Amand AL, Feldman RA, *et al*. Molecular-phylogenetic characterization of microbial community imbalances in human inflammatory bowel diseases. *Proc Natl Acad Sci U S A* 2007;104:13780–5.
7 Cucchiara S, Iebba V, Conte MP, *et al*. The microbiota in inflammatory bowel disease in different age groups. *Dig Dis* 2009;27:252–8.
8 Kotlowski R, Bernstein CN, Sepehri S, *et al*. High prevalence of Escherichia coli belonging to the B2+D phylogenetic group in inflammatory bowel disease. *Gut* 2007;56:669–75.
9 Martinez-Medina M, Aldeguer X, Lopez-Siles M, *et al*. Molecular diversity of Escherichia coli in the human gut: new ecological evidence supporting the role of adherent-invasive E. coli (AIEC) in Crohn's disease. *Inflamm Bowel Dis* 2009;15:872–82.
10 Jakobsen L, Garneau P, Kurbasic A, *et al*. Microarray-based detection of extended virulence and antimicrobial resistance gene profiles in phylogroup B2 Escherichia coli of human, meat and animal origin. *J Med Microbiol* 2011;60(Pt 10):1502–11.
11 Unno N, Fink MP. Intestinal epithelial hyperpermeability. Mechanisms and relevance to disease. *Gastroenterol Clin North Am* 1998;27:289–307.
12 Zeissig S, Bürgel N, Günzel D, *et al*. Changes in expression and distribution of claudin-2, -5 and -8 lead to discontinuous tight junctions and barrier dysfunction in active Crohn's disease. *Gut* 2007;56:61–72.
13 Gitter AH, Wullstein F, Fromm M, *et al*. Epithelial barrier defects in ulcerative colitis: characterization and quantification by electrophysiological imaging. *Gastroenterology* 2001;121:1320–8.
14 Taddei CR, Fasano A, Ferreira AJ, *et al*. Secreted autotransporter toxin produced by a diffusely adhering Escherichia coli strain causes intestinal damage in animal model assays. *FEMS Microbiol Lett* 2005;250:263–9.
15 Boisen N, Ruiz-Perez F, Scheutz F, *et al*. Short report: high prevalence of serine protease autotransporter cytotoxins among strains of enteroaggregative Escherichia coli. *Am J Trop Med Hyg* 2009;80:294–301.
16 Uhlén P, Laestadius A, Jahnukainen T, *et al*. Alpha-haemolysin of uropathogenic E. coli induces Ca^{2+} oscillations in renal epithelial cells. *Nature* 2000;405:694–7.
17 Songserm T, Zekarias B, van Roozelaar DJ, *et al*. Experimental reproduction of malabsorption syndrome with different combinations of reovirus, Escherichia coli, and treated homogenates obtained from broilers. *Avian Dis* 2002;46:87–94.
18 Raimondi F, Kao JP, Kaper JB, *et al*. Calcium-dependent intestinal chloride secretion by Vibrio parahaemolyticus thermostable direct hemolysin in a rabbit model. *Gastroenterology* 1995;109:381–6.
19 Hutto DL, Wannemuehler MJ. A comparison of the morphologic effects of Serpulina hyodysenteriae or its beta-hemolysin on the murine cecal mucosa. *Vet Pathol* 1999;36:412–22.
20 Troeger H, Richter JF, Beutin L, *et al*. E. coli alpha-hemolysin induces focal leaks in colonic epithelium—a novel mechanism of bacterial translocation. *Cell Microbiol* 2007;9:2530–40.
21 Günzel D, Florian P, Richter JF, *et al*. Restitution of single-cell defects in the mouse colon epithelium differs from that of cultured cells. *Am J Physiol Reg Integr Comp Physiol* 2006;290:R1496–507.
22 Nagy G, Altenhoefer A, Knapp O, *et al*. Both alpha-haemolysin determinants contribute to full virulence of uropathogenic Escherichia coli strain 536. *Microbes Infect* 2006;8:2006–12.
23 Diard M, Garry L, Selva M, *et al*. Pathogenicity-associated islands in extraintestinal pathogenic Escherichia coli are fitness elements involved in intestinal colonization. *J Bacteriol* 2010;192:4885–93.
24 Araki A, Kanai T, Ishikura T, *et al*. MyD88-deficient mice develop severe intestinal inflammation in dextran sodium sulfate colitis. *J Gastroenterol* 2005;40:16–23.
25 Katakura K, Lee J, Rachmilewitz D, *et al*. Toll-like receptor 9-induced type I IFN protects mice from experimental colitis. *J Clin Invest* 2005;115:695–702.
26 Bürgel N, Bojarski C, Mankertz J, *et al*. Mechanisms of diarrhea in collagenous colitis. *Gastroenterology* 2002;123:433–43.
27 Bratz K, Bücker R, Gölz G, *et al*. Experimental infection of weaned piglets with Campylobacter coli—excretion and translocation in a pig colonisation trial. *Vet Microbiol* 2013;162:136–43.
28 Amann RI, Binder BJ, Olson RJ, *et al*. Combination of 16S rRNA-targeted oligonucleotide probes with flow cytometry for analyzing mixed microbial populations. *Appl Environ Microbiol* 1990;56:1919–25.
29 Bartosch S, Fite A, Macfarlane GT, *et al*. Characterization of bacterial communities in feces from healthy elderly volunteers and hospitalized elderly patients by using real-time PCR and effects of antibiotic treatment on the fecal microbiota. *Appl Environ Microbiol* 2004;70:3575–81.
30 Sepehri S, Khafipour E, Bernstein CN, *et al*. Characterization of Escherichia coli isolated from gut biopsies of newly diagnosed patients with inflammatory bowel disease. *Inflamm Bowel Dis* 2011;17:1451–63.
31 Vingadassalom D, Kazlauskas A, Skehan B, *et al*. Insulin receptor tyrosine kinase substrate links the E. coli O157:H7 actin assembly effectors Tir and EspF(U) during pedestal formation. *Proc Natl Acad Sci U S A* 2009;106:6754–9.
32 Wiles TJ, Dhakal BK, Eto DS, *et al*. Inactivation of host Akt/protein kinase B signaling by bacterial pore-forming toxins. *Mol Biol Cell* 2008;19:1427–38.
33 Bücker R, Krug SM, Rosenthal R, *et al*. Aerolysin from Aeromonas hydrophila perturbs tight junction integrity and cell lesion repair in intestinal epithelial HT-29/B6 cells. *J Infect Dis* 2011;204:1283–92.
34 Martin FP, Rezzi S, Philippe D, *et al*. Metabolic assessment of gradual development of moderate experimental colitis in IL-10 deficient mice. *J Proteome Res* 2009;8:2376–87.
35 Opal SM, Cross AS, Gemski P, *et al*. Aerobactin and alpha-hemolysin as virulence determinants in Escherichia coli isolated from human blood, urine, and stool. *J Infect Dis* 1990;161:794–6.
36 Jakobsen L, Garneau P, Bruant G, *et al*. Is Escherichia coli urinary tract infection a zoonosis? Proof of direct link with production animals and meat. *Eur J Clin Microbiol Infect Dis* 2012;31:1121–9.
37 Schultsz C, Moussa M, van Ketel R, *et al*. Frequency of pathogenic and enteroadherent Escherichia coli in patients with inflammatory bowel disease and controls. *J Clin Pathol* 1997;50:573–9.
38 Schultsz C, Van Den Berg FM, Ten Kate FW, *et al*. The intestinal mucus layer from patients with inflammatory bowel disease harbors high numbers of bacteria compared with controls. *Gastroenterology* 1999;117:1089–97.
39 Kleessen B, Kroesen AJ, Buhr HJ, *et al*. Mucosal and invading bacteria in patients with inflammatory bowel disease compared with controls. *Scand J Gastroenterol* 2002;37:1034–41.
40 Swidsinski A, Ladhoff A, Pernthaler A, *et al*. Mucosal flora in inflammatory bowel disease. *Gastroenterology* 2002;122:44–54.
41 Vejborg RM, Hancock V, Petersen AM, *et al*. Comparative genomics of Escherichia coli isolated from patients with inflammatory bowel disease. *BMC Genomics* 2011;12:316.

GUT

α-Haemolysin of *Escherichia coli* in IBD: a potentiator of inflammatory activity in the colon

Roland Bücker, Emanuel Schulz, Dorothee Günzel, et al.

Gut published online February 17, 2014
doi: 10.1136/gutjnl-2013-306099

Supplemental Information

Supplemental calculation. Size estimation of focal leaks. Within the total tissue area of the Ussing chamber (0.049 cm2 = 4,900,000 µm²), 1 to 4 leaks were identified in the *E. coli*-536-mouse colon. These leaks added up to a mean leak area of 54,000 µm² which is about 1% of the respective tissue area. The quantitation of leak size revealed an increase in each of the 3 mouse models in *E. coli*-536 versus HDM colonization (manuscript figure 6). To assess if the overall leak area in an epithelium can explain the degree of epithelial barrier function impairment observed in Ussing chamber experiments (manuscript figures 2 & 3), we carried out the following calculations for epithelial conductance (G):

$$G_{epi\,leak} = \left(G_{epi} \cdot (100\% - \%\,leak\ area) + G_{leak} \cdot \%\,leak\ area\right)$$

where G*epi* leak indicates the conductance of the focal leak-affected epithelium, G*epi* the conductance of an epithelium without focal leaks and G*leak* the conductance within a leak area. Under control conditions, impedance measurements indicated epithelial conductances G*epi* of 20 mS/cm^2 (resistance of 50 Ω·cm^2) in epithelia without leaks. Using conductance scanning, Günzel et al. (2006) estimated a single-cell leak to amount to a total conductance of 1.73 µS.[21] Assuming a cell radius of about 5 to 7 µm, conductivity of the leak area would be about 1,000 to 2,000 mS/cm^2. Using the more conservative estimate for G*leak* of about 1,000 mS/cm^2 , the above equation yields:

$$G_{epi\,leak} = \left(20\,mS/cm^2 \cdot (100\% - 1\%\,leak\ area) + 1000\,mS/cm^2 \cdot 1\%\,leak\ area) = 29.8\,mS/cm^2\right)$$

Consequently, resistance of the leak-affected epithelium (R*epi leak*) is estimated to amount to:

$$R_{epi\,leak} = {}^{1000}\!/_{G_{epi\,leak}} = {}^{1000}\!/_{29.8\ mS/cm^2} = 33.6\ \Omega\ cm^2$$

Thus, the estimated value of R*epi leak* is in good agreement with the measured values in impedance analysis (manuscript figure 2, right panel).

TABLE S1. Patients and healthy controls for biopsy sampling

Diagnosis	n	Age (mean ± SD)	Gender (Females / Males)
Healthy controls	12	53.4 ± 13.9	5 / 7
Crohn's diease, active inflammation	9	43.9 ± 15.2	3 / 6
Ulcerative colitis, inactive	11	50.6 ± 15.3	4 / 7
Ulcerative colitis, active inflammation	11	45.7 ± 10.9	4 / 7

TABLE S2. PCR Primers

Target	Primer	Sequences	Reference
UPEC-like *hlyA*	HlyA536F	TTCTGCTGTGACACTGGCAA	This study
	HlyA536R	TAACAGCACCTACCAGTGCG	
EHEC-like *hlyA*	HlyA59F	TGCAGCCTCCAGTGCATCCCTC	Kotlowski et al. 2007 [8]
	HlyA59R	CTTACCACTCTGACTGCGATCAGC	
Total bacteria	UniF340	ACTCCTACGGGAGGCAGCAGT	Amann et al. 1990 [28]
	UniR514	ATTACCGCGGCTGCTGGC	
E. coli	Eco1457F	CATTGACGTTACCCGCAGAAGAAGC	Bartosch et al. 2004 [29]
	Eco1652R	CTCTACGAGACTCAAGCTTGC	

TABLE S3. Primer specificity

Strain	Pathovar	PCR primer HlyA536 (this study)	PCR primer HlyA59 (Kotlowski, 2007) [8]
E. coli 536	UPEC	+	
E. coli UMNK88	ETEC	+	
E. coli ABU83972	UPEC-like, asymptomatic bacteriuria	+	
E. coli O26NM	EHEC	+	
E. coli ABU37	UPEC-like, asymptomatic bacteriuria	+	
E. coli ABU27	UPEC-like, asymptomatic bacteriuria	+	
E. coli O83:K24:H31	commensal	+	
E. coli J96	UPEC	+	
E. coli 83-75	STEC/EHEC		+
E. coli O157:H7	EHEC		+
E. coli O111:H8	EHEC		+
E. coli O103:H2	EHEC		+
E. coli O26:H11	EHEC		+
E. coli EH41	EHEC		+

Note. Table shows positive PCR products for *E. coli* HlyA calculated by Primer-BLAST. Pairwise alignment with BLAST for *HlyA* e.g. between UPEC *E. coli* 536 and EHEC *E. coli* O157:H7 showed only 70% identity in nucleotide sequence.

Supplemental Methods to qPCR conditions. Amplification and detection of DNA by real-time PCR was performed with ABI-7900HT (Applied Biosystems) using optical grade 96-well plates. Duplicate samples were routinely used for the determination of DNA by real-time PCR. The PCR reaction was performed in a total volume of 25 µl using the SYBR Green PCR Master Mix (Applied Biosystems), containing 100 nM of each of the forward and reverse primers. The reaction conditions for amplification of DNA were 95°C for 10 min and 40 cycles of 95°C for 15 s and 60°C for 1 min. Afterwards dissociation curves were performed to check for unspecific amplification products. Absolute quantification was calculated by a concentration curve of known DNA / CFU ratios.

Confocal endomicroscopy in human colon in combination with *ex vivo* immunofluorescence microscopy revealed colocalisation of microlesions and HlyA-positive *E. coli*. Haemolysin-carrying *E. coli* can be identified in human mucosa from UC patients with mild inflammation. In order to investigate endoscopically the changes of the colon mucosa, we used video *chromo*endoscopy in combination with confocal *endo*microscopy (CEM) for visualisation. Forceps biopsies were taken (whole mount stainings) and C-LSM with 40x water-immersion objective for *E. coli* and HlyA as well as E-cadherin, occludin and F-actin. In the endoscopic observation healthy areas were noticed as well as lamina propria infiltrates around the crypts with concomitant swelling (edema), an increase of submucosal vascularisation and/or microlesions (figure S1 A). The same mucosal areas examined by CEM were removed by forceps biopsy for subsequent IF staining. C-LSM identified similar signals around or in microlesions, reflecting focal leaks as found in the animal models. IF stainings of these areas could be assigned to the CEM pictures *in vivo* (figure S1 B). In IF staining of the specimens signals of *E. coli* or HlyA were visible together with more diffuse signals of E-cadherin or F-actin, whereas clear TJ meshwork patterns could be found in endogenous control stainings of healthy mucosal areas from the same patient (fig. S1 C). The diffuse signals of occludin or E-cadherin were most prominent around affected areas reflecting barrier disturbance, similar to the focal leaks observed in cell culture, rat colon (Troeger et al., 2007)[20] or mouse colon colonised by *E. coli*-536 (manuscript fig. 5).

Figure S1 ***human coloscopy, biopsies***

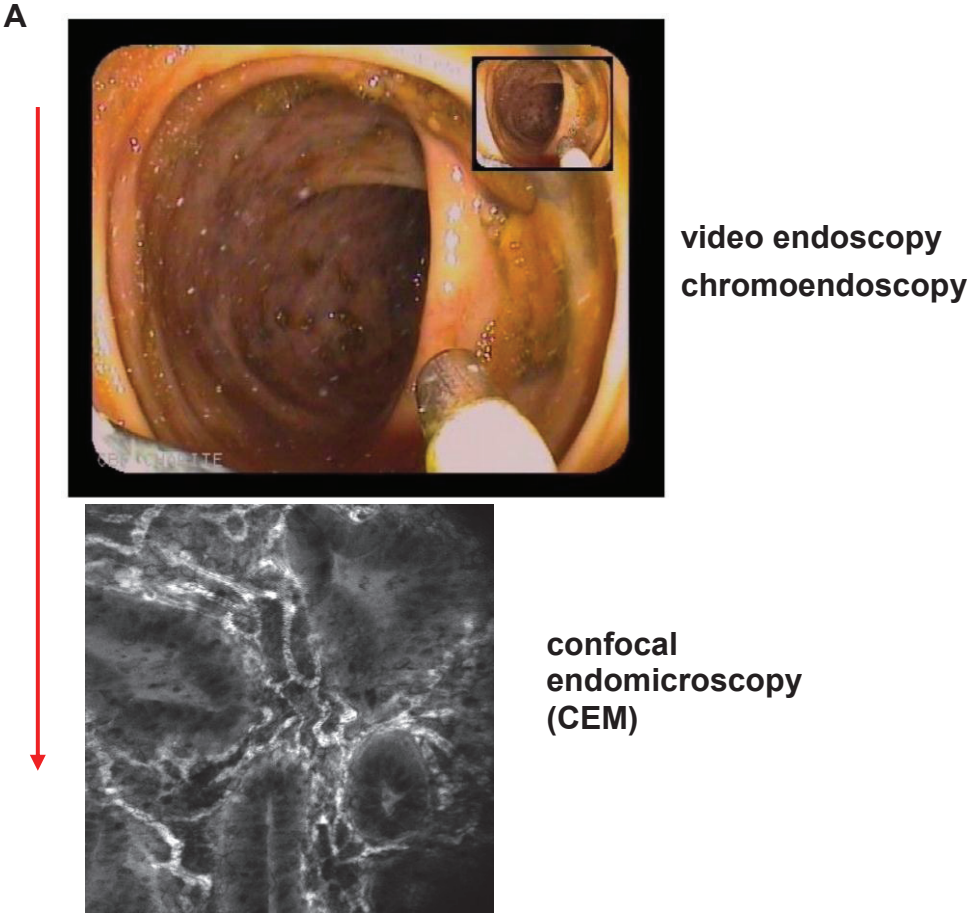

B

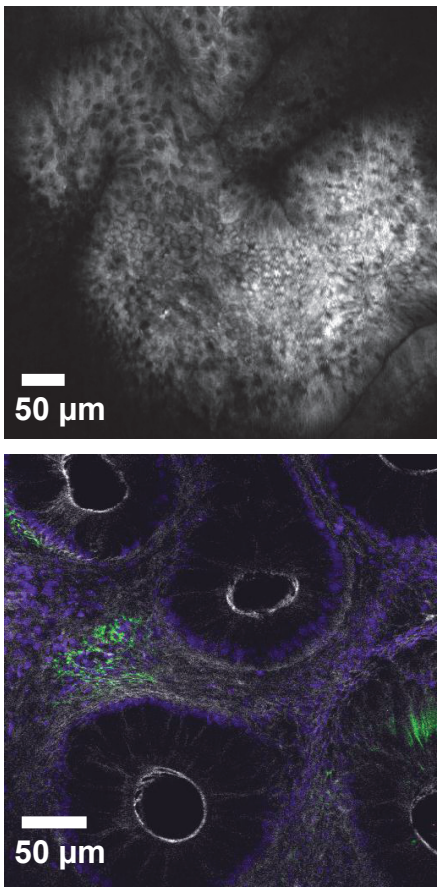

CEM

IF C-LSM

C *IF C-LSM, human UC biopsy*

HlyA | nuclei | E-cadherin

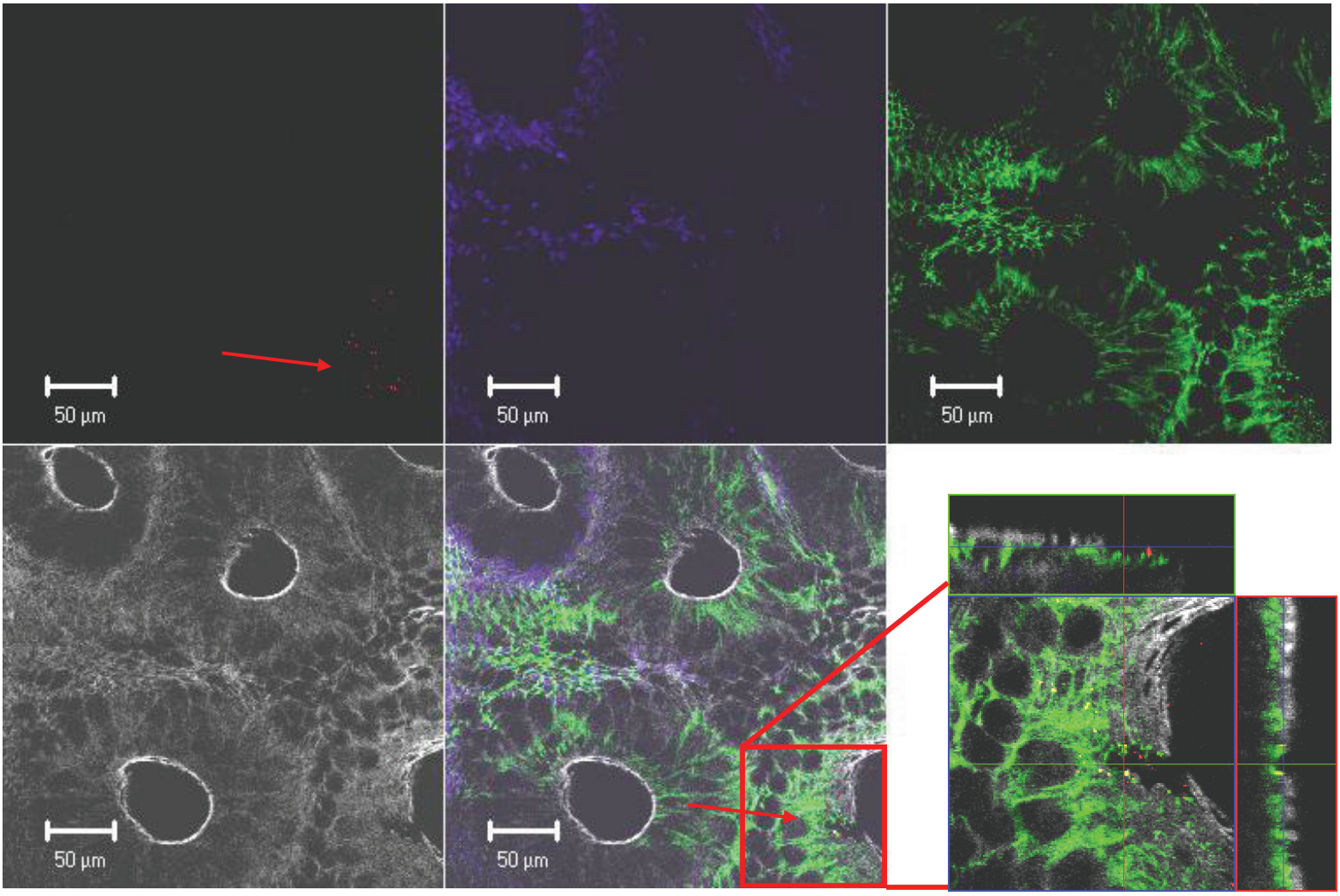

F-actin | merge | detail, orthogonal display, corresponding to fig. 7C

Observation of intracellular HRP. Generally, 44 kDa HRP (horseradish peroxidase) is a marker for larger epithelial lesions and may also be taken up by transcytosis, while it cannot pass the TJ, even if TJ structure is seriously impaired. Large tracer molecules like HRP can enter the organism via lesions or focal leaks but increased transcytosis is also supposable. To prove if HRP up-take by enterocytes is increased via the transcellular route, we microscopically investigated the colon after assessing HRP fluxes in 536-infected mice for this feature. HRP was histochemically stained according to manufacturer's protocol using 3,3',4,4'-Tetra-aminobiphenyl tetrahydrochloride (Carl Roth, Karlsruhe, Germany). Light microscopic images of stained HRP in mouse colon revealed intracellular accumulation of HRP signals, but without any obvious difference between HDM control and 536 HlyA-infected animals (figure S2). The cell count of HRP-positive epithelial cells was similar in MA wild type group (61.7% ± 1.7% HRP^+ cells in $HlyA^+$ mouse colon versus 64.7%± 4.5% HRP^+ cells in HDM control colon, *not significant*, n = 3). That endocytosis in non-inflamed tissues is not affected by HlyA indicates that HRP may primarily translocate through focal leaks. In contrast, measurements with the smaller tracer fluorescein (332 Da) were not suitable for characterisation of focal leaks in our models, because several effects can influence this tracer flux (e.g. TJ composition).

Figure S2 ***mouse colon after HRP flux***

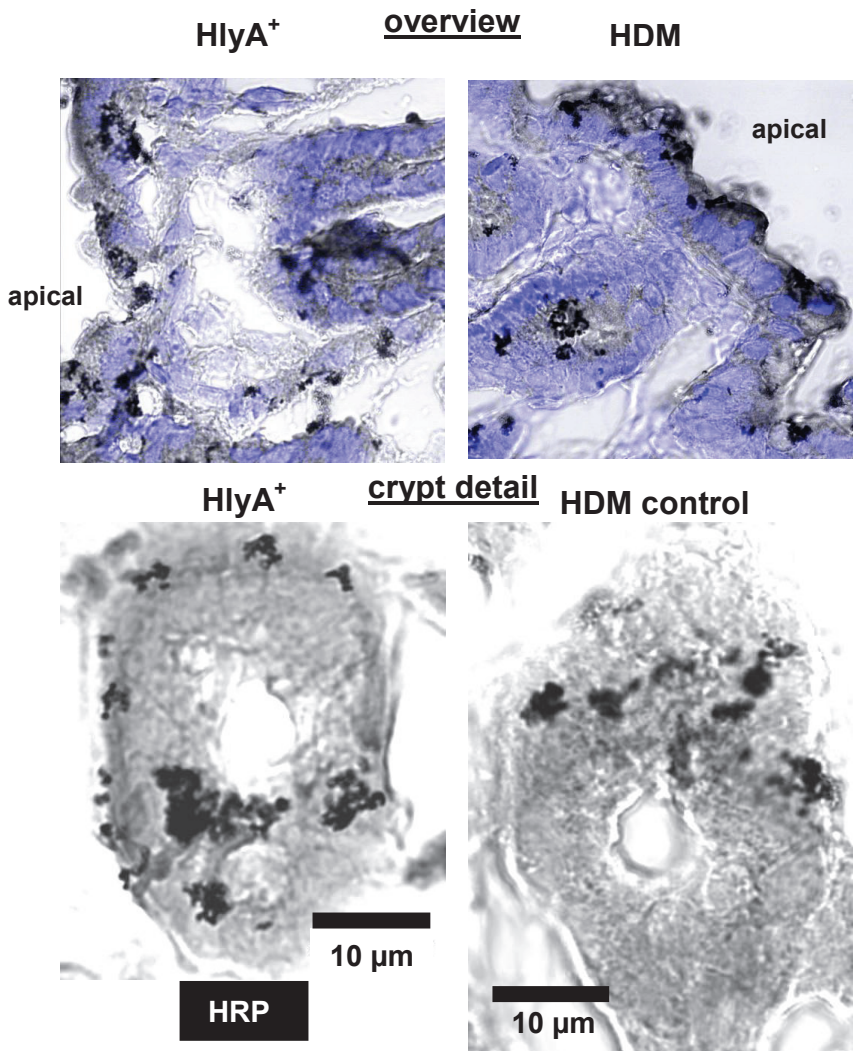

Figure S3 ***mouse colon, cLSM***

Apical view with more diffuse occludin signals (green) around the red HlyA signal and concomitant condensed F-actin (white). Mouse colon was stained 4 days after infection with *E. coli* 536. HlyA or occludin was antibody-labeled and immunostained with either secondary antibody AlexaFluor488 or AlexaFluor594. Cytoskeletal F-actin is coloured by Atto-phalloidin-647N staining. DAPI was used to mark the nuclei (blue). The white circles were added to highlight the affected area.

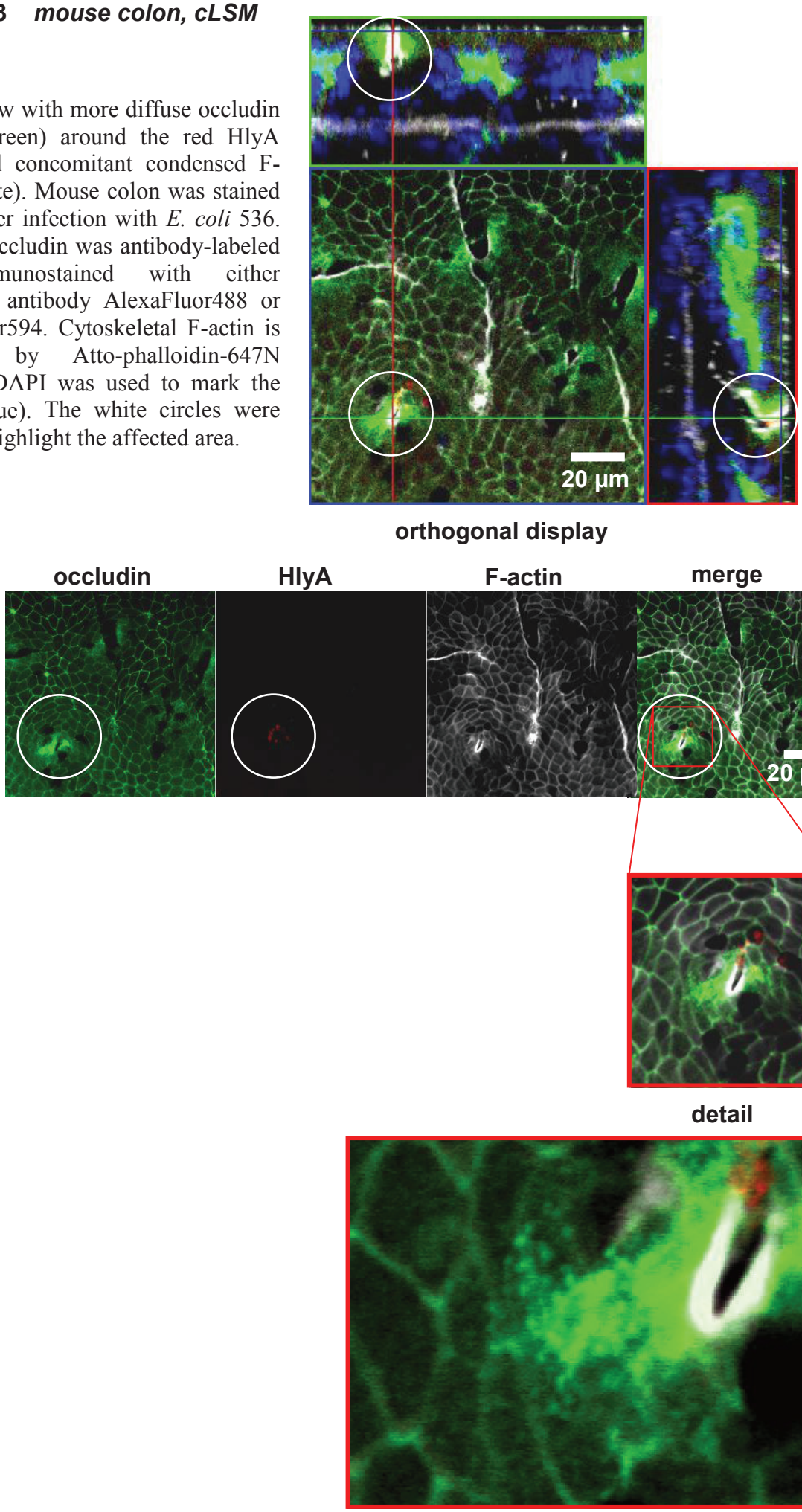

Figure S4 Tight junction protein quantification in *mouse colon*

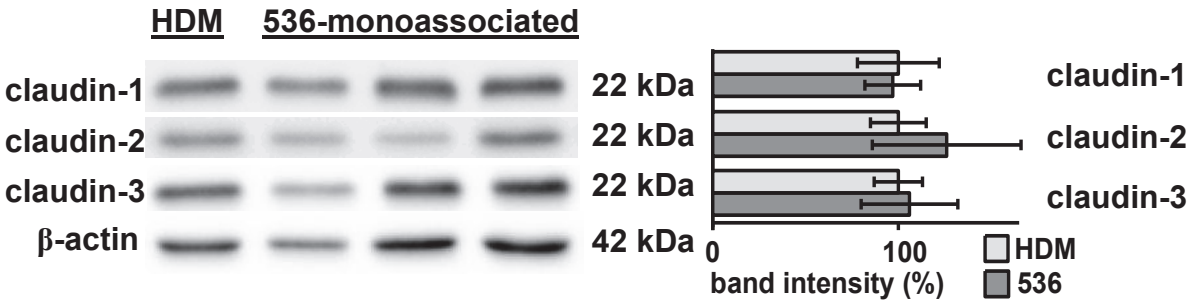

Densitometry from Western blots (n=4 each) performed as described previously [12]. Briefly, lysates were passed through a needle and insoluble material was removed by centrifugation (350 g, 5 min, 4°C). The supernatant was centrifuged at 43 000 g for 30 min at 4°C, and pellets were resuspended in lysate buffer. Aliquots of 5 mg were separated by polyacrylamide gel electrophoresis and transferred to a poly(vinylidene difluoride) membrane. Blots were blocked for 2 h in 5% milk powder in phosphate-buffered saline and overnight in 5% bovine serum albumin in phosphate-buffered saline (at 4°C) before incubation with primary antibodies for 90 min at room temperature. Primary rabbit polyclonal immunoglobulin (Ig)G antibodies were directed against claudins 1, 2 and 3. Peroxidase-conjugated goat antirabbit IgG and the chemiluminescence detection system Lumi-LightPLUS (Roche, Mannheim, Germany) were used to detect bound antibodies. Densitometric comparison was carried out on the same immunoblot.

Figure S5 *Akt protein kinase B activity.*

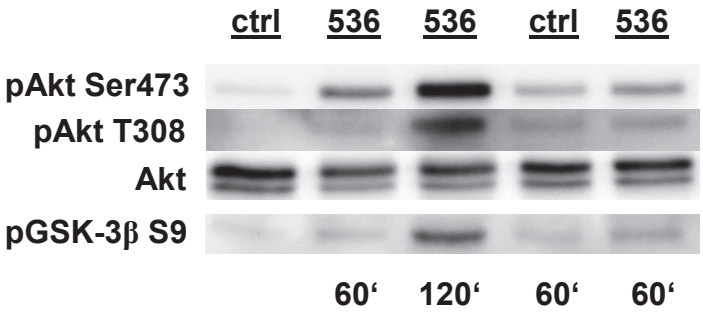

PI3K/Akt signaling was determined after samples were immunoblotted with an antibody against the active (phosphorylated) form of Akt (Akt-P). To ensure that equal amounts of samples were used, b-actin was used as loading control. Phosphorylation of Akt-P(Ser473), Akt-P(Thr308) and GSK3b was determined using phospho-specific anti-GSK3b, Akt-P(Ser473) and Akt-P(Thr308) antibodies. To analyze time-dependent phosphorylation, HT-29/B6 monolayers were exposed to HlyA for 60 and 120 minutes.

Supplemental Methods

Endoscopy, chromoendoscopy and confocal endomicroscopy. Endoscopic observation and imaging was performed as described earlier (Günther et al., 2011). Briefly, a contrast-enhanced chromoendoscopy with indigo carmine was performed. Indigo carmine was applied onto the mucosa as a watery solution with a concentration of 0.2% (Akorn Inc., Lake Forrest, USA). Confocal endomicroscopy (CEM) was developed by Pentax, Tokyo (EC-3870CIFK) and Optiscan, Australia (Hurlstone et al., 2008). Video endoscopy and CEM are possible with one instrument. For visualisation of cellular and subcellular structures, 5 ml fluorescein sodium 10% (Alcon Pharma, Germany) was injected intravenously (Ethics approval number EA4/098/09). Colon mucosa was scanned from 0 to 250 µm depth. Subsequently, random biopsies were taken for routine histology and the endomicroscopic pictures were recorded separately for comparison.

Günther U, Kusch D, Heller F, et al. Surveillance colonoscopy in patients with inflammatory bowel disease: comparison of random biopsy vs. targeted biopsy protocols. Int. J. Colorectal Dis. 2011;**26**(5):667-72.

Hurlstone DP, Kiesslich R, Thomson M, et al. Confocal chromoscopic endomicroscopy is superior to chromoscopy alone for the detection and characterisation of intraepithelial neoplasia in chronic ulcerative colitis. Gut 2008;**57**:196 – 204.

Intestinal colonization model of α-haemolysin-carrying *Escherichia coli*-536. We used *E. coli*-536 as a model organism for the *in vivo* investigation of pore-forming toxin-producing intestinal *Enterobacteriacea*. *E. coli*-536 pUC18 and *E. coli*-536-HDM were pre-cultured in LB medium containing ampicillin over night (100 $mg \cdot ml^{-1}$, MP Biomedicals, Illkirch, France). Infection of mice with $2 \cdot 10^6$ *E. coli*-536 or *E. coli*-536-HDM in 200 µl per os revealed colonisation of the gastrointestinal tract between 10^6 and 10^8 CFU/g feces 48h after infection. The mice were pre-treated with 5 g/l streptomycin in drinking water for one week to reduce the coliform flora, in order to gain an efficient colonization of the intestine according to Diard and co-workers (Diard et al., 2010).[23] Colonisation was not stable in the wild type mouse model with conventional microbiota as already reported without the use of antibiotics (Diard et al., 2010).[23] Pre-treatment with streptomycin led to higher bacterial numbers in the intestinal content and the infection lasted longer. With this technique the colitis model *IL-10*$^{-/-}$ and wild type (WT) mice were successfully colonized. In our facility *IL-10*$^{-/-}$ mice develop colitis after the 14th postnatal week. We assessed the colon of treated mice in the pre-inflammatory stage of disease in week 13 to 14 for subsequent electrophysiological and immunhistological investigations. After infection no antibiotics were applied anymore to ensure that no antibiotics-related effects are measured during the colonisation trial. Germ-free mice were colonised with a lower infectious dose of $2 \cdot 10^5$ bacteria in 200 µl resulting in an

intestinal colonisation with up to 10^8 bacteria/g faeces. The length of the colon as well as the length of the small intestine was not changed after treatment. **Colitis Score. Clinical Score.** No weight loss scored as 0, weight loss of 1% to 5% from baseline as 1; 5% to 10% as 2; 10% to 20% as 3; and more than 20% as 4. For stool consistency, a score of 0 points was assigned for well-formed pellets, 2 points for pasty and semiformed stools that did not adhere to the anus, and 4 points for liquid stools that did adhere to the anus. For bleeding, a score of 0 points was assigned for no blood, 2 points for positive hemoccult, and 4 points for gross bleeding. These scores were added together and divided by three, resulting in a total clinical score ranging from 0 (healthy) to 4 (maximal activity of colitis) (Araki, et al., 2005).[24] **Histological score.** The information on epithelial damage is coded with a score given between 0 and 6 (0 = normal; 1 = hyperproliferation, irregular crypts, and goblet cell loss; 2 = mild to moderate crypt loss (10-50%); 3 = severe crypt loss (50-90%); 4 = complete crypt loss, surface epithelium intact; 5 = small- to medium-sized ulcer (<10 crypt width); 6 = large ulcer (>10 crypt width)). The information on the tissue infiltration with inflammatory cells is coded separately for the mucosa with a score between 0 and 3 (0 = normal; 1 = mild; 2 = modest; 3 = severe), the submucosa with a score between 0 and 2 (0 = normal, 1 = mild to modest; 2 = severe) and the serosa with a score between 0 and 1 (0 = normal; 1 = moderate to severe) (Katakura, et al., 2005).[25]

Impedance spectroscopy. The total transepithelial resistance (R^t) of the intestinal barrier consists of two components, epithelial (R^{epi}) and subepithelial resistance (R^{sub}). By means of impedance spectroscopy it is possible to distinguish between R^{epi} and R^{sub} as previously described (Bürgel, et al., 2002).[26] Briefly, intestinal mouse colon samples, placed into Ussing chambers with Ringer's bathing solution were measured by alternating currents. Impedance spectra were calculated after exposure of the samples to sinusoidal currents in frequencies from 1 Hz to 65 kHz, that were provided by a programmable frequency response analyzer (402, Beran Instruments, Devon, UK) in combination with an electrochemical interface (1286, Solartron Schlumberger, Farnborough, UK). R^{epi} is short-circuited under high frequency currents that reveal the R^{sub}. R^{epi} is calculated from R^{sub} and R^t values.

3. Diskussion

Die Funktion der Darmbarriere im Rahmen von gastrointestinalen Infektionen ist für die medizinische Grundlagenforschung und Pathophysiologie des Darmtrakts von besonderer Bedeutung. Hierbei sind generell zwei Blickwinkel von Interesse. Zum Einen stellt das Darmepithel die größte Kontaktfläche des Körpers zur Umwelt dar und ist eine physikalische Barriere zur Limitation des Eindringens von Erregern und Antigenen, zum Anderen ist es mit seinen Barriereeigenschaften und Transportfunktionen auch Wirkort bakterieller Toxine oder Zielstruktur von gastrointestinalen Erregern, wobei es zur Aktivierung von Sekretionsprozessen oder mit der Störung der Barrierefunktion zur klinischen Symptomatik wie einer Diarrhö kommen kann. Dabei verfügen Pathogene individuell über ganz verschiedene Eigenschaften, die z.T. bis heute immer noch unbekannt oder nur partiell charakterisiert sind. Im Zentrum des Interesses steht hier die epitheliale Barrierestörung, die mit der *Leaky Gut*-Hypothese als Mechanismus für entzündliche Darmerkrankungen den Weg des Eindringens von Antigenen in den Organismus beschreibt und mit dem Leckflux-Mechanismus eine Erklärung für die Entstehung von Diarrhö liefert.

3.1 Leckflux als Pathomechanismus und die Pathogenität der *Campylobacteraceae*

Im Thementeil 2.1 wurde auf die potentiell pathogenen Veränderungen durch Bakterien aus der *Campylobacteraceae*-Familie eingegangen und es konnte erstmals ihr Diarrhömechanismus beleuchtet werden. Die Mechanismen von Diarrhöen, die auf Gram-negative Bakterien der Ordnung der *Campylobacterales* aus der Klasse der Epsilonproteobacteria zurückzuführen sind, wurden am Beispiel der „emerging human pathogens“ *C. concisus* und *A. butzleri* erstmals beschrieben. Dabei wurde ein Vergleich mit der bekannteren Spezies *C. jejuni* angestellt. Durch die Arbeiten liegt nun ein starkes Argument für die Pathogenität dieser „emerging human pathogens“ vor und man kann die eingangs gestellte erste Frage, ob diese Bakterien eine schädigende Wirkung auf humane Epithelzellen zeigen, bejahen. Allerdings müssen die Koch’schen Postulate noch *in vivo* erfüllt werden, um ihre Pathogenität abschließend zu belegen. Das relative Ausmaß der Pathogenität, also die Virulenz der untersuchten Stämme untereinander, war dabei sehr ähnlich. Die Frage nach den Pathomechanismen dieser Erreger konnte am Epithelzellmodell im Thementeil 2.1 näher beleuchtet werden:

Während der experimentellen Infektion mit dem Bakterium *A. butzleri* im humanen Kolonzellmodell HT-29/B6 konnte eine Barrierestörung aufgezeigt werden, wobei der transepitheliale elektrische Widerstand (R^t) vermindert und parallel dazu auch die parazelluläre Permeabilität für kleine Makromoleküle gesteigert war. Es fand sich eine reduzierte Expression von *Tight Junction*-Proteinen im infizierten Monolayer, sowie eine subzelluläre *Tight Junction*-Protein-Umverteilung (Bücker et al., 2009 *J. Infect. Dis.*

Arcobacter butzleri induces barrier dysfunction in intestinal HT-29/B6 cells). Der zugrundeliegende Pathomechanismus wurde demnach als Leckflux identifiziert und spiegelt den transsudativen Charakter der Diarrhö bei *Arcobacter*-Patienten mit vornehmlich wässriger Diarrhö wieder. Abzugrenzen ist die Leckfluxdiarrhö von der exsudativen Diarrhö, die ebenfalls von invasiven Bakterien ausgelöst werden kann, deren Leitsymptom aber die Beimengung von Proteinen, Schleim und Blut im Stuhl (Exsudat) darstellt.

Bisher ist es noch nicht gelungen putative *Arcobacter*-Virulenzgene zu identifizieren, die für die Pathogenität des Bakteriums verantwortlich sein könnten, allerdings konnten einige Hinweise dafür gefunden werden, dass u.a. das *Campylobacter*-Virulenzhomolog CiaB (invasion antigen B) oder CadF (fibronectin-binding protein) bei der Invasion oder Adhäsion der Bakterien eine Rolle spielen könnte (Levican et al., 2013; Karadas et al., 2013). Das Vorkommen von *Arcobacter* spp. im Gastrointestinaltrakt von Nutztieren wie z.B. dem Schwein ist häufig, wobei die Spezies *A. butzleri* und *A. cryaerophilus* die prominenten Vertreter sind (De Smet et al., 2012). Auch in Stühlen von Diarrhöpatienten sind diese Spezies zu finden, allerdings mit einer geringen Prävalenz von ca. 1% in einer Studie aus Neuseeland (Mandisodza et al., 2012). Interessanterweise konnte aber auch in einer Studie, in der experimentell eine osmotische Diarrhö erzeugt wurde, ein steigender Anteil von Proteobacteria im Stuhl der Probanden gemessen werden, in der *Arcobacter* spp. neben *Pseudomonas* spp. und *Acinetobacter* spp. als opportunistische Pathogene auftauchen (Gorkiewicz et al., 2013). Dies spricht dafür, dass *Arcobacter* spp. auch im menschlichen Mikrobiom in geringer Anzahl integriert sein kann und dabei keine gastrointestinalen Symptome auslöst.

Neben der *Arcobacter*-Enteritis mit eher sporadischen Ausbrüchen und niedriger Prävalenz ist die Infektion des nächsten verwandten Bakteriums *Campylobacter* spp., mit der *Campylobacter*-Enteritis, die häufigste Zoonose und die häufigste bakterielle Gastroenteritis. Das klinische Bild der *Campylobacter*-Infektion mit wässrigen bis blutigen Durchfällen ist ähnlich dem der *Arcobacter*-Infektion, aber eben nicht exakt gleich und unterscheidet sich z.T. sogar auch innerhalb des Genus *Campylobacter* in ihren Auswirkungen. In den untersuchten Patienten mit *C. jejuni*-Enteritis war der prozentuale Anteil der Fälle mit Stuhlbeimengung von Schleim und Blut höher als bei den *C. concisus*-Patienten (Nielsen, ..., Bücker, et al., 2012, *Clin. Microbiol. Infect.* Short-term and medium-term clinical outcomes of Campylobacter concisus infection.). Hier deutet auch das klinische Erscheinungsbild bei *C. concisus*-Durchfallpatienten auf eine epitheliale Barrierestörung hin, die durch ihren eher wässrigen Charakter auf eine sekretorische oder Leckflux-bedingte Störung schließen lässt. Auch die langanhaltende Diarrhöen durch *C. concisus* mit wenig Fieber und mit geringerer CRP-Erhöhung, also einer geringeren systemischen Immunaktivierung verglichen mit der *C. jejuni*-Infektion, zeigen nicht den entzündlichen und exsudativen Charakter wie er für die

C. jejuni-Infektion bekannt ist. Bislang fehlen allerdings noch pathophysiologische Untersuchungen an Patienten, um die Diarrhö-Mechanismen direkt zu analysieren. Hingegen konnte von unserer Arbeitsgruppe bei einer Norovirus-Epidemie an Patientenproben solche Untersuchungen durchgeführt werden. Bei Norovirus-Patienten mit akuter Infektion konnten funktionelle Messungen an Darmbiopsaten eine epitheliale Barrierestörung nachweisen und einen Leckflux-Mechanismus mit *Tight Junction*-Beteiligung als pathogenetischen Faktor identifizieren (Troeger et al., 2009). Darüber hinaus zeigte sich bei diesen Patienten in den Duodenalbiopsien eine aktive Anionensekretion und eine gesteigerte Anzahl von zytotoxischen T-Zellen im Epithel. Hier ist also eine sekretorische und wahrscheinlich auch eine entzündliche Komponente an der Entstehung der Diarrhö beteiligt (Troeger et al., 2009).

Auch durch den Parasiten *Giardia lamblia* ausgelöste Diarrhöen konnten an Patienten mit chronischer Lambliasis in unserer Klinik hinsichtlich des Diarrhömechanismus charakterisiert werden (Troeger et al., 2007b). Hier konnte an Biopsien aus dem Duodenum ein Leckflux-Mechanismus durch Apotoseinduktion und *Tight Junction*-Herabregulation von Claudin-1 dargestellt werden, allerdings trat die Diarrhö auch durch Malabsorption in Natrium-Glukose-Cotransportuntersuchungen und als sekretorische Störung mit aktiver elektrogener Chlorid-Sekretion zu Tage (Troeger et al., 2007b).

Die Beschreibung der Mechanismen der *C. jejuni*-Infektion am menschlichen Darm ist bisher nicht erfolgt, ist aber Gegenstand aktueller Forschung unserer Arbeitsgruppe. Die pathologischen Veränderungen, die für die Barrierestörung und Diarrhö bei der *C. concisus*-Infektion verantwortlich sind, konnten dagegen in unserem Zellmodell bereits beleuchtet werden (Nielsen, ..., Bücker, 2011). Ähnliche Resultate zur Invasivität und Pathogenität *von C. concisus* und anderen *Campylobacter*-Spezies haben auch anderen Gruppen an Zellsystemen wie z.B. Caco-2-Zellen zeigen können (Man et al., 2010). Für die experimentelle *C. jejuni*–Infektion konnten auch *Tight Junction*-Veränderungen in der humanen T84-Kolonzelllinie dargestellt werden. So konnte eine Verminderung von Claudin-1 als barriererelevant aufgezeigt werden (Chen et al., 2006). Eine detaillierte Darstellung von weiteren Claudinen während der Infektion mit *C. jejuni* steht allerdings noch aus. Zuvor konnte zusätzlich zur *Tight Junction*-Beteiligung bei der *C. jejuni*-Infektion gezeigt werden, dass die Flüssigkeitsabsorption im Caco-2-Zellmodell gestört war (MacCallum et al., 2005). Dass die Invasivität des Bakteriums mit den barriere- und zellschädigenden Effekten korreliert, scheint plausibel, wurde allerdings noch nicht eindeutig in Zusammenhang gebracht. Daten von anderen invasiven Erregern weisen auf einen besonderen Mechanismus bei der Invasion in die Epithelzelle hin. So zeigen *Shigella*-Bakterien ein gehäuftes Eindringen in die Zielzellen über trizelluläre Kontaktpunkte und auch eine Verbreitung zwischen den Zellen über die trizelluläre *Tight Junction* (Fukumatsu et al., 2012). Hierbei fungiert das *Tight Junction*-Protein Tricellulin anscheinend als ein Rezeptor für die

Internalisierung des Bakteriums in die Zielzelle, was mit dem experimentellen Knock-down von Tricellulin evident wurde (Fukumatsu et al., 2012). In wieweit die *Tight Junction*-Proteinverteilung während der Internalisierung von Bakterien gestört wird, ist ebenfalls Gegenstand aktueller Forschung. Die Signalwege, die bei der Invasion von z.B. *C. jejuni* über Clathrin-unabhängige Endozytose aktiviert werden (Wooldridge et al., 1996), sind ebenfalls für die Regulation der *Tight Junction* über das Assembly/Disassembly von *Tight Junction*-Proteinen von Bedeutung, so z.B. über den Endozytose-Signalweg mit Aktivierung von Cdc42 (Rojas et al., 2001, Krause-Gruszczynska et al., 2007). Eine Interferenz der invasiven Bakterien mit dem intrazellulären Vesikel-Membran-Trafficking von *Tight Junction*-Proteinen ist denkbar. Daneben zeigten Studien, dass Umverteilungs- und Phosphorylierungsvorgänge von *Tight Junction*-Proteinen z.B. durch enteropathogene *E. coli* verursacht werden können (Mc Namara et al., 2001; Simonovic et al., 2000). Auch ist die Spaltung von *Tight Junction*-Molekülen durch bakterielle Proteasen als Pathomechanismus belegt (Sears, 2000). Als ein weiteres Beispiel für die *Tight Junction* als Zielstruktur von Pathogenen konnte dargestellt werden, dass das Hepatitis-C Virus Claudin-1 als Rezeptor zum Eindringen in Hepatozyten benutzt (Evans et al., 2007).

Für *C. concisus* wurde bisher allerdings nur eine lose Assoziation der Bakterien mit den Zellgrenzen von Caco-2-Zellen in elektronenmikroskopischen Aufnahmen aufgezeigt (Man et al., 2010). Die bakterielle Pathogenität von *C. concisus* im humanen HT-29/B6-Zellkulturmodell zeigte bei unseren elektrophysiologischen Messungen ähnliche Ausprägungen der Barrierestörung wie durch *A. butzleri*. Der molekulare Mechanismus der Barrierestörung ist aber auf fokale Epithelschädigungen zurückzuführen, in denen eine Caspase-aktivierte Apoptoseinduktion, sowie eine Herabregulation des *Tight Junction*-Proteins Claudin-5 gefunden wurde. Die epitheliale Barrierestörung durch *C. concisus* ist dabei hauptsächlich durch fokale apoptotische Leck-Bildung bei gleichzeitigem Vorhandensein der Bakterien bedingt, was zusammen mit den *Tight Junction*-Veränderungen auf einen Leckflux-Mechanismus der Diarrhö hindeutet. Hierbei waren keine pathogenen Unterschiede zwischen verschiedenen *C. concisus*-Isolaten aus dem Mundraum oder dem Stuhl von Patienten messbar, was auf ein generelles pathogenes Potential der Bakterienspezies schließen lässt und damit die Störungen nicht nur von einem Referenzstamm hervorgerufen werden können (Nielsen,..., Bücker. 2011, *PLoS ONE* Oral and fecal Campylobacter concisus strains perturb barrier function by apoptosis induction in HT-29/B6 intestinal epithelial cells.). Die Infektion von der basalen Seite des Monolayers jedoch zeigte bei allen Stämmen einen schnelleren und stärkeren Abfall des R^t, verglichen zur apikalen Infektion der Monolayer. Bakterienkulturüberstände zeigten keine Wirkung. Dies weist darauf hin, dass die Bakterien nach erfolgreicher Invasion des Epithels die Barriere von basal mehr schwächen können und der Barrieredefekt bei der *Campylobacter*-Infektion eher

durch direkte Zell-Zell-Wirkung zustande kommt als durch lösliche sezernierte Faktoren. Eine erhöhte Apoptoserate, die durch vermehrte Zytokinfreisetzung oder intraepitheliale Lymphozyten induziert werden kann, könnte als weiterer Faktor zum Krankheitsgeschehen beitragen.

Insgesamt wurden sechs orale und acht fäkale *C. concisus*-Stämme aus Diarrhöpatienten in unserem HT-29/B6-Zellmodell eingesetzt. Alle Stämme waren invasiv im konfluenten Monolayer und störten die epitheliale Barrierefunktion in einer ähnlichen Dosisabhängigkeit. Auch mit oral isolierten Stämmen aus gesunden Kontrollpatienten fanden wir immer ein ähnliches Pathogenitätspotential der Bakterien (d.h. ähnliche Invasivität plus R^t-Abfall), wodurch anzunehmen ist, dass das Bakterium neben der fäkal-oralen Übertragungsweise ebenfalls oral-oral von Mensch zu Mensch oder auch durch Selbstinfektion in den Darm gelangt. Ein definiertes Tierreservoir, wie es für andere *Campylobacer*-Spezies bekannt ist, konnte bislang nicht gefunden werden, allerdings gibt es Hinweise dafür, dass *C. concisus* in Nutztieren vorkommen kann und somit als Zoonose in Betracht kommen könnte (Scanlon et al., 2013).

Während für Menschen eine relativ niedrige Infektionsdosis mit *C. jejuni* nach kurzer Inkubationszeit zu schweren Durchfällen führen kann, scheint die Kolonisation von Nutztieren hingegen (z.B. Hühner mit *C. jejuni* oder Schweine mit *C. coli*) mit keiner offensichtlichen klinischen Symptomatik bei den erwachsenen Tieren verbunden zu sein. Die *Campylobacter*-Infektion hat im veterinärmedizinischen Kontext unter zwei Gesichtspunkten eine erhöhte Relevanz. Zum Einen stellt die bakterielle Besiedlung von Tieren, die für den Verzehr bestimmt sind, durch ihr zoonotisches Potential ein gesundheitliches Risiko für Menschen dar, zum Anderen ist eine bakterielle Überbesiedlung unter bestimmten Haltungsumständen für die Tiere selbst und insbesondere für Jungtiere eine gesundheitliche Gefahr.

In einer weiteren Studie zur experimentellen Infektion von Ferkeln mit *C. coli* konnten wir feststellen, dass die Bakterien in der Lage waren, ausgehend von einer adäquaten natürlichen Kolonisationsdichte im Darm, über die Darmwand in den Organismus einzutreten. Die Translokation der Bakterien führte aber nicht zu klinischen Symptomen oder pathologischen epithelialen Veränderungen. Die Tiere zeigen auch eine immunologische Toleranz gegenüber diesen Bakterien. Die Bakterien konnten mit selektiver Anzucht, PCR und durch mikroskopischen Nachweis in verschiedenen Organen (z.B. jejunalen Lymphknoten, Tonsillen, Milz, Gallenblase) der Tiere nachgewiesen werden und insbesondere beim Übertritt in der Darmmukosa durch eine spezielle Immunfluoreszenz-Färbetechnik (*Whole Mount Staining*) verfolgt werden (Bratz, Bücker, et al. 2013). Die alternative Darstellung ganzer Präparate mit ‚*Whole Mount Staining'* ohne Schneiden der fixierten, eingebetteten Organe oder Zellkulturen ermöglicht eine exakte räumliche

Darstellung der Bakterienverteilung und dabei auch etwaiger Epithelveränderungen, die dann im Weiteren mit der konfokalen Laser-Scanning Mikroskopie aufgelöst werden können. Dabei wird das Präparat unter dem Mikroskop optisch „geschnitten“ und digital zu einem dreidimensionalen Bild zusammengesetzt. Mit Hilfe dieser Technik ist es möglich fokale Effekte durch barrierebrechende Erreger sichtbar zu machen.

3.2 Fokale Effekte und porenbildende Toxine

Die fokalen Effekte im infizierten HT-29/B6-Monolayer, wie die apoptotischen Areale, die von *C. concisus* invadiert waren, konnten mit der Immunfluoreszenzfärbung und konfokaler Laser-Scanning-Mikroskopie dargestellt werden (Seite 32, Abbildung Fig.5 und supplemental movie, www.plosone.org, http://www.plosone.org/article/info%3Adoi%2F10.1371%2Fjournal.pone.0023858#s5). Diese Fokalität des bakteriellen Übertritts kann auch bei anderen Bakterien beobachtet werden wie z.B. bei der *Y. enterocolitica*-Infektion (Hering, ..., Bücker, et al., 2011). Hierbei kam es zu lokalen Veränderungen der epithelialen Leitfähigkeit mit einer Herabregulation von *Tight Junction*-Proteinen Claudin-3 und -8 im HT-29/B6-Monolayer. Die Bakterien bilden sogenannte Mikrokolonien, die auch durch Induktion von nekrotischem Zelltod konduktive Lecks im Zellverband erzeugen (Hering, ..., Bücker, et al., 2011).

Auch war der fokale Charakter bakterieller Translokation über die epitheliale Barriere besonders bei HlyA-tragenden uropathogenen *Escherichia coli* (UPEC) zu beobachten, wobei der von unserer Gruppe beschriebene Pathomechanismus der Entstehung von *Focal Leaks* im Epithelmodell (Troeger et al., 2007a), nun unter definierten Bedingungen in der Maus *in vivo* weiter charakterisiert werden konnte (Bücker et al. 2014 *GUT,* α-Haemolysin of Escherichia coli in IBD: a potentiator of inflammatory activity in the colon.). Die zweite Hauptfrage dieser Habilitationsschrift nach der Rolle von PFTs bei der Induktion einer epitheliale Barrierestörung und darüber hinaus bei der Induktion von epithelialen Läsionen *in vivo* im Falle von HlyA konnte am Kolon des experimentellen Modells im Thementeil 2.2 beantwortet werden (Seite 56, Abbildung Fig.5, Supplemental movie; http://gut.bmj.com, http://gut.bmj.com/content/early/2014/02/17/gutjnl-2013-306099/suppl/DC1). So konnte der Zusammenhang zwischen der in der Impedanzspektroskopie gemessenen funktionellen Barrierestörung bei *E. coli* 536-infizierten Mäusen und der HlyA-induzierten Bildung von *Focal Leaks* dargestellt werden. Als entscheidendes Ergebnis zeigte sich bei der Barrierestörung eine erhöhte Permeabilität des *E. coli*-infizierten Mauskolons gegenüber Proteinen wie HRP. Das Markermolekül HRP besitzt bei der Darstellung der Transzytose oder Translokation durch das Darmgewebe zwei vorteilhafte Eigenschaften: Es diffundiert aufgrund der Molekülgröße nicht parazellulär durch intakte *Tight Junctions* und man kann den HRP-Gehalt enzymatisch bestimmen. Damit misst man nur intaktes HRP und keine

Fragmente, die z.B. durch den lysosomalen Abbau entstehen können. In der Darstellung der Transzytose von HRP in Mauskolonozyten, konnte keine Steigerung der Transzytoserate über das Kolon HlyA-behandelter Mäuse festgestellt werden (Seite 65, Abbildung Supplemental Fig. S2, Intracellular HRP). Folglich kann die Zunahme des HRP-Fluxes nur durch die HlyA-induzierten *Focal Leaks* erklärt werden. Desweiteren betrug die akkumulierte Fläche von *Focal Leaks* im Durchschnitt 1% der untersuchten Kolonoberflächen HlyA-infizierter Mäuse. Diese Läsionsfläche ist auch rechnerisch groß genug, um die gemessene epitheliale Widerstandserniedrigung zu erklären (Seite 61, Supplemental calculation).

Die Läsionen vom *Focal Leak*-Typ, die durch HlyA vermittelt werden, scheinen nicht mit typischen A/E (attaching & effacing)-Läsionen durch Bakterien, wie sie von enteropathogenen *E. coli* (EPEC) oder enterohämorrhagischen *E. coli* (EHEC) hervorgerufen werden, vergleichbar zu sein. Den UPEC 536 fehlen die nötigen Virulenzfaktoren der Pathogenitätsinsel LEE (locus of enterocyte effacement) und wir konnten auch keine typischen A/E-Aktinausstülpungen an unseren Zellen oder Gewebsproben bei der Induktion von Läsionen durch HlyA beobachten.

Ob das HlyA aus den in der Studie verwendeten UPEC 536 überhaupt eine Relevanz im humanen Kolon oder in Patienten mit Colitis hat, wurde ebenfalls analysiert. Bei CED-Patienten – insbesondere bei Patienten mit Colitis ulcerosa – ist die Zusammensetzung der Mikrobiota im Schub verändert, was sich u.a. in einer erhöhten Zahl von *Enterobacteriaceae* äußert. Dabei konnten in endoskopisch entnommenen Biopsien vermehrt Hämolysin-tragende *E. coli* detektiert werden (Bücker et al., 2014). In der Literatur findet sich dazu bisher zum Einen eine Prävalenzangabe von 30% zur phylogenetischen Gruppe B2 gehörender *E. coli* im gesunden Kolon und bei Morbus Crohn (Martinez-Medina et al., 2009) und zum Anderen eine Vermehrung von *E. coli* der Phylogruppe B2 bei Colitis ulcerosa (Kotlowski et al., 2007). Hämolysin-tragende UPEC gehören meist zur Phylogruppe B2. In einer vergleichenden Genomstudie an *E. coli*-Isolaten konnte mit Chiptechnologie auch in 2 von 5 Biopsien aus Colitis ulcerosa-Patienten das Gen *hlyA* detektiert werden (Vejborg et al., 2011). Allerdings konnte in zwei weiteren Arbeiten der Virulenzfaktor HlyA bei Colitis ulcerosa überhaupt nicht detektiert werden (Kotlowski et al., 2007; Sepehri et al., 2011).

In unseren Untersuchungen fanden wir heraus, dass die zur PCR-Detektion von HlyA verwendeten Primer in diesen beiden zuletzt genannten Publikationen nur eine Isoform des HlyA in der Untergruppe der EHECs identifizieren können, was das negative Resultat dieser beiden Publikationen erklärt. Die zur Phylogruppe B2 gehörenden *E. coli* jedoch, die zu den klassischen „kommensalen“ bzw. UPECs zählen, fanden sich in der PCR aber nur mit den von uns neu hergestellten und validierten Primern, womit dann auch das *E. coli*-Hämolysin HlyA in der Phylogruppe B2 detektiert werden konnte (Seite 62, Tabelle S3, Supplement). Ein Alignment von HlyA-Sequenzen aus EHEC und UPEC mittels BLAST zeigt auch nur eine

66% Homologie in der Aminosäuresequenz und nur eine 70% Übereinstimmung in der DNA-Sequenz der verschiedenen HlyA-Typen. Dies bedeutet also, dass sich die Einschätzung durch unseren aktuellen Befund signifikant ändert. Entgegen der momentanen Datenlage, wo wohl eine Zunahme der *E. coli* B2-Phylogruppe bei Colitis ulcerosa beobachtet werden konnte, allerdings ohne dass eine Hämolysin-Expression detektiert wurde, konnten wir jetzt erstmals mittels quantitativer real-time PCR zeigen, dass HlyA vom UPEC-Typ in der Mukosa von Patienten mit Colitis ulcerosa im akuten Schub im Vergleich zu Kontrollen vermehrt ist. Die Methodik beinhaltet PCR-Messungen an mukosalen Biopsaten, wobei die Extraktion der bakteriellen DNA direkt aus den Patientenproben durchgeführt wurde, ohne dass es eine vorherige Anzucht von Bakterienkolonien bedurfte und somit keine anzuchtbedingte Selektion stattfand. Überraschenderweise liegt die *E. coli* HlyA-Prävalenz dabei in beiden Gruppen bei 90%. Allerdings fand sich die HlyA-Genhäufigkeit (Bakterienzahl) bei Colitis ulcerosa im akuten Schub gegenüber den nicht-entzündeten Kontrollen 10-fach erhöht (Seite 58, Abbildung Fig. 7). Das *E. coli* α-Hämolysin zählt zur Familie der RTX (Repeats in toxin)-Toxine, die sich durch mehrere Calciumbindestellen auszeichnen, welche für die extrazelluläre Aktivierung der Toxine relevant sind und C-terminal wiederholende Signalpeptidsequenzen zur Sekretion über das bakterielle Typ 1-Sekretionssystem besitzt.

Die zelluläre Antwort auf sublytische Konzentrationen von Hämolysinen sind vielgestaltig und reichen von leichten Verschiebungen in der Ionenhomöostase bis hin zu Zelllyse. Bakterielle Hämolysine gehören zu den PFTs, die in der Wirtszellmembran integrieren und dort Kanäle von ca. 10 Å Durchmesser bilden, die meist für Kationen leitfähig sind. Ihre Wirkungsweise auf die intestinale epitheliale Barrierefunktion konnte auch beim Hämolysin, Aerolysin, von *A. hydrophila* genauer molekular charakterisiert werden. Es konnte hierbei erstmals gezeigt werden, dass das hämolytische Aerolysin in sublytischen Konzentrationen eine *Tight Junction*-Proteinumverteilung in der Epithelzelle auslöst und dass – anders als erwartet – nicht dem transzellulären Weg durch die Porenbildung des Hämolysins der Hauptanteil am erniedrigten epithelialen Widerstand zugesprochen werden muss (Seite 40, Abbildung Fig. 2). Die Anwendung der neuen Technik der Zwei-Wege-Impedanzspektroskopie kam bei der Analyse der Aerolysin-induzierten Störung eine methodische Schlüsselfunktion zu. Bei dieser Methode am Epithelzellmonolayer kann der parazelluläre Anteil des epithelialen elektrischen Widerstands, der durch die *Tight Junction* bestimmt wird, von dem transzellulären Anteil des Widerstands, der durch die Zellmembran zustande kommt, unterschieden werden (Krug, et al., 2009b).

Darüber hinaus konnten wir zeigen, dass durch das Aerolysin eine Aktivierung der MLCK als Folge einer Erhöhung des intrazellulären Calcium erfolgt. Diese MLCK-Aktivierung führt zu einer Kontraktion des perijunktionalen Zytoskeletts, wodurch eine schnelle Umverteilung der

Tight Junction-Proteine aus der *Tight Junction* heraus in intrazelluläre Kompartimente der Zelle hinein stattfindet. Als Folge davon erhöhte sich auch die Permeabilität des Zellmonolayers gegenüber Molekülmarkern wie Fluoreszein und 4 kDa FITC-Dextran. In Folge der *Tight Junction*-Proteinumverteilung und der Zytoskelettveränderungen war gleichzeitig die Restitution von epithelialen Einzelzellläsionen gestört, was die Barrierestörung des Monolayers weiter intensiviert. Die experimentelle Einzelzellläsion mit ihrer Relevanz für epitheliale Barrierestörungen samt der Erfassung der Restitution dieser Läsionen durch den „purse-string" Mechanismus (bzw. die Störung der Restitution durch bakterielle Toxine) ist gleichzeitig ein adäquates Modell für die Analyse einer gestörten Wundheilung, wofür *A. hydrophila* ebenfalls bekannt ist (Bücker et al., 2011 *J. Infect. Dis.* „Aerolysin from Aeromonas hydrophila perturbs tight junction integrity and cell lesion repair in intestinal epithelial HT-29/B6 cells.").

Der „purse-string" Restitutionsmechanismus mit seinem kontraktilen Aktinring, der durch die um die experimentell geschädigte Zelle herumliegenden Epithelzellen gebildet wird, dient dem schnellen Verschluss kleiner epithelialer Läsionen. Diesem Phänomen wird für die mukosale Integrität eine hohe Bedeutung beigemessen (Seite 47/48; Bücker et al., 2011 *J. Infect. Dis.* 204; Cover Image), da auch natürliche apoptotische Lecks sofort wieder verschlossen werden müssen. Die durch Aerolysin induzierte Restitutionsstörung konnte durch die Behandlung der Zellen mit Zink-Ionen unterbunden werden (Bücker et al., 2011). Hierbei liegt die Wirkung von Zink wahrscheinlich in der Interferenz bei der Oligomerisierung des Aerolysins während der Porenbildung in der Zellmembran (Wilmsen et al., 1990).

3.3 Leaky Gut-Hypothese und Perspektiven

Ein dichtes Epithel, wie im Dickdarm physiologischerweise vorhanden, schützt den Organismus vor der luminalen bakteriellen Außenwelt. Im Falle einer Schädigung oder einer Fehlregulation der Barrierefunktion kommt es zur Undichtigkeit des Epithels: Es wird leck und Wasser und Solute strömen ins Darmlumen (Leckflux-Diarrhö). Meist findet diese Fehlregulation über die dynamische und stark-regulierte epitheliale *Tight Junction* statt. Auf der anderen Seite können durch das leck-gewordene Epithel Antigene in die Mukosa eindringen und dort eine Entzündung induzieren (*Leaky Gut*). Durch die hier präsentierte Publikation über das *E. coli* HlyA und seine Wirkung auf die epitheliale Barriere konnte ein möglicher Zusammenhang zwischen dem vermehrten Vorkommen des Virulenzfaktors und einer gesteigerten entzündlichen Aktivität bei Colitis ulcerosa und im experimentellen Mausmodell dargestellt werden. Die *Leaky Gut*-Hypothese könnte somit als weiterer Erklärungsansatz zum Verständnis der Entstehung bzw. Aufrechterhaltung von entzündlichen Darmerkrankungen beitragen und auch bei der Pathogenese infektiöser

Gastroenteritiden könnte diese Hypothese eine Rolle spielen, was allerdings noch experimentell geprüft werden muss.

Die humanpathogenen Bakterien aus der Bakterienordnung der *Campylobacterales*, wie *Arcobacter* spp. und *Campylobacter* spp. sind für ihre Invasivität bekannt und induzieren bei der Translokation über das Darmepithel je nach Oberflächenantigenausstattung und immunmodulatorischer Virulenzausstattung definierte Immunreaktionen, die auch über Zytokinfreisetzung zu Diarrhö und Darmentzündung führen können. Der Anteil Zytokin-vermittelter Barriere-Effekte bei diesen Infektionen muss in weiterführenden Analysen an Patientenproben oder im Tiermodell erst noch beleuchtet werden. Auch ist die mögliche Beteiligung von *C. concisus* an der Ätiologie der *Mikroskopischen Kolitis* ein interessantes Forschungsprojekt, wie auch die Beteiligung von *Campylobacter* spp. an der Entstehung des postinfektösen Reizdarmsyndroms in der aktuellen Forschung verfolgt wird.

Bei pathologischer Translokation von luminalen Antigenen und Bakterien über eine geschädigte Dickdarmmukosa ist allerdings bereits allein aufgrund der enormen Größe der intestinalen Mikrobioms im Dickdarm in Zahl ($>10^{14}$ Bakterien) und Diversität (>1000 Bakterienspezies) eine Entzündungsinduktion wahrscheinlich. Die Translokation von Bakterien in sterile Körperhöhlen ist ein kritisches Ereignis. Sie kann z.B. während oder nach operativen Eingriffen oder bei einer Pankreatitis erfolgen und in Sepsis oder in SIRS resultieren. Transloziert werden u.a. *E. coli*-Stämme, die als Teil der physiologischen Darmmikrobiota zunächst als nicht-pathogen einzustufen sind. Unter bestimmten Bedingungen einer beeinträchtigten Barrierefunktion sind sie dann aber durchaus in der Lage, die epitheliale Barriere zu überwinden und im o.g. Sinne Pathogenität zu entwickeln (Pathobionten oder opportunistische Pathogene). Die Relevanz von sogenannten Pathobionten konnte kürzlich auch für das fakultativ pathogene Bakterium *Klebsiella oxytoca* und ihres Toxins Tilivallin als Auslöser der Antibiotika-assoziierte Kolitis aufgezeigt werden (Högenauer et al., 2009; Schneditz, ..., Bücker, et al., 2014). Enteropathogene Bakterien, die nicht Bestandteil der Mikrobiota des Dickdarms sind, müssen noch wesentlich mehr Barrieren überwinden bevor sie über das Darmepithel translozieren können: Sie müssen die gastrale Barriere aus Säure und Pepsin überleben, einer Kontrolle durch das Immunsystem im Dünndarm (Peyer's Patches, Mucosa-associated lymphoid tissue) entgehen, dann mit der residenten Mikrobiota um Metabolite und Lebensraum konkurrieren, um schließlich im Dickdarm die Mukusbarriere mit Defensinen und anderen molekularen Abstandshaltern zu überwinden. Erst nach Translokation über das dichte Kolonepithel und in dem Vorhandensein einer ausreichenden Anzahl an Bakterien auf der serosalen Seite des Epithels kann eine Entzündungsreaktion ausgelöst werden. Trotz der erheblichen Barrieren des Organismus gegen Pathogene schafft es z.B. *C. jejuni* allein in Deutschland in mehr als 60.000 registrierten Fällen pro Jahr, eine infektiöse Diarrhö auszulösen.

Eine Kolonisationsresistenz gegen *C. jejuni* wurde kürzlich auch für den menschlichen Darm beschrieben, wobei zum Einen eine bestimmte Komposition der Mikrobiota gegen *C. jejuni* schützt, zum Anderen kann die Mikrobiota aber auch durch eine vorangegangene Infektion nachhaltig in ihrer Zusammensetzung verändert werden (Dicksved et al., 2014).

Neben den invasiven darmpathogenen Bakterien wie *C. jejuni* können sezernierte bakterielle Toxine die Darmwand direkt schädigen und wie am Beispiel der Hämolysine HlyA aus *E. coli* oder Aerolysin ausgeführt zu lecken Epithelien führen. Die Bedeutung der PFTs wie HlyA ist für das *Leaky Gut*-Konzept wahrscheinlich noch von größerer Relevanz, da die Faktoren auch in der residenten Mikrobiota des gesunden Menschen vorhanden sind und im Falle einer bakteriellen Fehl- oder Überbesiedlung (Dysbiose), z.B. nach Einnahme von Antibiotika, ein gewöhnlicher kommensaler Bakterienstamm zu einem Pathobionten werden kann. Das bedeutet die kommensale Mikrobiota enthält, neben den immunogenen Oberflächenantigenen wie LPS, Virulenzfaktoren wie HlyA, die unter Umständen zu entzündlichen Erkrankungen führen oder diese unterhalten können.

Es kann abschließend zusammengefasst werden, dass invasive bakterielle Pathogene (wie *C. concisus*) oder Hämolysin-tragende Bakterien (wie *E. coli* 536) fokale Läsionen entweder durch Induktion vermehrter Apoptose oder durch Bildung von *Focal Leaks* in Zellmodellen und auch im nativen Kolon erzeugen können. Darüber hinaus konnte gezeigt werden, dass extra-intestinal pathogene *E. coli* in hohen Kolonisationsdichten im Darm als Pathobionten Entzündungsreaktionen induzieren oder als Mediator der Kolitis fungieren können. Daher können Läsionen bis hin zu Erosionen und Ulzerationen, wie sie bei Colitis ulcerosa beobachtet werden, in Zusammenhang mit Apoptose-induzierenden Bakterien oder Mediatoren wie HlyA gebracht werden.

Perspektivisch können nun weitere alternative therapeutische Möglichkeiten bei der Behandlung von CED in Betracht gezogen werden. So ist die Bakterientherapie bei Colitis ulcerosa, z.B. mit nicht-pathogenen bzw. probiotischen *E. coli*-Stämmen eine Option. Es könnten sogar Ansätze angedacht werden, die eine Vakzinierung gegen bestimmte pathobionte bzw. pathogene *Enterobacteriaceae* zum Ziel hat, wie sie z.B. bei rezidivierenden Infekten der Blase als Therapiemöglichkeit bereits angewendet wird. Bei der *chronischen Zystitis* kann mit dem zugelassenen Impfstoff StroVac, welcher inaktivierte *E. coli*-Stämme und weitere *Enterobacteriaceae* enthält, die Infekthäufigkeit reduziert werden (Moriel & Schembri, 2014).
Für den Ansatz der Bakterientherapie spricht, dass eine Supplementation der residenten Mikrobiota mit probiotischen Bakterien wie etwa mit *E. coli* Nissle 1917 förderlich sein kann. In klinischen Studien mit Nissle-Präparaten konnte für die Colitis ulcerosa die gleiche remmissionserhaltende Wirkung erzielt werden, wie durch die Behandlung mit Mesalazin (5-ASA) (Kruis et al, 2004).

Da *E. coli* Nissle 1917 auch zum Phylogruppe B2 gehört und dem genetischen Profil eines ursprünglichen UPECs entspricht (Dobrindt et al., 2010, Vejborg et al., 2011), kann man annehmen, dass diese Bakterien in der Lage sind, andere *E. coli* im residenten intestinalen Mikrobiom zu verdrängen. Die Bakterien konkurrieren dann kompetitiv um Metabolite also um eine ökologische Nische. Neben dem Effekt der Verdrängung von pathogenen *E. coli*-Stämmen durch den apathogenen *E. coli* Nissle 1917, zeigt dieser aber auch zusätzlich immunmodulatorische Eigenschaften z.B. durch TcpC (Toll/Interleukin-1 receptor domain-containing protein), einem bakteriellen Faktor, der durch die direkte Interaktion mit dem *Myeloid Differentiation Factor 88* (MyD88) in der Wirtszelle zu einer Reduktion der Zytokinsekretion führen kann, indem der Toll-like Rezeptor-abhängige Signalweg supprimiert wird (Cirl et al., 2008). TcpC zeigt neben der Interaktion des MyD88 Signalweges und somit seiner immunsuppressiven Wirkung aber auch barrierefördernde Eigenschaften an Epithelzellen. So konnte gezeigt werden, dass TcpC über eine Heraufregulation von Claudin-14 durch eine Aktivierung der atypischen Proteinkinase C-zeta (PKC-ζ) die Integrität der epithelialen Barriere stärkt (Hering, ..., Bücker, et al. 2014).

Eine weitere Option bei der Behandlung von infektiösen Diarrhöen und CED ist die Anwendung von Zink als anti-diarrhöischem Therapeutikum. Zinkoxid wird in der Pädiatrie eingesetzt und ist, wie auch in Cochrane Metaanalysen deutlich wurde, effektiv gegen infektiöse Diarrhöen im Kindesalter (Lazzerini & Ronfani, 2013; Mayo-Wilson et al., 2014). Die Weltgesundheitsorganisation WHO empfiehlt gerade für Länder wo Unterernährung und somit eine Unterversorgung mit Zink eine Rolle spielt, bei der Behandlung von Diarrhöen bei Kindern zwischen 6 Monaten und 14 Jahren eine Tagesdosis von 20 mg Zinksupplementation für 10-14 Tage (10 mg pro Tag für Kinder unter sechs Monaten). Freie Zink-Ionen können die Wirkung von Hämolysinen inhibieren. Ein weiterer Wirkmechanismus von Zink kann also die Hemmung dieser Virulenzfaktoren sein und es könnte dadurch eine schnellere Abheilung einer Diarrhö begünstigen. Zu diesem Teilaspekt der Zinktherapie laufen aktuelle Untersuchungen durch unsere Gruppe.

4. Zusammenfassung

Gastroenteritiden, die durch invasive Bakterien hervorgerufen werden können, wurden am Beispiel von „emerging human pathogens“ aus der *Campylobacteraceae*-Familie hinsichtlich ihrer Diarrhö-auslösenden Mechanismen untersucht und mit Infektionen der bekannteren Spezies *Campylobacter jejuni* verglichen. So konnte erstmals beschrieben werden, dass die Bakterienspezies *Campylobacter concisus* und *Arcobacter butzleri* ein pathogenes Potential besitzen, was sie befähigt, barrierebrechende Eigenschaften an Zellkulturmodellen zu entwickeln, die sich durch den Leckflux als Diarrhö-Mechanismus erklären lassen. Beim Leckflux zeigt sich eine Schwächung der epithelialen Barriere des Darms z.B. durch eine Expressionsänderung von abdichtenden oder kanalbildenden *Tight Junction*-Proteinen und/oder eine Umverteilung ihrer subzellulären Lokalisation. Darüber hinaus kann die Erhöhung der Anzahl von Apoptosen in einem Epithel oder ein gestörter Verschluss von Einzelzellläsionen zum Leckflux beitragen. Bei der Leckflux-Diarrhö wird die Permeabilität des Epithels gegenüber Wasser und Soluten heraufgesetzt, was sich in der Folge eines gesteigerten Flüssigkeitsausstroms in das Darmlumen hinein als Diarrhö äußert. Dass *C. concisus* auch klinische Relevanz hat, konnte in einer vergleichenden Arbeit zu den akuten Symptomen bei der *C. concisus*-Infektion in Relation zu *C. jejuni*-infizierten Patienten dargestellt werden. Patienten mit *C. concisus*-Besiedlung des Darms entwickelten langanhaltende Diarrhöen mit geringerer systemischer Immunaktivierung (weniger CRP und Fieber) als bei der *C. jejuni*-Enteritis.

Das pathogene Potential von *A. butzleri* und *C. concisus* zeigte sich auch experimentell mit der Invasion der Bakterien im humanem Kolonzellmodell HT-29/B6 mit der Folge eines reduzierten transepithelialen elektrischen Widerstands. Während bei *A. butzleri* eine Labilisierung der *Tight Junction*-Integrität durch die verminderte Expression von definierten barrierebildenden Claudinen prägnant in Erscheinung trat, zeigte sich bei *C. concisus* vornehmlich eine Induktion von epithelialen Apoptosen als Hauptmerkmal der Barrierestörung, wobei auch *Tight Junction*-Veränderungen messbar waren, die sich aber eher lokal um die apoptotischen Bereiche herum manifestierten.

Bei diesen invasiven Bakterien scheint die fokale apoptotische Leck-Bildung bei gleichzeitigem Vorhandensein der Bakterien im betroffenen Areal des Epithels ursächlich für die Barrierestörung zu sein. Dagegen können andere Bakterien der *Enterobacteriaceae*-Familie eine Leckfluxstörung allein durch sezernierte Toxine induzieren. So konnte durch das porenbildende Toxin Aerolysin AerA von *Aeromonas hydrophila* eine Permeabilitätsstörung im HT-29/B6-Modell gemessen werden, die vornehmlich auf die Umverteilung von *Tight Junction*-Proteinen als Folge einer Aktivierung von Calcium-Signalwegen der Kolonozyten zurückzuführen war. Zur Pathogenese durch die Toxinwirkung wurde bisher eine sekretorische Störung oder der Zelluntergang bei hohen Toxinkonzentrationen als ursächlich

angesehen. Hier konnte aber, vermittelt durch sublytische Konzentrationen dieses porenbildenden Toxins, der Leckflux-Mechanismus als initiales und irreversibles Prinzip erstmals dargestellt werden. Die Blockade der Restitution epithelialer Läsionen konnte ebenfalls als ein weiterer Mechanismus bei der Epithelschädigung durch Aerolysin identifiziert werden.

Es können aber auch epitheliale Läsionen durch andere sezernierte porenbildende Toxine, wie das α-Hämolysin HlyA von *Escherichia coli*, direkt induziert werden. Das mit HlyA-produzierenden *E. coli* behandelte lecke HT-29/B6-Epithel zeigte fokale Läsionen, so genannte *Focal Leaks*, durch die sogar ganze Bakterien eindringen konnten. Ob das HlyA bei der Pathogenese am Epithel des Darms auch *in vivo* eine Rolle spielt, wurde in einer experimentellen Studie und an humanen Darmproben untersucht.

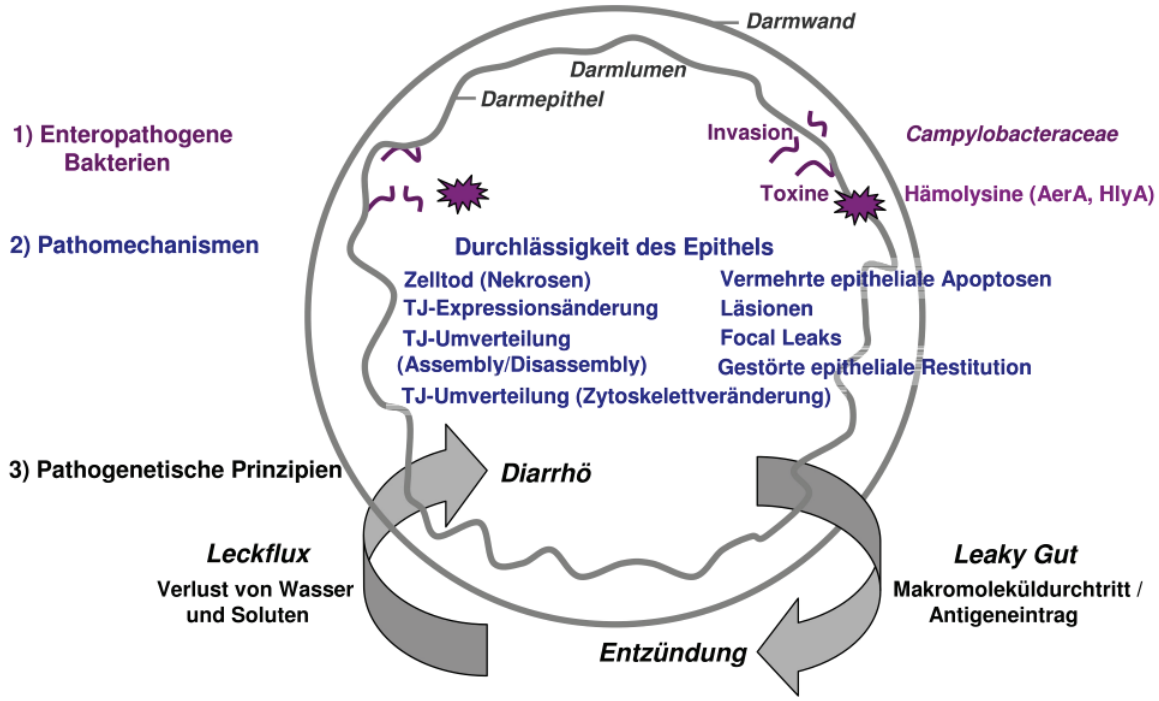

Schematische Darstellung des Habilitationsthemas an einem Darmquerschnitt:

1) **Provokation der Integrität des intestinalen Epithels durch pathogene Bakterien, die invasiv sind (*Campylobacter* spp., *Arcobacter* spp.) oder porenbildende Toxine sezerniern (*E. coli*-HlyA, *Aeromonas*-AerA).**
2) **Erhöhte Permeabiltät des Epithels, mediiert durch verschiedene Pathomechanismen, die Zellverlust, Tight Junction (TJ)-Veränderungen und/oder Läsionen umschreiben.**
3) **Als pathogenetische Prinzipien beschreibt die *Leckflux-Diarrhö* den passiven Ausfluss in das Darmlumen, der hauptsächlich durch TJ-Veränderungen ausgelößt wird, wohingegen der Influx größerer Moleküle, die aus dem Lumen stammen, durch den *Leaky Gut* mit der Folge einer Induktion von proinflammatorischen Zytokinen und Entzündung beschrieben wird.**

Die Prävalenz der HlyA-tragenden Bakterienstämme in Darmbiopsaten des Kolons von Darmgesunden und Patienten mit chronisch-entzündlicher Darmerkrankung war erstaunlich hoch und die *E. coli*-Bakterienzahl und HlyA-Genhäufigkeit bei Colitis ulcerosa im akuten Schub war gegenüber den nicht-entzündeten Kontrollen erhöht. Darüber hinaus konnte *in vivo* im Mausmodell gezeigt werden, dass der neuartige Pathomechanismus der *Focal Leak*-

Induktion durch vermehrte Translokation von Antigenen in den Organismus eine inflammatorische Antwort zur Folge hat.

Die Rolle des α-Hämolysin als bakterieller Virulenzfaktor bei intestinalen Entzündungen und als ein Prototyp für die *Leaky Gut*-Hypothese konnte so dargestellt werden. Die *Leaky Gut*-Hypothese ist ein bedeutender Erklärungsansatz für die Entstehung von entzündlichen Darmerkrankungen wie Colitis ulcerosa, aber insbesondere auch für gastrointestinale Infektionserkrankungen mit Entzündungsreaktionen durch barrierebrechende Erreger.

Die hier beschriebenen Pathomechanismen, die zu einer Undichtigkeit des intestinalen Epithels und somit zu Diarrhö und/oder Entzündung führen können, umfassen somit: i) die Fehlregulation von bestimmten *Tight Junction*-Proteinen auf Expressionsebene, ii) die subzelluläre Umverteilung von *Tight Junction*-Proteinen, iii) die zytoskeletale Kontraktion mit schneller Umverteilung der *Tight Junction*, iv) die Restitutionsstörung von kleinen Läsionen, v) die Entstehung von größeren fokalen Läsionen, vi) die Erhöhung der epithelialen Apoptoserate, sowie vii) die Leckbildung durch vermehrte fokale Apoptose-Ereignisse oder Zellverlust. Dabei ist auch eine Kombination der verschiedenen Pathomechanismen zu beobachten. Eine mögliche Erhöhung der Transzytoserate von Makromolekülen oder eine etwaige Erhöhung der kanalbildenden *Tight Junction*-Proteine wie z.B. Claudin-2 als weitere Pathomechanismen der Barrierestörung wurden durch die hier untersuchten Pathogene nicht ausgelöst. Aus den dargestellten Arbeiten lassen sich die Kernaussagen so zusammenfassen, dass die Störung der epithelialen Barrierefunktion des Darms durch bakterielle Pathogene als ein wichtiger Mechanismus für die Entstehung von Diarrhö und Entzündung, vornehmlich über die Veränderung der *Tight Junction*-Regulation, aber auch durch vermehrten epithelialen Zelltod und durch Restitutionsstörung verursacht wird. Als pathogenetische Prinzipien wurden der Leckflux-Mechanismus der Diarrhö und das Konzept des *Leaky Gut* herausgearbeitet und ersterer in die wissenschaftliche Literatur eingeführt.

5. Literaturverzeichnis

Amasheh S, Meiri N, Gitter AH, Schöneberg T, Mankertz J, Schulzke JD, Fromm M. (2002) Claudin-2 expression induces cation-selective channels in tight junctions of epithelial cells. *J Cell Sci.* 115(Pt 24): 4969-76

Bereswill S, Kist M. (2003) Recent developments in Campylobacter pathogenesis. *Curr Opin Infect Dis.* 16(5): 487-91

Black RE, Levine MM, Clements ML, Hughes TP, Blaser MJ. (1988) Experimental Campylobacter jejuni infection in humans. *J Infect Dis.* 157(3): 472-9

Bojarski C, Gitter AH, Bendfeldt K, Mankertz J, Schmitz H, Wagner S, Fromm M, Schulzke JD. (2001) Permeability of HT-29/B6 colonic epithelium as a function of apoptosis. *J. Physiol.* (Lond.) 535: 541-552

Bratz K, Bücker R, Gölz G, Zakrzewski SS, Janczyk P, Nöckler K, Alter T. (2013) Experimental infection of weaned piglets with Campylobacter coli--excretion and translocation in a pig colonisation trial. *Vet Microbiol.* 162(1): 136-43

Bücker R, Troeger H, Kleer J, Fromm M, Schulzke JD. (2009) Arcobacter butzleri induces barrier dysfunction in intestinal HT-29/B6 cells. *J Infect Dis.* 200(5): 756-64

Bücker R, Schumann M, Amasheh S, Schulzke JD. (2010) Claudins in intestinal function and disease. Current Topics in Membranes 65: 195-227, Chapter 9. published in Claudins, *Current Topics in Membranes*, Volume 65, edited by Alan S.L. Yu, Elsevier Inc. USA

Bücker R, Krug SM, Rosenthal R, Günzel D, Fromm A, Zeitz M, Chakraborty T, Fromm M, Epple HJ, Schulzke JD. (2011) Aerolysin from Aeromonas hydrophila perturbs tight junction integrity and cell lesion repair in intestinal epithelial HT-29/B6 cells. *J Infect Dis.* 204(8): 1283-92

Bücker R, Schulz E, Günzel D, Bojarski C, Lee IF, John LJ, Wiegand S, Janßen T, Wieler LH, Dobrindt U, Beutin L, Ewers C, Fromm M, Siegmund B, Troeger H, Schulzke JD. (2014) α-Haemolysin of Escherichia coli in IBD: a potentiator of inflammatory activity in the colon. *Gut*. doi: 10.1136/gutjnl-2013-306099 [Epub ahead of print]

Chen ML, Ge Z, Fox JG, Schauer DB. (2006) Disruption of tight junctions and induction of proinflammatory cytokine responses in colonic epithelial cells by Campylobacter jejuni. *Infect Immun.* 74(12): 6581-9

Cirl C, Wieser A, Yadav M, Duerr S, Schubert S, Fischer H, Stappert D, Wantia N, Rodriguez N, Wagner H, Svanborg C, Miethke T. (2008) Subversion of Toll-like receptor signaling by a unique family of bacterial Toll/interleukin-1 receptor domain-containing proteins. *Nat Med.* 14(4): 399-406

De Smet S, De Zutter L, Houf K. (2012) Spatial distribution of the emerging foodborne pathogen arcobacter in the gastrointestinal tract of pigs. *Foodborne Pathog Dis.* 9(12):1097-103

Dicksved J, Ellström P, Engstrand L, Rautelin H. (2014) Susceptibility to Campylobacter infection is associated with the species composition of the human fecal microbiota. *MBio.* 5(5): e01212-14

Dobrindt U, Chowdary MG, Krumbholz G, Hacker J. (2010) Genome dynamics and its impact on evolution of Escherichia coli. *Med Microbiol Immunol*. 199(3): 145-54

Ellis WA, Neill SD, O'Brien JJ, Ferguson HW, Hanna J. (1977) Isolation of *Spirillum/Vibrio*-like organisms from bovine fetuses. *Vet Rec*. 100: 451–2

Epple HJ, Mankertz J, Ignatius R, Liesenfeld O, Fromm M, Zeitz M, Chakraborty T, Schulzke JD. (2004) Aeromonas hydrophila beta-hemolysin induces active chloride secretion in colon epithelial cells (HT-29/B6). *Infect Immun.* 72(8): 4848-58

Evans MJ, von Hahn T, Tscherne DM, Syder AJ, Panis M, Wölk B, Hatziioannou T, McKeating JA, Bieniasz PD, Rice CM. (2007) Claudin-1 is a hepatitis C virus co-receptor required for a late step in entry. *Nature.* 446(7137): 801-5

Fasano A, Baudry B, Pumplin DW, Wasserman SS, Tall BD, Ketley JM, Kaper JB. (1991) Vibrio cholerae produces a second enterotoxin, which affects intestinal tight junctions. *Proc Natl Acad Sci* U S A. 88(12): 5242-6

Fukumatsu M, Ogawa M, Arakawa S, Suzuki M, Nakayama K, Shimizu S, Kim M, Mimuro H, Sasakawa C. (2012) Shigella targets epithelial tricellular junctions and uses a noncanonical clathrin-dependent endocytic pathway to spread between cells. *Cell Host Microbe*. 11(4): 325-36

Giaffer MH, Holdsworth CD, Duerden BI. (1992) Virulence properties of Escherichia coli strains isolated from patients with inflammatory bowel disease. *Gut*. 33(5): 646-50

Gitter AH, Bendfeldt K, Schulzke JD, Fromm M. (2000) Leaks in the epithelial barrier caused by spontaneous and TNFα-induced single-cell apoptosis. *FASEB J.* 14: 1749-1753

Gorkiewicz G, Thallinger GG, Trajanoski S, Lackner S, Stocker G, Hinterleitner T, Gülly C, Högenauer C. (2013) Alterations in the colonic microbiota in response to osmotic diarrhea. *PLoS One.* 8(2): e55817

Günzel D, Fromm M. (2012) Claudins and other tight junction proteins. *Compr Physiol.* 2(3): 1819-52

Günzel D, Yu AS. (2013) Claudins and the modulation of tight junction permeability. *Physiol Rev.* 93(2): 525-569

Hecht G, Koutsouris A, Pothoulakis C, LaMont JT, Madara JL. (1992) Clostridium difficile toxin B disrupts the barrier function of T84 monolayers. *Gastroenterology*. 102(2): 416-23

Heller F, Florian P, Bojarski C, Richter JF, Christ M, Hillenbrand B, Mankertz J, Gitter AH, Bürgel N, Fromm M, Zeitz M, Fuss I, Strober W, Schulzke JD. (2005) Interleukin-13 is the key effector Th2 cytokine in ulcerative colitis that affects epithelial tight junctions, apoptosis and cell restitution. *Gastroenterology.* 129(2): 550-564

Hering NA, Richter JF, Krug SM, Günzel D, Fromm A, Bohn E, Rosenthal R, Bücker R, Fromm M, Troeger H, Schulzke JD. (2011) *Yersinia enterocolitica* induces epithelial barrier dysfunction through regional tight junction changes in colonic HT-29/B6 cell monolayers. *Lab. Invest.* 91(2): 310-324

Hering NA, Richter JF, Fromm A, Wieser A, Hartmann S, Günzel D, Bücker R, Fromm M, Schulzke JD, Troeger H. (2014) TcpC protein from E. coli Nissle improves epithelial barrier function involving PKCζ and ERK1/2 signaling in HT-29/B6 cells. *Mucosal Immunol.* 7(2): 369-78

Högenauer C, Langner C, Beubler E, Lippe IT, Schicho R, Gorkiewicz G, Krause R, Gerstgrasser N, Krejs GJ, Hinterleitner TA. (2006) Klebsiella oxytoca as a causative organism of antibiotic-associated hemorrhagic colitis. *N Engl J Med*. 355(23): 2418-26

Ikenouchi J, Furuse M, Furuse K, Sasaki H, Tsukita S, Tsukita S. (2005) Tricellulin constitutes a novel barrier at tricellular contacts of epithelial cells. *J Cell Biol.* 171(6): 939-45

Janda JM, Kokka RP. (1991) Three-year prevalence of enteropathogenic bacteria in an urban patient population in Germany. *FEMS Microbiol Lett.* 69(1): 29-33

Karadas G, Sharbati S, Hänel I, Messelhäußer U, Glocker E, Alter T, Gölz G. (2013) Presence of virulence genes, adhesion and invasion of Arcobacter butzleri. *J Appl Microbiol.* 115(2): 583-90

Kiehlbauch JA, Brenner DJ, Nicholson MA, Baker CN, Patton CM, Steigerwalt AG, Wachsmuth IK. (1991) Campylobacter butzleri sp. nov. isolated from humans and animals with diarrheal illness. *J Clin Microbiol.* 29(2): 376-85

Kotlowski R, Bernstein CN, Sepehri S, Krause DO. (2007) High prevalence of Escherichia coli belonging to the B2+D phylogenetic group in inflammatory bowel disease. *Gut*. 56(5): 669-75

Krause-Gruszczynska M, Rohde M, Hartig R, Genth H, Schmidt G, Keo T, König W, Miller WG, Konkel ME, Backert S. (2007) Role of the small Rho GTPases Rac1 and Cdc42 in host cell invasion of Campylobacter jejuni. *Cell Microbiol.* 9(10): 2431-44

Kruis W, Fric P, Pokrotnieks J, Lukás M, Fixa B, Kascák M, Kamm MA, Weismueller J, Beglinger C, Stolte M, Wolff C, Schulze J. (2004) Maintaining remission of ulcerative colitis with the probiotic Escherichia coli Nissle 1917 is as effective as with standard mesalazine. *Gut*. 53(11): 1617-23

Krug SM, Amasheh S, Richter JF, Milatz S, Günzel D, Westphal JK, Huber O, Schulzke JD, Fromm M (2009a) Tricellulin forms a barrier to macromolecules in tricellular tight junctions without affecting ion permeability. *Mol Biol Cell.* 20: 3713-3724

Krug SM, Fromm M, Günzel D (2009b) Two-path impedance spectroscopy for measuring paracellular and transcellular epithelial resistance. *Biophys J.* 97: 2202-2211

Krug SM, Günzel D, Conrad MP, Lee IF, Amasheh S, Fromm M, Yu AS. (2012) Charge-selective claudin channels. *Ann N Y Acad Sci.* 1257: 20-8

Levican A, Alkeskas A, Günter C, Forsythe SJ, Figueras MJ. (2013) Adherence to and invasion of human intestinal cells by Arcobacter species and their virulence genotypes. *Appl Environ Microbiol.* 79(16): 4951-7

Ma TY. Intestinal epithelial barrier dysfunction in Crohn's disease. (1997) *Proc Soc Exp Biol Med.* 214(4): 318-27

Mayo-Wilson E, Junior JA, Imdad A, Dean S, Chan XH, Chan ES, Jaswal A, Bhutta ZA. (2014) Zinc supplementation for preventing mortality, morbidity, and growth failure in children aged 6 months to 12 years of age. *Cochrane Database Syst Rev*. 5: CD009384

Lazzerini M, Ronfani L. (2013) Oral zinc for treating diarrhoea in children. *Cochrane Database Syst Rev*. 1: CD005436

Liesenfeld O, Weinke T, Hahn H. (1993) Three-year prevalence of enteropathogenic bacteria in an urban patient population in Germany. *Infection.* 21(2):101-5

MacCallum A, Hardy SP, Everest PH. (2005) Campylobacter jejuni inhibits the absorptive transport functions of Caco-2 cells and disrupts cellular tight junctions. *Microbiology.* 151(Pt 7): 2451-8

Macutkiewicz C, Carlson G, Clark E, Dobrindt U, Roberts I, Warhurst G. (2008) Characterisation of Escherichia coli strains involved in transcytosis across gut epithelial cells exposed to metabolic and inflammatory stress. *Microbes Infect.* 10(4): 424-31

Man SM, Kaakoush NO, Leach ST, Nahidi L, Lu HK, Norman J, Day AS, Zhang L, Mitchell HM. (2010) Host attachment, invasion, and stimulation of proinflammatory cytokines by Campylobacter concisus and other non-Campylobacter jejuni Campylobacter species. *J Infect Dis.* 202(12): 1855-65

Mandisodza O, Burrows E, Nulsen M. (2012) Arcobacter species in diarrhoeal faeces from humans in New Zealand. *N Z Med J.* 125(1353): 40-6

Mankertz J, Amasheh M, Krug SM, Fromm A, Amasheh S, Hillenbrand B, Tavalali S, Fromm M, Schulzke JD (2009) TNFalpha up-regulates claudin-2 expression in epithelial HT-29/B6 cells via phosphatidylinositol-3-kinase signaling. *Cell Tiss Res.* 336(1): 67-77

Mankertz J, Tavalali S, Schmitz H, Mankertz A, Riecken EO, Fromm M, Schulzke JD (2000) Expression from the human occludin promoter is affected by tumor necrosis factor α and interferon γ. *J Cell Sci.* 113(Pt 11): 2085-2090

Martinez-Medina M, Aldeguer X, Lopez-Siles M, González-Huix F, López-Oliu C, Dahbi G, Blanco JE, Blanco J, Garcia-Gil LJ, Darfeuille-Michaud A. (2009) Molecular diversity of Escherichia coli in the human gut: new ecological evidence supporting the role of adherent-invasive E. coli (AIEC) in Crohn's disease. *Inflamm Bowel Dis.* 15(6): 872-82

Masanta WO, Heimesaat MM, Bereswill S, Tareen AM, Lugert R, Groß U, Zautner AE. (2013) Modification of intestinal microbiota and its consequences for innate immune response in the pathogenesis of campylobacteriosis. *Clin Dev Immunol.* 2013: 526860

Matysiak-Budnik, T, Moura IC, Arcos-Fajardo M, Lebreton C, Menard S, Candalh C, Ben-Khalifa K, Dugave C, Tamouza H, van Niel G, Bouhnik Y, Lamarque D, Chaussade S,

Malamut G, Cellier C, Cerf-Bensussan N, Monteiro RC, Heyman M (2008) Secretory IgA mediates retrotranscytosis of intact gliadin peptides via the transferrin receptor in celiac disease. *J Exp Med.* 205(1): 143-154

McNamara BP, Koutsouris A, O'Connell CB, Nougayréde JP, Donnenberg MS, Hecht G. (2001) Translocated EspF protein from enteropathogenic Escherichia coli disrupts host intestinal barrier function. *J Clin Invest.* 107(5): 621-9

Moriel, DG, Schembri, MA. (2014) Vaccination approaches for the prevention of urinary tract infection. *Curr Pharm Biotechnol*. 14(11): 967-74

Nielsen HL, Engberg J, Ejlertsen T, Bücker R, Nielsen H (2012a) Short-term and medium-term clinical outcomes of *Campylobacter concisus* infection. *Clin Microbiol Infect.* 18: E459-465

Nielsen HL, Ejlertsen T, Engberg J, Nielsen H (2012b) High incidence of *Campylobacter concisus* in gastroenteritis in North Jutland, Denmark: a population-based study. *Clin Microbiol Infect.* 48: 633-635

Nielsen HL, Nielsen H, Ejlertsen T, Engberg J, Günzel D, Zeitz M, Hering NA, Fromm M, Schulzke JD, Bücker R. (2011) Oral and fecal Campylobacter concisus strains perturb barrier function by apoptosis induction in HT-29/B6 intestinal epithelial cells. *PLoS One.* 6(8): e23858

Packey CD, Sartor RB. (2008) Interplay of commensal and pathogenic bacteria, genetic mutations, and immunoregulatory defects in the pathogenesis of inflammatory bowel diseases. *J Intern Med*. 263(6): 597-606

Peralta Soler A, Mullin JM, Knudsen KA, Marano CW. (1996) Tissue remodeling during tumor necrosis factor-induced apoptosis in LLC-PK1 renal epithelial cells. *Am J Physiol.* 270(5 Pt 2): F869-79

Porras M, Martín MT, Yang PC, Jury J, Perdue MH, Vergara P. (2006) Correlation between cyclical epithelial barrier dysfunction and bacterial translocation in the relapses of intestinal inflammation. *Inflamm Bowel Dis*. 12(9): 843-52

Raleigh DR, Marchiando AM, Zhang Y, Shen L, Sasaki H, Wang Y, Long M, Turner JR. (2010) Tight junction-associated MARVEL proteins marveld3, tricellulin, and occludin have distinct but overlapping functions. *Mol Biol Cell.* 21(7): 1200-13

Rojas R, Ruiz WG, Leung SM, Jou TS, Apodaca G. (2001) Cdc42-dependent modulation of tight junctions and membrane protein traffic in polarized Madin-Darby canine kidney cells. *Mol Biol Cell.* 12(8): 2257-74

Rosenthal R, Milatz S, Krug SM, Oelrich B, Schulzke JD, Amasheh S, Günzel D, Fromm M. (2010) Claudin-2, a component of the tight junction, forms a paracellular water channel. *J Cell Sci.* 123(Pt 11): 1913-21

Samie A, Obi CL, Barrett LJ, Powell SM, Guerrant RL. (2007) Prevalence of Campylobacter species, Helicobacter pylori and Arcobacter species in stool samples from the Venda region, Limpopo, South Africa: studies using molecular diagnostic methods. *J Infect*. 54(6): 558-66

Sánchez-Pulido L, Martín-Belmonte F, Valencia A, Alonso MA. (2002) MARVEL: a conserved domain involved in membrane apposition events. *Trends Biochem Sci.* 27(12): 599-601

Scanlon KA, Cagney C, Walsh D, McNulty D, Carroll A, McNamara EB, McDowell DA, Duffy G. (2013) Occurrence and characteristics of fastidious Campylobacteraceae species in porcine samples. *Int J Food Microbiol.* 163(1): 6-13

Schmitz H, Fromm M, Bentzel CJ, Scholz P, Bode H, Epple HJ, Riecken EO, Schulzke JD (1999) Tumor necrosis factor-α (TNFα) regulates the epithelial barrier in the human intestinal cell line HT-29/B6. *J Cell Sci.* 112: 137-146

Schneditz G, Rentner J, Roier S, Pletz J, Herzog KA, Bücker R, Troeger H, Schild S, Weber H, Breinbauer R, Gorkiewicz G, Högenauer C, Zechner EL. (2014) Enterotoxicity of a nonribosomal peptide causes antibiotic-associated colitis. *Proc Natl Acad Sci U S A.* 111(36): 13181-6

Schumann M, Richter JF, Wedell I, Moos V, Zimmermann-Kordmann M, Schneider T, Daum S, Zeitz M, Fromm M, Schulzke JD. (2008) Mechanisms of epithelial translocation of the a2-gliadin-33mer in celiac sprue. *Gut.* 57(6): 747-754

Schumann M, Günzel D, Buergel N, Richter JF, Troeger H, May C, Fromm A, Sorgenfrei D, Daum S, Bojarski C, Heyman M, Zeitz M, Fromm M, Schulzke JD. (2012) Cell polarity-determining proteins Par-3 and PP-1 are involved in epithelial tight junction defects in coeliac disease. *Gut.* 61(2): 220-8

Sears CL. (2000) Molecular physiology and pathophysiology of tight junctions V. assault of the tight junction by enteric pathogens. *Am J Physiol Gastrointest Liver Physiol.* 279(6): G1129-34

Sepehri S, Khafipour E, Bernstein CN, Coombes BK, Pilar AV, Karmali M, Ziebell K, Krause DO. (2011) Characterization of Escherichia coli isolated from gut biopsies of newly diagnosed patients with inflammatory bowel disease. *Inflamm Bowel Dis.* 17(7): 1451-63

Shen L, Turner JR. (2006) Role of epithelial cells in initiation and propagation of intestinal inflammation. Eliminating the static: tight junction dynamics exposed. *Am J Physiol Gastrointest Liver Physiol.* 290(4): G577-82

Shen L, Weber CR, Raleigh DR, Yu D, Turner JR. (2011) Tight junction pore and leak pathways: a dynamic duo. *Ann Rev Physiol.* 73: 283-309

Simonovic I, Rosenberg J, Koutsouris A, Hecht G. (2000) Enteropathogenic Escherichia coli dephosphorylates and dissociates occludin from intestinal epithelial tight junctions. *Cell Microbiol.* 2(4): 305-15

Suzuki H, Nishizawa T, Tani K, Yamazaki Y, Tamura A, Ishitani R, Dohmae N, Tsukita S, Nureki O, Fujiyoshi Y. (2014) Crystal structure of a claudin provides insight into the architecture of tight junctions. *Science.* 344: 304-7

Troeger H, Richter JF, Beutin L, Günzel D, Dobrindt U, Epple HJ, Gitter AH, Zeitz M, Fromm M, Schulzke JD. (2007a) Escherichia coli alpha-haemolysin induces focal leaks in colonic epithelium: a novel mechanism of bacterial translocation. *Cell Microbiol.*; 9(10): 2530-40

Troeger H, Epple HJ, Schneider T, Wahnschaffe U, Ullrich R, Burchard GD, Jelinek T, Zeitz M, Fromm M, Schulzke JD. (2007b) Effect of chronic *Giardia lamblia* infection on epithelial transport and barrier function in human duodenum. *Gut.* 56(3): 328-335

Troeger H, Loddenkemper C, Schneider T, Schreier E, Epple HJ, Zeitz M, Fromm M, Schulzke JD. (2009) Structural and functional changes of the duodenum in human norovirus infection. *Gut*. 58(8):1070-7

Turner JR, Buschmann MM, Romero-Calvo I, Sailer A, Shen L. (2014) The role of molecular remodeling in differential regulation of tight junction permeability. *Semin Cell Dev Biol*. pii: S1084-9521(14) 00277-8

Vandamme P, Falsen E, Rossau R, Hoste B, Segers P, Tytgat R, De Ley J. (1991) Revision of *Campylobacter, Helicobacter,* and *Wolinella* taxonomy: emendation of generic descriptions and proposal of *Arcobacter* gen. nov. *Int J Syst Bacteriol.* 41: 88–103

Vejborg RM, Hancock V, Schembri MA, Klemm P. (2011) Comparative genomics of Escherichia coli strains causing urinary tract infections. *Appl Environ Microbiol.* 77(10): 3268-78

Wesley IV, Baetz AL, Larson DJ. (1996) Infection of cesarean-derived colostrum-deprived 1-day-old piglets with Arcobacter butzleri, Arcobacter cryaerophilus, and Arcobacter skirrowii. *Infect Immun.* 64(6): 2295-9

Wooldridge KG1, Williams PH, Ketley JM. (1996) Host signal transduction and endocytosis of Campylobacter jejuni. *Microb Pathog.* 21(4): 299-305

Young CR, Harvey R, Anderson R, Nisbet D, Stanker LH. (2000) Enteric colonisation following natural exposure to Campylobacter in pigs. *Res Vet Sci.* 68(1):75-8

Appendix

Abbreviations in publications

2PI	Two-path impedance spectroscopy
A/E	Attaching & effacing lesions
AerA	Aerolysin (Toxin from *Aeromonas hydrophila*)
β-PFT	Beta-barrel pore-forming toxin
BAPTA-AM	1,2-bis-(2-amino-phenoxy)-ethane-N,N,N',N'-tetraacetic acid acetoxymethyl ester (= intracellular calcium chelator)
cAMP	Cyclic adenosine monophosphate
CC	Collagenous colitis
CD	Crohn's disease
CEM	Confocal endomicroscopy
CFU	Colony forming unit
CI	Confidence interval
CPE	*Clostridium perfringens* enterotoxin
CRP	C-reactive protein
DAPI	4′,6-diamidino-2-phenylindole, 4′,6-Diamidin-2-phenylindol
EGTA	Ethylenglycol-bis(aminoethylether)-N,N,N′,N′-tetraacetic acid
EHEC	Enterohaemorrhagic *Escherichia coli*
EPEC	Enteropathogenic *Escherichia coli*
FITC	Fluorescein isothiocyanate
GI	Gastrointestinal
GPI	Glycosylphosphatidylinositol
HDM	Haemolysin-deficient mutant
HlyA	Alpha-haemolysin
HRP	Horseradish peroxidase
HT-29/B6	B6-clon from the human colon carcinoma cell line HT-29
HU	Haemolytic unit
IBD	Inflammatory bowel diseases
IBS	Irritable bowel syndrome
ICD	International statistical classification of diseases and related health problems
IF	Immunofluorescence
IL-10$^{-/-}$	Interleukin-10-deficient mouse model
IQR	Interquartile range
I_{SC}	Short-circuit current

LDH	Lactatdehydrogenase
LSM	Laser-scanning microscopy
MA	Monoassociation
MC	Microscopic colitis
ML-7	Inhibitor of the myosin-light-chain-kinase
MLC	Myosin-light-chain
MLCK	Myosin-light-chain-kinase
MOI	Multiplicity of infection
MTT	3-(4,5-Dimethylthiazol-2-yl)-2,5-diphenyltetrazoliumbromid (= assay for viable cell count)
PFT	Pore-forming toxin
PPI	Proton pump inhibitor
qPCR	Quantitative real-time polymerase-chain-reaction
ReA	Reactive Arthritis
R^{epi}	Epithelial resistance
ROCK	Rho-associated protein kinase
R^{para}	Paracellular resistance
RPP	Relative prevalence proportion
RR	Relative risk
R^{sub}	Subepithelial resistance
R^{t}	Transepithelial resistance (= TER)
R^{trans}	Transzellular resistance
RTX	Repeats in toxin
spp.	Species (plural)
TJ	Tight Junction
TNFα	Tumor necrosis factor-alpha
TUNEL	Terminal deoxynucleotidyl transferase (TdT)-mediated dUTP nick end labeling
UC	Ulcerative colitis
UPEC	Uropathogenic *Escherichia coli*
WT	Wildtyp
Y-27632	Inhibitor of the Rho/ROCK signalling pathway
ZO-1	Zonula occludens-protein-1
ZOT	Zonula occludens-toxin
Z-VAD-FMK	N-benzyloxycarbonyl-Val-Ala-Asp-fluoromethyl-ketone (= Caspase-Inhibitor)

Danksagung

Mein herzlicher Dank gilt Prof. Dr. Jörg-Dieter Schulzke für die Einführung in das Forschungsfeld. Seine persönliches Engagement, die stetige Unterstützung, sowie die guten Diskussionen und vielen Ideen waren für mich sehr wertvoll.

Bedanken möchte ich mich auch bei Prof. Dr. Michael Fromm, der mir ebenfalls immer mit Rat und Tat zur Seite stand.

Ein herzlicher Dank geht auch an die Ärzte der Gastroenterologie Dr. Hanno Tröger, PD Dr. Christian Bojarski, PD Dr. Hans-Jörg Epple, Dr. Christian Barmeyer, Dr. Michael Schumann und Prof. Dr. Britta Siegmund für ihre tatkräftige Hilfestellung.

Bei Elisabeth Schultze, In-Fah Maria Lee, Claudia Heldt, Britta Jebautzke und Detlef Sorgenfrei, sowie insbesondere bei Anja Fromm, möchte ich mich für die professionelle Unterstützung in und um die Laborabeit bedanken. Insbesondere schwierige technische Details sind auf diese Weise für mich lösbar geworden.

Für die hervorragende Zusammenarbeit danke ich herzlich PD Dr. Rita Rosenthal, PD Dr. Dorothee Günzel, Stephanie Wiegand, Dr. Silke Zakrzewski und Dr. Susanne Krug, die mir mit ihrem Know-how in zahlreichen Versuchen helfen konnten. Ebenso bedanke ich mich bei meinen dänischen Kollegen Dr. Hans Linde Nielsen und Prof. Dr. Henrik Nielsen aus Aalborg und meinen österreichischen Kooperationspartnern Georg Schneditz, Prof. Dr. Christoph Högenauer, Prof. Dr. Ellen Zechner und PD Dr. Gregor Gorkiewicz aus Graz.

Den Kollegen aus der Infektiologie Dr. Verena Moos und Prof. Dr. Dr. Thomas Schneider sei ebenfalls recht herzlich für die gemeinsame Lehre und die fruchtbaren wissenschaftlichen Diskussionen gedankt. Bedanken möchte ich mich auch bei den Kollegen aus der Veterinärmedizin der FU Berlin, Prof. Dr. Thomas Alter und Dr. Greta Gölz, sowie Prof. Dr. Lothar Wieler für die gute Zusammenarbeit.

Für die gemeinsame Zeit im Institut für Klinische Physiologie mit reger kollegialer Interaktion danke ich auch den ehemaligen Kollegen Prof. Dr. Salah Amasheh, Dr. Nina Hering, Dr. Dana Kuntzsch, Dr. Lena John, Dr. Theresa Bergann und Dr. Svenja Plöger.

Einen besonderen Dank möchte ich an meinen Doktoranden Emanuel Schulz richten, der mich während seiner experimentellen Doktorarbeit substantiell unterstützt hat.

Meinen Eltern und Geschwistern und insbesondere meinen Kindern Lore und Kilian sowie meiner Frau Maxi möchte ich für die liebevolle Unterstützung danken.

Erklärung

§ 4 Abs. 3 (k) der HabOMed der Charité

Hiermit erkläre ich, dass

- weder früher noch gleichzeitig ein Habilitationsverfahren durchgeführt oder angemeldet wurde,
- die vorgelegte Habilitationsschrift ohne fremde Hilfe verfasst, die beschriebenen Ergebnisse selbst gewonnen sowie die verwendeten Hilfsmittel, die Zusammenarbeit mit anderen Wissenschaftlern/Wissenschaftlerinnen und mit technischen Hilfskräften sowie die verwendete Literatur vollständig in der Habilitationsschrift angegeben wurden,
- mir die geltende Habilitationsordnung bekannt ist.

Ich erkläre ferner, dass mir die Satzung der Charité – Universitätsmedizin Berlin zur Sicherung Guter Wissenschaftlicher Praxis bekannt ist und ich mich zur Einhaltung dieser Satzung verpflichte.

…….
Datum

……..
Unterschrift